PROTEINASE 3 ACTIVITY AS A BIOMARKER FOR DISEASE SEVERITY IN CHRONIC OBSTRUCTIVE PULMONARY DISEASE: A NOVEL MODEL OF THE PROTEINASE/ANTI-PROTEINASE BALANCE.

by HELENA ANNE CRISFORD.

A thesis submitted to the University of Birmingham for the degree of DOCTOR OF PHILOSOPHY.

Institute of Inflammation and Ageing

College of Medical and Dental Sciences

University of Birmingham

January 2022

ABSTRACT

Background

Alpha-1 antitrypsin (AAT) deficiency (AATD) represents a subset of chronic obstructive pulmonary disease (COPD) which is a progressive, inflammatory disease of the lungs. COPD presents a significant global health burden; however, its heterogeneity means its pathogenesis remains poorly understood.

AATD is caused by mutation in the anti-proteinase AAT, which results in little/no production of AAT and consequently uninhibited action of destructive proteinases, including proteinase 3 (PR3) and neutrophil elastase (NE). PR3 and NE are implicated in the pathophysiological development of emphysema and biomarkers of their activity (Aα-Val^{541} and Aα-Val^{360} respectively) correlate to disease severity and progression.

Methods

A novel *in vitro* neutrophil/fibrinogen-buffer model of the proteinase/anti-proteinase balance observed in AATD was validated for use within in-house PR3 and NE proteinase activity immunoassays to determine whether proteinase activity footprints (Aα-Val^{541} and Aα-Val^{360}) could be used as pharmaceutical biomarkers in disease.

Results and Conclusions

A reduction in proteinase activity within the model following AAT treatment was observed which supported the significance of the putative 11 μM AAT clinical threshold. The model was also validated to assess drug efficacy. For the first time, AZD9668 was demonstrated to reduce NE activity *in vitro* and evidence was presented to suggest it worked synergistically with AAT. These data support the application of the novel model presented in this thesis as a method to determine the effect of inhibitors on proteinase activity footprints and as a biomarker of pharmaceutical efficacy.

ACKNOWLEDGEMENTS

Firstly, I would like to express my thanks to my supervisors Professor Elizabeth Sapey, Professor Rob Stockley and Paul Newby for the support, guidance, and opportunities that they have given me through every stage of the research project. I really appreciate the time you've given to me.

I would also like to thank my past and present colleagues within the Respiratory lab for their support and friendship both in the lab and beyond. I owe you many more coffees in thanks than I can ever repay!

Finally, I wish to thank my family, particularly my Mum, my Dad, Sandi, Amy, my Grandma and my Grandad, for their love and support. Thank you for believing in and encouraging me. I could not have done this without you.

CONTENTS

LIST OF FIGURES

LIST OF TABLES

ABBREVIATIONS

$[E]_T$	Total enzyme
[S]	Substrate
7-AAD	7-aminoactineomycin
A2M	Alpha-2-macroglobulin
AAT	Alpha-1 antitrypsin
AATD	Alpha-1 antitrypsin deficiency
ADAPT	Antitrypsin Deficiency Assessment and Programme for Treatment
ANOVA	Analysis of variance
ANV	Annexin V
BPI	bacterial/permeability-increasing protein
BSA	Bovine serine albumin
C5a	Complement component 5a
CaI	Calcium ionophore
CD	Cluster of differentiation
CF	Cystic fibrosis
CT	Computer tomography
COPD	Chronic obstructive pulmonary disease
CRP	C-reactive protein
DAMPs	Damage associated molecular patterns.
DMSO	Dimethyl sulphoxide
DNA	Deoxyribonucleic acid
ECM	Extracellular matrix
ELISA	Enzyme-linked immunosorbent assay

ER	Endoplasmic recticulum
FEV_1	Forced expiratory volume in one second
fMLP	N-formylmethionyl-leucyl-phenylalanine
FVC	Forced vital capacity
GOLD	Global Initiative for Chronic Obstructive Lung Disease
GRN	Granulin
hCAP	Human cationic antimicrobial protein
HIV	Human immunodeficiency virus
HLA	Human leukocyte antigen
IL	Interleukin
IQR	Interquartile range
K_{ass}	Association rate
K_{cat}	Catalytic efficiency of enzyme
K_m	Michaelis constant
LFA-1	Lymphocyte function-associated antigen 1
Mac-1	Macrophage-1 antigen
MAMPs	Microbial associated molecular patterns
MMP	matrix metalloproteinase
MNEI	Monocyte/neutrophil elastase inhibitor
MPO	Myeloperoxidase
mRNA	messenger RNA
MSaavpN	N-methoxysuccinyl-ala-ala-pro-val-p-nitroanilide
NE	Neutrophil elastase
NETs	Neutrophil extracellular traps

NICE	National Institute for Health and Care Excellence
NREC	National Research Ethics Committee
NSP	Neutrophil serine proteinase
PBMC	Peripheral blood mononuclear cell
PBS	Phosphate buffered saline
PDB	Protein database
PE	Phycoerythrin
PGRN	Progranulin
Pi*XX*	Proteinase inhibitor *(allele 1, allele 2)*
PMN	Polymorphonuclear
PMSF	Phenylmethylsulfonyl fluoride
PPE	Porcine pancreatic elastase
PR3	Proteinase 3
PS	Phophatidylserine
PSA	Prostate specific antigen
RAGE	Receptor for advanced glycation end-products
RBC	Red blood cells
RCF	Relative centrifugal force
RCL	Reactive centre loop
RNA	Ribonucleic acid
ROS	Reactive oxygen species
RPMI	Roswell Park Memorial Institute
SD	Standard deviation
SDF	Stromal cell-derived factor

SEM	Standard error of the mean
Serpin	Serine proteinase inhibitor
SlaaapN	N-succinyl-Ala-Ala-Ala-p-nitroanilide
SLPI	Secretory leukocyte proteinase inhibitor
sRAGE	soluble receptor for advanced glycation end-products
TNFα	Tumour necrosis factor-α
v	Velocity
V_{max}	Maximum rate of reaction
WHO	World Health Organisation

CHAPTER 1: INTRODUCTION TO THE THESIS

The following outputs relate to this chapter:

Crisford, H. Sapey, E. Stockley, R.A. (2018). Proteinase 3; a potential target in chronic obstructive pulmonary disease and other chronic inflammatory diseases. *Respiratory Research.* **19**

Crisford, H. Sapey, E. Rogers, G.B. Taylor, S.L. Nagakumar, P. Lokwani, R. and Simpson, J.L. (2021). Neutrophils in Asthma: The good, the bad and the bacteria. *Thorax.***76(8).**

1.1. Chronic Obstructive Pulmonary Disease

1.1.1. Physiology of the Healthy Lung

The healthy lung is a complex organ consisting of a branching bronchial system that delivers air into the gas-exchanging terminal bronchioles and alveoli (Weibel, 1963). In these structures, pulmonary capillaries permit gas exchange into peripheral venous blood across a capillary endothelium and alveolar epithelium for uptake of oxygen and removal of excess carbon dioxide (Weibel, 1963). Air is inhaled through a bronchial tree via negative intrathoracic pressure and exhaled by passive recoil (Mead *et al.*, 1967).

Due to exposure to the external environment, the lung has also evolved a complex system of defence to trap and remove foreign particles via a mucociliary escalator (Bustamante-Marin *et al.*, 2017), and the local and systemic immune system to protect against infection by inhaled pathogens (Martin *et al.*, 2005).

The healthy lung consists of many different tissue layers: beneath a superficial liquid layer, there is an epithelial layer (consisting of ciliated cells in the larger airways and submucosal goblet cells), on top of the basement membrane and the lamina propria. Below this is the smooth muscle, submucosa (including cartilage and mucus glands) and the adventitial coat (Murray *et al.*, 2010). More peripherally, the airways become thinner and less complex with no cartilaginous support or submucosal glands, due to reduced exposure to large particles and hence less need for effective mucociliary clearance. Smaller particles in these peripheral airways are removed by phagocytes in

the tissues (Poulter, 1997; James, 2002), assisted by surfactant in larger airways (Han *et al.*, 2015).

These peripheral bronchioles end in the alveoli which are lined with squamous epithelium (type I and II pneumocytes) which produce essential surfactants whilst allowing for gas exchange (Guillot *et al.*, 2013; Knudsen *et al.*, 2018). Below this is a complex extracellular matrix (ECM); and structural fibres, including collagen, fibrinogen, and elastin. This matrix is on top of the endothelial cells of the pulmonary capillaries where most gas exchange occurs.

Dysfunction of these delicate mechanisms may result in the development of pathophysiological change associated with diseases such as Chronic Obstructive Pulmonary Disease (COPD).

1.1.2. Physiology of the COPD lung

The Global initiative for chronic Obstructive Lung Disease (GOLD) defines COPD as "a common, preventable and treatable disease that is characterised by persistent respiratory symptoms and airflow limitation due to airway and/or alveolar abnormalities usually caused by significant exposure to noxious particles or gases" (Global Initiative for Chronic Obstructive Lung Disease, 2021).

Thus, COPD describes a group of conditions characterised by an expiratory problem from loss of compliance and increased resistance due to damage of the small airways and delicate gas exchanging compartments, and compromise of the immune integrity

of the major airways (Singh, 2017; McGrath *et al.*, 2018). Although the condition is common the pathophysiology remains largely unclear.

Airflow obstruction is predominantly contributed to by changes in the small airways and lack of support due to connective tissue damage as part of emphysema which often co-exists with COPD to a varying extent (Hogg, 2004). Disease phenotypes may include chronic bronchitis, and a subset of patients have bronchiectatic change often in areas of emphysema (O'Donnell, 2011; Kim *et al.*, 2013). Both contribute to differences in clinical phenotype.

Small airway dysfunction is a slow, progressive problem that is thought to be caused by chronic inflammation leading to airway narrowing, mucus plugging, and fibrosis as a result of local tissue damage and defective repair (Allen, 2010). However, small airways are the main site of airway obstruction, and such changes often precede the development of emphysema (Hogg, 2004).

Chronic bronchitis is, by definition, inflammation of the bronchi and clinically manifests as cough and sputum production - due to excess mucus production by the goblet cells. This impairs mucociliary clearance which can be enhanced by epithelial damage and remodelling (Kim *et al.*, 2013), leading to microbial retention and chronic colonisation.

Bronchiectasis is primarily a pathological diagnosis of irreversibly dilated airways. More recently the widespread use of computer tomography (CT) scanning detects such changes in up to 50% of patients with a diagnosis of COPD (O'Brien *et al.*, 2000; Bafadhel *et al.*, 2011; Jin *et al.*, 2018). The dilatation also contributes to impairment of mucociliary clearance and sputum retention, and is often associated with persistent microbial colonisation with pathologically relevant bacteria (Currie *et al.*, 1987; Ni *et*

al., 2015), and increased likelihood of exacerbations and death (Patel *et al.*, 2004; Martínez-García *et al.*, 2011).

1.1.1.1. *Emphysema*

Emphysema is characterised by a permanent dilation and coalescence of the most peripheral airspaces from the terminal bronchioles (Gough, 1965). It is widely thought that these changes reflect connective tissue destruction by proteolytic enzymes. A key component of the alveolar structure is the lung elastin, but with emphysematous changes, elastin loses its fibrillary nature and is unable to provide a foundation for the alveolar epithelium or support for the small airways during expiration (Black *et al.*, 2008). The loss of essential lung elasticity from the disrupted tissue microarchitecture results in poor aeration and gas retention, which is associated with enlargement, coalescence and loss of shape in the alveoli, and results in dynamic collapse of the small airways during expiration, poor gas exchange and air trapping (Liu *et al.*, 2017) (**Figure.1.1**).

The role of elastin in this process is supported by extensive animal models of emphysema targeting this component for damage and defective repair (see later). Emphysema is associated with a more rapid decline of forced expiratory volume in one second (FEV_1), increased mortality and an increased likelihood of lung cancer (Oelsner *et al.*, 2016).

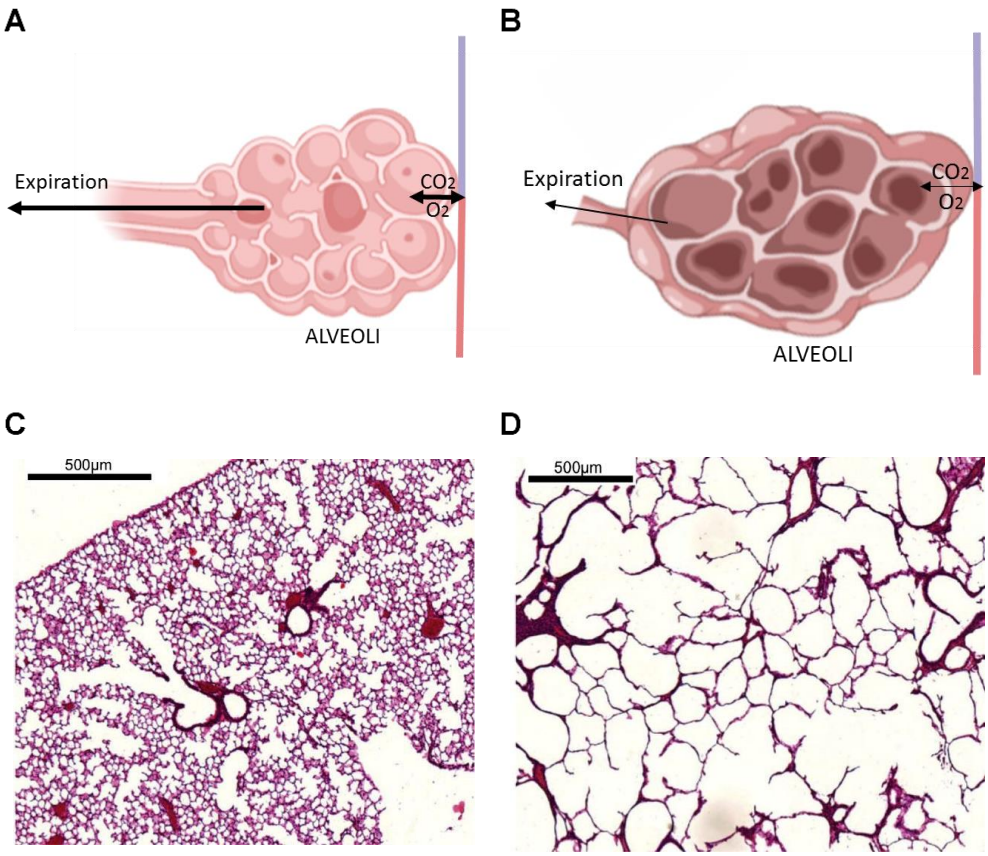

Figure.1.1. Diagram of alveoli with and without emphysematous changes and visualisation of emphysematous changes to lung structure.

A healthy alveolus with normal expiration and gaseous exchange; **B** alveolus with emphysematous changes resulting in impaired expiration and gaseous exchange. Arrows indication air movement within the alveoli, thinner lines portray reduced action or flow; **C** histological image showing healthy lung alveoli and terminal bronchioles stained with Meyer's H&E embedded within paraffin; **D** Histological image showing lung alveoli from a patient with COPD stained with Meyer's H&E embedded within paraffin with loss of normal architecture and airspace enlargement; Diagrams produced using BioRender.com, and histological images used with permission (Schleede *et al.*, 2012) (Permission for use granted by PNAS).

Air trapping causes further enlargement of alveolar spaces and contributes towards the hyperinflation observed in COPD patients (Thomas *et al.*, 2013; Gagnon *et al.*, 2014).

McDonough *et al.* (2011) found that gradual narrowing obstruction of the bronchioles culminating in small airway loss is observed in early-stage COPD, prior to the development of emphysematous changes.

1.1.3. Diagnostic criteria

Despite the high clinical, physiological and pathological heterogeneity, there are established diagnostic criteria for COPD.

According to GOLD, COPD is defined by airflow limitation with spirometry showing that the FEV_1 to forced vital capacity (FVC) ratio is less than the fixed value of 0.7 (Global Initiative for Chronic Obstructive Lung Disease, 2021).

Spirometry is undertaken as a forced airflow manoeuvre, so it is effort dependent and there is significant intra-patient variability (Hruby *et al.*, 1975; Magnussen *et al.*, 2017). It is also dependent upon age, sex, height, and ethnicity so it is usually normalised for all these factors and expressed as a % predicted (Ostrowski *et al.*, 2006; Global Initiative for Chronic Obstructive Lung Disease, 2021).

Airflow obstruction also becomes more prevalent with ageing (Halbert *et al.*, 2006; Mercado *et al.*, 2015) and is a feature of other diseases including asthma (Postma *et al.*, 2014) and bronchiectasis (Roberts *et al.*, 2000). More recently it has been recognised that many of the biological features of COPD can be identified before

airflow obstruction crosses the 80% diagnostic threshold for FEV_1 and FEV_1/FVC ratio of 0.7 (see later) (Miller *et al.*, 2011; Şerifoğlu *et al.*, 2019).

These lung function thresholds may act as indicators of clinical features including exercise capacity and premature mortality (Torén *et al.*, 2020). However, the mainstay of therapy is to alleviate symptoms and hence GOLD proposes clinicians' direct treatment predominantly at improving current symptoms as well as preventing recurrent exacerbations.

COPD exacerbations are defined as acute worsening of respiratory symptoms requiring further treatment (Global Initiative for Chronic Obstructive Lung Disease, 2021). The episodes may be mild, moderate or severe depending on the treatment required, with severe episodes reflecting hospitalisation (Miravitlles *et al.*, 1999).

In addition to the symptoms above, cough and sputum production are also relatively common (~30% of patients) and makes exacerbations more likely (Global Initiative for Chronic Obstructive Lung Disease, 2021). Other common symptoms include wheezing, chest pain and chest tightness, disturbed sleep (Global Initiative for Chronic Obstructive Lung Disease, 2021). In addition, there are other less common features of COPD including, fatigue, weight loss, anorexia, cough syncope, and depression as well as increased likelihood of co-morbidities including type 2 diabetes, cardiovascular disease, osteoporosis, lung cancer and periodontitis (Global Initiative for Chronic Obstructive Lung Disease, 2021).

1.1.4. Risk Factors

COPD is a highly multifactorial disease and demonstrates high heterogeneity. Indeed, individuals may be exposed to multiple risk factors but still retain lung function in the normal range, whereas others may have limited exposures but still develop COPD indicating the current limitations in knowledge of pathophysiological process and susceptibility.

Contributing factors to COPD development include:

- Classically in western culture, there is usually a history of exposure to tobacco smoking/passive smoking or to environmental pollutants (Saetta *et al.*, 1994; Halbert *et al.*, 2006; Jayes *et al.*, 2016).

  Cigarette smoke exposure induces an inflammatory state which leads to neutrophil recruitment to the airways (Totti *et al.*, 1984; Shoji *et al.*, 1995); increasing cell life span and impairing neutrophil clearance (Quint *et al.*, 2007). These changes appear to continue in patients with/or susceptible to COPD even after smoking cessation (Willemse *et al.*, 2005; Louhelainen *et al.*, 2009), suggesting a disease-specific continuation.

  Current smokers aggravate pulmonary inflammation when they smoke (Lee *et al.*, 2012). Patients who continue to smoke, therefore have a greater likelihood of progression of disease in general (Pride, 2001).

- Other high-risk exposures include urban air pollution (Berend, 2016), occupational exposures which could include mining or industrial fumes (Baur *et al.*, 2010; Sadhra *et al.*, 2017), concurrent cannabis smoking (Ribeiro *et al.*, 2016) and biomass fuel

pollution (Siddharthan *et al.*, 2018). Further, household exposure may account for a 41% increase in likelihood of developing COPD (Siddharthan *et al.*, 2018). Emerging longitudinal and existing animal models also suggests that e-cigarettes may have a role in COPD development (Phillips *et al.*, 2015; Bals *et al.*, 2019; Bhatta *et al.*, 2020).

- Increasing evidence provides support that older patients are more likely to develop emphysematous changes in the lung associated with progressive age-related decline in lung function, termed inflamm-ageing (Mercado *et al.*, 2015). A global meta-analysis found that up to 10% of over 40-year-olds may have physiologically definable COPD (Halbert *et al.*, 2006). Further, GOLD found multiple worldwide studies indicating an increase in COPD prevalence with age (Global Initiative for Chronic Obstructive Lung Disease, 2021).

- The same meta-analysis also reported a higher prevalence of COPD in males (Halbert *et al.*, 2006) and similarly, the Burden of Obstructive Lung Disease identified a prevalence of COPD at 11.8% in males and 8.5% in females (Lamprecht *et al.*, 2011).

  Recent literature has implied that although they have a lower prevalence, women may be more susceptible to developing COPD. Females are reported to develop more severe disease from lower cigarette smoke exposure (Sørheim *et al.*, 2010; Barnes, 2016a). It is suggested that this is because women generally have smaller airways and therefore are exposed to a greater local concentration of tobacco smoke (Barnes, 2016a). Although, evidence suggests that women are less likely to

develop emphysema and more likely to develop small airway disease as the dominant feature of their COPD (Barnes, 2016a). It may also be proposed that hormonal differences may also play a role (Barnes, 2016a).

- Any process affecting foetal, infant, and adolescent lung development (for example diet, physiological damage or birth complications) may cause a reduction in spirometrically measured maximal lung function obtained in adulthood. The 2020 GOLD report termed these “childhood disadvantage factors”. A systematic review by Savran *et al.* found that factors of relevance included foetal/infant tobacco exposure, low birth weight and, lower respiratory tract infections and asthma in childhood (Savran *et al.*, 2018).

- There are many links between socioeconomic status and COPD. Those with lower socioeconomic status have an increased likelihood of developing disease (Gershon *et al.*, 2011; Beran *et al.*, 2015; Townend *et al.*, 2017). Lower socioeconomic status is also associated with low birth weight, malnutrition, exposure to higher levels of pollution and crowding which may be the cause.

- Studies have found that people with pre-existing asthma are 12x more likely to develop COPD than those without asthma, and that 20% of asthmatics were likely to develop irreversible airway obstruction (Vonk *et al.*, 2003; Silva *et al.*, 2004). Although it must be noted that asthma endotype was not considered in the analysis of these studies.

- Infections affecting the lung, including pneumonia or tuberculosis and generalised infections related to human immunodeficiency virus (HIV), are associated with increased risk of COPD development (Byrne *et al.*, 2015; Bigna *et al.*, 2018), particularly when these infections occur in childhood (Hayden *et al.*, 2015).

- Diabetes and cardiovascular disease are among diseases that can coexist with COPD as common comorbidities. It is suspected that immune dysfunction and/or abnormal inflammation pathways may be shared between these conditions (Sevenoaks *et al.*, 2006; Hughes *et al.*, 2020). However, this may reflect common causation, such as smoking and environmental/socioeconomic factors.

A further factor is genetic predisposition to develop obstructive lung disease, as COPD is recognised to run in families. The most widely recognised genetic association is alpha-1 antitrypsin deficiency (AATD) which is described in detail in **1.4 Alpha-1 Antitrypsin Deficiency.**

Whilst the factors described above are widely implicated in the development of COPD, not all such exposed individuals develop the condition suggesting a susceptibility with a gene/environment aetiology or factors not currently recognised.

1.1.5. Global health and economic burden

Globally there are estimated to be 384 million people living with COPD, although many are believed to remain undiagnosed, and approximately 2.9 million people die each year with the condition (Adeloye *et al.*, 2015). Case finding studies have estimated that approximately 10% of the global adult population have COPD (at GOLD stage II or higher) (Buist *et al.*, 2007; Adeloye *et al.*, 2015).

A meta-analysis of COPD between 1990 and 2014 found that numbers were highest in the Americas (15.2% in 2010), with lower reported prevalence in Southeast Asia (9.7%) (Adeloye *et al.*, 2015). The prevalence increased most rapidly in the Eastern Mediterranean area (+118.7%) over this period especially in urban rather than rural populations. More recently these prevalence figures have been confirmed worldwide (as categorised into Europe, Africa, America, Asia and Oceania) (Blanco *et al.*, 2019).

Of note, the locations with a higher prevalence of COPD are also areas that have been demonstrated to have/have had higher proportions of smokers (Jha *et al.*, 2002; Ng *et al.*, 2014).

In 2014, it was estimated that COPD costs the United Kingdom health service £2108/patient per year, with individual costs rising with each exacerbation especially those leading to hospital admission, giving an overall total cost of approximately £1.9 billion per year (Punekar *et al.*, 2014).

1.1.6. Treatment

There is no cure for COPD, but recently, clinicians have aimed to target ‘treatable traits’ of COPD, referring to phenotypic characteristics of an individual’s disease emphasising the heterogeneity of the disease.

Depending on the disease stage, severity, or rate of progression – inhaled therapies are aimed at treating symptoms predominantly of breathlessness, reduced exercise tolerance, and preventing exacerbations with the aim of improving quality of life and potentially preventing further damage, although few clinical trials demonstrate an effect on disease progression (The Torch Study Group, 2004; Calverley *et al.*, 2007). Rehabilitation is advised for most patients especially with moderate to severe disease and can also improve symptoms. Other palliative approaches may have individual roles in specific patients (as demonstrated in **Figure 1.2**) (Global Initiative for Chronic Obstructive Lung Disease, 2021).

It is argued that in this complex disease, biological characteristics should be considered as a treatable trait. This would include focussing on neutrophils which are present in higher numbers both in the bronchi and alveoli in COPD (O'Shaughnessy *et al.*, 1997; Saetta *et al.*, 1997; Stone *et al.*, 2012) and are suggested to be responsible for driving both inflammation and damage.

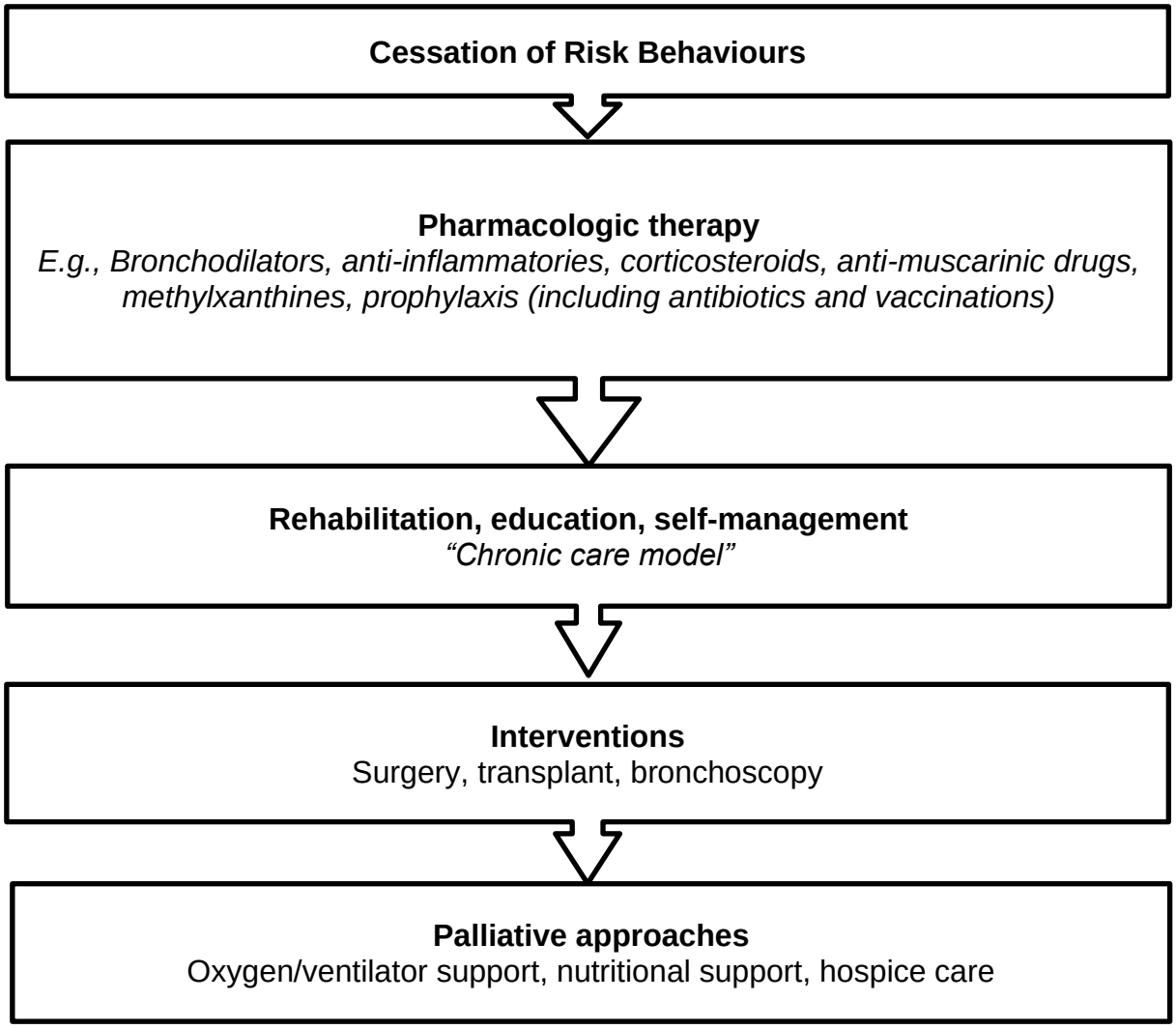

Figure 1.2. Progression of treatment options available for patients with COPD.

Treatment pathway for patients diagnosed with COPD. Generated using information from GOLD (Global Initiative for Chronic Obstructive Lung Disease, 2021).

1.2. The neutrophil in COPD

The following section pertains to a published review paper; ***Crisford, H.*** *Sapey, E. Rogers, G.B. Taylor, S.L. Nagakumar, P. Lokwani, R. and Simpson, J.L. (2021). Neutrophils in Asthma: The good, the bad and the bacteria. Thorax.* ***76(8).***

Neutrophils are multi-lobular, innate immune cells and make up the majority of circulating polymorphonuclear (PMN) leukocytes (also referred to as granulocytes) (Amulic *et al.*, 2012). The normal concentration is 2.5-7.5x10^6 cells/ ml, approximately accounting for 70% of circulating white blood cells (Li *et al.*, 2002; Sapey, 2010; Amulic *et al.*, 2012). Following maturation from haematopoietic stem cells (da Silva *et al.*, 1994), neutrophils have a short circulating half-life of less than 24 hours (Dancey *et al.*, 1976; Suratt *et al.*, 2001) and therefore a turnover of 5-10 x10^{10} neutrophils/day is required to maintain neutrophil homeostasis (Summers *et al.*, 2010).

Once released into the circulation from the bone marrow, neutrophils patrol the blood vessels and navigate towards inflammation by sensing chemotactic gradients, such as interleukin (IL)-8, which are released by the affected tissues mainly due to the interaction of microbial or damage-associated molecular patterns (M/D-AMPs) (Amulic *et al.*, 2012). During this process, neutrophils utilise cellular polarity, regulated by Rho guanosine triphosphatases, to perform amoeboid movement to reach the site of inflammation accurately (Norberg *et al.*, 1977; Amulic *et al.*, 2012).

Once near the site of infection or inflammation, they undergo a process of rolling along the endothelium, firm adhesion with surface receptors, including LFA-1 and Mac-1 which are upregulated in activated neutrophils (Ding *et al.*, 1999), before shedding

Cluster of differentiation (CD)62L and transmigrating through tissues (Gane *et al.*, 2012; Tak *et al.*, 2017).

To enable migration through dense extracellular matrices, neutrophils release proteinases from the granular cytoplasm, such as neutrophil elastase (NE) and proteinase 3 (PR3), to cleave components of the ECM such as elastin, fibronectin, vitronectin, laminin and collagen (Amulic *et al.*, 2012).

Neutrophils are often maintained in a neutral quiescent or primed state, but when activated have the potential to carry out 3 functions rapidly: (1) phagocytosis of particulates, especially if opsonised, (2) degranulation and/or (3) release of neutrophil extracellular traps (NETs) (Amulic *et al.*, 2012).

1. At the site of inflammation, neutrophils engulf smaller target material by phagocytosis, such as the respiratory relevant pathogens *Haemophilus influenzae* (Ahmed *et al.*, 1993) or *Streptococcus pneumoniae* (Hof *et al.*, 1980; Thore *et al.*, 1985). Engulfed microbes are contained within a phagolysosome to protect the cell and then destroyed through pH change, and exposures to reactive oxygen species (ROS) and cytotoxic/hydrolytic enzymes released by the granules into the phagolysosomes (Lee *et al.*, 2003).

2. Besides phagocytosis, neutrophils can also kill microbes by degranulation, a process in which neutrophils release cytotoxic ROS and proteolytic enzymes such as NE/PR3 into the extracellular medium at the site of infection (Korkmaz *et al.*, 2010; Crisford *et al.*, 2018) where they are also able to destroy invading pathogens (Amulic *et al.*, 2012). These externalised granules also facilitate tissue penetration

and have evolved the ability to degrade the surrounding tissues preventing the spread of infection (Amulic *et al.*, 2012). There are 3 types of granules released by neutrophils, each containing different proteins (**Figure 1.3**). This process results in a region of obligate tissue damage due to proteinase degradation, described in greater detail later (**1.3. Neutrophil Serine Proteinases**).

3. The last neutrophilic mechanism is the release of neutrophil extracellular traps (NETs) as a final action of the cell. These are web-like structures consisting of cytosolic granule proteins embedded on a scaffold of decondensed chromatin (Brinkmann *et al.*, 2004; Papayannopoulos, 2018). NETs capture pathogens within the chromatin fibres, then high concentrations of neutrophil serine proteinases (NSPs) and ROS destroy the trapped microbes without the process of phagocytosis (Amulic *et al.*, 2012).

The release of NETs from neutrophils in normal conditions, termed vital NETosis, is controversial (Yipp *et al.*, 2013; Brinkmann, 2018), however their production in high stress situations, termed suicidal NETosis, is clearly demonstrated *in vitro* (Brinkmann *et al.*, 2004; de Bont *et al.*, 2018) leading to cytotoxic damage to the microenvironment (Narasaraju *et al.*, 2011; Lefrançais *et al.*, 2018). The exact function of NETs is subject to much debate and, at the time of writing, no consensus has been achieved as to the method to create NETs *in vitro*.

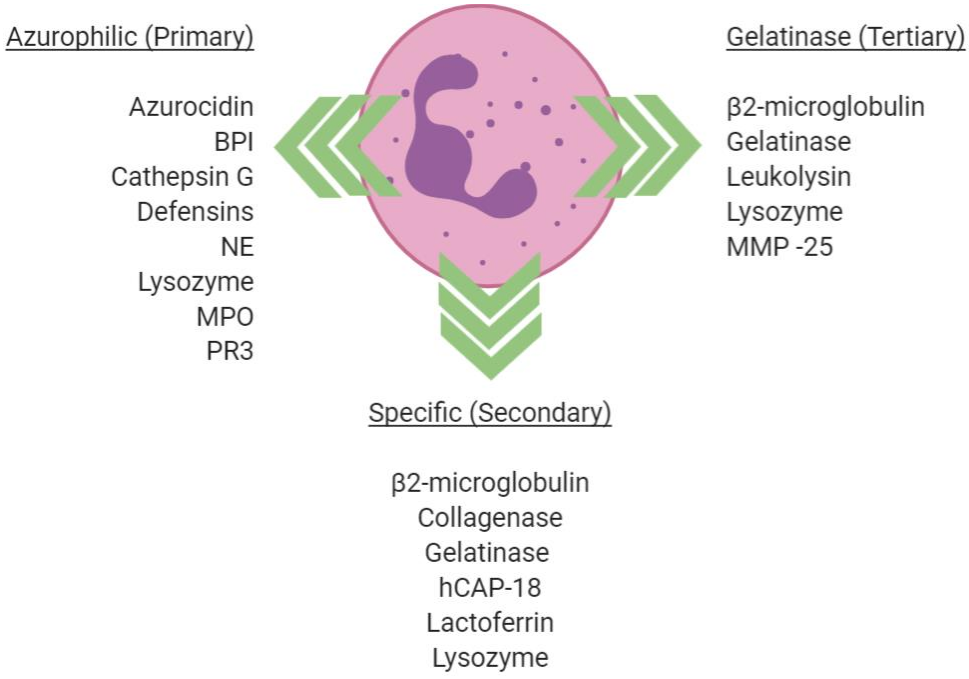

Figure 1.3. Proteins released from within the primary, secondary, and tertiary granules.

Diagram of proteins released from within the neutrophil granules during degranulation. Image shows a neutrophil. BPI=bacterial/permeability-increasing protein, NE= neutrophil elastase, MPO=myeloperoxidase, PR3=proteinase 3, MMP=matrix metalloproteinase, hCAP=human cationic antimicrobial protein. Produced using BioRender.com. (Amulic *et al.*, 2012).

Following transmigration to sites of inflammation and fulfilling their function, neutrophils either move back into the circulation (via a process called reverse transmigration, which is thought to be uncommon) (Hughes *et al.*, 1997; Mathias *et al.*, 2006), are phagocytosed by macrophages (termed efferocytosis) (deCathelineau *et al.*, 2003; Grabiec *et al.*, 2016), or in the case of the lung transported along the bronchial tree by the mucociliary escalator to the oropharynx and swallowed or expectorated as sputum (Singh *et al.*, 2010; Amulic *et al.*, 2012).

Previously, the understanding was that some neutrophils may be sequestered within the vasculature of the lungs (O'Shaughnessy *et al.*, 1997) to provide a more rapid immune response to the host-environment interface in the airways (Lien *et al.*, 1991; Kuebler *et al.*, 1999). However, recent studies have indicated that this does not occur, with neutrophils only retained transiently within the lung vasculature when primed (Summers *et al.*, 2014; Tregay *et al.*, 2019). Neutrophils have a large diameter when compared to narrow pulmonary capillaries and it has hence recently been shown that passage through the tight vasculature in the lung can also de-prime activated neutrophils (Vogt *et al.*, 2018).

Studies suggest that neutrophil functions change as the host ages. In older age, there is a decline in cellular function, including reduced migratory accuracy (Sapey *et al.*, 2014), NETs generation (Hazeldine *et al.*, 2014), and phagocytosis (Butcher *et al.*, 2000), but increased spontaneous ROS production (Ogawa *et al.*, 2008), and decreased ROS production following stimulation (Sauce *et al.*, 2017). The cells from older adults may therefore predispose to a less effective pathogen clearance but increased bystander tissue damage, which may be further exaggerated during severe infections (Sapey *et al.*, 2017).In COPD, neutrophil functions can also be altered.

Patients with COPD display upregulation of neutrophil α-defensins (Wang *et al.*, 2008), proteinases (Damiano *et al.*, 1986; Lacoste *et al.*, 1993; Linden *et al.*, 1993) and increased NET formation (Obermayer *et al.*, 2014; Grabcanovic-Musija *et al.*, 2015; Pedersen *et al.*, 2015; Wright *et al.*, 2016).

In addition, neutrophils isolated from patients with COPD display dysfunctional migration - with impaired directional accuracy as a result of defective cellular signalling (Sapey *et al.*, 2011) - and some evidence of reduced phagocytic ability (Fietta *et al.*, 1988) *in vitro* compared to healthy matched controls. These changes are reminiscent of the “ageing” dysfunction observed in later life.

Although less well studied, increased airway neutrophils are associated with airflow obstruction breathlessness, and a faster subsequent decline in FEV_1 (Boulet *et al.*, 2003). NSPs have been implicated in airway mucus gland hyperplasia, mucus secretion, airway smooth muscle cell proliferation and impaired ciliary function which is described in greater detail later (Smallman *et al.*, 1984; Voynow *et al.*, 2004; Park *et al.*, 2005; Domon *et al.*, 2018).

NE, PR3 and cathepsin G are the three main NSPs stored within the primary granules (Pham, 2006; Amulic *et al.*, 2012). They are classified by the presence of an active site serine residue activated by scissile bond cleavage, marked by their catalytic triad of residues (His57, Asp102 and Ser195), and can hydrolyse key structural proteins including elastin and collagen (Rao *et al.*, 1991; Lombard *et al.*, 2005; Korkmaz *et al.*, 2008; Hajjar *et al.*, 2010; Chelladurai *et al.*, 2012; Twigg *et al.*, 2015). They can be found on the cell surface of mature neutrophils, especially following activation (Csernok *et al.*, 1994; Baici *et al.*, 1996).

It is believed that when these NSPs are initially released, the amount exceeds the ability of local inhibitors to inactivate them (see local inhibitors in **Figure 1.4**), a cycle of neutrophilic inflammation begins that can lead to progressive tissue damage thought to be central to the pathophysiology of diseases such as COPD (Stockley, 2001; 2002; Pham, 2006; Crisford *et al.*, 2018). NE has long been suspected as the major contributor to the development of COPD and is supported by a plethora of in vitro and animal studies, however more recent studies have also highlighted a similar and significant role for PR3 (Gudmann *et al.*, 2018; Newby *et al.*, 2019; Schouten *et al.*, 2021).

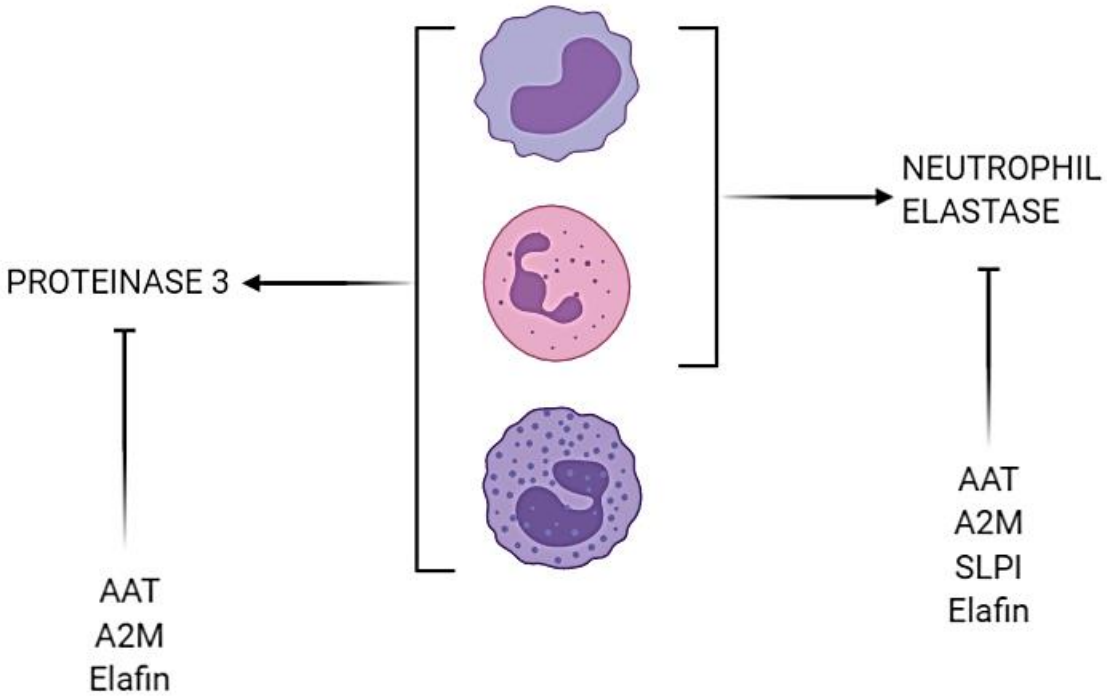

Figure 1.4. Endogenous inhibitors of PR3 and NE.

Endogenous inhibitors of PR3 and NE following release from a cellular source. Cells illustrated (top to bottom): monocyte, neutrophil, basophil. PR3 is released by monocytes, neutrophils, and basophils, whereas NE is only released from monocytes and neutrophils. Alpha-1 antitrypsin (AAT), alpha-2-macroglobulin (A2M) and Elafin inhibit both NE (Laurent *et al.*, 1989; Ying *et al.*, 1993; Janciauskiene *et al.*, 2018) and PR3 (Duranton *et al.*, 2003; Zani *et al.*, 2004; Sinden *et al.*, 2015). NE is also inhibited by the lung derived inhibitor secretory leukocyte protease inhibitors (SLPI) (Bergenfeldt *et al.*, 1992). Image created using BioRender.com.

1.3. Neutrophil Serine Proteinases

The following section reflects a published review paper; ***Crisford, H.*** *Sapey, E. Stockley, R.A. (2018). Proteinase 3; a Potential Target in Chronic Obstructive Pulmonary Disease and Other Chronic Inflammatory Diseases. Respiratory Research.* ***19:*** *180.*

As mentioned previously, the NSP PR3 (also known as myeloblastin, azurophil granule protein-7 or p29b) is an enzyme released from the azurophilic granules during neutrophilic inflammation and can cleave many targets including key structural proteins of the lung.

A second NSP NE (also referred to as leukocyte elastase or serine elastase) is also released from the azurophilic granules during neutrophilic inflammation and shares many of the same properties as PR3.

This section focuses on PR3 and NE as these have been shown to produce emphysema in animal models and may be more relevant to airflow obstruction of COPD. Both enzymes are thought to play central roles in COPD pathophysiology as they can replicate many of the structural changes of the disease and hence a potential target for therapeutic manipulation, described in detail in **1.3.5 The role of proteinases in COPD**.

1.3.1. Proteinase 3 specificity

PR3 is a highly abundant neutrophil protein that is transcribed in primitive myeloid and monocytic progenitor cells, and expressed in cells of both granulocyte and monocyte

lineage, especially neutrophils, but also to a lesser extent in mast cells and basophils (Zimmer *et al.*, 1992; Baici *et al.*, 1996; Korkmaz *et al.*, 2008; Karatepe *et al.*, 2015). In the neutrophil, it is primarily located within the azurophilic granules of the mature cell but is also present in specific granules, secretory vesicles, and on the cell surface (Csernok *et al.*, 1994; Witko-Sarsat *et al.*, 1999). It is expressed constitutively on the cell membrane by naïve neutrophils in peripheral blood of healthy individuals (known as “constitutive” PR3) and increases with cell priming by tumour necrosis factor (TNF)α (van Rossum *et al.*, 2004), and is secreted into extracellular milieu during neutrophil activation following granule translocation to the cell membrane (known as “induced” PR3) and exocytosis (Csernok *et al.*, 1994; Halbwachs-Mecarelli *et al.*, 1995; Korkmaz *et al.*, 2009; Korkmaz *et al.*, 2013).

The protein is encoded by the gene *PRTN3* which is located at human chromosome 19p13.3 and spans 6.57 kb pairs, including 5 exons and 4 introns. It consists of 222 amino acids that fold to form the 29 kDa glycoprotein (**Figure 1.5**).

PR3 is classified within the family of “chymotrypsin”-like NSP, which are characterised by their highly conserved catalytic triad (His57, Asp102 and Ser195; using chymotrypsinogen numbering) that defines the proteolytic specificity and classified by their active site serine residue (Korkmaz *et al.*, 2008; Hajjar *et al.*, 2010). PR3, like other NSPs, possesses an enlarged binding site with high specificity (Hajjar *et al.*, 2010), but differs by 4 main subsites, S2, S1’, S2’ and S3’ (**Figure 1.6.**). PR3 specificity is further defined by differences in residues that alter subsite specificities (subsites shown in **Figure 1.6.**).

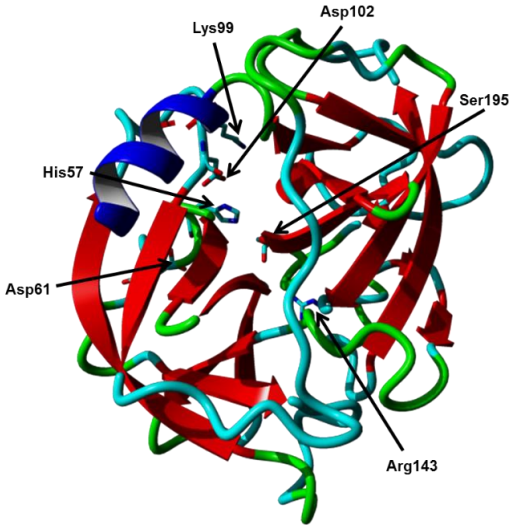

Figure 1.5. Three-dimensional visualisation of Proteinase 3 by ribbon plot.

Ribbon plot of PR3 with the catalytic triad and PR3-specific residues stylised in a stick representation and annotated. Image developed from the Proteinase 3 Protein Data Bank entry (PDB ID: 1FUJ) (Fujinaga *et al.*, 1996; Berman *et al.*, 2000) using YASARA (Krieger *et al.*, 2014). *(Published in Crisford et al.,* 2018).

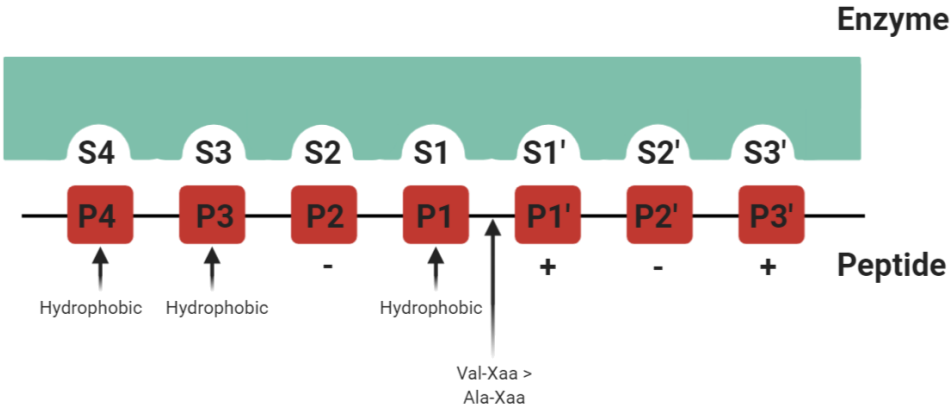

Figure 1.6. Substrate binding sites of Proteinase 3.

Representation of the substrate-binding pockets S4-S3' of PR3 with substrate cleavage positions P4-P3', according to Schechter and Berger enzyme-ligand binding site numbering convention (Schechter *et al.*, 1967). Arrows indicate sites for Val/Ala containing peptide cleavage and hydrophobic residue binding sites, whilst + indicates a positive and – a negative residue binding site (Hajjar *et al.*, 2006). *(Adapted from Crisford et al.,* 2018*)*.

Substrate specificities are determined by:

- Amide hydrogens on Gly193 and Ser195 which stabilises charge during catalysis (Guarino *et al.*, 2018).

- 3 charged residues: Lys99, Asp61, and Arg143 within the active site region.

Positioning of the solvent accessible Lys99, which borders the S2 and S4 sites and makes the S2 subsite deeper and more polar, in addition to reducing its hydrophobicity, which determines preferential binding of negative and polar residues, such as Asp (Fujinaga *et al.*, 1996; Hajjar *et al.*, 2010; Guarino *et al.*, 2018).

Asp61 brings the proteins negatively charged side chain closer to the S1' and S'3 subsites, making the subsites smaller and more polar, thereby encouraging binding of basic residues at P1' and P'3 (Hajjar *et al.*, 2010; Korkmaz *et al.*, 2010).

Arg143 (and Pro151) increase the polarity of the S2' subsite which creates a basic S2' subsite that binds acidic residues (Hajjar *et al.*, 2010; Korkmaz *et al.*, 2010).

Asp213 (compared to Ala213 in NE) restricts the S1 binding site causing it to bind small hydrophobic residues at P1 preferentially, which includes alanine, serine, valine, norvaline, and methionine (Rao *et al.*, 1991; Brubaker *et al.*, 1992; Hajjar *et al.*, 2010; Korkmaz *et al.*, 2010; Guarino *et al.*, 2018).

Ile217 allows small hydrophobic residues at P4 to bind with Trp218, creating a more hydrophobic S5 subsite (Hajjar *et al.*, 2010; Korkmaz *et al.*, 2010; Guarino *et al.*, 2018).

1.3.2. Neutrophil elastase specificity

NE is transcribed, and expressed in the same manner as PR3, although NE is not expressed by basophils. In the neutrophil, NE is also stored within primary azurophilic granules and can be mobilised to the cell surface and nuclear envelope.

It is encoded by the gene *ELANE* which is located, near *PRTN3*, at human chromosome 19p13.3 and spans 5 exons and 4 introns (Takahashi *et al.*, 1988). In NE, 218 amino acids fold to form its 29.5 kDa glycoprotein structure (Bode *et al.*, 1986).

Like PR3, NE is also a “chymotrypsin”-like NSP, with a catalytic triad, and an active site serine residue. It also possesses two N-glycosylation sites (Bode *et al.*, 1986).

NE specificity is defined by:

- A small hydrophobic residue at the P1 position, similarly to PR3 (Korkmaz *et al.*, 2008).

- Val190, Phe192, Ala213, Val216, Phe228 and the Cys191-220 disulphide bridge, which results in a hemispherical and hydrophobic S1 pocket which preferentially cleaves hydrophobic residues (Navia *et al.*, 1989).

- Bordering of the S2 subsite with Phe214, Leu99 and His57 resulting in a shallower S2 pocket than seen in PR3, and preferential medium hydrophobic side chains (Navia *et al.*, 1989).

- Hydrophobic S1’ and S2’ subsites from Cys42-Cys58, Phe41 and Leu143 positioning (Navia *et al.*, 1989).

1.3.3. NSP transcription and storage

Both PR3 and NE are initially transcribed as inactive precursors, referred to as zymogens, and then undergo a two-stage posttranslational modification to become active (Korkmaz *et al.*, 2008).

Firstly (via signal peptidase), there is N-terminal signal peptide cleavage, followed by cleavage of the N-terminal pro-di-peptide by the cysteine proteinase, cathepsin C leading to enzymatic activity (Korkmaz *et al.*, 2010).

Secondly, they undergo pro-peptide cleavage at the C terminus which is crucial for granule packaging (Hajjar *et al.*, 2010). This forms the catalytic triad of residues and the final conformation of the mature proteinase.

The active enzymes then remain stored within the neutrophil azurophilic granules until release.

1.3.4. NSP release

There is estimated to be 3 pg of PR3 and 1.1 pg of NE stored in each neutrophil, alongside other key NSPs (Campbell *et al.*, 2000b). Although this quantification is shown to be highly variable between individuals (Halbwachs-Mecarelli *et al.*, 1995).

Release of NSPs can occur either constitutively or via granule translocation.

Externalisation of NE occurs through electrostatic, charge-dependent interactions with proteoglycans, whereas PR3 membrane binding relies upon a hydrophobic surface patch.

Once released from the granule, NSPs can act enzymatically in both an intracellular and extracellular manner. Their activity is localised through inactivation by inhibitors (both reversibly and irreversibly), including **ser**ine **p**roteinase **in**hibitors (Serpins), chelonianin inhibitors and alpha-2-macroglobulin (A2M) (Zani *et al.*, 2004; Loison *et al.*, 2014; Yang *et al.*, 2017).

1.3.5. The role of proteinases in COPD

NSPs have many functions. Their primary roles are described below. Dysfunction of these systems has long been associated with the development or progression of several chronic inflammatory diseases, including COPD.

1.1.1.2. *Tissue Remodelling*

It is believed that NSPs play a key role in the tissue damage leading to emphysema, especially in subjects with genetic deficiency of alpha-1 antitrypsin (AAT).

When a migrating neutrophil degranulates *in vitro*, it releases PR3 and NE from the azurophilic granules. Some enzyme becomes membrane-bound and more resistant to inhibition, and some enzyme becomes free (Campbell *et al.*, 2000b).

Many biochemical studies have shown that NSPs cleave ECM proteins, including elastin, fibronectin, vitronectin, laminin and collagen, at a GXXPG site within a β-fold conformation resulting in protein degradation (Rao *et al.*, 1991; Lombard *et al.*, 2005; Joo *et al.*, 2010; Chelladurai *et al.*, 2012; Kristensen *et al.*, 2015).

These proteins are important components of tissue structures and, it is the degradation of the ECM (particularly elastin) which results in the interstitial damage leading to emphysema, in animal models and reflected *in vivo* by biomarkers in COPD.

The role of NE in this process is widely accepted inducing emphysema in animal models (Janoff *et al.*, 1977; Mehraban *et al.*, 2020) as well as mucous gland hyperplasia, mucus secretion, ciliary dysfunction and damage to many aspects of the innate and secondary immune systems (Smallman *et al.*, 1984; Stockley, 1995; Voynow *et al.*, 2004; Park *et al.*, 2005; Domon *et al.*, 2018).

Furthermore, PR3 has also been shown to have many of the same effects *in vivo* including the development of emphysema (Kao *et al.*, 1988; Borel *et al.*, 2018).

1.1.1.3. *Cytokines*

As well as causing direct tissue damage, NSPs can potentially amplify the cytokine-induced inflammation associated with COPD.

The NSPs are known to modulate a variety of cytokine functions, which impact processes such as metabolism and inflammasome generation (Sorensen *et al.*, 2001; Popa *et al.*, 2007; Ren *et al.*, 2009; Domon *et al.*, 2018) – see **Table 1.1**. The enzymes facilitate increased production and/or modulation of pro-inflammatory cytokines. Many of which have also been implicated in other inflammatory diseases.

All these cytokines can act through autocrine, paracrine and endocrine pathways to activate pro-inflammatory cascade responses and upregulate pro-inflammatory genes and transcription factors leading to a heightened inflammatory state (Zhang *et al.*, 2007). The products of these key inflammatory pathways can further induce feedback loops to perpetuate and enhance chronic inflammation (Robache-Gallea *et al.*, 1995; Kessenbrock *et al.*, 2011; Nemeth *et al.*, 2016).

Therefore, proteinases can play multiple roles in the initiation and amplification of inflammation, as demonstrated *in vitro* and hence likely are involved in similar processes *in vivo*.

Table 1.1. Summary of the cytokines acted on by proteinase 3 and neutrophil elastase.

Cytokine	Role of PR3	Role of NE
IL-1α	Processes and activates through cleavage at Ala101	
IL-6	Functionally inactivates and degrades the soluble IL-6 receptor (sIL-6R) – exact mechanisms unknown.	
IL-36	Proteolytically processes and activates	
IL-1β	Proteolytically activates extracellular pro-forms to be cleaved into active counterparts.	Inactivates mature p17 where IL-1α is active
IL-8	Truncates stored IL-8 (77) into more potent chemoattractant IL-8 (70) through Ala-Lys cleavage.	No known action
IL-17	Stimulation increases cytokine production	No known action
IL-18	Activation of pro-forms through proteolytic cleavage	No known action
IL-32	Cleaves IL-32 at IL-32α to a more bioactive form	No known action
IL-33	Processes and activates through proteolytic cleavage. Supresses NE activation.	Enhances activity
SDF-1α	No known action	Cleaves the N-terminal tripeptide Lys1-Pro2-Val3 decreasing activity.
TNFα	Cleaves precursor to bioactive form (via hypothesised cleavage sites at Ala15-Leu16 or Val77-Arg78)	Reports are conflicted as to the effect of NE on TNFα.

Legend. Table showing proteinase action on cytokines. Adapted from (Crisford *et al.*, 2018). IL=interleukin, TNFα=tumour necrosis factor-α, SDF=stromal cell-derived factor. (Keatings *et al.*, 1996; Coeshott *et al.*, 1999; Hurst *et al.*, 2001; Sugawara *et al.*, 2001; Valenzuela-Fernández *et al.*, 2002; McLoughlin *et al.*, 2004; Kim *et al.*, 2005; Calabrese *et al.*, 2008; Afonina *et al.*, 2011; Lefrancais *et al.*, 2012; Alfaidi *et al.*, 2015; Rani *et al.*, 2015; Henry *et al.*, 2016).

1.1.1.4. *Inflammatory mediators*

More recently, both NE and PR3 have been also found to degrade the anti-inflammatory mediator progranulin (PGRN), resulting in the generation of granulin (GRN) peptides *in vitro* (Couto *et al.*, 1992; Kessenbrock *et al.*, 2008; Kessenbrock *et al.*, 2011; Ungers *et al.*, 2014). PGRN degradation causes increased neutrophil infiltration, activation of ROS, pro-inflammatory cytokine production and anti-inflammatory pathway inhibition, which sustains an inflammatory state in several inflammatory diseases (Baker *et al.*, 2006). GRN molecules are also known to accumulate and release the chemoattractant IL-8 amplifying neutrophil recruitment (Couto *et al.*, 1992; Zhu *et al.*, 2002). In clinically stable COPD, the concentration of PR3 in airway secretions is a strong predictor of PGRN levels, because of its high neutrophil concentration and hence greater secretory activity.

PR3 is also able to act in a pro-inflammatory manner by interacting with the complement pathway. It can fragment the neutrophil surface complement component 5a (C5a) receptor (C5aR), resulting in the loss of the N-terminus and an inability to bind C5a (van der Berg *et al.*, 2014). In cystic fibrosis (CF), the lack of C5aR signalling contributes towards inefficient clearance of microbial infections *in vitro* and also inactivates signalling and stimulates neutrophils to degranulate (van der Berg *et al.*, 2014). This potentially results in a cycle of dysfunctional neutrophils thereby perpetuating the bacterial-stimulated inflammatory signals and further neutrophil recruitment. Although there is no direct evidence, it is likely that C5aR inhibition by PR3 also has a role in COPD leading to elevated levels of C5a in the sputum of patients and correlations with circulating C5a, physiological gas transfer and the degree of

emphysema (Marc *et al.*, 2004). Further research is clearly indicated to determine any importance of this mechanism in COPD.

An additional mechanism implicated in the pathophysiology of COPD involves the receptor for advanced glycation end-products (RAGE) and soluble RAGE (sRAGE) (Stockley *et al.*, 2019). In prostate cancer cell lines, PR3 has been shown to bind to RAGE both promoting cell activation and preventing its cleavage which escalates inflammation (Sukkar *et al.*, 2012; Kolonin *et al.*, 2017). Furthermore, decreased levels of sRAGE have been implicated in emphysema development (Sukkar *et al.*, 2012; Yonchuk *et al.*, 2015), and sRAGE concentration is lower with increasing severity (by GOLD stage) (Cockayne *et al.*, 2012) and the rate of decline in FEV_1/FVC (Iwamoto *et al.*, 2014).

1.1.1.5. *Microbicidal Clearance*

Despite the potential to impede bacterial clearance, it has also been reported that NSPs possess bactericidal properties.

PR3 acts through cleavage of the pro-microbicidal protein hCAP-18 (human cathelicidin) into the antibacterial peptide, mucus inducer and neutrophil chemo-attractant LL-37 (Campanelli *et al.*, 1990; Dasaraju *et al.*, 1996; Sorensen *et al.*, 2001; Zhang *et al.*, 2014; Kuroda *et al.*, 2015). Furthermore, levels of LL-37 in sputum are related to disease severity in patients with COPD suggesting an indirect role for PR3 which is worthy of further investigation (Jiang *et al.*, 2012).

Similarly, NE is involved in the activation of antibacterial cathelicidins (Cole *et al.*, 2001), which act against Staphylococcus, *E. coli*, *Pseudomonas aeruginosa* and

Candida species, and protegrins from inactive pro-protegrins in porcine models, with increased activity against *Listeria* species (Shi *et al.*, 1998).

As described previously, NSPs can adhere to NETs contributing towards the destruction of bacteria (Kessenbrock *et al.*, 2009; Urban *et al.*, 2009; Delgado-Rizo *et al.*, 2017). However, many respiratory-relevant bacteria, such as *Streptococcus pneumoniae* and *Haemophilus influenzae,* have evolved NET evasion mechanisms that may overcome this potential clearance mechanism (Beiter *et al.*, 2006; Hong *et al.*, 2009). It has also been noted that patients with *P. aeruginosa* infection are more susceptible to poor outcomes when lacking sufficient proteinase inhibition and patients with AATD are at particularly high risk of respiratory infection and lung damage as other natural proteinase inhibitors are unable to compensate for low AAT levels (Benarafa *et al.*, 2007; Sinden *et al.*, 2013).

It has further been reported that PR3 can inactivate secretory leukocyte protease inhibitors (SLPI), by cleaving at the Ala-16 site within the N-terminal and preventing SLPI/enzymes complex formation which would indirectly amplify the local activity of other NSPs, including NE (Rao *et al.*, 1993) that would normally be controlled (at least in part) by SLPI.

1.1.1.6. *Cellular signalling*

PR3 and NE have roles in the efficacy of neutrophil transmigration (Wang *et al.*, 2005; Kuckleburg *et al.*, 2012). PR3 acts through interaction with the cell surface receptor NB1 (CD177) which acts with PECAM-1 (CD31) during trans-endothelial migration of neutrophils (Wiedow *et al.*, 2005; Kuckleburg *et al.*, 2012).

In CF, this is supported by a positive relationship between PR3 activity and neutrophil migration effectiveness (Twigg *et al.*, 2015). The interaction of PR3 with NB1 and PECAM-1 is confirmed *in vitro* in endothelial cells, where it inhibits activation and upregulation of these adhesion molecules (Saragih *et al.*, 2014).

Recent data quantifying proteinase specific cleavage of elastin and fibrinogen in COPD provides more direct evidence of ongoing PR3 activity (Carter *et al.*, 2013; Newby *et al.*, 2017; Gudmann *et al.*, 2018; Schouten *et al.*, 2021).

1.1.1.7. *Proteinase/anti-proteinase balance theory*

The pathophysiology of COPD is considered to reflect an imbalance between proteinases and anti-proteinases in the lung that results in the predominance of uncontrolled enzyme activity.

Generally, activated proteinases have the potential to cause direct tissue damage (as described above), whereas anti-proteinases protect this process. In heath, a homeostatic balance is largely maintained in the lungs, with the exception of a region of quantum proteolysis closely surrounding migrating and degranulating neutrophils which is greater in patients with AATD explaining the increased susceptibility of these

subjects to developing features of COPD (Campbell *et al.*, 2000a) – described in more detail in **1.4.2 Alpha-1 Antitrypsin Deficiency.**

Sinden *et al.* produced mathematical evidence to support a greater potential role for PR3 in tissue damage in a three-dimensional reaction diffusion lung interstitium model (Sinden *et al.*, 2015). The authors demonstrated that active proteinase diffusion distance following release from a neutrophil varies depending on concentrations of the released enzyme and local concentration of inhibitors (Sinden *et al.*, 2015).

Obligate proteolysis in the immediate cell vicinity reflects the high concentrations of NSPs released from the granules compared to the available concentration of the physiological inhibitors. As the NSPs diffuse away from the neutrophil, the concentration falls exponentially until it equals that of the surrounding inhibitors when activity ceases (Campbell *et al.*, 2000a). It is believed that when numbers of NSPs exceed the number of protective anti-proteinases, such as AAT, excessive damage to lung tissue and other proteinase effects are facilitated (Stockley, 1999).

The theory of a proteinase/anti-proteinase imbalance is supported by further, recent evidence that SerpinA1 paralog-deficient murine models (a murine homolog) develop spontaneous emphysema (Borel *et al.*, 2018).

In addition, NSP-knockout murine models are protected against developing emphysema induced by cigarette smoke. Mice only deficient in NE are less susceptible but still develop emphysema-like changes when exposed to cigarette smoke, implying that either cathepsin G or PR3 also play an important role (Guyot *et al.*, 2014).

It should be noted that an imbalance can also be a result of excess neutrophil migration, where the release of enzyme exceeds the ability of local inhibitors to minimise the area of obligate proteolysis, and this has been implicated in the pathophysiology of COPD in subjects with normal AAT (Burnett *et al.*, 1987; Owen *et al.*, 1995) and patients with bronchiectasis with or without cystic fibrosis (Sandhaus *et al.*, 2013).

1.4. Alpha-1 Antitrypsin Deficiency

The term COPD refers to a heterogeneous group of physiological and pathological conditions. As previously described, AATD is one widely recognised risk factor for the development of COPD with an implicated genetic basis.

The concept of the proteinase/anti-proteinase balance originated from this observational link. Such individuals can develop COPD in the absence of any recognised external risk factors and are thought to reflect the increased obligate proteolysis of degranulating neutrophils due to a critical reduction in the surrounding AAT inhibition.

Due to its specific aetiology, it is argued that AATD should be considered a treatable trait and should be targeted for treatment by biologics or other compounds that can redress the balance (van Dijk *et al.*, 2020).

1.4.1. Alpha-1 Antitrypsin

AAT is a 52 kDa circulating Serpin produced and released predominantly by hepatocytes, but also in smaller amounts by airway epithelium and some phagocytes (Koj *et al.*, 1978; Mornex *et al.*, 1986; Cichy *et al.*, 1997). From the liver, it is then secreted into the circulation, diffuses into tissues and provides essential protection from excessive proteinase activity.

AAT can rapidly and irreversibly inhibit NSPs (Beatty *et al.*, 1980; Korkmaz *et al.*, 2008). It is highly active in the lung and is considered to be a major mediator of the proteinase/anti-proteinase balance.

Usually, AAT exists as a single polypeptide chain that undergoes extensive folding before secretion consisting of an exposed reactive centre loop (RCL) alongside three beta-sheets and nine alpha-helices (Irving *et al.*, 2000)**.**

The RCL consists of 20 amino acid residues that mimic the proteinase substrate site (Belorgey *et al.*, 2007).

AAT acts on NSPs with non-covalent binding occurring between the RCL, and P1-P1' (In Schechter-Berger notation (Schechter *et al.*, 1967)) on the enzyme to form a Michaelis-like complex (Gettins, 2002; Janciauskiene *et al.*, 2018). The enzyme is then translocated and the proteinase active site serine reacts by first cleaving the inhibitor RCL at Met358-Ser359, forming an acyl ester linkage against the inhibitor RCL in its β-sheet A (Gettins, 2002). This action results in a conformational change to the enzyme, with disruption of the P1 side chain from S1, movement of the catalytic Ser195 from His57 and loss of its oxyanion hole, ultimately preventing catalytic efficacy and resulting in inhibition of proteinase activity (Gettins, 2002).

AAT covalently binds active proteinases. Inhibition of NE occurs at 1:1 stoichiometry (Korkmaz *et al.*, 2008), although this can be affected by environmental factors (Shock *et al.*, 1988). AAT has a 10X higher association rate (K_{ass}) with NE than with PR3 which suggests its first activity is to inhibit NE.

AAT is the major inhibitor of destructive NSPs, contributing significantly towards the proteinases/anti-proteinase balance which protects the lung. It is generally accepted that a lack of AAT is central to the inflammatory airway disease associated with AATD and the cause of the pathophysiological emphysema (Stockley, 1999).

1.4.2. Alpha-1 Antitrypsin Deficiency

AATD is the only widely recognised genetic cause of COPD. It is caused by mutations in the SERPINA1 gene, which encodes AAT (Kidd *et al.*, 1983; Gettins, 2002). In AATD, mutations result in premature stop codons preventing the production of the whole functional protein or amino acid substitutions which can alter the conformation of AAT by changing structural interactions. This potential for conformational change is the most recognised mechanism especially in the Z genotype (see below) which results in spontaneous polymerisation causing retention and failure of adequate secretion from the hepatocytes or proteasome destruction (McCarthy *et al.*, 2016).

Mutation with polymerisation results in low serum concentrations (2.5-7 μM in the Z homozygote variant compared to a normal level of 20-48 μM in the usual M variants (American Thoracic Society/European Respiratory Society, 2003)). Genetic defects resulting in values below 11 μM are thought to predispose subjects to emphysematous lung disease and is termed the putative “at-risk threshold” (Wewers *et al.*, 1987) (**Figure 1.7**).

There are over 120 deficient genotypes described, and patients may be heterozygous or homozygous (Richardson *et al.*, 1969). Phenotypes are named Pi for proteinase inhibitor then alleles are lettered according to protein migration speed along an isoelectric gradient, with Z very slow, S slow and, M (being the central letter of the alphabet) medium (Sinden, 2012).

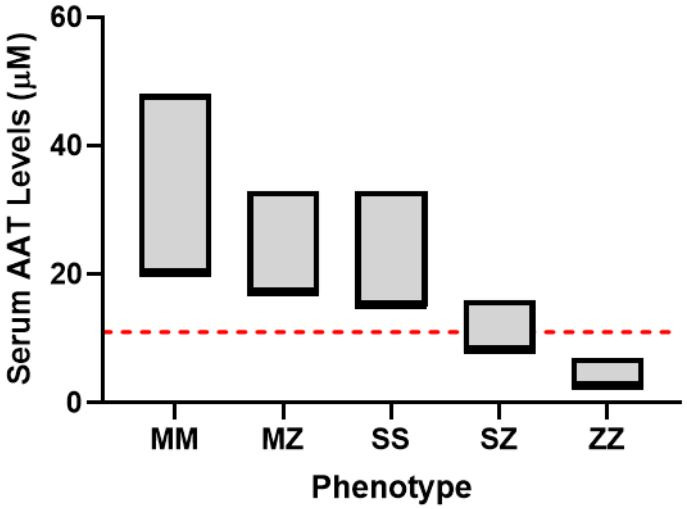

Figure 1.7. Phenotype serum concentrations of alpha-1 antitrypsin

Visualisation of the usual range of serum alpha-1 antitrypsin (AAT) concentrations, µM, from different AAT deficient phenotypes. The putative AAT threshold of 11 µM, below which there is generally an accepted increased predisposition to the development of emphysematous lung disease, is indicated by a dotted red line. Values obtained from American Thoracic Society/European Respiratory Society consortium guidelines (American Thoracic Society/European Respiratory Society, 2003).

It is now becoming widely accepted to refer to AAT variants by their genotype. Exact genetic defects have been characterised for most of the known variants. Some defects lead to no gene transcription, and hence translation and secretion, so cannot be phenotyped by isoelectric focussing making genetic nomenclature essential. For instance, a Znull genotype only transcribes the Z gene. So Znull phenotyping will only identify the Z protein and may mistakenly be interpreted as being a ZZ heterozygote in the absence of confirmative family studies (Abboud *et al.*, 2011; Tubío-Pérez *et al.*, 2018).

The normal genotype (~90% of all humans) is PiMM (Sveger *et al.*, 1995; Thelin *et al.*, 1996), whereas PiZZ causes the most prevalent severe deficiency with only 15% of the normal serum AAT levels (**Figure 1.7**) (Sveger, 1976; Zorzetto *et al.*, 2008). A PiZZ genotype is predominantly present in Caucasian populations at a prevalence of up to 1 in 1600 in Scandinavia (Sveger, 1976; Hutchison, 1998) but with decreasing prevalence consistent with early human migration patterns (Stockley *et al.*, 2013b).

Z protein variant is the result of the substitution of lysine 342 for glutamine, following an exon 5 mutation in *SerpinA1* (Carrell *et al.*, 2003).

This results in defective folding causing loop-sheet polymerisation with the active site of one molecule linking with the RCL β-sheet A of a second molecule (Lomas *et al.*, 1992; Nyon *et al.*, 2012). It must be noted that although alternative hypotheses of polymerisation, including the β-hairpin (Yamasaki *et al.*, 2008) and C-terminal (Yamasaki *et al.*, 2011) theories, have been suggested, that subsequent biochemical analysis tends to support the loop-fold hypothesis (Tsutsui *et al.*, 2008; Ekeowa *et al.*, 2010; Nyon *et al.*, 2012; Faull *et al.*, 2020).

Usually, the accumulation of mutant protein within the cell triggers a degradation pathway, called the unfolded protein response (Ron *et al.*, 2007), during which Ire1-Xbp1 coordinates endoplasmic reticulum(ER)-associated degradation cascades (Yoshida *et al.*, 2003), however, the Z mutant has also been demonstrated to also have a reduced rate of degradation (Wu *et al.*, 2003; Haq *et al.*, 2016) which enhances its retention.

Aggregated undegraded AAT protein can be visualised as inclusion bodies in the endoplasmic reticulum of hepatocytes (Graham *et al.*, 1990) and is believed to result in the instigation of a heat shock response causing localised tissue damage leading to clinically important liver disease in some subjects (Qizilbash *et al.*, 1983; Janciauskiene *et al.*, 2004).

In particular, homozygous Z genotypes (Jugniot *et al.*, 2018) may be accompanied with disease of the liver, such as cirrhosis, due to the aggregation of these polymerised proteins (Tanash *et al.*, 2019). Indeed, Qizilbash and Young-Pong (1983) identified periportal aggregations associated with AATD from a cohort of 500 deceased patients, and furthermore 71% of cases with these periportal aggregations presented with cirrhosis.

Furthermore, it has been shown in a murine model of PiZ-induced liver injury, that high concentrations of aggregations correlate with increased levels of autophagy and apoptotic cellular death (Lindblad *et al.*, 2007).

Initially, the subsequent low AAT concentrations due to the impaired hepatocyte release were considered to be solely responsible for emphysema and lung creating a proteinase/anti-proteinase imbalance in the lung.

This AAT has also been demonstrated to aggregate within the lung tissues which may in part reflect the local release of AAT by lung epithelial cells (Mulgrew *et al.*, 2004; Mahadeva *et al.*, 2005; Blanco, 2014). Cigarette smoke has been shown to exacerbate the polymerisation of AAT in the airways which may reflect an oxidation process (Alam *et al.*, 2011). This may play an additional role in the development of disease as polymers trigger inflammation cascades and localise neutrophils to the tissues where they can release ROS and proteinases, exacerbating local proteinase activity (McElvaney *et al.*, 1997; Mahadeva *et al.*, 2005; Janciauskiene *et al.*, 2018).

More rarely AATD is associated with necrotising cutaneous panniculitis of adipose tissue, inflammatory bowel disease, kidney disease such as glomerulonephritis, or vascular conditions including granulomatosis with polyangiitis (Esnault *et al.*, 1993; Montanelli *et al.*, 2002; Stone *et al.*, 2014; Blanco *et al.*, 2016) however this thesis focuses on its role in lung disease.

The second most common AAT genotype associated with some deficiency is the *SerpinA1* S mutation. The S variant of AAT is a result of the substitution of glutamine at position 264 with valine (Long *et al.*, 1984). S allele genotypes also have a lower secretion from hepatocytes, have a shorter half-life and are degraded more quickly (Long *et al.*, 1984).

However, AAT levels in homozygous S genotype (PiSS) individuals are about 60% of normal concentrations (15-33 μM in S compared to 20-48 μM in M homozygotes) (American Thoracic Society/European Respiratory Society, 2003). The S variant is not thought to present an increased health risk. Patients with S variants rarely present with

clinical disease and, if so, it is not considered attributed to their AAT (de Serres *et al.*, 2006; McGee *et al.*, 2010).

However, intermediate heterozygous AATD genotypes are also reported such as SZ or MZ genotypes. In these genotypes, the S or M allele at least partly compensates for the reduction in secretion caused by a Z mutant (Ferrarotti *et al.*, 2012). Heavy smoking in these heterozygotes has been related to a slight risk of COPD (Turino *et al.*, 1996; Franciosi *et al.*, 2020; Franciosi *et al.*, 2021). Although, those with an SZ genotype closest to the putative protective threshold seem to have disease radiologically and clinically similar to COPD in those with a MM genotype rather than that of ZZ subjects (Holme *et al.*, 2009; Green *et al.*, 2015). Recent work indicates that some patients with the SZ genotype have values below the 11 μM threshold but no increased risk in the absence of smoking suggesting the true threshold may be lower although it is a reasonable target for largely restoring effective AAT/NE balance (Franciosi *et al.*, 2020).

An SZ genotype represents 4% of symptomatic AATD pathologies (Brantly *et al.*, 1988) although evidence suggests it may be underdiagnosed. Individuals with an SZ genotype have serum concentrations between 8-16 μM (American Thoracic Society/European Respiratory Society, 2003). Using the putative threshold of 11 μM, it has been estimated that 20% of individuals with an SZ genotype may be at risk of lung disease, particularly those with a history of smoking or exposure to airborne pollutants (Stoller *et al.*, 1993; de Serres *et al.*, 2006).

The risk for MZ heterozygotes (serum concentrations between 17-33 μM) is similarly debated with recent studies indicating patients with this genotype may also have an

increased risk of developing emphysematous lung disease (de Serres *et al.*, 2006; Sørheim *et al.*, 2010; Al Ashry *et al.*, 2017). In studies to overcome selection bias, Molloy *et al.* (2014) confirmed that heavy smokers with the MZ genotype are more likely to develop COPD than a non-smoking sibling who unlike some ZZ individuals do not develop 'spontaneous' disease.

In a similar study with SZ subjects and their siblings (Franciosi *et al.*, 2020), only heavy smokers were at risk of developing COPD and this did not reflect the AAT level or putative "protective" threshold and likely reflects the Z contribution and possible pro-inflammatory signal from Z polymers (Stockley, 2020b).

Thus, recent literature has questioned the simplistic approach of attributing low risk to intermediate phenotypes and the clinical use of an 11 μM threshold (Brantly *et al.*, 1991). McElvaney *et al.* (2020) argue that clinical response and guidance should centre upon risk factors and the manifestation of disease rather than an arbitrary value (McElvaney *et al.*, 2020). That said, studies of quantum proteolysis *in vitro* (Campbell *et al.*, 2000a) and successful use of the threshold as a target in AAT augmentation therapies (discussed later) (Brantly *et al.*, 2018) have proved supportive of a safe target for treatment.

It must be noted that rarer genotypes have been observed in patients with COPD, such as those with a PiNull genotype (with no detectable plasma AAT) who seem to develop worse disease than ZZ subjects (Fregonese *et al.*, 2008), suggesting AAT concentration is also important even without the Z genotype.

1.4.3. Mechanisms of AATD progression

Despite the evidence presented above, the exact mechanisms of disease development in patients with AATD remain unclear since many ZZ patients retain normal lung function throughout life.

However, it is well accepted that in patients with clinical disease, a lack of AAT in the bloodstream disrupts the proteinase/anti-proteinase balance adversely in the tissues, leaving proteinase activity relatively unopposed and able to cleave major ECM proteins, such as elastin, collagen and fibrinogen (Rao *et al.*, 1991).

This ECM cleavage is believed to be the likely cause of the pathophysiological irreversible emphysematous changes associated with patients with AATD (Stockley, 1999), indeed it has been demonstrated that emphysematous changes can reoccur in patients post successful lung transplantation as the genetic defect persists (Ataya, 2020).

PR3 has a lower association rate with AAT than NE which means that PR3 is even more poorly regulated in AATD, and persistent PR3 activity is detectable in lung secretions (Korkmaz *et al.*, 2005; Sinden *et al.*, 2013). This implies the proteinase/anti-proteinase balance may be influenced to a greater extent by PR3 than NE, and hence PR3 may play a greater role in disease pathophysiology than previously considered.

In addition to this proteinase/anti-proteinase imbalance, neutrophilic mechanisms contributing to AATD also include increased neutrophilic burden (and hence proteinase load), but with evidence of abnormal recruitment, migration, and degranulation (McCarthy *et al.*, 2016); as well as premature neutrophilic apoptosis (McCarthy *et al.*, 2016) (**Figure 1.8**).

There is also increasing evidence of changes in monocyte-derived populations (Belchamber *et al.*, 2020). Macrophages from patients with AATD have been demonstrated *in vitro* to have impaired efferocytosis (Lee *et al.*, 2020) and phagocytosis (Belchamber *et al.*, 2021), and evidence of AAT polymer accumulation within the cell (Mornex *et al.*, 1986; Bazzan *et al.*, 2018), whilst a small study indicated that there is a reduction in human leukocyte antigen (HLA)-DR phenotype monocytes (Stolk *et al.*, 2019) which are responsible for the production of anti-proteinase messenger ribonucleic acid (mRNA) (Perlmutter *et al.*, 1988) and potential mediation of inflammation (Thomas *et al.*, 2015a) (**Figure 1.8**). The role of monocytes/macrophages will not be explored further in this thesis.

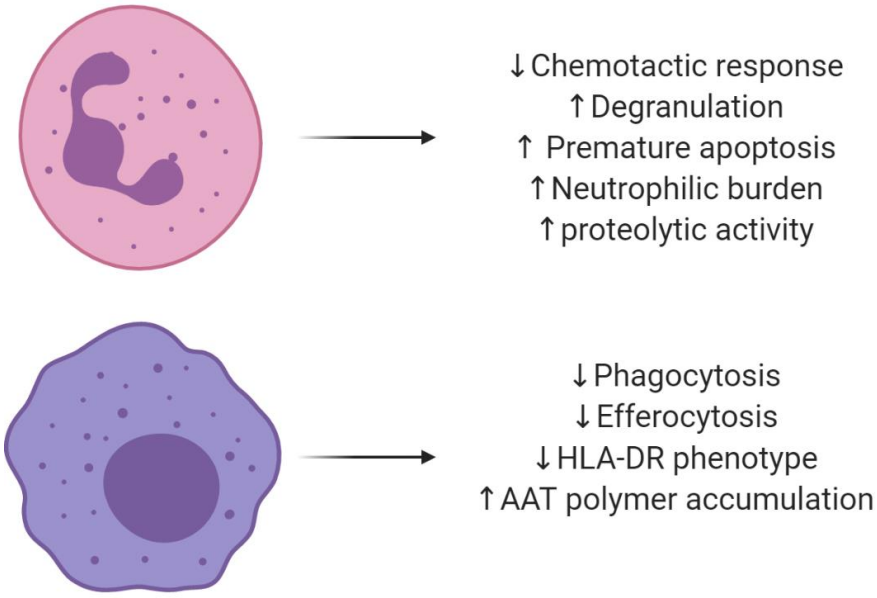

Figure 1.8. Summary of the changes in neutrophil and macrophage function in individuals with AATD.

Diagram of a neutrophil (top) and macrophage (bottom) with change in functions listed to the left. The upwards arrow (↑) indicates an increase in function, and the downwards arrow (↓) indicates a decrease in function.

1.4.4. Diagnosis of AATD

AATD presents generally with similar features to non-deficient COPD patients although more likely with a lower zone localisation of emphysema rather than the apical distribution seen in non-deficient disease (Miravitlles *et al.*, 2015). The same initial diagnostic pathway is used, although patients often present at a younger age (Campos *et al.*, 2005) and with lesser or no cigarette smoke exposure (Yang *et al.*, 2008), as well as earlier onset breathlessness than in usual COPD, family history or evidence of liver involvement (Miravitlles *et al.*, 2015). Patients with suspected AATD should undergo genetic testing to identify specific mutations.

1.4.5. Treatment options

Current clinical treatments for AATD concentrate on the management of symptoms and risk factors to minimise disease progression as for usual COPD, but in many countries, AAT augmentation therapy is available and utilised in line with national guidelines.

Augmentation of AAT plasma-derived protein, to retain physiological concentrations above the putative AAT protective threshold, was considered as the simplest way to resolve AATD/proteinase imbalance.

However, the ability of intravenous augmentation therapy to prevent disease progression is not conclusive, and variation between study measurements and outcomes makes assessment difficult (Miravitlles *et al.*, 2017). Augmentation therapy is not routinely used in the United Kingdom, although this varies globally. The global use of augmentation therapy is discussed in further detail in **Chapter 5**. Studies have also investigated whether alternative delivery of AAT for example through inhalation is effective or more effective than the intravenous route.

Alternatively to increasing lung AAT to restore the balance as with exogenous AAT augmentation, some strategies aim to reduce proteinase activity pharmacologically. The use of proteinase inhibitors, such as Alvelestat (Stevens *et al.*, 2011; Gunawardena *et al.*, 2013), and other small molecule drugs to target protein polymerisation (Quinn *et al.*, 2020) have been proposed for use in patients with AATD and formal studies of inhibitors are currently underway.

In pharmaceutical inhibitor therapies that target the proteinase/anti-proteinase imbalance, it is important to determine concentrations that allow for physiological proteinase activity to occur whilst limiting excessive action. It is necessary to have a validated biomarker of the process to determine relevant efficacy before phase II clinical studies, before embarking on expensive, definitive phase III studies.

1.5. Biomarkers

A biomarker was initially defined by the World Health Organisation (WHO) 1993 as “almost any measurement reflecting an interaction between a biological system and a potential hazard, which may be chemical, physical, or biological” and stated that “the measured response may be functional and physiological, biochemical at the cellular level, or a molecular interaction” (WHO, 1993). In 2001 the American National Institute of Health formed a Biomarkers Definitions Working Group that refined the definition to “a characteristic that is objectively measured and evaluated as an indicator of normal biological or pathogenic processes.

Due to being indicative of a disease, biomarkers can be used for diagnosis, determination of disease progression or staging, and even to determine the effectiveness of therapeutics. Indeed, this latter approach was used to support the use of augmentation therapy to increase AAT levels above a protective level (Gadek *et al.*, 1981). Often multiple biomarkers are used for diagnosis, for example, prostate size and prostate-specific antigen (PSA) levels in the diagnosis of prostate cancer (Candas *et al.*, 2000).

Molecular biomarkers are effective for the diagnosis of many chronic diseases, even prior to the development of clinical symptoms. The use of molecular biomarkers means those deemed at risk can be identified and monitored enabling disease and its progression to be detected at an earlier stage.

COPD exemplifies one disease where the use of molecular biomarkers would be beneficial as it is a slowly progressive and currently irreversible condition, and most people do not present until significant damage has been caused (Smith, 2015). Despite

the importance of detecting the disease at the earliest opportunity, there is currently no agreed strategy to detect COPD before the development of significant lung damage which occurs before airflow obstruction becomes spirometrically sufficient to cross the COPD diagnostic threshold (Johns *et al.*, 2014). The introduction of a validated biomarker reflecting the early stages would address this issue.

Physiological biomarkers, such as lung function, effectively diagnose the condition but at a late stage and not in the prodromal stage before the diagnostic threshold is achieved (Yu *et al.*, 2013), although recent interest in tests of small airways dysfunction may fulfil this role (Stockley *et al.*, 2017; Alobaidi *et al.*, 2020).

Many molecular biomarkers are of interest in COPD detection and progression, from specific protein degradation products to broader markers of inflammation, as summarised in **Table 1.2.**

Six key criteria for a successful biomarker in COPD were proposed by Stockley (2007); the biomarker should be pathophysiologically central **(1)**, directly reflect this process **(2)**, be stable **(3)**, relate to disease severity **(4)**, predict progression **(5)**, and respond to therapies and interventions effecting progression **(6)**.

Table 1.2. Biomarkers proposed for COPD diagnosis and monitoring.

Biomarker	Indicates	Benefits	Pitfalls
Lung function (Mannino *et al.*, 2015)	Airway obstruction	Easy to obtain Reproducible	Major lung damage already occurred Doesn't distinguish phenotype/activity
Pro-inflammatory cytokines (Barnes, 2016b; Bradford *et al.*, 2017)	Inflammation	Difference reported in abnormal to healthy	Non-specific marker of inflammation Cannot differentiate source or role
White blood cells (Koo *et al.*, 2017)	Inflammation	Easy to obtain	Non-specific marker of inflammation Cannot differentiate the source More useful during exacerbation
CRP (Dahl *et al.*, 2007)	Tissue injury	Correlates with severity	Non-specific tissue damage
Club cell 16 (Lomas *et al.*, 2008)	Tissue injury	Correlates with disease development	Affected by demographics including gender and age
Desmosine/ isodesmosine (Luisetti *et al.*, 2008)	Lung breakdown	Correlates with lung function Able to predict mortality	Non-specific marker of inflammation Cannot differentiate source as it is widely distributed
ECM cleavage products (Carter *et al.*, 2015; Gudmann *et al.*, 2018)	Lung breakdown	More specific Phenotype-specific	Difficult to obtain
Fibrinogen (Kim *et al.*, 2008; Duvoix *et al.*, 2013)	Lung breakdown	Indicated mortality and hospitalisation	Non-specific inflammation Possible marker of multimorbidity
Surfactant protein D (Zaky *et al.*, 2014)	Lung breakdown	Indicates the risk of acute exacerbation Correlates with lung function	Cannot differentiate the source Raised in stable disease
RAGE (Pouwels *et al.*, 2019)	Inflammation	Correlates with D_{LCO} and emphysema	Non-specific, raised in comorbidities Reduced in smoking and exacerbations

Legend. A non-exhaustive list of biomarkers proposed for the diagnosis and monitoring of COPD, and their associated effect and pitfalls. CRP=C-reactive protein, ECM=extracellular matrix, RAGE=receptor for advanced glycation end-products.

1.5.1. Proteinase activity as a Biomarker of Disease Pathophysiology

*The following section refers to a published data methods paper: Newby, P.R. … **Crisford, H.** …Stockley, R.A. (2019). A specific proteinase 3 activity footprint in α1-antitrypsin deficiency. European Respiratory Journal Open Research.*

The involvement of proteinases in disease development is due to the activity of the enzyme and the disruption of the proteinase/anti-proteinase balance, not their overall presence. Therefore, to determine the impact of NSPs in COPD, it is not necessary to measure the direct quantity, but rather evidence of the enzymatic activity.

To quantify the activity of proteinase, it is necessary to determine the amount of uninhibited enzyme and to distinguish individual proteinase activity from the activity of other NSPs. Recent advances have led to the production of free reagents that can determine this. However, as mentioned earlier, this only quantifies the amount of uninhibited enzyme and does not monitor its pre-inhibition activity.

Fibrinogen cleavage was proposed as a suitable marker for the activity assays, due to specific peptide formation and evidence that neutrophils migrate alongside fibrinogen strands even into the alveoli (Burns *et al.*, 2003). This proximity permits proteinases released from activated neutrophils to degrade fibrinogen prior to inhibition by inhibitors present in the surrounding milieu.

Carter *et al.* recently studied NE footprint assays to measure pre-inhibition activity (Carter *et al.*, 2013) based on a NE-specific fibrinogen cleavage site at Val^{360}, and predicted a PR3-specific fibrinogen cleavage site at Val^{541} using matrix-assisted laser desorption ionisation mass spectrometry analysis (Carter, 2013). This allowed the generation of a specific poly-clonal antibody and development of a further assay which

measured specific PR3 epitope released by cleavage of fibrinogen and therefore their pre-inhibition activity (Carter, 2013; Carter *et al.*, 2013; Newby *et al.*, 2019).

Carter *et al.* and Newby *et al.* validated these assays for use in plasma (Carter, 2013; Newby *et al.*, 2019). This included titration experiments to determine optimum concentrations of anti-serum, PR3 cleaved fibrinogen and the generation of a cleavage peptide up to valine 541 of the protein amino acid chain for use in a standard curve (Newby *et al.*, 2019). Furthermore, the authors modified the standard with C-terminal extensions/deletions to confirm the specificity of the terminal Valine, assessed cross-reactivity of the NE footprint peptide and used fibrinogen spiking to assess inhibition of the antibody (Newby *et al.*, 2019).

Control samples with known NE activity footprint or with high and low PR3 activity footprints were included in every assay and results were only accepted if the controls were within mean +/- 2SD of the inter-plate coefficient of variation (Newby *et al.*, 2019).

It was observed that in patients with AATD, quantification of the cleavage product Aα-Val^{360} reflected disease severity, although not disease progression except in early disease (Carter, 2013; Carter *et al.*, 2013), and Aα-Val^{541} reflected disease severity (Carter, 2013; Newby *et al.*, 2019).

The detection of NE and PR3 activity footprints allows a better understanding of current proteinase activity reflecting the pathophysiology of COPD, as well as the relationship to individual patients and their disease severity and progression. If these biomarkers are raised in patients with COPD, including those in the early stage of the disease, it may lead to diagnosis before extensive lung damage has developed, as well as enabling subsequent personalisation of treatments.

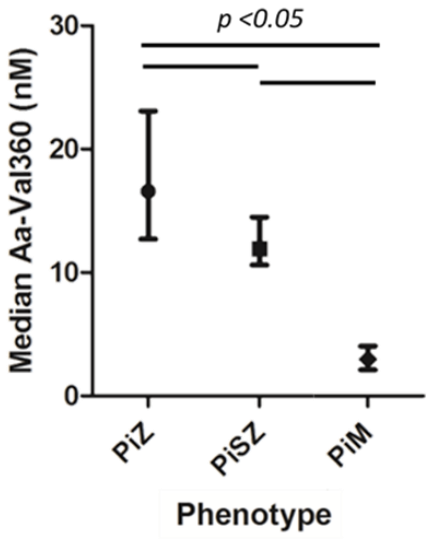

Figure 1.9. Neutrophil elastase activity footprints in AATD phenotypes.

Neutrophil elastase activity footprint (y-axis) present in the plasma of patients with the AATD phenotypes PiMM, PiSZ and PiZZ (x-axis). Error bars median +/- IQR. (Carter, 2013). Used with permission.

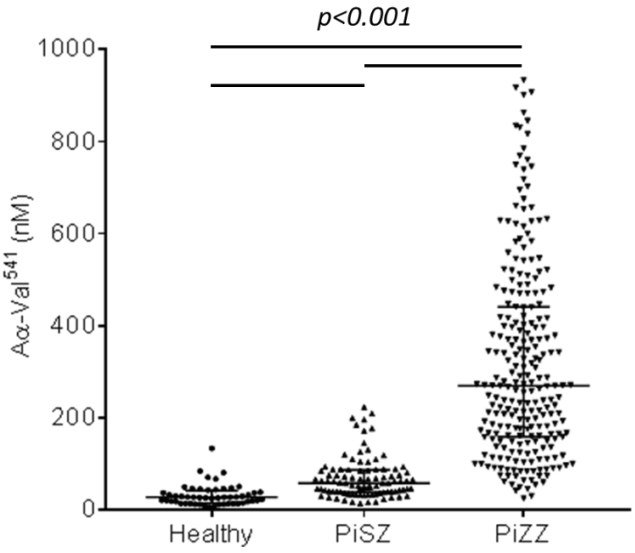

Figure 1.10 Proteinase 3 activity in healthy subjects or individuals with AATD.

Proteinase 3 activity footprints (y-axis) for healthy subjects and PiSZ and PiZZ alpha-1 antitrypsin deficient patients (x-axis) ($p<0.001$ between all groups; tested by the Mann-Whitney U-test). Each point represents the result for a single subject. Error bars median +/- IQR. (Newby *et al.*, 2019). Used with permission.

1.6. Summary and structures of this thesis

The role of NSPs in the pathogenesis of AATD is becoming more abundantly clear, with literature suggesting major roles for both NE and PR3 in both the proteinase/anti-proteinase balance observed in disease cross-sectionally, and longitudinally.

This background resulted in the concept that a cell model of this balance could be developed *in vitro,* allowing exploration of the impact of this balance/imbalance on pathophysiology in patients with AATD*,* and enabling the study of the role of intrinsic and therapeutic inhibitors.

As such, the main aims of this thesis were to:

1. Facilitate the development of a novel cell model of the proteinase/anti-proteinase balance relevant to patients with AATD and measure the resulting proteinase activity footprints with two in-house immunoassays of PR3 and NE activity (**Chapter 3**).
2. Validate this model to assess the *in vitro* effect of natural inhibitors on NSPs activity and extrapolate our findings to expand understanding of the putative anti-proteinase thresholds (with a focus on AAT); and how this relates to our understanding of disease pathophysiology (**Chapter 4**).
3. Measure the impact of therapeutic inhibitors on proteinase activity and determine whether the model data could be utilised as a pharmaceutical biomarker of efficacy and likely clinical benefit (**Chapter 5**).
4. Adapt the validated cell model to use in “whole blood” as a more physiologically accurate model of the disease state (**Chapter 6**).

CHAPTER 2: GENERAL METHODOLOGY

This chapter provides a comprehensive overview of the general methodology used throughout this thesis. Chapter specific methods are described in more detail at the relevant point.

2.1. Ethical Considerations

All biological material used to obtain the data described in this thesis was collected from donors and patients with written informed consent, and all research activities had specific ethical approvals.

Healthy, young (<35 years old) non-smokers blood and plasma were collected with ethical approval under “Investigations of the ageing immune system” (ERN_12-1184) held by Professor Janet Lord, Institute of Inflammation and Ageing, University of Birmingham.

AATD PiZZ blood and archived PiZZ plasma was collected with ethical approval as part of the Antitrypsin Deficiency Assessment and Programme for Treatment (ADAPT) programme established by Professor Robert Stockley and approved by the National Research Ethics Committee (NREC) West Midlands- South Birmingham (LREC Ref: 3359a).

AATD PiMM plasma was collected from volunteers with ethical approval under “Neutrophil and Macrophage Phagocytosis in Alpha-1 Antitrypsin Deficiency.” led by Professor Elizabeth Sapey, Institute of Inflammation and Ageing, University of Birmingham, and approved by the NREC West Midlands- South Birmingham (REC 18/WM/0365).

COPD plasma was collected with ethical approval under the “Accelerated ageing as a cause of disease pathogenesis, progression and multi-morbidity in COPD” study, as approved by the NREC West Midlands- Solihull (REC 18/WM/0097).

All research conformed to regulations set out by the Health Research Authority and Human Tissue Authority, and followed Good Clinical Practice guidelines.

2.2. Change in methodology due to SARS-CoV-2 Pandemic

To account for any variation in data, the methodology changes adapted during/following the SARS-CoV-2 pandemic are recorded in this sub-section.

Blood (and subsequent blood products) were treated assuming live virus was present in the sample according to University of Birmingham risk assessments AG 20_36 and AG 20_32.

Blood vacutainers were decontaminated with 70% ethanol, prior to being placed in Biosafety Level 2 cabinets. All work with blood products were confined to biosafety hoods. During the transfer, centrifuge or incubation steps which necessitated removal from biosafety hoods, samples were kept in secondary containment with absorbent material and containment devices decontaminated before removal from the hoods.

Specific procedures used to mitigate risk are described in detail in the publication by Walker *et al.* (2020) (Walker *et al.*, 2020).

2.3. Plasma and Serum preparation

2.3.1. Plasma preparation

Blood obtained by vacutainer (lithium heparin vacutainer; BD, USA) was stood upright for 30 minutes at room temperature, then spun in a centrifuge at 1000 *xg* for 10 minutes (at room temperature).

Plasma was removed from the vacutainer, with care not to disrupt the cellular layer underneath, and pipetted in 1 ml aliquots into 1.5 ml sample tubes. Samples were labelled with study ID numbers and date of collection, then frozen at -20°C, before being transferred to a -80°C freezer for long term storage.

2.3.2. Serum preparation

Similarly, blood obtained by vacutainer (clot activator tubes/CAT vacutainer; BD, US) was sat upright for 30 minutes at room temperature, then spun in a centrifuge at 1000 *xg* for 10 minutes (at room temperature).

Serum was removed from the vacutainer, and the same protocol was followed as described in **2.3.1. Plasma preparation**.

2.4. Neutrophil Isolation

The method was broadly that described by Jepsen and Skottun for neutrophil isolation (Jepsen *et al.*, 1982). In brief, blood was collected from donors using a heparin vacutainer system (BD, US) and then mixed within 10 minutes with 2% dextran (1 g powdered dextran; 0.9% NaCl; Sigma-Aldrich; filter sterilised) at a ratio of 6:1 and left for 45 minutes to sediment.

The buffy coat was then removed and layered on top of a Percoll gradient; produced by layering 80% Percoll (90% isotonic Percoll; 0.9% NaCl; Sigma-Aldrich) beneath 56% Percoll (90% isotonic Percoll; 0.9% NaCl). This was then placed into a centrifuge at 470 *xg* (brake, 0; acceleration, 1) for 20 minutes, producing a separation gradient (**Figure 2.1**).

The peripheral blood mononuclear cell (PBMC) layer and plasma were removed and then the PMN leukocytes (including neutrophils) were extracted and washed in phosphate-buffered saline (PBS) (sterile; Sigma-Aldrich), centrifuged (250 *xg*; 10 minutes; 21°C; brake, 9; acceleration, 9) and the pellet resuspended in 5 ml Roswell Park Memorial Institute media 1640 (RPMI; Sigma-Aldrich; with L-glutamine and sodium bicarbonate) supplemented with Penicillin-streptomycin (1% v/v; Sigma-Aldrich). Neutrophils were counted in a 10 µl aliquot, under light microscopy, with no dye using a haemocytometer. Cells were then adjusted to the desired concentration, either by dilution with RPMI or concentrating by centrifugation to obtain a pellet and resuspended in an appropriate volume of RPMI.

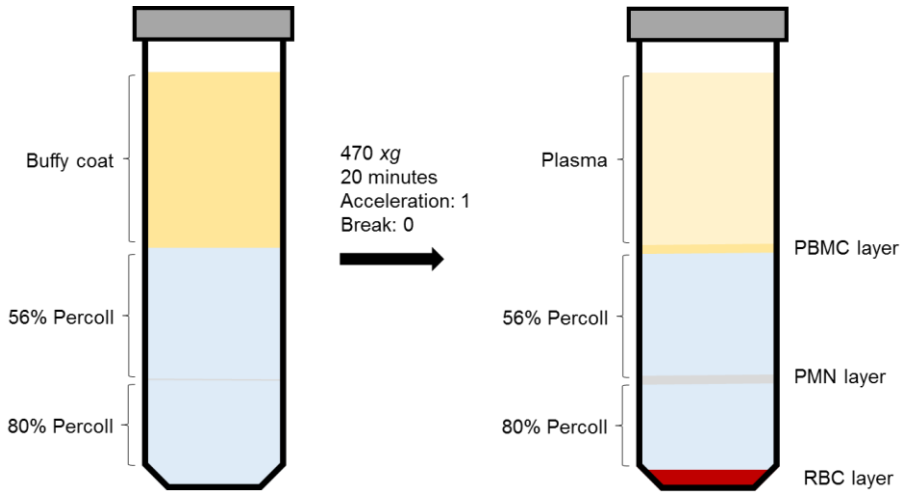

Figure 2.1. Diagram showing process of polymorphonuclear leukocyte isolation from a buffy coat.

Separation gradient produced by a buffy coat (produced via red blood cell sedimentation from whole blood with 2% dextran) following centrifugation (at 470 xg; 20 minutes; acceleration: 1; braking: 0) down a 56%:80% Percoll gradient as described by Jepsen and Skottun (Jepsen *et al.*, 1982). PBMC = peripheral blood mononuclear cells; PMN = polymorphonuclear leukocytes; RBC = red blood cells.

2.5. Neutrophil Purity

Neutrophil purity was determined using a Cytospin procedure.

Funnels were set up with a Shandon (UK) filter card and a microscope slide – as detailed in **Figure 2.2**.

Isolated cells (50 µl) were inserted into the funnel and spun at 30 relative centrifugal force (RCF) for 5 minutes (Shandon cytospin; at room temperature). Cells were then labelled for 20 seconds each with diff-quik stains: methanol fixative, xanthene and thiazine/methyline blue/azure A (all Reastain, Reagena, Finland). This method stains neutrophils light pink with a purple nucleus.

Cells were then visually assessed under light microscopy. Neutrophils were identified through colour from diff-quik stain, their size (larger than monocytes, erythrocytes and platelets) and morphology- intra-cellular granules within the cytoplasm and presence of a segmented nucleus (3-5 lobes is considered normal) (**Figure 2.3**). Neutrophils of different maturity were observed.

The other PMNs isolated by the Jepsen/Skottun method were differentiated by colour with eosinophils staining a darker red and basophils blue.

Neutrophil purity was determined by differential count.

$$\%\, purity = \frac{number\ of\ labelled\ neutrophils}{total\ number\ of\ cells} \times 100$$

Preparations with less than 85% purity or visibly abnormal morphology were discarded.

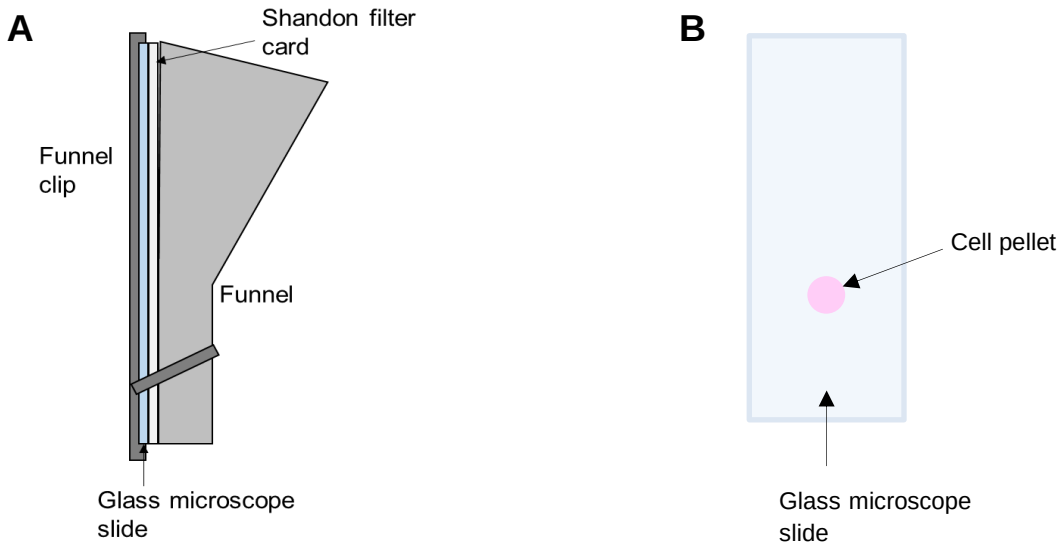

Figure 2.2. Cytospin funnel system

A Set up of components used for Cytospin with labelled components; **B** Output from Cytospin run, grey=slide, pink=cell pellet following dye with Reastain diff-quik staining.

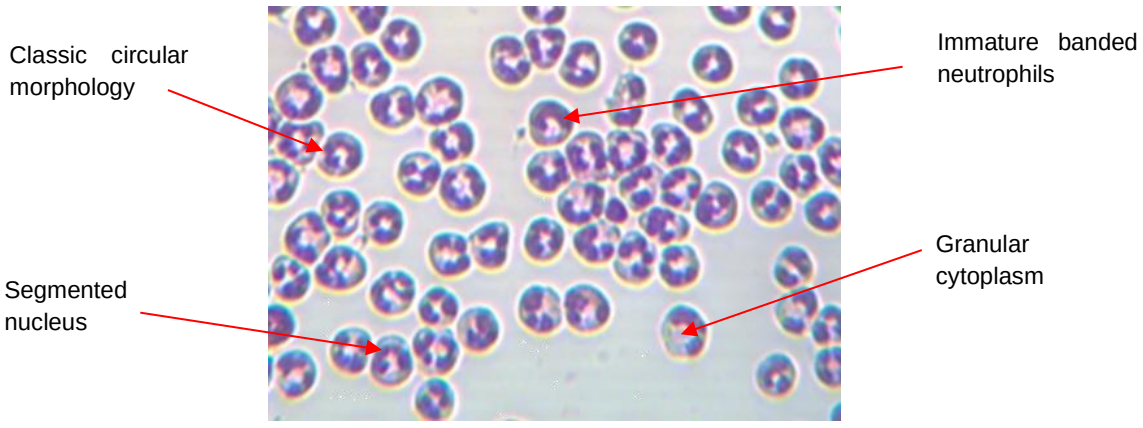

Figure 2.3. Morphology of neutrophils.

Example visualisation of isolated neutrophils under a light microscope following Cytospin and Reastain diff-quik staining. Key features for neutrophil recognition are indicated with red arrows.

2.6. Fibrinopeptide proteinase activity assays

2.6.1. Aα-Val^{541} assay

The following methodology has been published; Newby, P.R… Crisford, H…. Sapey, E. and Stockley, R.A. (2019). A specific proteinase 3 activity footprint in α$_1$-antitrypsin deficiency. ERJ Open Research. 5(3).

Coating buffer (15 mM Na_2CO_3; 35 mM $NaHCO_3$; pH 9.6; BDH Chemicals Ltd, UK) was combined with PR3-cleaved human fibrinogen (Calbiochem, US; prepared by incubation at a 200:1 enzyme to fibrinogen molar ratio for 30 minutes at 37°C, then inhibited 1:1 with trifluoroacetic acid (Merck, US)) at 1:16000 in coating buffer and 50 µl applied to 93 wells of a 96-well high binding plate (Corning Costar) with 3 empty as negative controls. The plate was placed in the centrifuge (1 minute; 172 x*g*; room temperature), then refrigerated at 4°C overnight on a shaker (Luckham R100 Rotatest, UK; setting 2.5).

A valine 541 cleavage peptide COMLGEFV (Alta Biosciences, UK) standard curve was produced in a polypropylene 96-well plate (Nunc U-96 0.5 ml) in duplicate in block buffer (1% bovine serine albumin (BSA) (Sigma-Aldrich, US) and 0.05% Tween20 (Sigma-Aldrich) in 10% TBS (Fisher Bioreagents, US)), as a 1:2 dilution series with the highest concentration of 500 nM and the lowest concentration of 2 nM. The pre-selected 32 samples, diluted at 1:5 in block buffer (60 µl buffer: 15 µl sample), were then plated in duplicate, alongside 3 wells containing 75 µl block buffer only as positive controls. Aα-Val^{541} antibody (rabbit serum; R3839; bleed 2; Alta Biosciences) was

added at 75 µl to every well, giving a total sample concentration of 1:10, and then the plate was incubated overnight at 4°C.

After overnight incubation, the high binding plate was washed 3 times; with 300 µl of wash buffer (0.05% Tween20 in 10% TBS) put into each well using a multichannel pipette and after each wash, the excess tapped out onto clean paper tissue. Each well was then filled with 300 µl block buffer, the plate was sealed and left to incubate at 37°C for 60 minutes. All following incubations were at room temperature.

The plate was again washed 3 times with wash buffer and 100 µl of each sample-antibody was stirred and transferred from the polypropylene plate into the corresponding wells on the high binding plate. The plate was sealed and incubated for 2 hours with shaking at a 2.5 setting.

After this further incubation, the plate was again washed 3 times, and 100 µl Eu-N1-anti-rabbit IgG antibody (806 ng/ml; Perkin Elmer, US) pipetted into each well. The plate was then sealed and incubated for 60 minutes with shaking at a 2.5 setting.

Following the incubation, the plate was again washed 3 times and then 100 µl enhancement solution (warmed to room temperature; Perkin Elmer) was pipetted into each well. The plate was incubated in the dark for 20 minutes with shaking at a 2.5 setting.

After 20 minutes, the plate was read at 25°C by Biotek Synergy 2 (BioTek, US) at an excitation of 340 nm and an emission of 620 nm at 25°C. An auto-scale sensitivity of 200 was used for the negative control wells.

Fluorescent readings were converted into cleavage product concentrations by interpolating from a sigmoidal standard curve in Microsoft Excel (**Figure 2.4**). Data was then transferred into GraphPad Prism and interpolated values were adjusted, as necessary, prior to statistical analysis.

2.6.2. Aα-Val^{360} assay

Coating buffer was combined with NE-cleaved human fibrinogen (prepared by incubation at a 200:1 enzyme to fibrinogen molar ratio with neutrophil elastase for 30 minutes at 37°, then inhibited 1:1 with 10 μM L-910 (Merck, US)) at 1:1000 in coating buffer and 50 μl applied to 93 wells of a 96-well high binding plate with 2 empty as negative controls. The plate was placed in the centrifuge (1 minute; 172 x*g*; room temperature), then refrigerated at 4°C overnight on a shaker at setting 2.5.

A valine 360 peptide CJTSESSV (Alta Biosciences) standard curve was produced in a polypropylene 96-well plate in duplicate in block buffer, as a 1:2 dilution series with the highest concentration of 250 nM and the lowest concentration of 2.0 nM. The pre-selected 36 samples, diluted at 2:1 in block buffer, were then plated in duplicate, alongside 3 wells containing 75 μl block buffer only as positive controls. Aα-Val^{360} antibody (rabbit serum; GN17-120; bleed 3; Alta Biosciences) was added at 75 μl to every well, and then the plate was incubated overnight at 4°C.

The assay was then completed using the same procedure as described in **2.6.1 Aα-Val541 assay** with the standard (**Figure 2.5**)**.**

Due to the inverse nature of the immunoassays, for clarity of the methodology, the core underlying biological process and binding of epitopes and antibodies for both assays are outlined visually in **Figure 2.6**.

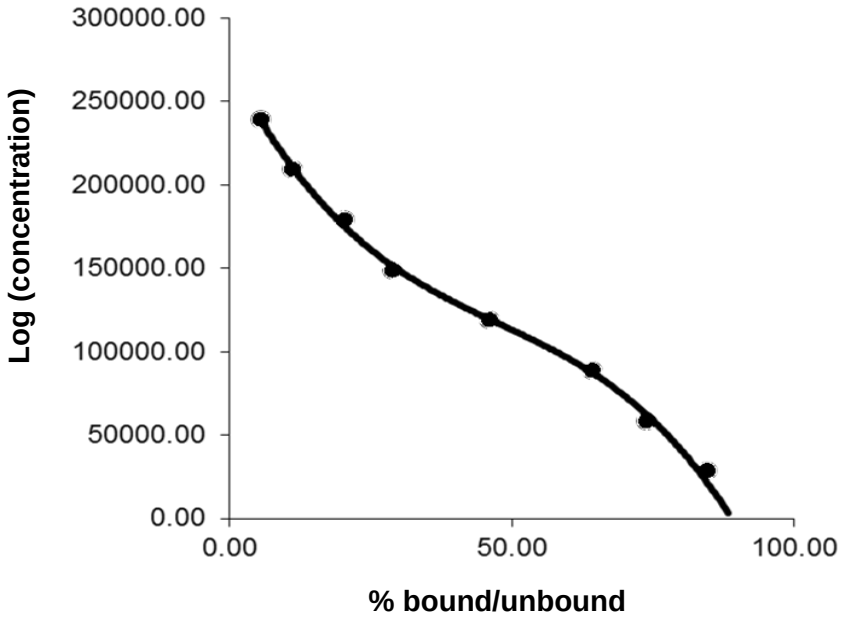

Figure 2.4. Proteinase 3 activity assay standard curve

Representative sigmoidal curve of standards with known concentrations of Aα-Val^{541} peptide utilised for graphical interpolation of sample results.

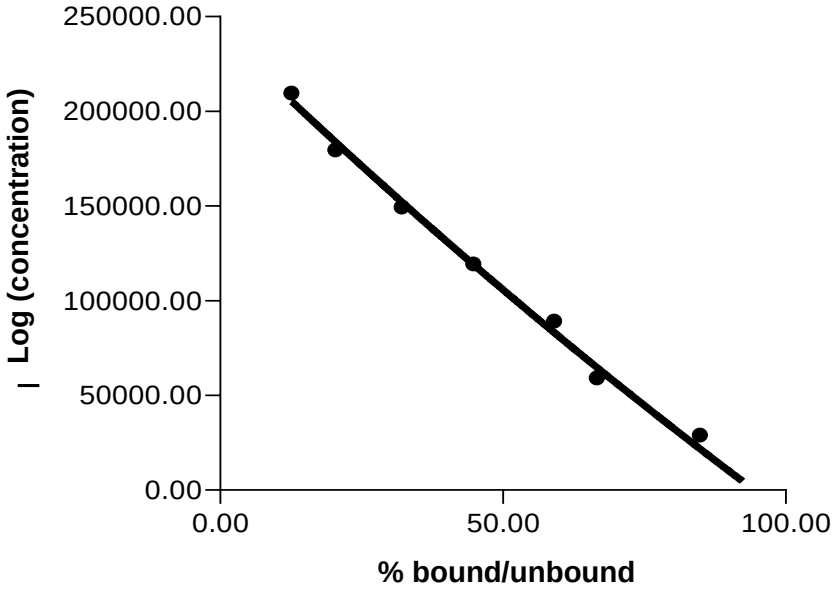

Figure 2.5. Neutrophil elastase activity assay standard curve.

Representative sigmoidal curve of standards with known concentrations of Aα-Val^{360} peptide used for graphical interpolation of sample results.

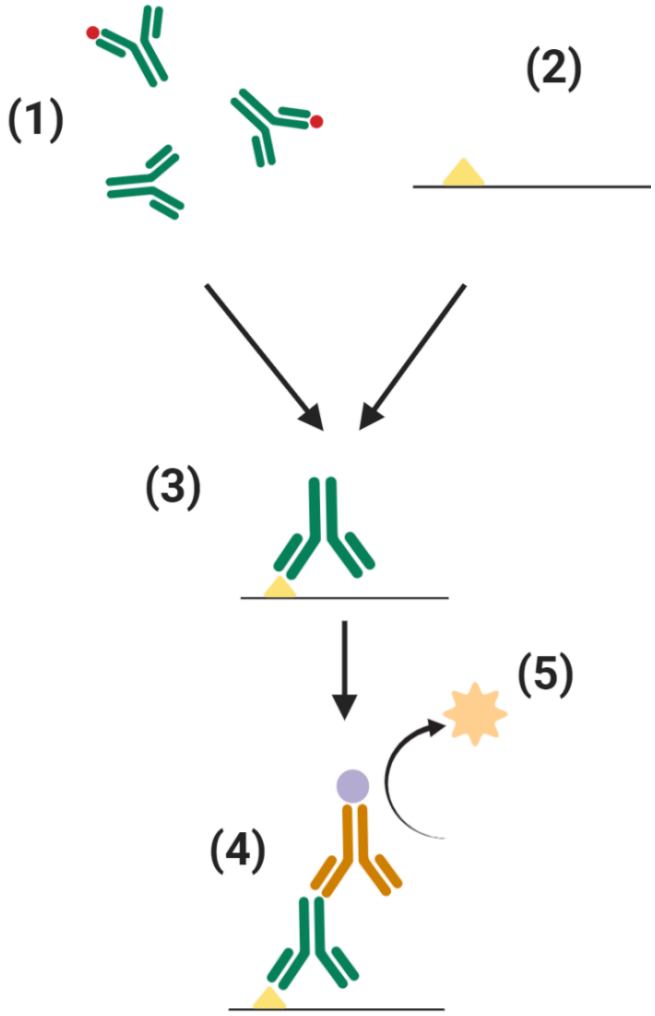

Figure 2.6. Annotated diagram detailing the proteinase activity assay procedure.

(1) Specific Aα-Val antibody - Aα-Val^{541} for PR3, Aα-Val^{360} for NE - was incubated in a polypropylene plate with the sample/standard overnight; (2) High binding plates coated with PR3/NE cleaved fibrinogen were incubated overnight; (3) The antibody/sample mixture was transferred into the coated plate. The unbound Aα-Val antibody binds to the fibrinogen coated on the plate, whereas the pre-bound antibody was washed away; (4) Anti-rabbit IgG Europium was used for detection; (5) The europium fluoresces when exposed to enhancement solution, and fluorescence is measured by time-resolved fluorometry. Representative image created using BioRender. A result for each single sample was taken from the average of the duplicate assays.

2.7. Proteinase/anti-proteinase balance model

Neutrophils were isolated as described above and $2.5x10^6$ cells/ml were incubated in RPMI with fibrinogen (550 nM) with and without stock calcium ionophore (CaI; A23187; 19.1 mM; Sigma-Aldrich; in dimethyl sulphoxide (DMSO)) at 0.9 µM or stock N-formylmethionine-leucyl-phenylalanine (fMLP; 1 mM; Sigma-Aldrich; in DMSO) at 10 µM for 60 minutes at 37°C. Incubation occurred in a closed, sterile 0.5 ml Eppendorf tube with $5x10^5$ cells/tube.

The number of replicates used is provided in each experiment.

Cells were then spun down (350 *xg*; 5 minutes; room temperature), and the supernatants were removed and frozen at -80°C for future analysis.

During the addition of inhibitors and other therapeutic treatments, compounds were incubated with isolated cells in RMPI (with L-glutamine and sodium bicarbonate; supplemented with 1% v/v Penicillin-streptomycin) for 15 minutes at 37°C prior to the addition of uncleaved fibrinogen and stimuli before the 60-minute incubation step described above.

Compound concentrations for dose-response curves were determined using concentrations described in current literature or supplied by the compound manufacturer.

2.8. Statistical Analysis

Statistical analysis was completed using the GraphPad Prism 9 statistical package for Windows.

Each dataset underwent a normality test after which it was subject to the appropriate (parametric/non-parametric) statistical and ad-hoc tests. The normality test used was D'Agostino and Pearson test. The decision sequence for the choice of statistical tests is shown in **Figure 2.7.**

Throughout this thesis, parametric data are presented as the mean +/- the standard error of the mean (SEM) and non-parametric data are presented as the median with the interquartile range (IQR).

$p \leq 0.05$ was considered a statistically significant result and statistical significance was reported on graphs as * = $p \leq 0.05$, ** = $p \leq 0.01$, *** = $p \leq 0.001$. No symbol indicates no significance.

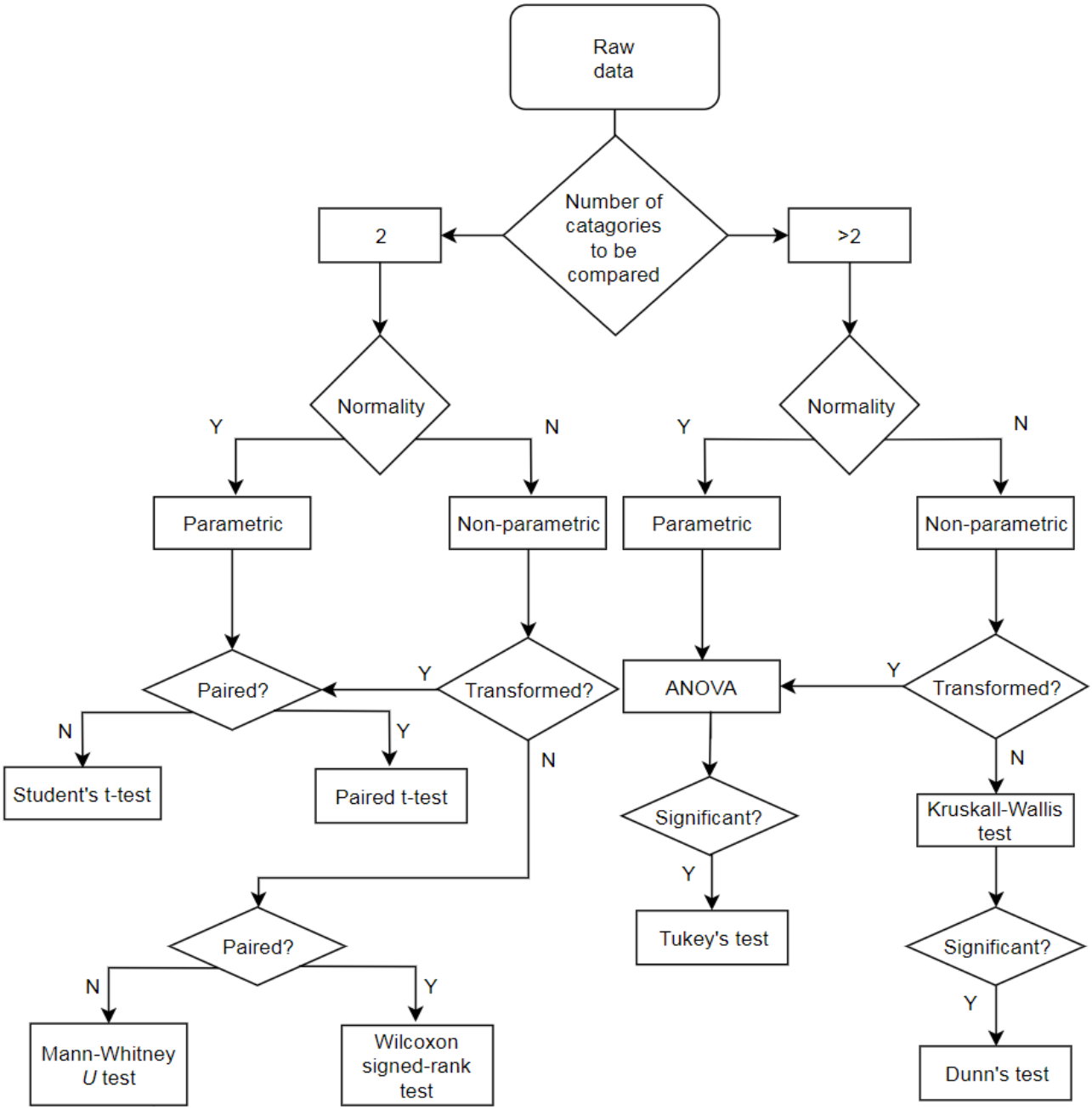

Figure 2.7. Statistical Decision Chart.

Flow chart demonstrating decisions behind statistical tests utilised throughout this thesis. Statistical tests not used in this thesis are not represented. Produced using draw.io.

CHAPTER 3: DEVELOPMENT OF A PROTEINASE/ANTI-PROTEINASE BALANCE MODEL

The following outputs relate to the data obtained in this chapter:

ABSTRACT. H Crisford, E Sapey, RA Stockley. (2020). Validation of an *in vitro* Model of the Proteinase/Anti-proteinase Imbalance observed in Alpha-1 Antitrypsin Deficiency. American Journal of Respiratory and Critical Care Medicine. **201:** A4080

3.1. Brief Introduction

3.1.1. Background

Recent development of *in vivo* proteinase activity footprint immunoassays for NE and PR3, based upon detection of enzyme-specific fibrinogen cleavage products in plasma, has supported the theory that there is a proteinase/anti-proteinase imbalance in AATD and a largely unrecognised role for PR3 (Carter *et al.*, 2015; Newby *et al.*, 2019).

These studies have demonstrated that different genotypes of AATD are related to different proteinase activity footprints, which have the potential to be used as molecular biomarkers for disease severity, activity and treatment efficacy or progression (Carter *et al.*, 2013; Carter *et al.*, 2015; Newby *et al.*, 2019).

AATD plasma samples measured for NE or PR3 activity footprints demonstrated increased levels when compared to healthy smoking volunteers and demonstrated differentiated profiles between AAT genotypes that likely reflect the underlying pathophysiological processes (Carter *et al.*, 2015; Newby *et al.*, 2019).

The work described in this chapter builds upon these previously described immunoassays by measuring and assessing proteinase activity in a novel *in vitro* model of the proteinase/anti-proteinase balance as observed in AATD.

3.1.2. Hypotheses and aims

It was hypothesised that a proof-of-concept model could be developed which would enable assessment of the physiological and therapeutic impact of the proteinase/anti-proteinase balance with the specific characterisation of the effect of AATD and its management.

This chapter aims to determine parameters needed to create a physiologically relevant model of proteinase/anti-proteinase balance, representative of the uninhibited proteinase-activity system in those with different AATD genotypes and particularly study the influence of inhibitors.

3.2. Specific Methodology

3.2.1. Neutrophil/fibrinogen-buffer model

To assess the putative role of PR3 and NE in disease and determine the effectiveness of therapeutics for pre-clinical studies related to clinical trial data, a cell-based model was designed, as described in **2.7. Proteinase/anti-proteinase balance model**. To determine robust parameters for this model, each aspect was individually investigated, including the period of incubation of isolated neutrophils, cell numbers required, the concentration of fibrinogen, and the effect of external stimulants (**Figure 3.1**). Experiments were completed within Eppendorf tubes in aliquots of $5x10^5$ cells diluted to $1x10^6$/ml or, following validation, $2.5x10^6$/ml.

The number of replicates used is shown for each experiment to assess cell-to-cell variations. Data are presented as a percentage or fold change to overcome the variation in cell sample activity.

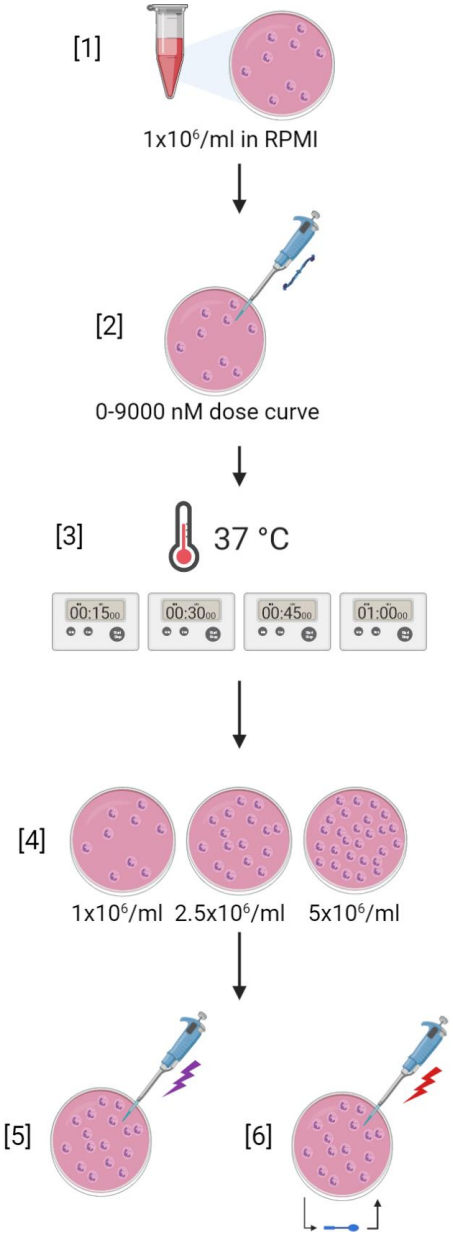

Figure 3.1. Diagram of the methodological processes for the development of the neutrophil/fibrinogen-buffer model.

[1] Neutrophils were isolated from whole blood (collected in a lithium-heparin vacutainer) using a Jepsen-Skottun method. Parameters for [2] fibrinogen concentration, [3] incubation period (0, 15, 30, 45 or 60 minutes) and [4] neutrophil concentration ($1x10^6$/ml, $2.5x10^6$/ml or $5x10^6$/ml) were determined. The effect of stimulation by [5] 0.3-2.4 µM CaI or [6] 1-10 µM fMLP was then measured, with priming of fMLP-stimulated neutrophils with 250 U/ml TNFα. Stimulation is indicated by a lightning bolt, purple=CaI, red=fMLP. Created using Biorender.com.

3.2.1.1. *Analyte limits of the PR3 and NE assays when using cell supernatants*

To assess the lowest concentrations at which the proteinase activity immunoassays can reliably measure the proteinase activity footprints, the Limit of Detection (LoD; the ability of the assay to differentiate between no signal and a signal), the Lower limit of the Quantification (LLoQ; the lowest reading where the assay can accurately quantify the amount of signal) and the Coefficient of variation (CV) were calculated (n=10).

The LoD was calculated as:

$$LoD = Limit\ of\ the\ Blank + 1.645(SD_{lowest\ analyte})$$

The Limit of the Blank (LoB) is defined as the highest value expected to be measured from blank samples with no analyte present.

The LLoQ was calculated as:

$$LLoQ = LoB + 10(SD_{lowest\ analyte})$$

The coefficient of variation (CV; %) was based upon repeated measures (n=10) using the same control samples.

Inter-assay variation was calculated as:

$$Inter\text{-}assay\ CV = (\frac{SD}{Mean}) \times 100$$

Whereas, intra-assay variation was calculated as:

$$Sample\ CV = (\frac{Sample\ SD}{Sample\ Mean}) \times 100$$

$$Intra\text{-}assay\ CV = \frac{Sum\ of\ all\ sample\ CV}{Number\ of\ Samples}$$

3.2.1.2. *Determining Fibrinogen Concentrations*

Physiological fibrinogen levels in healthy adults vary, with an average systemic concentration of 8797 nM reported (299 mg/dl) (Chao *et al.*, 1974; Oswald *et al.*, 1983; Muller *et al.*, 2007; Bolliger *et al.*, 2009; Valvi *et al.*, 2012; Swarowska *et al.*, 2014; Pedrazzani *et al.*, 2016) .

To reflect potential physiological levels in a cell-based model, fibrinogen (Calbiochem, CA USA) concentrations of 17 nM, 34 nM, 69 nM, 137 nM, 275 nM, 550 nM, 1099 nM, 2199 nM, 4399 nM or 8797 nM diluted in RPMI (Sigma-Aldrich, MO US) were used (or no fibrinogen as a baseline). Fibrinogen, at these concentrations, was added to neutrophils and incubated for 60 minutes at 37°C, following which, the supernatant was removed, centrifuged (300 *xg*, 5 minutes) and stored at -80^{o}C until analysed (**Figure 3.2**).

Figure 3.2. Change in fibrinogen concentration.

Isolated neutrophils (1x10^6/ml) were suspended in RPMI in an Eppendorf tube. Fibrinogen was added at concentrations between 17-8797 nM, then the neutrophil/fibrinogen-buffer mix was incubated for 60 minutes at 37°C. Created using Biorender.com.

3.2.1.3. *Proteinase Inhibitors*

To confirm the resulting activity footprint was related to specific proteinase activity, a cocktail of proteinase inhibitors - 100 mM β-glycerophosphate (β-GP), 20 mM sodium fluoride (NaF), 100 mM sodium orthovanadate (Na_3VO_4), 1 mM phenylmethylsulfonyl fluoride (PMSF) and 1:100 commercial proteinase inhibitor cocktail (MS-SAFE Protease and Phosphatase Inhibitor) (all Sigma-Aldrich) - were either added to supernatants at the end of the cellular incubation period or to the neutrophils prior to the incubation phase (**Figure 3.3**). Inhibitor concentrations were validated by running a dose-response curve (based upon manufacturer recommended concentrations) before use within the model.

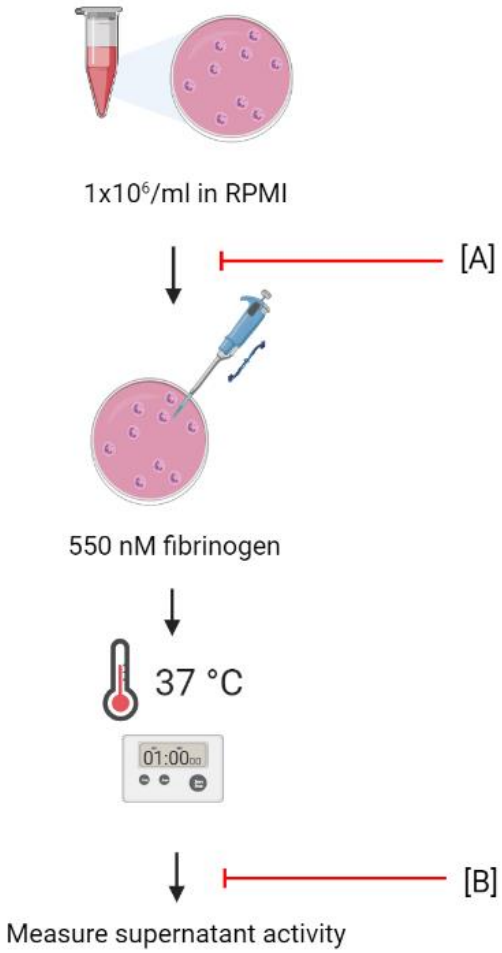

Figure 3.3. Addition of proteinase inhibitors

Isolated neutrophils (1x10^6/ml) were suspended in RPMI in an Eppendorf tube. Fibrinogen was added at 550 nM, then the neutrophil/fibrinogen-buffer mix was incubated for 60 minutes at 37°C. Proteinase inhibitors were either added [A] directly to the isolated neutrophils before the addition of fibrinogen and incubation, or [B] to cell-free supernatant produced following incubation of neutrophils in fibrinogen-buffer. Created using Biorender.com.

3.2.1.4. *Determining Neutrophil Incubation time course*

The optimal incubation time for this model was determined by exposing fibrinogen (550 nM) to neutrophils for 0, 15, 30, 45 or 60 minutes (**Figure 3.4**).

Neutrophils were adjusted to approximately $1x10^6$ cells/ml in 5 tubes. The first tube was ‘timepoint zero’. The cells were immediately spun down (300 x*g*, 5 minutes) and the supernatant was removed then frozen at the timepoints described above.

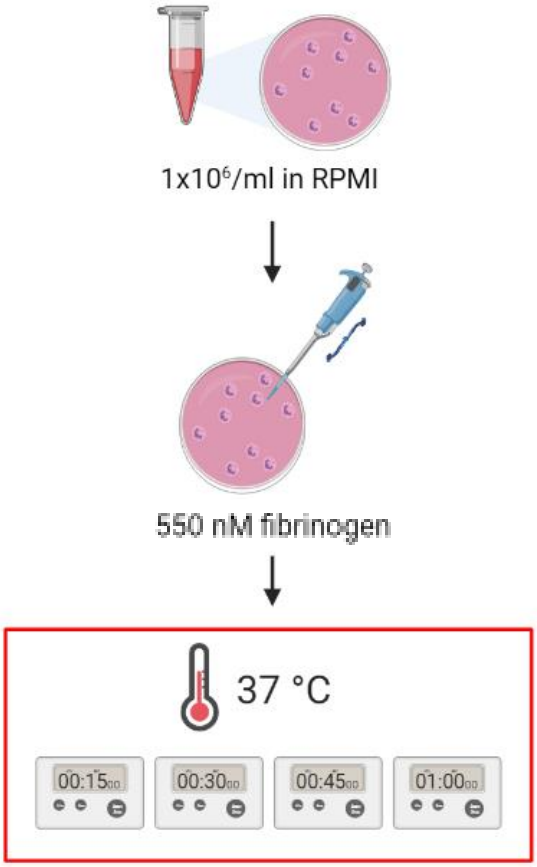

Figure 3.4. Change in length of neutrophil incubation.

Isolated neutrophils (1x10^6/ml) were suspended in RPMI in an Eppendorf tube. Fibrinogen was added at 550 nM, then the neutrophil/fibrinogen-buffer mix was incubated for either 15, 30, 45 or 60 minutes at 37°C. Created using Biorender.com.

3.2.1.5. *Determining Neutrophil Concentration*

To determine the optimal concentration of neutrophils to prevent substrate exhaustion, neutrophil concentrations of $1x10^6$, $2.5x10^6$, or $5x10^6$ cells/ml were incubated with 550nM fibrinogen for 60 minutes at 37°C (**Figure 3.5**).

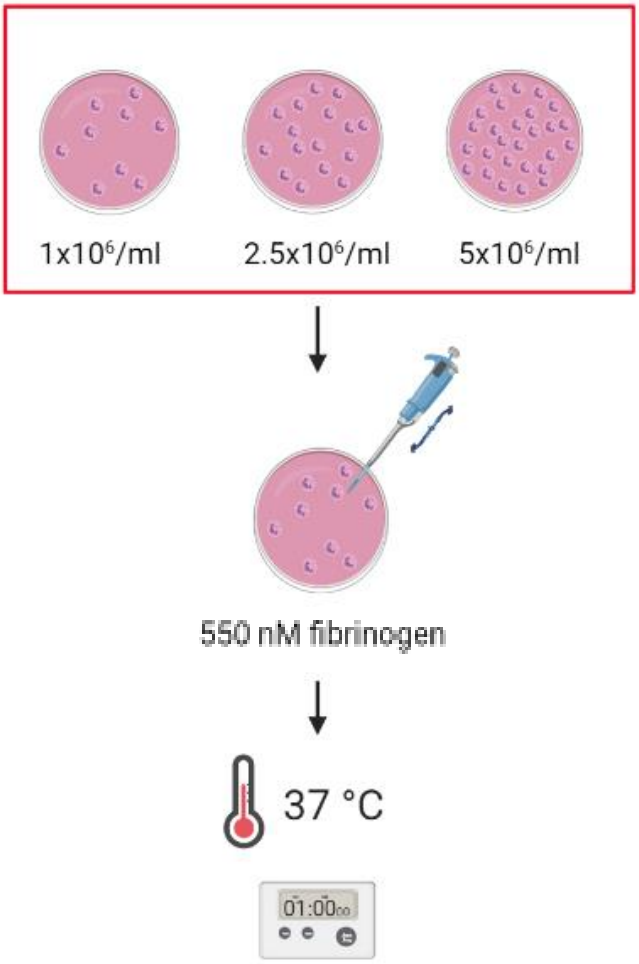

Figure 3.5. Change in neutrophil concentration.

Isolated neutrophils at concentrations of $1x10^6$/ml, $2.5x10^6$/ml or $5x10^6$/ml were suspended in RPMI in an Eppendorf tube. Fibrinogen was added at 550 nM, then the neutrophil/fibrinogen-buffer mix was incubated for 60 minutes at 37°C. Created using Biorender.com.

3.2.1.6. *Neutrophil Stimulation*

Neutrophils were stimulated with calcium ionophore (CaI; A23187; Sigma-Aldrich, UK) to calculate the potential activity footprint generated following the maximal release of proteinases from the granules. A dose-response was conducted at concentrations chosen based upon previous literature (Simchowitz *et al.*, 1980).

Neutrophils ($2.5x10^6$ cells/ml) were incubated with fibrinogen (550 nM) and with CaI (in dimethyl sulphoxide (DMSO; Sigma-Aldrich)) at concentrations of 0.3 μM, 0.6 μM, 0.9 μM, 1.2 μM, 1.5 μM, 1.8 μM, 2.1 μM and 2.4 μM for 15 minutes at 37°C.

In addition to CaI, neutrophils were also stimulated in separate studies with a pathologically relevant stimulus N-formyl-L-methionyl-L-leucyl-phenylalanine (Sigma-Aldrich; fMLP) A dose-response was performed using fMLP (in DMSO) at concentrations of 0.1 μM, 1 μM, 10 μM or negative control, with neutrophils ($2.5x10^6$ cells/ml) incubated with fibrinogen (550 nM) for 60 minutes at 37 °C.

fMLP concentrations were chosen to reflect pathologically relevant concentrations recorded in the literature (Palmer *et al.*, 1983; Chen *et al.*, 2001).

To assess whether priming the neutrophils with TNFα affected proteinase footprints, neutrophils were also incubated for 15 minutes prior to the addition of the fibrinogen (550 nM) and fMLP (10 μM) with 250 U/ml TNFα (R&D systems, MN USA) together with an unprimed control. The concentration of TNFα reflected the concentration used commonly within the literature for priming experiments (Gibbs *et al.*, 1990; Condliffe *et al.*, 1998; Cadwallader *et al.*, 2004) (**Figure 3.6**).

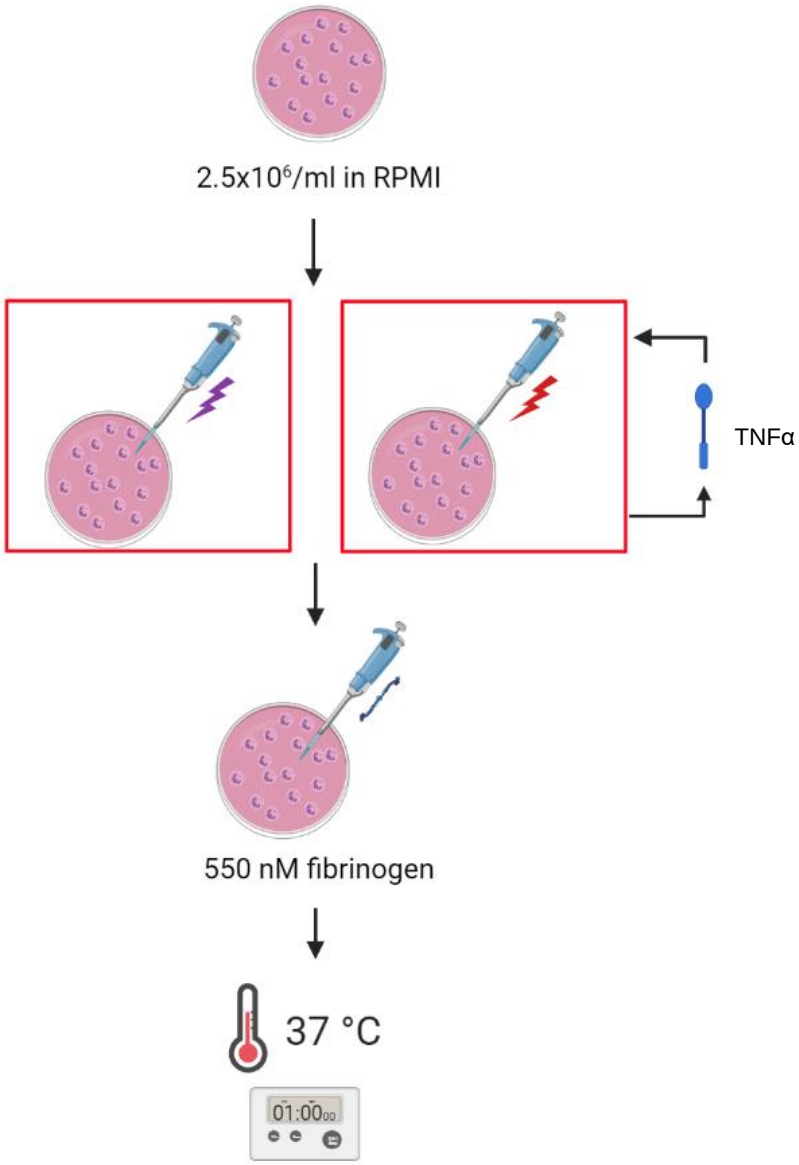

Figure 3.6. Neutrophil stimulation

Isolated neutrophils at concentrations of 2.5x10^6/ml were suspended in RPMI in an Eppendorf tube. Cells were stimulated with CaI (purple bolt) or fMLP (red bolt), with/without TNFα priming, then fibrinogen was added at 550 nM. The stimulated neutrophil/fibrinogen-buffer mix was incubated for 60 minutes at 37°C. Created using Biorender.com.

3.2.1.6.1. Flow cytometry to assess cellular viability and degranulation

Using flow cytometry software (BD Accuri C6 Software), neutrophil populations were initially identified and gated. Forward scatter (FSC) was plotted against side scatter (SSC) to visualise cellular populations within the sample. Doublet events were further identified and omitted, by assessing FSC against the cell width.

All samples were run through the machine using slow flow fluidics (14 µl/min; 10 µM core), and 10000 events were recorded.

3.2.1.6.2. Cellular Viability

To judge cellular viability, annexin V (ANV) (Biolegend, CA USA; phycoerythrin (PE)-conjugated) and 7-aminoactinomycin D (7-AAD) (Biolegend) staining were used.

ANV determines apoptotic changes in the cell by binding to the cell membrane marker phosphatidylserine (PS): PS is only present on the internal cytoplasmic membrane in live cells but is translocated to the external membranes during apoptosis (Bio-Rad, 2019). 7-AAD determines cellular death by binding to GC regions of DNA (deoxyribonucleic acid) exposed by the permeable membrane of dead cells (Modest *et al.*, 1974). When associated with DNA, the DNA/7-AAD complex experiences a spectral shift and fluoresces.

Pre-treated neutrophils were pelleted (300 x*g*, 5 minutes) and the supernatant removed. The pelleted cells were resuspended in 1 ml ANV buffer and 250 µl pipetted into a fresh Eppendorf.

These samples were then centrifuged again (300 x*g*, 5 minutes), and the pellet was resuspended in 100 µl ANV buffer with 5 µl ANV. Cells were then incubated for 15 minutes at room temperature in the dark.

The conjugated fluorescent algal pigment PE was then used to indicate ANV presence.

Following incubation, cells were washed with ANV buffer, then resuspended in 200 µl ANV buffer with 10 µl 7-aminoactinomycin D (7-AAD) and incubated for a further 5 minutes in the dark.

Cells were then vortexed and read on a validated BD Accuri (BD Biosciences, NJ USA). Controls were run as appropriate (**Table 3.1**)**.**

Using a gated neutrophil population, characteristics of live, apoptotic, dead or necrotic cells were identified and appropriate gates were introduced, allowing viability to be determined. The PE fluoresces in the FL2 channel and the DNA/7-AAD fluoresces in the FL3 channel. Compensation was introduced as 22.5% in FL2 and 4.0% in FL3. Gating strategy for cellular viability assay is shown in **Figure 3.7.**

Table 3.1. Dye conditions for cell viability staining.

	Dye	
Conditions	ANV	7-AAD
Untreated control		
Untreated apoptosis control	X	
Untreated necrosis control		X
Untreated	X	X
Treatment	X	X
…further treatments…	X	X

Legend. The dye conditions required for cellular viability assay performed by flow cytometry. The shaded box denotes the use of dye within the sample. X indicates the use of dye.

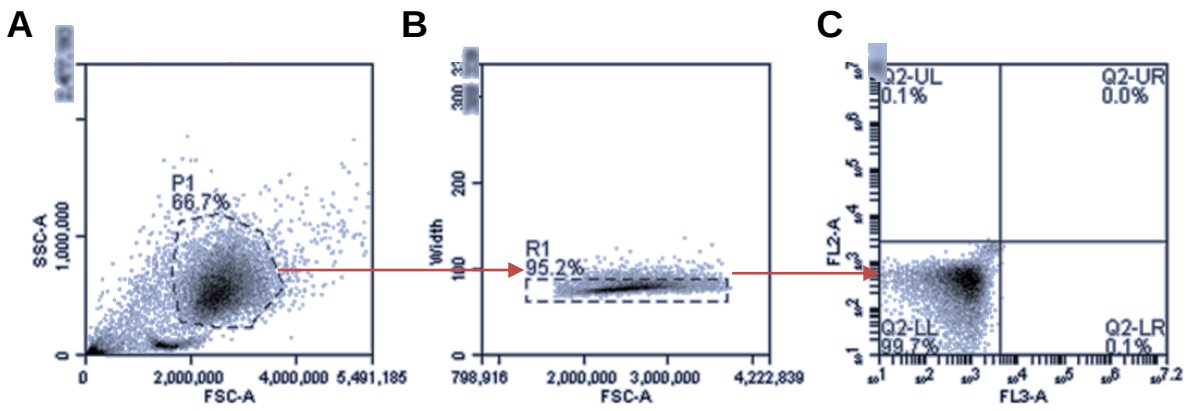

Figure 3.7. Neutrophil gating strategy for cellular viability.

Example graphs of the neutrophil gating strategy for flow cytometry using unstained and untreated cells ($2.5x10^6$ /ml) following incubation with fibrinogen (550 nM) for 60 minutes at 37°C. The neutrophil population was identified and gated, FSC versus SSC; B Single-cell events were selected for, FSC versus width; C unstained neutrophils were identified as live cells, FL3 versus FL2 channels. Lower left quadrant=alive cells, upper left= apoptotic, upper right= dead, lower right= non-apoptotic death/necrotic.

3.2.1.6.3. Degranulation

Neutrophil degranulation was assessed using flow cytometry.

Pre-treated neutrophils were spun down (300 x*g*, 5 minutes) and the supernatant removed. Cell pellets were resuspended in 1 ml PBS-BSA (2% bovine serum albumin (Sigma-Aldrich) in phosphate-buffered saline) buffer and 50 µl pipetted into a fresh Eppendorf.

Cells were put on ice, and 5 µl anti- cluster of differentiation (CD) 63 antibody (anti-human; IgG1κ; fluorescein isothiocyanate-conjugated (FITC); Biolegend) was added. CD63 is a protein component of the membranes of primary/azurophilic granules released by degranulating neutrophils (Kallquist *et al.*, 2008). Anti-CD63 antibody binds to the exposed CD63 on these granules and therefore acts as a marker of neutrophilic degranulation. Conjugating the antibody with FITC produces a green fluorescence upon binding (Bio-Rad 2019).

As appropriate, isotype controls (anti-mouse; IgG1κ; Dako, Denmark) and unstained controls were run simultaneously.

Cells were incubated for 20 minutes on ice in the dark, then washed twice with PBS-BSA (or PBS-BSA-EDTA where cells were stimulated with high concentration CaI) to limit cellular adhesion/clumping. Cells were then vortexed and immediately read on a validated BD Accuri.

The neutrophil population was gated, then in this subset population (an unstained, unstimulated control) a boundary line for degranulation marker CD63 was drawn, and a gate added for subsequent analysis. The FITC fluoresces in the FL1 channel and was plotted against cell count. Movement across this gate indicated presence of the marker. Isotype controls confirmed validity of this threshold. The gating strategy is shown in **Figure 3.8**. The number of replicates used for each experiment is indicated.

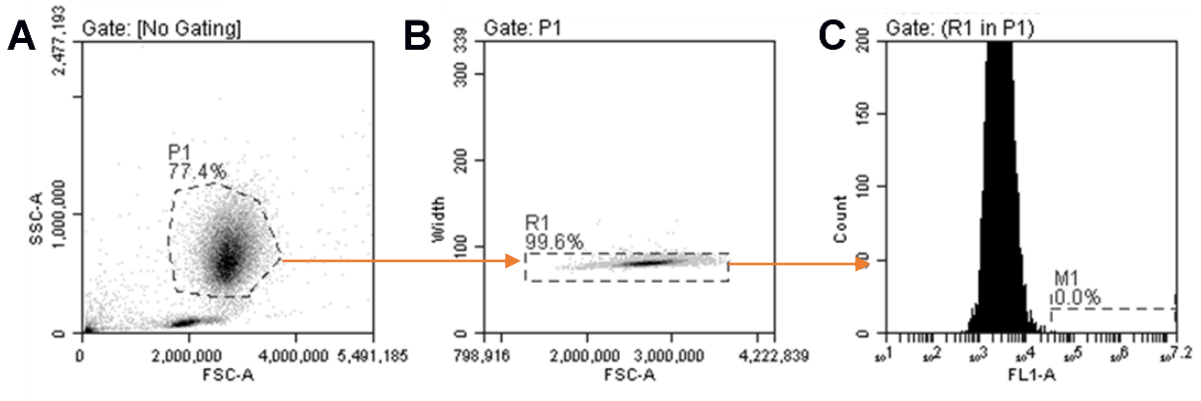

Figure 3.8. Neutrophil gating strategy for degranulation.

Representative graph of the neutrophil gating strategy for flow cytometry using cells ($2.5x10^6$ /ml) following incubation with fibrinogen (550 nM) for 60 minutes at 37°C. **A** neutrophil populations were identified and gated; **B** Single-cell events were selected for; **C** untreated neutrophils shown not to have degranulated.

3.2.2. Validation of Supernatants within the Assay

To validate the use of the model supernatants within the assay, experiments were undertaken to assess the effect of spiking of model products.

A supernatant sample with a known low proteinase activity footprint was spiked with a sample with a known high proteinase activity footprint. Aliquots were created with increasing proportions of a high sample within the low sample at ratios of *known low: known high* at 1:1, 1:2 and 1:4. The mixed supernatants were then measured in the proteinase assays, as described in **2.6. Fibrinopeptide proteinase activity assays.**

3.3. Results

3.3.1. Testing the PR3 and NE activity footprint assays when used on cell supernatants.

First, the lower limits of detection and quantification, as well as the co-efficient of variation for the PR3 and NE activity assay were determined using cell supernatants as opposed to plasma, which was used to validate the assays originally. The analyte limits and the Coefficient of Variation are displayed in **Table 3.2**.

For the PR3 footprint, the limit of detection was 6.52 nM, and for the NE footprint, it was 1.02 nM. Values falling below these limits of detection were read as zero, or where possible the assay repeated with a less dilute sample such that it was above the limit and a dilution corrected factor added to the result.

For the PR3 footprint, the limit of quantification (LoQ) was 8.33 nM, and 5.37 nM for the NE footprint. Again, values falling below the LoQ were repeated at lower sample dilution and classified as zero if still below the LoQ.

For samples exceeding the upper limit of the footprint activity standard curve, dilution of the sample was repeated until the result fell within the defined range and the result adjusted for the degree of dilution.

The use of model supernatants within the assays produced inter-assay CV values of 42.9% for PR3 and 21.6% for NE, and intra-assay CV values of 15.9% for PR3 and 13.7% for NE. Therefore, where it was possible, analysis for the samples pertaining to each experiment was analysed from within the same assay plate.

Table 3.2 Analyte Limits of in-house Proteinase Activity Assays.

	PR3 Assay	**NE Assay**
Mean Blank, nM	6.17 (+/- 9.29)	0.16 (+/- 0.43)
Mean of Lowest Analyte, nM	1.11 (+/- 0.22)	0.64 (+/- 0.52)
Limit of the Blank, nM	0	0
Lower Limit of Detection, nM	6.52	1.02
Lower Limit of Quantification, nM	8.33	5.37
Upper limit of Quantification, nM	2500	375
Inter-assay CV, %	42.9%	21.6%
Intra-assay CV, %	15.9%	13.7%

Legend. Calculated limits of the in-house NSP activity footprint assays (n=10) using adapted methodology by (Armbruster *et al.*, 2008). Limit of the Blank (LoB) calculated as $mean_{blank}+1.645(SD_{blank})$; Limit of Detection calculated as $LoB+1.645(SD_{lowest\ analyte})$. Mean values +/- SEM; Lower limit of the Quantification calculated as $LoB+10(SD_{lowest\ analyte})$. The coefficient of variation (%, CV) was calculated as *inter-assay CV = mean sample CV* and *intra-assay CV = (SD/mean)*100.* n=10.

3.3.2. Model development

In order to generate a footprint model of proteinase/anti-proteinase balance, each parameter involved in model development was individually assessed. Throughout this thesis, PR3 activity data is represented graphically as filled in circles "●" and/or greyed bars and NE activity data is represented as outlined circles "o" and/or outlined bars.

3.3.2.1. *Change in fibrinogen concentration*

To select an optimal fibrinogen concentration, neutrophils ($1x10^6$/ml) were incubated with increasing concentrations of uncleaved fibrinogen. NSP activity footprint was measured and Aα-Val^{360} or Aα-Val^{541} are expressed in nM. Controls contained no neutrophils.

Initial experiments showed a fibrinogen dose-dependent increase in activity footprint by neutrophils (**Figure 3.9**)**.** A fibrinogen concentration of 550 nM was selected for the next series of experiments as it produced an easily measurable signal for both footprints that remained below the upper limit of detection in the working assays without requiring dilution.

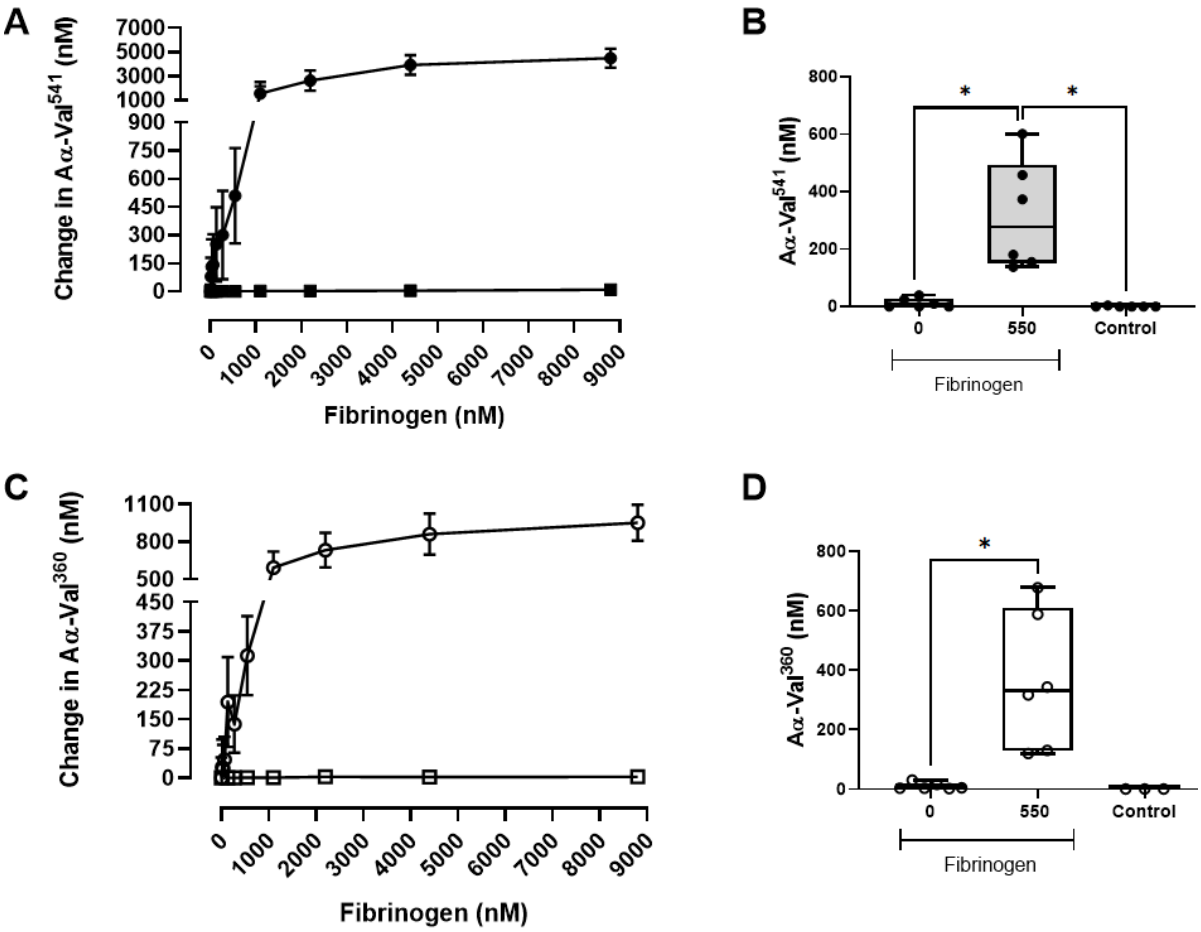

Figure 3.9 Increasing fibrinogen within a closed model increases NSP activity footprints**.**

A Change in Aα-Val^{541} (y-axis) produced by neutrophils (1x10^6/ml) incubated with increasing concentrations of fibrinogen (x-axis) over 60 minutes; ●= with neutrophils, n=6; ■ = without neutrophils, n=3; error bars median +/- SEM; **B** Focused comparison of the amount of Aα-Val^{541} (x-axis) produced by neutrophils (1x10^6/ml) in fibrinogen buffer (550 nM) [as shown in A] compared to neutrophils with no fibrinogen (0) and fibrinogen with no neutrophils (y-axis) ; n=6; * = p ≤ 0.05 determined by Kruskal-Wallis test; error bars median +/- IQR; **C** Change in Aα-Val^{360} levels produced by neutrophils (1x10^6/ml) when incubated with increasing concentrations of fibrinogen over 60 minutes; O= with neutrophils, n=6; □ = without neutrophils, n=3; error bars mean +/- SEM; **D** Focused comparison of the amount of Aα-Val^{360} produced by neutrophils (1x10^6/ml) in fibrinogen buffer (550 nM) [as shown in C], n=6, to controls with no fibrinogen (0), n=6, and no neutrophils, n=3; * = p ≤ 0.05 determined by Wilcoxon matched-pairs signed rank test; error bars median +/- IQR.

3.3.2.2. *Addition of proteinase inhibitors*

The effect of adding commercial, non-physiological proteinase inhibitors to the model was assessed. NSP activity results are described as a percentage change in Aα-Val^{360}/ Aα-Val^{541}.

3.3.2.2.1. Effect of proteinase inhibitors on incubating neutrophils

Proteinase inhibitors were added to isolated neutrophils (1x10^6/ml; in RPMI) alongside fibrinogen (550 nM) at working concentrations suggested by the manufacturer and literature then incubated at 37°C at 60 minutes. Working concentrations used were sodium fluoride (NaF; 20 mM), sodium orthovanadate (Na_3VO_4; 100 mM), beta-glycerophosphate (β-GP; 100 mM), phenylmethylsulfonyl fluoride (PMSF; 1 mM) and a commercial proteinase inhibitor cocktail (1:100; MS-SAFE Protease and Phosphatase Inhibitor; Sigma).

The addition of proteinase inhibitors resulted in a marked reduction in PR3 activity footprint from 100% with fibrinogen alone to 13.8% (IQR: 10.64-21.12) in the presence of the proteinase inhibitors (p=0.03; Wilcoxon test) (**Figure 3.10**).

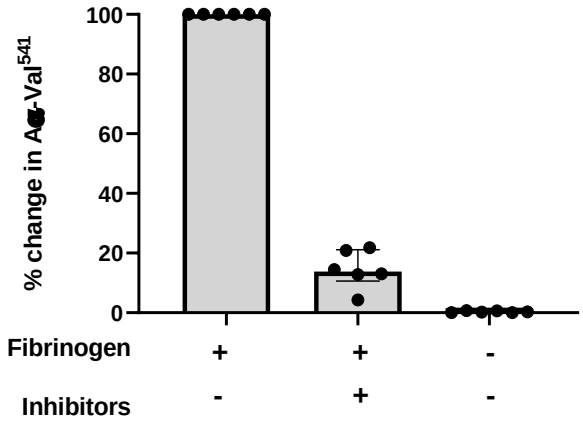

Figure 3.10. Change in PR3 footprint following the addition of proteinase inhibitors to incubating neutrophils in fibrinogen buffer.

Percentage change in the Aα-Val^{541} levels (y-axis) produced by unstimulated neutrophils (1x10^{6}/ml) incubated for 60 minutes at 37°C with proteinase inhibitors added alongside fibrinogen buffer (550 nM) (x-axis); 100% is control; n=6; error bars median +/- IQR.

3.3.2.2.2. Effect of proteinase inhibitors added into the activity assays

To ensure NSP activity was stopped at the end of the incubation time before measuring the PR3 footprint, proteinase inhibitors were added directly to aliquots of the supernatant at the end of each timepoint or to the total assay before processing and the activity footprint measured after processing.

In the PR3 activity assay, adding proteinase inhibitors into the sample at the end of the incubation period did not alter the activity footprint (**Figure 3.11**).

Na_3VO_4 and βGP resulted in no change of PR3 activity footprint, with the signal at 104.0% and 100.7% respectively, whereas the total inhibitor cocktail resulted in a 15.4% average reduction in activity to 84.6%. These changes were considered to be within the error of the assays Newby *et al.* (2019) and Carter *et al.* (2015).

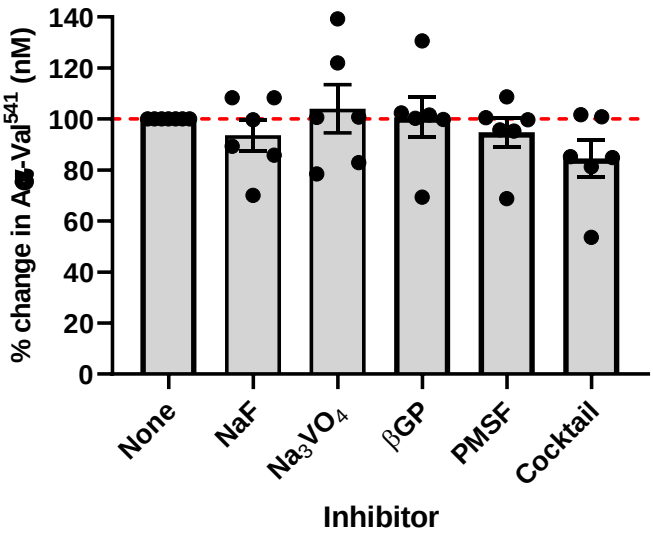

Figure 3.11. Change in PR3 footprint following the addition of proteinase inhibitors at the end of the incubation period and before measuring the PR3 footprint.

Percentage change in Aα-Val^{541} levels (y-axis) following the addition of proteinase inhibitors (x-axis) into the supernatant from neutrophils (1x10^{6}/ml) incubated for 60 minutes at 37°C in a fibrinogen-buffer (550 nM)) before measurement in the Aα-Val^{541} assay; n=6; error bars mean +/- SEM.

3.3.2.3. *Increasing Incubation Length has No Significant Effect on Activity Footprint*

Extending the period of incubation of neutrophils with fibrinogen before removal of supernatant did not have a significant effect upon the activity footprint, representing maximal degranulation (**Figure 3.12**).

For PR3, at the baseline time point, there was evidence of fibrinogen cleavage with a median concentration of the PR3 footprint of 200.0 nM (IQR: 200.0-216.9). This likely represented proteinase cleavage of fibrinogen during the processing and transfer of cleavage products. After 15 minutes incubation, activity increased significantly to 1244.0 nM (900.4-2311.0) (p=0.048, Dunn's multiple comparison) and then plateaued. Beyond this point, the length of incubation had no further effect (p=0.4634; Kruskal-Wallis test).

For NE, at the baseline time point, there was also some evidence of fibrinogen cleavage with a median concentration of the NE footprint of 8.1 nM (IQR: 4.8-10.7). After 15 minutes incubation, activity increased to 77.3 nM (23.2-127.2) (p=0.383, Dunn's multiple comparison). After 30 minutes, activity was 118.0 nM (70.6-172.2) with no change in activity footprint after this time period.

Neutrophil controls with no fibrinogen, fibrinogen buffer alone and RPMI controls all gave results of <15 nM.

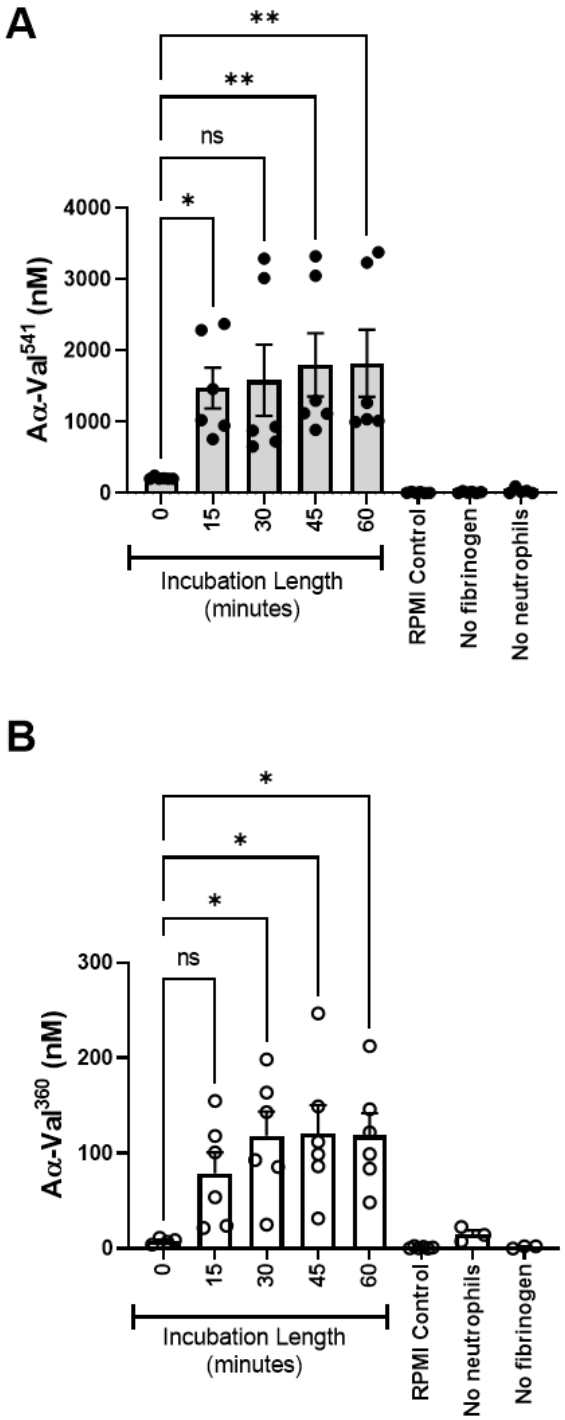

Figure 3.12. Effect of Incubation Length on Proteinase footprints.

Proteinase footprint levels (y-axis) following incubation of unstimulated neutrophils ($2.5x10^6$/ml) with fibrinogen (550 nM) at 15-minute intervals over 60 minutes (x-axis) **A** Aα-Val^{541} levels; n=6; **B** Aα-Val^{360} levels; n=6, 0 minutes n=4. Controls n=3. ●= PR3 activity footprint, o= NE activity footprint. Median histograms +/- IQR bars. * = $p \leq 0.05$, ** = $p \leq 0.01$ determined by Kruskal-Wallis Test.

3.3.2.4. *Increasing Neutrophil Concentration has No Significant Effect on Activity Footprints*

To confirm if the results seen in experiment **3.3.2.1 Change in fibrinogen concentration** represented maximal degranulation, the numbers of neutrophils were increased.

Changing the number of neutrophils did not significantly increase the activity footprints, but there was significant variability in individual neutrophil preparations (**Figure 3.13**).

The median PR3 activity footprint increased from 1028 nM (IQR: 837.6-1305.0) in the presence of $1x10^6$/ml neutrophils to 1143.0 nM (673.9-1616.0) with $2.5x10^6$/ml neutrophils and to 1535.0 nM (751.6-1667.0) with $5x10^6$/ml neutrophils, but these changes were not statistically significant. The activity footprint was increased at all concentrations of neutrophils compared to the control (p=0.0029, Kruskal-Wallis test).

The median NE activity footprint increased from 28.4 nM (3.8-64.5) to 59.3 nM (21.6-127.4), and to 114.3 nM (16.8-175.2) using the same increasing concentrations of neutrophils as described above, respectively. There was a significant difference between the control and both $2.5x10^6$/ml (p=0.004, Kruskal-Wallis test) and $5x10^6$/ml (p=0.0012, Kruskal-Wallis test) to the control.

From these data, at $2.5x10^6$/ml neutrophils were chosen for future experiments, unless stated otherwise, as this was both practical in terms of blood volume required for experiments and provided a measurable NSP activity footprint.

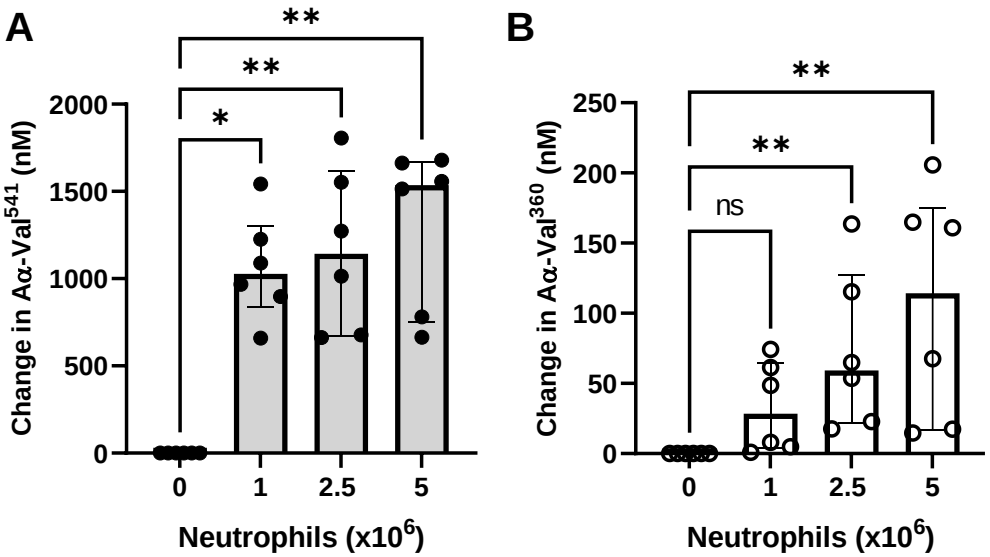

Figure 3.13. Effect of change in neutrophil concentration on NSP activity footprint.

NSP activity levels (y-axis) following incubation of unstimulated neutrophils at 1/2.5/5x10^6/ml (x-axis) with fibrinogen (550 nM) over 60 minutes, **A** Aα-Val^{541} levels, n=6; **B** Aα-Val^{360} levels, n=6; ●= PR3 activity footprint, o= NE activity footprint. Error bars median +/- IQR. * = $p \leq 0.05$, ** = $p \leq 0.01$. determined by Kruskal-Wallis test.

3.3.2.5. *Calcium Ionophore Exposure*

To determine what might represent maximal degranulation for $2.5x10^6$/ml neutrophils, and to determine if substrate exhaustion was possible in the assay, a potent stimulator of neutrophils, CaI (Lefrancais *et al.*, 2012), was added at baseline from 0.3-2.4 µM and the specific proteinase fibrinogen-cleavage product was measured (**Figure 3.14**).

The PR3 activity footprint increased in a dose-response as neutrophils were exposed to increasing concentrations of CaI, from 0 µM to 0.9 µM.

After 0.9 µM, the PR3 activity footprint plateaued, suggesting fibrinogen substrate exhaustion. The NE activity footprint continued to rise steadily across increasing concentrations of CaI.

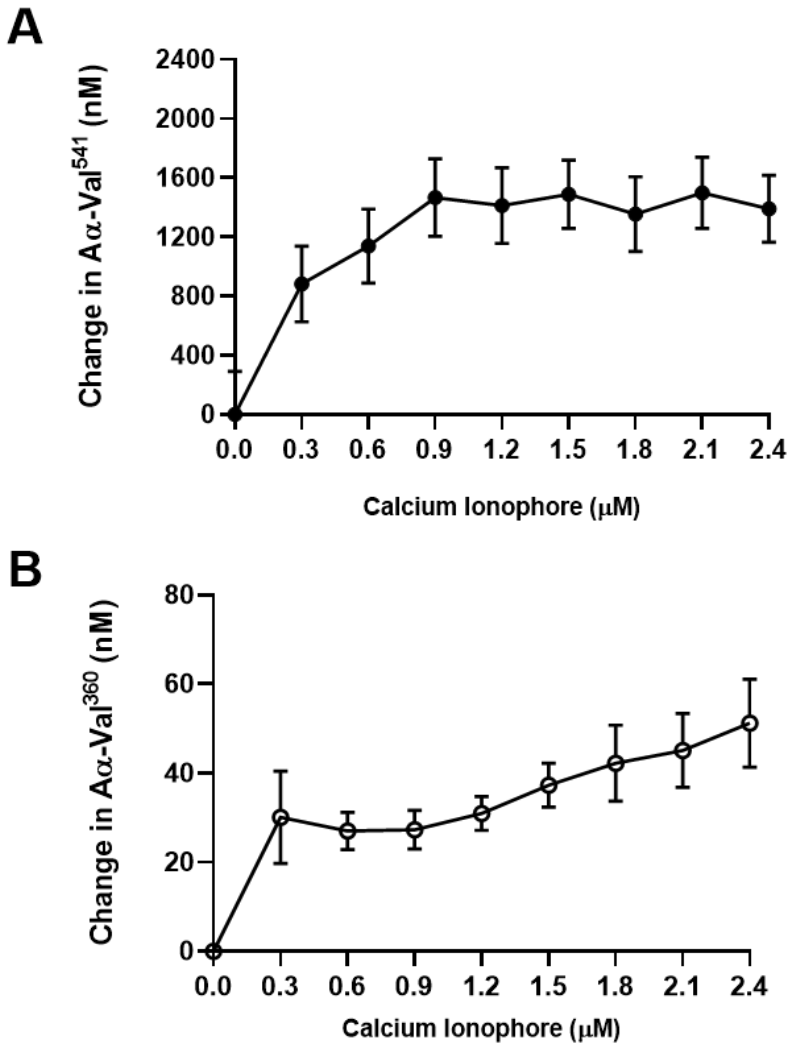

Figure 3.14. NSP activity footprint following stimulation of neutrophils with CaI.

Change in NSP activity footprint levels (y-axis) following stimulation of neutrophils at 2.5x10^6/ml with Calcium ionophore (CaI) at 0.3/0/6/0.9/1.2/1.5/1.8/2.1/2.4 µM (x-axis) with fibrinogen (550 nM) for 60 minutes; **A** Aα-Val^{541} levels, n=6; **B** Aα-Val^{360} levels, n=6. ●= PR3 activity footprint, o= NE activity footprint. Baseline set as unstimulated neutrophils, 0 µM.

Flow cytometry demonstrated that when stimulated with 0.9 µM CaI, 82.2% (75.2-83.9) of neutrophils had degranulated compared with 0.2% (0.1-0.3) of the unstimulated cells (p=0.041). Exposure to 1.8 µM CaI resulted in 84.4% (81.1-87.1) of neutrophils degranulating (p=0.002) (**Figure 3.15**).

No such effect was seen with isotype controls (as described in the methodology) (**Figure 3.16**).

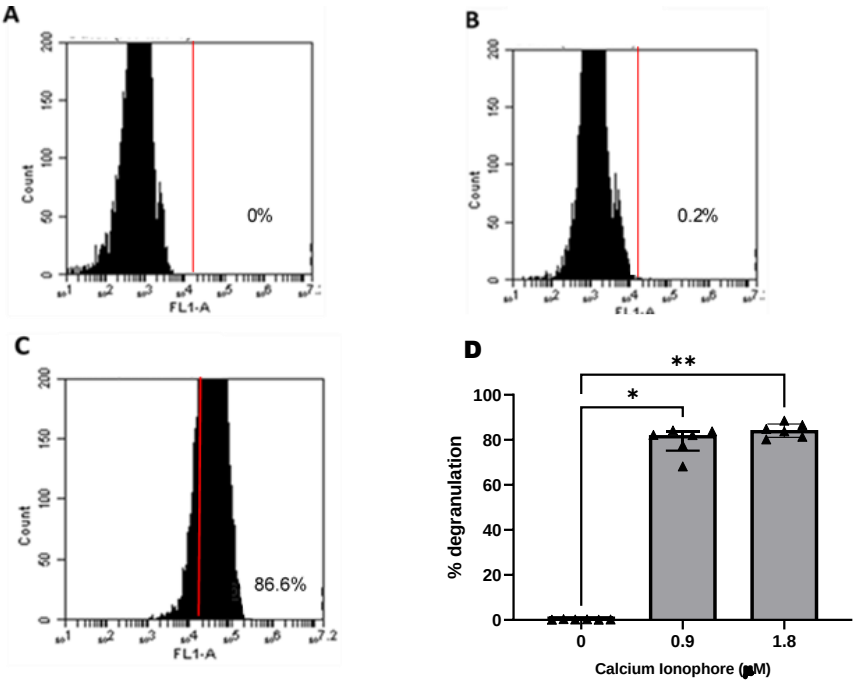

Figure 3.15. CD63 expression after CaI stimulation of neutrophils

A unstained (0%); **B** unstimulated (0.2%); **C** CaI stimulated (86.6%); n=1. Red line indicates gate. Graphs shown are a representative image. **D** Median percentage of degranulation (y-axis) from unstimulated or CaI stimulated (0.9 µM or 1.8 µM) cells (x-axis), n=6; error bars mean +/- SEM, * = p ≤ 0.05, ** = p ≤ 0.01 determined by Kruskal--Wallis.

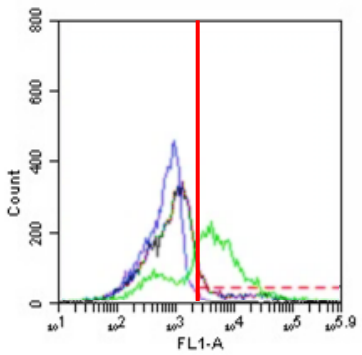

Figure 3.16. Representation of isotype control expression compared to positive antibody expression for degranulation.

Percentage degranulation present in the same sample following application of a CD63 antibody or an anti-mouse IgG1κ isotype control antibody, n=1. The blue histogram is the unstained neutrophils, the black histogram is the isotype control, the green histogram is the positive antibody expression. The red line indicates the gate.

Flow cytometry showed that exposure to 0.9 µM Cal had a variable impact on neutrophil viability between individuals, but mean viability remained high across the experimental replicates (**Figure 3.17**).

Mean data shows 66.5% (SEM: +/- 8.0) of cells remained viable with 29.8% (+/- 7.8) showing an apoptotic phenotype, whilst only 0.5% (+/- 0.3%) followed a non-apoptotic death pathway (Hereafter, all non-apoptotic death pathways are termed necrotic/necrosis) and 3.2% (+/- 1.4) appeared dead.

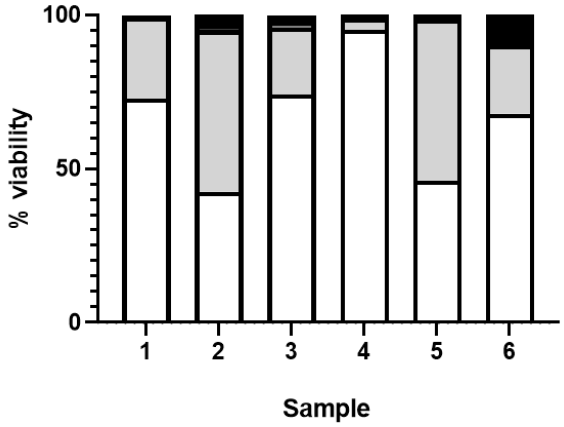

Figure 3.17. Viability of neutrophils following calcium ionophore stimulation.

Percentage neutrophil viability (y-axis) following stimulation at $2.5x10^6$/ml with CaI (0.9 µM) and incubation in fibrinogen-buffer for 60 minutes at 37°C; n=6 (x-axis); black=dead, dark grey=necrotic, light grey=apoptotic, white=viable.

To confirm that the activity footprints reflected the impact of the CaI, and not a vehicle effect, experiments were repeated with DMSO as an appropriate vehicle control (**Figure 3.18**). A higher concentration of CaI was used to ensure maximal stimulation.

Cellular viability remained similar across untreated, DMSO or CaI treatment groups (**Figure 3.18.D**),

The PR3 activity footprint was 3059.0 μM (SEM +/- 671.5) when neutrophils were treated with CaI in DMSO and 1312.0 (+/- 503.6) when treated with DMSO alone ($p=0.0013$; Wilcoxon test). While this number appears high, it is similar to that seen in unstimulated cells (**Figure 3.7**) indicating that DMSO was associated with a similar level of PR3 activity as seen in unstimulated cells (**Figure 3.18.E**).

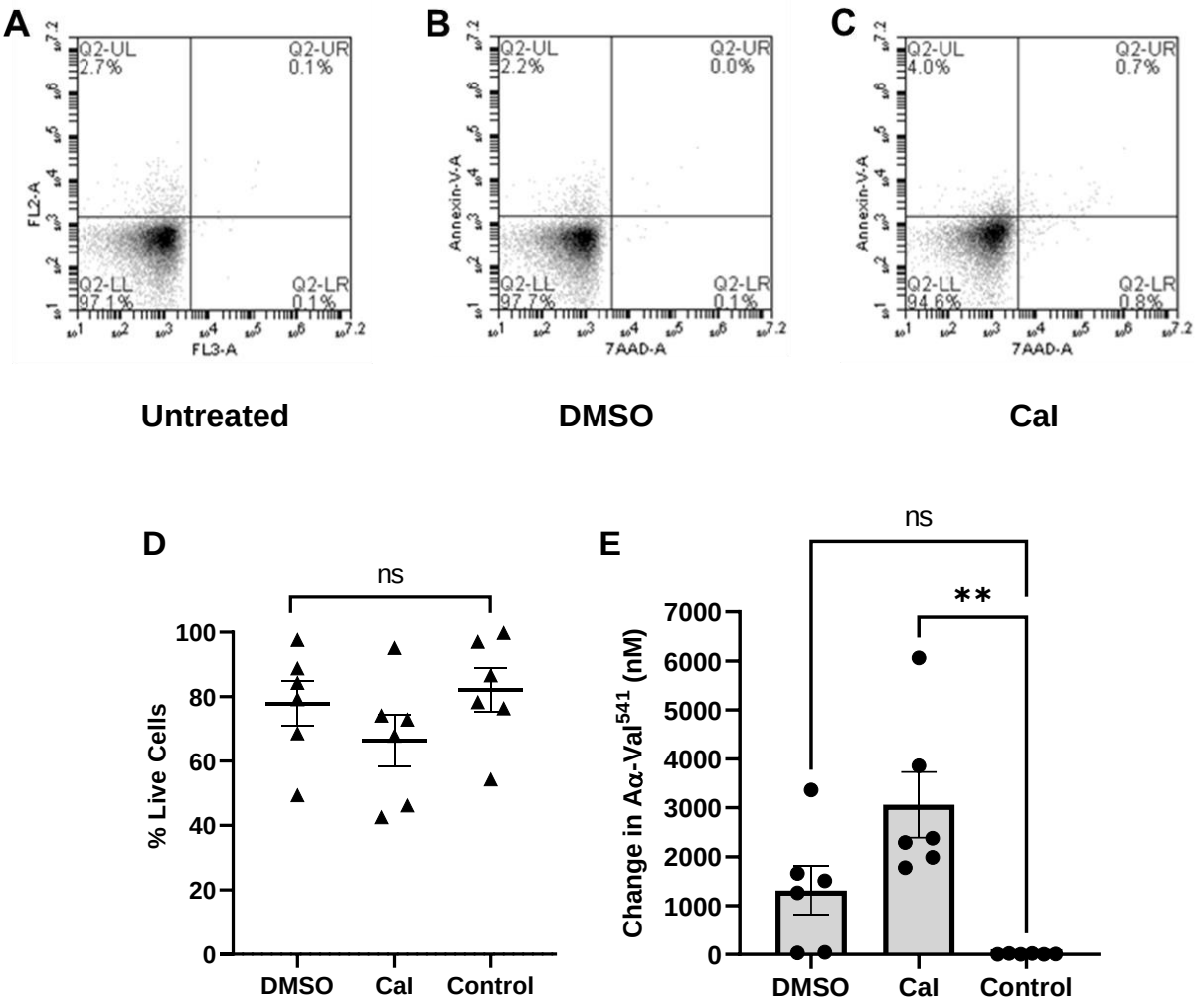

Figure 3.18. Cellular viability following CaI stimulation or a DMSO vehicle control.

Cellular viability following stimulation of neutrophils at 2.5x10^6/ml with calcium ionophore (7.5 µM) or a DMSO vehicle control and fibrinogen at 550 nM for 15 minutes. **A** untreated cells, **B** cells treated with DMSO, **C** cells treated with CaI, graphs shown are representative images; **D** neutrophil viability as a percentage (y-axis) in CaI-stimulated neutrophils, a DMSO control or negative control (x-axis), error bars mean +/- SEM, significance determined by Kruskal-Wallis, n=6; **E** baseline-corrected PR3 activity levels (y-axis) to a negative control compared to CaI-stimulated neutrophil or a DMSO control (x-axis), error bars mean +/- SEM, ** = $p \leq 0.01$ significance determined by Kruskal-Wallis, n=6.

3.3.2.6. *Fibrinogen Exhaustion Occurs Following CaI Stimulation*

The previous work suggested substrate exhaustion may be limiting PR3 activity footprint, as opposed to NSP activity being exhausted. To assess this, a fibrinogen titration curve was undertaken using stimulated neutrophils (**Figure 3.19**).

There was a significant increase ($p=0.0005$; ANOVA test) in the activity footprint produced by neutrophils (concentration $2.5x10^6$) when the concentration of uncleaved fibrinogen was doubled, from 550 nM to 1099 nM (**Figure 3.19.A**).

Furthermore, the fibrinogen titration curve (**Figure 3.19.B**), showed an increase in PR3 activity footprint at every concentration of fibrinogen when exposed to neutrophils.

This suggested that in **3.3.2.5. Calcium Ionophore Exposure**, the upper limit of footprint generation observed when CaI > 0.3 µM was introduced to the model was likely due at least in part to fibrinogen exhaustion (**Figure 3.14**).

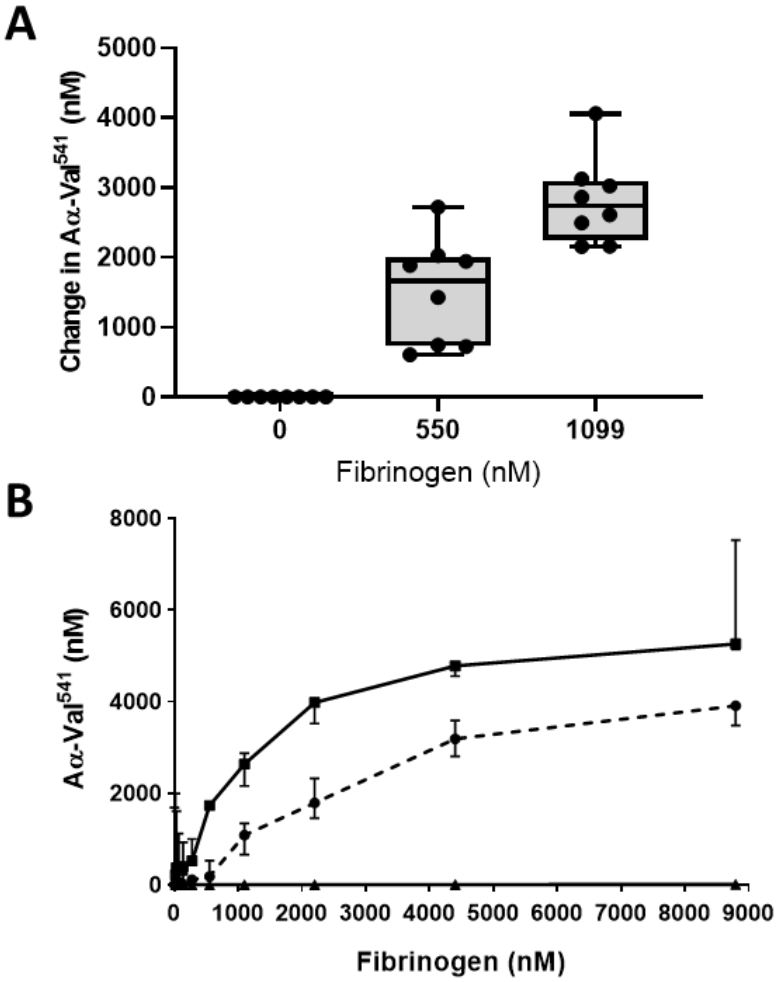

Figure 3.19. Test of fibrinogen exhaustion.

A Change in Aα-Val^{541} levels (y-axis) produced by CaI-stimulated (0.9 µM) neutrophils (2.5x10^{6}/ml) incubated with increasing concentrations of fibrinogen 550/1099 nM (x-axis) for 15 minutes; change from no fibrinogen control; error bars median with min-max; n=8; **B** Aα-Val^{541} levels (y-axis) produced by neutrophils (2.5x10^{6}/ml) incubated with increasing concentrations of fibrinogen (x-axis) for 15 minutes; square with solid line=0.9 µM CaI-stimulated, n=8; circle with dotted line =unstimulated, n=8; triangle with no line=cell free control, n=8.

3.3.2.7. *Stimulation with fMLP increases activity footprint*

In recognition of the non-pathophysiological nature of Cal, neutrophils were incubated with the bacterial peptide N-formyl-methionine-leucyl-phenylalanine (fMLP) (**Figure 3.20**). Concentrations chosen represented the range of physiological concentrations reported in published literature (Palmer et al., 1983; Chen et al., 2001).

There was an increase in the PR3 activity footprint following neutrophil stimulation with 0.1 to 1µM fMLP in the presence of 550 nM fibrinogen. Above 1 µM fMLP, the concentration of the PR3 activity footprint plateaued (**Figure 3.20.A**).

Similarly, significant changes in the NE activity footprint were seen following neutrophil stimulation with 0.1 µM and 1 µM fMLP in the presence of 550 nM fibrinogen, with only a slight further increase with 10 µM fMLP (**Figure 3.20.B**).

Given that the levels of proteinase activity footprint were lower than seen with Cal, this was not thought to be an artefact limited by substrate exhaustion, but rather the limit of the neutrophil response to fMLP. 10 µM was chosen for all subsequent fMLP experiments unless otherwise stated.

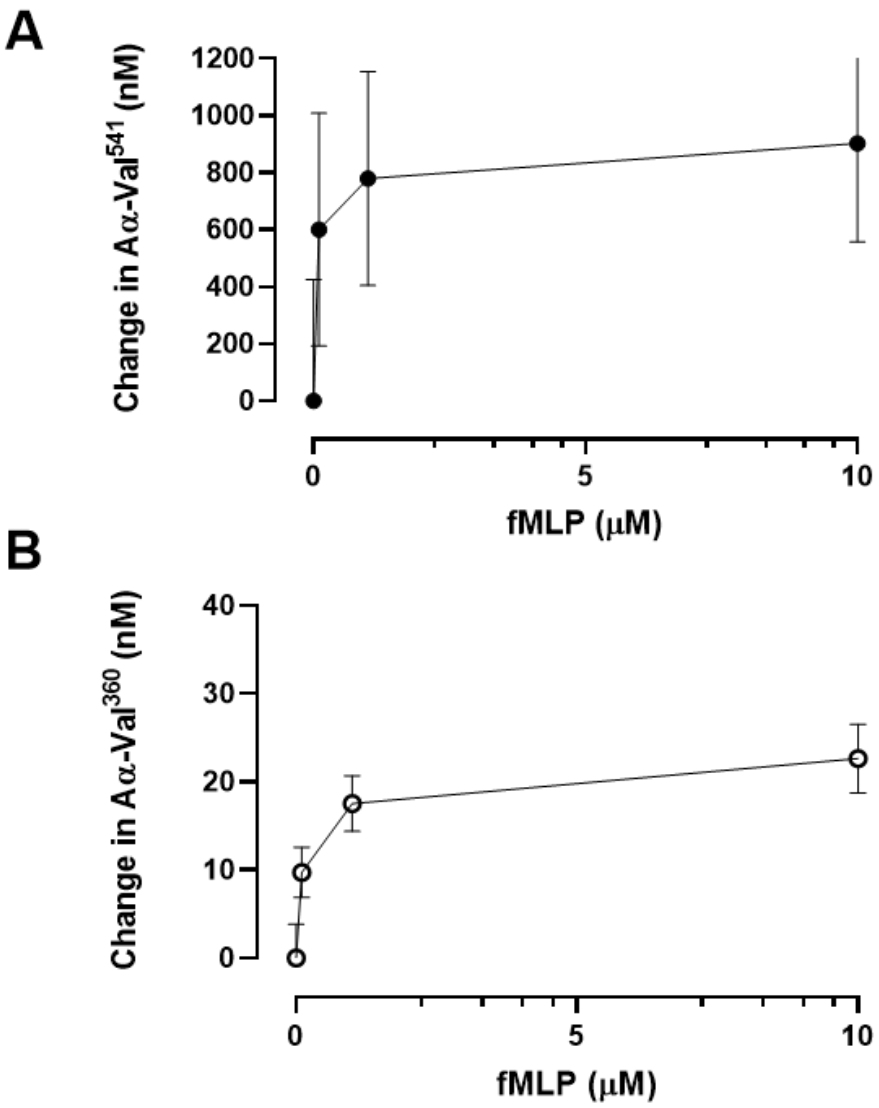

Figure 3.20. Proteinase activity following stimulation of neutrophils with fMLP.

Change in proteinase activity footprint (y-axis) following stimulation of neutrophils ($2.5x10^6$/ml) with 0, 0.1, 1 or 10 µM fMLP (x-axis) with fibrinogen (550 nM) for 15 minutes; **A** Aα-Val^{541}, n=6; **B** Change in Aα-Val^{360}, n=6. ●= PR3 activity footprint, o= NE activity footprint. Baseline set as unstimulated neutrophils, 0 µM. Error bars mean +/- SEM.

3.3.2.8. *Priming cells with TNFα*

Priming can potentiate neutrophil activation, and TNFα has been widely used as a priming agent (Gibbs *et al.*, 1990; Condliffe *et al.*, 1998; Cadwallader *et al.*, 2004).

To determine if priming alters proteinase activity footprints, neutrophils ($2.5x10^6$/ml) were primed with TNFα at 250 U/ml for 15 minutes (concentration based on literature quoted above) before the addition of fibrinogen (550 nM) and stimulation with fMLP to assess their effect on proteinase activity footprint (**Figure 3.21**)

Following priming, PR3 activity footprint increased from 319.2 nM (SEM: +/- 157.6) to 448.7 nM (+/- 28.1) but this failed to achieve significance (p=0.0952, ANOVA test), suggesting that the impact of priming neutrophils with TNFα before stimulation with fMLP on proteinase release was minimal in this model.

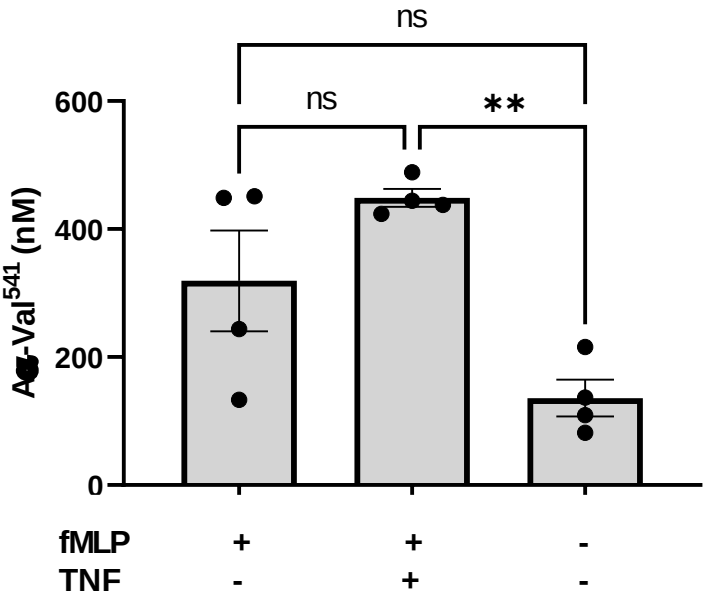

Figure 3.21 Effect of fMLP stimulation on neutrophils with and without priming with TNFα.

Change in Aα-Val^{541} levels (y-axis) following treatment of isolated neutrophils (2.5x10^{6}/ml) with TNFα (250 U/ml) for 15 minutes prior to addition of fibrinogen (550 nM) and stimulation with fMLP (10 μM) (x-axis) for 15 minutes, n=4. Error bars mean +/- SEM. ** = p ≤ 0.01 significance assessed by ANOVA.

3.3.2.9. *Degranulation Following Cellular Stimulation with fMLP*

Stimulation with 10 µM fMLP caused a greater proportion of cells to degranulate compared to vehicle control. In control conditions, a mean of 3.1% (+/- 1.3) neutrophils showed evidence of degranulation. This increased to 16.1% (+/- 6.9) with 0.1 µM fMLP, 16.6% (+/- 7.4) with 1 µM and 26.9% (+/- 9.8) with 10 µM (**Figure 3.22**)**,** suggesting that most neutrophils did not degranulate in the presence of fMLP but a sub-population did.

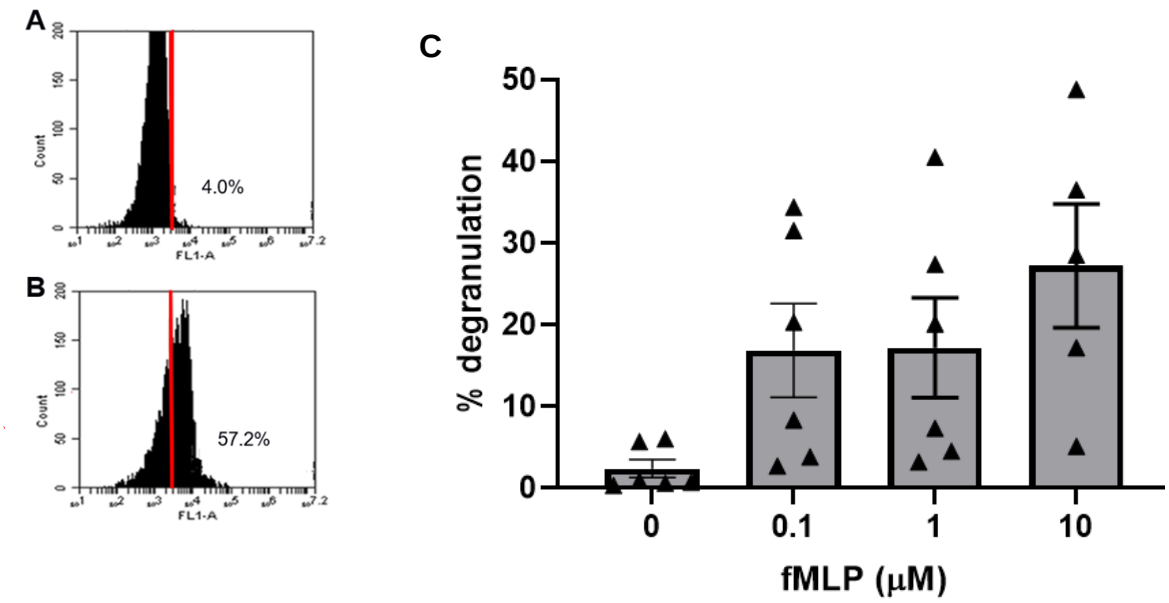

Figure 3.22 Neutrophil degranulation following stimulation with fMLP**.**

CD63 expression following stimulation of neutrophils at $2.5x10^6$ /ml in the presence of fibrinogen (550 nM) and with/without fMLP for 15 minutes; **A** unstimulated; **B** fMLP stimulated, single representative sample shown; **C** percentage of cells showing features of degranulation (y-axis) with increasing concentrations of fMLP, 0, 0.1, 1 µM (x-axis) n=6, 10 µM n=5; bars show mean +/- IQR.

3.3.2.10. *Cell Viability Remained High Following Cellular Exposure to fMLP*

Flow cytometry also showed that neutrophil viability remained high following fMLP stimulation (**Figure 3.23**) although individual sample responses were again variable.

Mean data shows 72.1% (SEM: +/- 7.6%) of cells remained viable and 24.7% (+/- 8.5%) appeared apoptotic, whilst 2.3% (+/- 2.0%) were necrotic and 1.0% (+/- 0.5%) appeared non-viable.

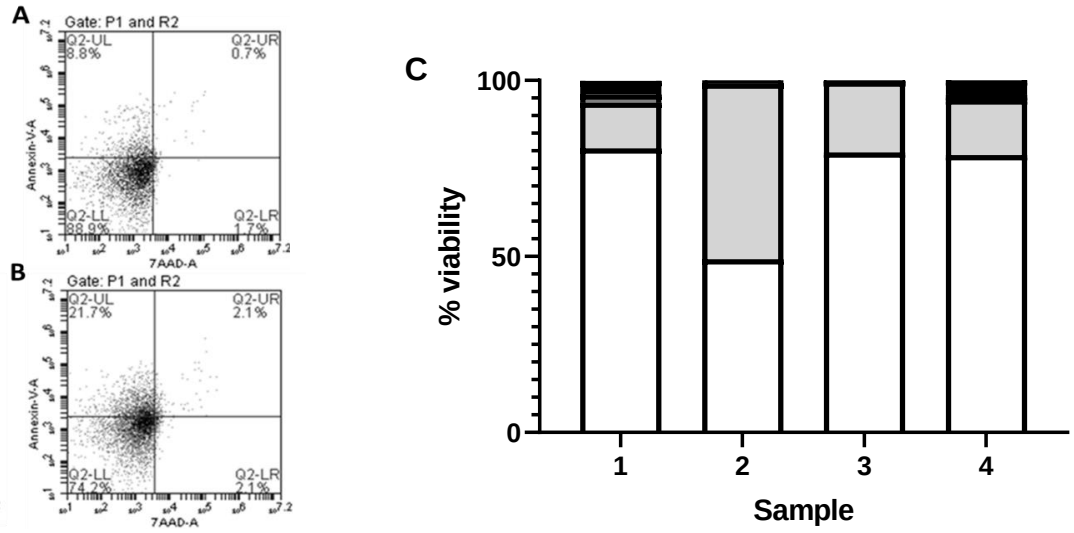

Figure 3.23. Neutrophil viability following stimulation with fMLP.

Cellular viability following stimulation (10 µM fMLP) of neutrophils ($2.5x10^6$ /ml) incubated with fibrinogen (550 nM) for 60 minutes, **A** with no treatment, **B** treated with fMLP; Graphs shown are a representative image; **C** Percentage neutrophil viability (y-axis) following stimulation of neutrophils at $2.5x10^6$/ml with CaI (0.9 µM) and incubation in fibrinogen-buffer for 15 minutes at 37°C; n=4 (x-axis); black=dead, dark grey=necrotic, light grey=apoptotic, white=viable.

3.3.3. Validation of Supernatants within the Assay

To determine whether the addition of a high activity footprint supernatant to an otherwise low activity supernatant would result in an expected intermediate activity footprint, a high activity footprint supernatant was added in increasing proportions to the low activity footprint sample and the resulting value for the mixtures were quantified.

As the ratio of the high activity sample increased, the proteinase activity footprints also increased (PR3: R^2= 0.99; NE: R^2= 0.95) (**Table 3.3**).

Table 3.3 Effect of mixing supernatants on proteinase activity footprints.

	Low Value, nM	High Value, nM	Ratio, H:L	Predicted value, nM	Actual Value, nM	% Accuracy	Linear Regression
PR3	0.8 (+/- 0.1)	1573.0 (+/- 367.6)	1:1	786.9	889.9 (+/- 321.0)	87	
			1:2	524.8	502.9 (+/- 238.2)	96	R^2= 0.99
			1:4	393.8	331.5 (+/- 88.5)	84	
NE	1.7 (+/- 0.4)	37.3 (+/- 3.6)	1:1	19.5	20.9 (+/- 5.4)	93	
			1:2	13.5	16.5 (+/- 6.7)	78	R^2= 0.95
			1:4	10.6	11.7 (+/- 5.9)	90	

Legend. Median proteinase activity footprints produced by high-value (nM) proteinase/anti-proteinase model supernatant diluted with a low-value supernatant (nM) at ratios of 1:1, 1:2 or 1:4 (mixed supernatants added at a total supernatant ratio of 1:10 within the PR3 activity assay, or 1:3 within the NE activity assay). Predicted values were calculated as a proportion of undiluted high/low values. Accuracy calculated as *(actual value/predicted value)*100.*

3.4. Discussion

3.4.1. Development of the Proteinase/anti-proteinase Cell Model

The work presented in this chapter has proposed a neutrophil-fibrinogen system as a potential model to study the proteinase/anti-proteinase balance for use in studying AATD and its response to therapy.

The activity assays used had been validated for plasma samples from patients but not for use in supernatants from an *in vitro* assay, and therefore initial validation was required to ensure the assays could be used in this model.

When developing the proteinase/anti-proteinase model, it was important to assess whether the model supernatants could be used accurately and consistently within the footprint assays. Hence, manipulation of neutrophil/fibrinogen-buffer supernatants and reporting the analytical parameters of the assay, including the limits of detection and quantification, were used to validate their use.

Initially, the effect of spiking the supernatant after harvesting from the model with global proteinase inhibitors, mixing low activity samples with high activity and adding diluent was assessed.

The addition of global inhibitors did not affect the footprint assays after harvesting. The mixing activities influenced the end result in a manner consistent with the expected result.

3.4.1.1. *Incubation with uncleaved fibrinogen*

An increase in fibrinogen concentration during neutrophil incubation increased proteinase footprint generation, for both NE and PR3. A concentration of 550 nM was selected for future studies as the generation of the footprint was well within the assay range and enabled assessment of a stimulated increase, without exceeding the upper analyte for the standard curve. However, when stimulated with high-dose CaI, fibrinogen exhaustion could occur.

3.4.1.2. *Addition of Proteinase Inhibitors*

Addition of commercially available, non-physiological proteinase inhibitors directly into the footprint assay with the neutrophil model supernatants showed no effect compared to the uninhibited result for PR3. This confirmed that there was no further cleavage occurring once the supernatants had been separated.

To determine whether the inhibitors were able to act effectively against fibrinogen cleavage by the proteinases, inhibitors were also added directly into the model at the start and incubated with the neutrophils. This resulted in flattening of PR3 activity footprint confirming the ability to abrogate the neutrophil-derived activity.

These data support the hypothesis that the model accurately demonstrates neutrophil-derived proteinase activity, causing specific fibrinogen cleavage occurring only during the model incubation phase.

3.4.1.3. *The length of incubation does not impact proteinase activity*

The data showed a small but insignificant increase in proteinase footprint generation by unstimulated cells over 60 minutes. This time point was also consistent with the use of longer time points in the literature (Abrams *et al.*, 1983; Naegelen *et al.*, 2015).

However, data from this thesis suggested that, following stimulation, the surface expression of markers of degranulation (anti-CD63 antibody binding of CD63 granule marker by flow cytometry) reached maximum concentrations by 15 minutes. Therefore, 15 minutes was revised as an optimal time-point for the assay post-stimulation.

A physiological concentration of $2.5x10^6$ neutrophils/ml was selected for the assay based on the dose responses published previously (Li *et al.*, 2002; Sapey, 2010; Amulic *et al.*, 2012).

3.4.1.4. *Stimulation of neutrophils in fibrinogen buffer increases proteinase activity*

3.4.1.4.1. Calcium ionophore stimulation

CaI is a potent stimulator of neutrophils (Bréa *et al.*, 2012) through facilitation of Ca^{2+} transfer across the cell membrane into the cytosol (Mahomed *et al.*, 2000).

Even at low concentrations, stimulation with CaI causes a rapid increase in proteinase footprint generation, however, it was observed that from 0.9 μM CaI the level did not increase further.

Flow cytometry was used to assess cellular viability and degranulation.

A combination of ANV and 7-AAD stains were used to determine cellular viability. Experimentation demonstrated that neutrophil viability remained high, and a high percentage of cells had undergone degranulation. Taken with the previous data this implies that either maximal degranulation and proteinases release or substrate exhaustion were occurring. Literature supports the theory of CaI inducing maximal degranulation (Kokot *et al.*, 1987; Brown *et al.*, 1991; Bréa *et al.*, 2012), however further investigation supported the likelihood of substrate exhaustion.

Excessive CaI induced degranulation was associated with fibrinogen exhaustion, indicating more proteinase released than required to cleave the available fibrinogen. Within this model, other neutrophil proteinases are also likely to be present and therefore different cleavage products may be generated in addition to the specific footprint being measured and may add to substrate exhaustion without generating

specific footprint epitopes. Since CaI stimulation is non-physiological, subsequent experiments were designed to lie within the linear part of the dose-response curve.

The effect of DMSO on proteinase activity footprints and neutrophil functionality was addressed by comparing the effect of treating neutrophils with DMSO alone compared to CaI in DMSO. DMSO alone produced an activity footprint similar to that of the untreated sample. This indicated that DMSO did not affect the proteinase activity footprint generation. To negate any change, it would be beneficial to standardise future samples by treating them with equal amounts of DMSO when comparing treatment groups.

In addition, the viability of cells was not affected by either DMSO or CaI in DMSO, as published previously (Beilke *et al.*, 1987) suggesting that the results for the model reflect largely physiological effects of the experimental conditions.

3.4.1.4.2. fMLP stimulation

fMLP acts as a physiological stimulus of neutrophils which is naturally produced by bacteria (Harris, 1954). It binds to G_{i2} protein-coupled receptors to activate intracellular signalling generating inflammation cascades (Iiri *et al.*, 1989), and acts as a chemoattractant and generator of superoxide production and degranulation (Brown *et al.*, 1991; Nick *et al.*, 1997; Sato *et al.*, 2013).

Stimulating with fMLP results in an increase of proteinase activity footprint generation by neutrophils compared to unstimulated cells, without reaching substrate exhaustion seen with calcium ionophore. Results were consistent with studies showing that above

a chemotactic concentration, fMLP stimulates neutrophil degranulation (Sato *et al.*, 2013).

Neutrophil priming is also considered an important cellular mechanism involved in cellular preparation for activation responses (Hallett *et al.*, 1995; Miralda *et al.*, 2017). Neutrophils can be primed by a variety of stimuli, including mechanical action, molecular agents, and environmental factors (Hallett *et al.*, 1995; Ekpenyong *et al.*, 2015).

Priming neutrophils with TNFα prior to fMLP stimulation, however, did not produce a significant increase in generation of the activity footprints by neutrophils. This was not expected, given polarisation and migration are increased at this dose (Amulic *et al.*, 2012). That said, the process of degranulation occurs at later phase of neutrophil activation than these other neutrophil functions (polarisation and migration) (Mottola *et al.*, 1982; Lacy, 2006) , therefore a longer period of incubation may be required. Furthermore, Klebanoff et al. (1986) found that TNFα-priming prior to zymosan stimulation with produced an increase in some, but not all, of the proteinases released during degranulation (Klebanoff *et al.*, 1986). There is no direct evidence that TNFα-priming prior to fMLP stimulation can increase PR3 or NE release or activity following degranulation.

3.5. Summary

This chapter describes the development of a novel *in vitro* fibrinogen-buffer cellular model of the proteinase/anti-proteinase balance observed with relevance to AATD.

Evaluation of the neutrophil/fibrinogen buffer model primarily identified that median PR3 and NE activity footprint generation increases with fibrinogen concentration; but not unstimulated neutrophil concentration or the period of cellular incubation; calcium ionophore and fMLP stimulate neutrophil degranulation, proteinase release and generation of the proteinase footprints; neutrophil stimulations were not affected by the DMSO vehicle; TNFα priming did not increase proteinase footprint generation following stimulation with fMLP; CaI was able to cause fibrinogen exhaustion up to a high fibrinogen concentration. These studies enabled the optimal concentration of fibrinogen, neutrophils and time course to be established within the assay parameters for interventional studies.

Data indicated that proteinase inhibitors were able to abrogate proteinase activity footprint when applied to the model.

This chapter validated the use of supernatants generated within the in-house proteinase footprint assays for stability at the chosen fixed point and that spiking individual samples with other high and low activity samples produced the expected intermediate values.

In conclusion, the validation described in this chapter allows confidence in the model, and permits its use for studying the role of intrinsic and therapeutic inhibitors to control proteinase activity from resting and stimulated neutrophils in both health and disease.

CHAPTER 4: VALIDATION OF A PROTEINASE/ANTI-PROTEINASE BALANCE MODEL

The following outputs relate to the data obtained in this chapter:

ABSTRACT. H Crisford, E Sapey, RA Stockley. (2020). Validation of an *in vitro* Model of the Proteinase/Anti-proteinase Imbalance observed in Alpha-1 Antitrypsin Deficiency. American Journal of Respiratory and Critical Care Medicine. **201:** A4080

4.1. Brief Introduction

4.1.1. Background

In healthy lung tissue, proteinase activity is modulated with proteinase inhibitors. The proteinases (especially NE) are released during neutrophil migration through tissues (Cepinskas *et al.*, 1999), as a result of granule release from activated neutrophils (Segal, 2005) and can localise within NETs (Urban *et al.*, 2009).

Endogenous inhibitors in the plasma can diffuse into the tissues and form complexes with active proteinases thereby inactivating them and curtailing proteolytic activity.

The inactivation of proteinases closely limits the enzyme activity to an area of quantum proteolysis directly around the cell which dissipates until inhibitor homeostasis is achieved (Campbell *et al.*, 2000a). Homeostasis allows for innate immune cell navigation to, and subsequent impact on, sites of an immune challenge but greatly limits excessive and potentially destructive proteolytic action.

In an imbalanced state, the excessive proteolytic activity of NE and PR3 are strongly implicated in the pathophysiology of airway disease, including COPD (Owen, 2008) and AATD (Stockley, 2020a). It has been demonstrated that specific fibrinogen cleavage products of these proteinases are detectable in the plasma and increased in disease, especially in AATD (Carter, 2013; Gudmann *et al.*, 2018; Newby *et al.*, 2019; Schouten *et al.*, 2021).

An increase of proteinase activity within the airways has been associated with irreversible emphysematous changes both *ex vivo* human studies (Damiano *et al.*, 1986; Pierce *et al.*, 1995) and *in vivo* murine models (Janoff *et al.*, 1977; Kao *et al.*, 1988) indicating that intratracheal administration of NSPs results in emphysematous changes (Janoff *et al.*, 1977; Kao *et al.*, 1988). NE and PR3 can establish a functional loss of terminal airways through ECM cleavage and can exacerbate the inflammatory state of the lung (Pandey *et al.*, 2017; Crisford *et al.*, 2018) leading to further damage.

The main anti-proteinase in the lung tissues is AAT derived from the circulation, however other locally produced anti-proteinases such as secretory leukocyte protease inhibitor (SLPI) also have a role in limiting proteinase action, especially in the airways (Stockley, 1999).

4.1.2. Physiological Inhibitors of Proteinases in the Airways

There are several endogenous proteinase inhibitors present in the airways that can inhibit NE and PR3, in addition to AAT. Some of the major NSP inhibitors identified in the lung are described below.

4.1.2.1. *Secretory leukocyte proteinase inhibitor*

SLPI is a cationic 11.7 kDa glycoprotein released by cells at mucosal surfaces, including the epithelium, alveolar type 2 cells, club cells and phagocytes within the airways (Sallenave *et al.*, 1997; Sallenave, 2002). As a chelonianin inhibitor, SLPI is a potent reversible inhibitor of NE, but it has no activity against PR3 (Bergenfeldt *et al.*,

1992). SLPI is known to be the major locally produced anti-proteinase in the lung and is dominant in the airway secretions in the absence of inflammation (Sinden *et al.*, 2013).

SLPI acts by NE P1 (Leu72i) occupying the S1 pocket then binding the C-terminal domain via intra-hydrogen bonds and electrostatic interactions at P2'-P3 and P5 (Koizumi *et al.*, 2008).

Dysfunction or deficiency of SLPI has been reported in lung disease including asthma (Raundhal *et al.*, 2015) and cystic fibrosis (Weldon *et al.*, 2009). Gene expression of SLPI is shown to be increased *in vitro* following exposure to NE (Sallenave *et al.*, 1994; Marchand *et al.*, 1997) and the protein found to be present in increased concentrations within epithelial cells (van Wetering *et al.*, 2000) and the neutrophil (Sallenave *et al.*, 1997). However, its concentration in inflamed secretions is reduced as indicated above (Hill *et al.*, 2000; Weldon *et al.*, 2009; Raundhal *et al.*, 2015).

4.1.2.2. *Monocyte/neutrophil elastase inhibitor*

Monocyte/neutrophil elastase inhibitor (MNEI) is a 42 kDa Serpin, with a similar conserved structure to AAT (Gettins, 2002). MNEI is found in the neutrophil cytoplasm, but it remains intracellular (Remold-O'Donnell *et al.*, 1989) where it is able to bind PR3 and NE irreversibly through binding at Phe343-Cys344 and Cys344-Met345 in the reactive centre loop (RCL) (Cooley *et al.*, 2001; Korkmaz *et al.*, 2008).

4.1.2.3. *Alpha-2-macroglobulin*

Alpha-2-macroglobulin (A2M) is 725 kDa glycoprotein (Virca *et al.*, 1984). A2M is primarily produced by hepatocytes and is present in the circulation (Petersen, 1993). The inhibitor can enter the airways by diffusion (Burnett *et al.*, 1981) although the size largely prevents this in the absence of inflammation. The protein irreversibly 'traps' PR3 and NE (Delain *et al.*, 1992) following binding of a bait region (Harpel, 1973). Although the enzymes retain proteolytic function against substrates able to penetrate the 'trap' (Sottrup-Jensen, 1989). The inhibitor also has wide-ranging activity against other classes of proteinases and it can be produced by macrophages, although the size limitation for diffusion from plasma suggests it has a limited anti-NSP role in the lung (Stone *et al.*, 1982).

4.1.2.4. *Elafin*

Elafin is a comparatively small chelonianin glycoprotein with a molecular weight of 6kDa (Sallenave, 2002). Elafin is produced locally in the lungs by alveolar cells (van Wetering *et al.*, 2000; Sallenave, 2002) and phagocytes (Sallenave *et al.*, 1997; Mihaila *et al.*, 2001). It can reversibly inhibit both NE and PR3, including cell-bound proteinase (Zani *et al.*, 2004; Zani *et al.*, 2009). Elafin is cleaved by NE reducing inhibitory function in high proteinase environments (Greene *et al.*, 2009). Direct studies have indicated its role in serine proteinase inhibition in the lung is relatively small (Sinden *et al.*, 2013).

4.1.3. Hypotheses and aims

It was hypothesised that the addition of specific physiological NSP inhibitors would influence proteinase activity within our model, enabling studies of the dose and response to therapeutic approaches *in vitro* as a predictor of efficacy *in vivo.* The addition of AAT should result in a decrease in both NE and PR3 activity footprint, whereas the addition of SLPI should result in a decrease only in NE footprint.

For initial validation of the model, increasing concentrations of the physiological inhibitors AAT and SLPI were added to the model.

This chapter aimed to provide data on the putative AAT “protective” threshold by a different mechanism to that established by Campbell *et al.* (2000).

4.2. Specific Methodology

4.2.1. Plasma preparation

Blood obtained by vacutainer (lithium heparin vacutainer; BD, US) was stood upright for 30 minutes at room temperature, then centrifuged at 1000 *xg* for minutes (at room temperature).

Plasma was removed from the vacutainer, with care not to disrupt the underlying cellular layer, and pipetted in 0.5 ml aliquots into sample tubes. Samples were labelled with study ID numbers and date of collection, then frozen at -20°C, before being transferred to a -80°C freezer until future use.

Defrost cycles of aliquots of frozen plasma were limited to two to prevent any possible freeze-thaw effects.

4.2.2. Neutrophil treatment with physiological proteinase inhibitors

Isolated neutrophils ($2.5x10^6$ cells/ml) in RPMI were incubated for 15 minutes at 37°C with AAT or SLPI (of known molar concentrations) in a dose-response based upon concentrations reported within the literature (Kida *et al.*, 1992; Kouchi *et al.*, 1993; Sluis *et al.*, 1994; American Thoracic Society/European Respiratory Society, 2003; Tsukishiro *et al.*, 2005). Fibrinogen was then added (550 nM) and cells stimulated with fMLP (10 µM), followed by incubation for 15 minutes at 37 °C (**Figure 4.1**.)

This method allows for stimulated degranulation to occur in the presence of the inhibitors likely to be present in the milieu *in vivo* alongside the fibrinogen substrate.

As an alternative model, isolated neutrophils ($2.5x10^6$ cells/ml) in fibrinogen-buffer (550 nM) were incubated for 15 minutes at 37°C with fMLP (10 μM) and AAT or SLPI. This was to determine if the late addition of inhibitors altered assay readings.

Both methods are visualised in **Figure 4.1**.

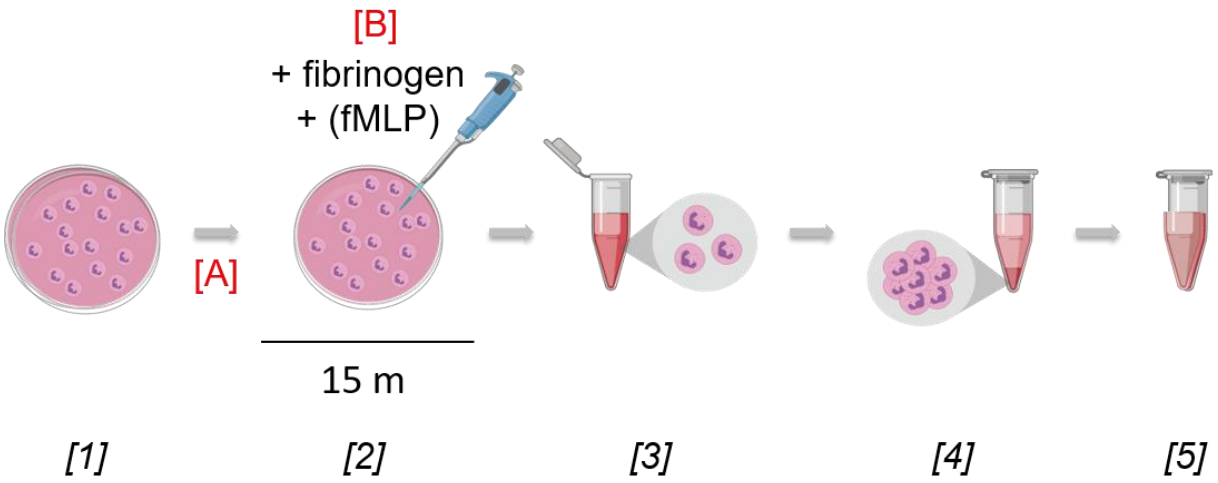

Figure 4.1. Visualisation of proteinase/anti-proteinase balance model methodology.

[1] Isolated neutrophils were plated at 2.5x10^6/ml; [2] fibrinogen and fMLP were added to the isolated neutrophils for a 15-minute incubation period; [3] treated cells were removed from the plate and centrifuged for 5 minutes at 300 x*g*; [4-5] supernatant was transferred to a clean Eppendorf and cells were discarded. Inhibitors were added at either of two points: with a 15-minute pre-incubation step at [A], or together with the substrate and stimulus at [B]. [A] indicates the point of inhibitor addition to isolated neutrophils (in RPMI) with a pre-incubation (15 minutes; 37°C) before the addition of fibrinogen and stimulus, and a further 15-minute incubation step; [B] indicates the point of inhibitor and stimulus addition together to isolated neutrophils in a fibrinogen buffer. Figure produced using Biorender.com.

4.2.3. Incubation of healthy neutrophils in patient plasma

Isolated neutrophils ($2.5x10^6$/ml) from healthy young donors were incubated in a plasma pool from patients with AATD, non-AATD COPD, or the plasma from age-matched donors with no chronic lung diseases (termed healthy elderly (HE) donors) for 15 minutes at 37°C. Plasma was used rather than serum as serum adversely affects neutrophil viability (Hughes, 2021). fMLP (10 μM) was added to the incubation mixture to stimulate the cells. After the incubation, the sample was centrifuged at 10000 *xg* for 10 minutes and the supernatant was removed. The proteinase footprints were measured.

The proteinase activity footprints of each cohort plasma pool were measured before use, and the baseline value was subtracted from the experimental footprint generated by neutrophils incubated in the relevant plasma pool.

Subject demographics are described in **Table 4.1**.

Inclusion and exclusion criteria were applied to the cohorts as described below.

- Healthy young donors that provided neutrophils for incubation were required to be 18-45 years old, have no smoking history within the last 10 years and a <10 pack-year smoking history, with no evidence of clinical disease or recent history (>6 weeks) of respiratory symptoms or acute illness.

- The healthy donor plasma pool was obtained from healthy older adults (≥45 years old) with no evidence of clinical disease or symptoms of current or recent respiratory disease.

- The AATD plasma pool was obtained from patients with a confirmed PiZZ AATD genotype and stable disease (no exacerbation in the previous 6 weeks). Exclusion criteria included evidence of lung cancer, haematological malignancy, previous lung resection, treatment with regular oral prednisolone or immunosuppressive medication.

- Patients included within the COPD cohort had stable proven COPD, at least a 10 pack-year smoking history and be older than 40 years. The exclusion criteria included a diagnosis of any alternative lung disease as diagnosed by a respiratory clinician i.e. asthma, interstitial lung disease or lung cancer, and recent exacerbation of disease (within the previous 6 weeks).

All donors and patients gave informed consent and were recruited under ethics described in **2.1 Ethical Considerations**.

Table *4.1*. Demographics of subjects providing plasma pools

	Healthy elderly donors	**Patients with stable COPD**	**Patients with PiZZ AATD**
Total, n	20	20	13
Age, mean (range)	71.5 (59-95)	70.8 (60-83)	60.9 (48-81)
Gender, % male	9, 45%	14, 70%	10, 77%
FEV_1 % predicted, mean (SD)	116.5 +/- 19.1	54.0 +/- 22.3	47.2 +/- 22.0
Current smokers, %	2, 10%	2, 10%	1, 7%
Ex-smokers, %	7, 35%	18, 90%	8, 62%
Mean pack year history +/- SD	7.2 +/- 11.7	54.1 +/- 53.7	18.0 +/- 11.3
Pooled plasma AAT concentration (μM)	13	29	7
Pooled plasma Aα-Val^{541} footprint (nM)	39.97	29.76	61.37
Pooled plasma Aα-Val^{360} footprint (nM)	9.76	7.68	10.76

Legend. Age, lung function and smoking status of patients/donors whose plasma was used to generate a pool for experimentation. Cohorts were healthy elderly donors (as reported by Walton (Walton, 2018)), stable patients with PiZZ genotype AATD, stable non-AATD COPD (as reported by Hughes (Hughes, 2021)). The AAT concentration (μM; determined by colorimetric ELISA), and PR3 and NE footprints of the pools.

4.2.4. Measurement of plasma pool AAT concentration

The AAT concentration of each plasma pool was measured using a commercial colorimetric AAT ELISA (Enzyme-linked immunosorbent assay) kit (ab108799, Abcam, UK).

AAT standard (27.5 ng) was reconstituted to 25 ng/ml (480.8 nM) in 1X Diluent N (10X Diluent N concentrate 1:10 in distilled (d)H_2O) then prepared in a 1:1 dilutional series to 0.391 ng/ml (7.5 nM). Plasma pools were diluted 200,000-fold in 1X Diluent N. Standard or sample were added at 50 µl to a 96-well microplate and incubated for 2 hours at room temperature. The plate was washed 5 times with 300 µl wash buffer (20X wash buffer concentrate 1:20 in dH_2O). Biotinylated AAT antibody (50X Biotinylated antibody stock diluted in 1X diluent N) was added at 50 µl to each well and incubated for 1 hour. The plate was again washed 5 times. Streptavidin-peroxidase conjugate (Streptavidin-peroxidase conjugate concentrate at 1:100 in 1X Diluent N) was added at 50 µl and incubated for 30 minutes. Chromogen substrate was added at 50µl to each well and incubated for 25 minutes, then 50 µl STOP solution (2N H_2SO_4) was added. Absorbance was measured on a BioTek Synergy HT machine at 450 nm with 570 nm correction.

The concentration of samples was obtained by interpolation from the standard curve using GraphPad Prism 8 software, then corrected for dilution (200,000-fold).

Values are recorded in **Table 4.1**.

4.2.5. Enzyme kinetics

As pure inhibitors were used for some of the experiment it was necessary to determine the exact inhibitory function of each. In order to do this an indirect method was used whereby known enzyme kinetics were determined for Porcine pancreatic elastase and used to assess the inhibitory activity of the purified AAT. This result was then used to determine the enzyme activity of purified NE and the last result used to determine the functional activity of SLPI.

There are several established methods that can be used to determine the activity of enzymes accurately. The protocols described below detail the methodology used throughout this thesis.

4.2.5.1. *Activity of Porcine Pancreatic Elastase*

N-succinyl-Ala-Ala-Ala-p-nitroanilide (SlaaapN; Sigma-Aldrich) was prepared at concentrations of 0.5-7.5 mM in porcine pancreatic elastase (PPE) substrate buffer (0.1 M HEPES, pH 7.5; 9.5% dimethyl sulphoxide (DMSO); Sigma-Aldrich). A flat-bottomed polystyrene 96-well plate had 247.5 µl of each concentration added to wells in duplicate.

PPE (Sigma-Aldrich) was then prepared at 10 µg/ml (386.1 nM) in PPE buffer (0.2 M Tris-HCl, pH 8.6; 0.1% v/v Triton X100; Sigma-Aldrich) and 2.5 µl was added to each well with the substrate (as described above),

Control wells without either substrate, PPE, or both were also prepared, and the volumes made up to 250 µl with buffer.

The plates were shaken for 8 seconds, then read every 30 seconds for 15 minutes at 410 nm by a spectrophotometer (BioTek Synergy HT).

Using Beer-Lambert Law $A = \varepsilon lc$ (where *A = absorbance; **ε** = molar extinction coefficient; l = path length; c = solution concentration*), the maximum reaction velocity (V_{max}) was determined and Michaelis-Menten (Example plot in **Figure 4.2**) and Lineweaver-Burk (Example plot in **Figure 4.3**) plots were produced (Michaelis *et al.*, 1913; Lineweaver *et al.*, 1934).

V_{max} = maximal reaction velocity K_m = Michaelis-Menten constant

V = reaction velocity [s] = substrate concentration

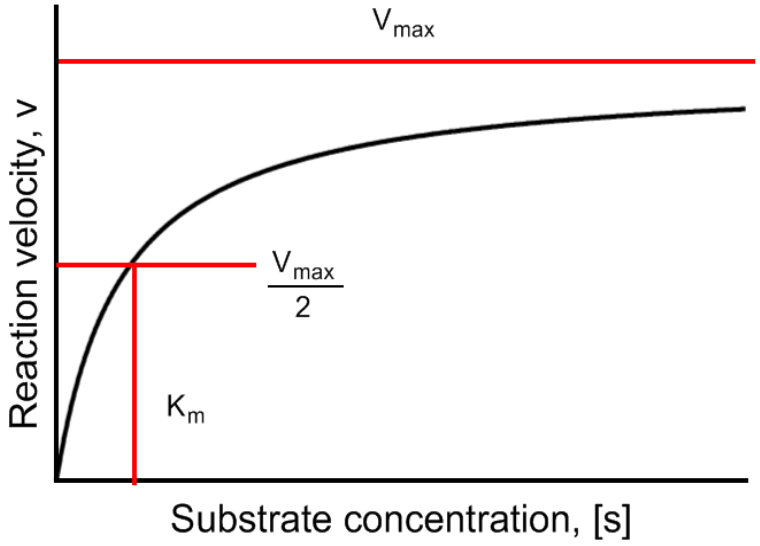

Figure 4.2. Michaelis-Menten plot.

Graphical representation of a Michaelis-Menten plot, with key mathematical parameters indicated.

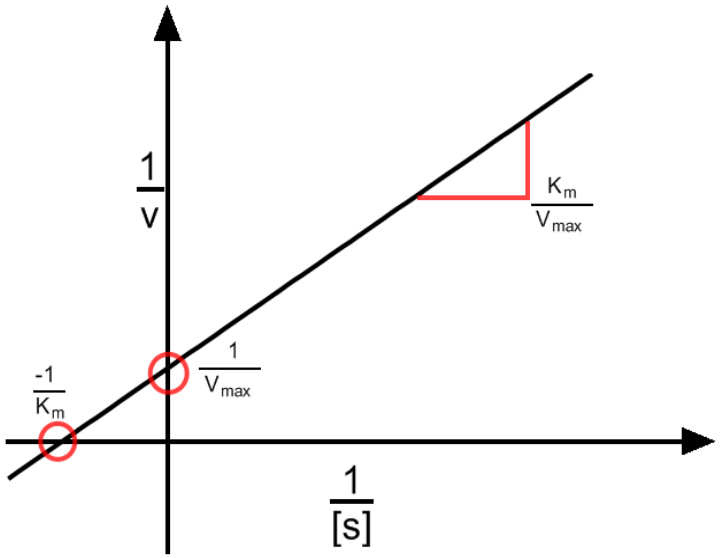

Figure 4.3. Lineweaver-Burk Plot.

Graphical visualisation of a Lineweaver-Burk plot, with key mathematical parameters indicated. The y-intercept indicates $\frac{\mathbf{1}}{\mathbf{V_{max}}}$ and the x-axis intercept indicates $\frac{\mathbf{-1}}{\mathbf{K_m}}$.

The input of kinetic values into the GraphPad Prism statistical software package produced computerised, accurate values for x-intercept and y-intercept on the Lineweaver-Burk plot, and V_{max} and K_m values on the Michaelis-Menten plot. The use of computational measurements removed any human error in the visual interpretation of these intercepts and constants.

Enzyme activity was then calculated using:

$$\frac{V_{max}}{K_{cat}} = active\ enzyme\ concentration\ ([E]_T)$$

$$1\ mg/ml\ \times \frac{1\ L}{Molecular\ weight\ Da} = total\ enzyme\ concentration\ (Mol\ L^{-1})$$

$$\frac{active\ molar\ concentration}{total\ molar\ concentration} \times 100 = percentage\ activity$$

This activity was translated into molar concentration for all future studies but also cross-checked using a normal plasma sample as detailed below.

Plasma collected from 5 healthy individuals with known PiMM genotype and AAT serum concentration were used initially. Although a plasma pool consisting of the same donors was also produced and used.

Increasing amounts of PPE buffer was added to wells in a flat-bottomed polystyrene 96-well plate starting from 82 µl to 100 µl in 3 µl increments. Each well condition was run in duplicate.

PiMM AAT plasma was diluted at 1:200 in PPE buffer and added to the above wells to make a volume of 100 µl.

Then 10 µl of PPE (10 µg/ml; 386.1 nM) was added to each well. The plate was then incubated at 37°C with gentle shaking for 20 minutes.

Post-incubation, SlaaapN was prepared to 1 mg/ml (2.22 mM) in PPE substrate buffer, and 100 µl was added to each well.

Again, control wells lacking substrate, plasma, or both were prepared, and the volumes made up to 210 µl with buffer.

The plate was shaken for 8 seconds, then read every minute for 20 minutes by a spectrophotometer (410 nm).

Normal plasma has a functional AAT concentration of approximately 25 µM. Individual AAT concentrations were determined using a pathological serum assessment. Using these values, PPE molar ratios to AAT were estimated.

Molar ratio was then plotted against percentage enzyme activity and the intercept on the x-axis was used to confirm this was close to the 1:1 molar ratio.

4.2.5.2. *Activity of Alpha-1 Antitrypsin*

Having confirmed the PPE activity, the inhibitory function of a purified batch of AAT (Athens Research & Technology, GA US) was determined. AAT is able to act as an effective inhibitor of PPE by forming a stable 1:1 complex by peptide linkage at Ser and Val residues of the amino-terminal end (James *et al.*, 1978).

AAT activity for all subsequent experiments was identified as follows.

Increasing amounts of PPE buffer was added to wells in a flat-bottomed polystyrene 96-well plate starting from 75 µl to 100 µl in 5 µl increments and each well was in duplicate.

Pure AAT was diluted to 20 µg/ml (384.6 nM) in lyophilisation buffer (30 mM sodium phosphate, pH 6.5; 300 mM sodium chloride; Athens Research and Technology), then increasing volumes of the AAT (5-25 µl) was added to the above wells with buffer to establish a dose-response and a total volume of 100 µl.

Then 10 µl of PPE at 10 µg/ml (386.1 nM) was added to each well and the plate was incubated at 37°C with gentle shaking for 20 minutes.

SlaaapN was prepared to 1 mg/ml (2.2 mM) in PPE substrate buffer, and 100 µl was added to each well. Again, control wells lacking in substrate, plasma, or both were prepared, and the final volumes were made up to 210 µl with buffer.

The plate was shaken for 8 seconds, then read every 5 minutes for 1 hour by a spectrophotometer (410 nm).

Molar ratio of AAT was then plotted against percentage enzyme activity and the intercept on the x-axis was used to determine AAT functional activity.

$$\frac{known\ PPE\ activity}{x\ axis\ intercept} = AAT\ activity$$

4.2.5.3. *Activity of NE*

SLPI activity was determined using NE as SLPI has only weak inhibitory effect on PPE (Thompson et al., 1986; Masuda et al., 1994).

NE (10 µg/ml) was incubated at increasing concentrations (with gentle shaking; in a polystyrene 96-well plate; in the dark) with a fixed amount of AAT (10 µg/ml; at known activity) for 20 minutes at 37°C. Wells were topped up to 110 µl using NE activity buffer (0.01 M Tris-HCl, 0.5 M NaCl, 0.1% Triton X100, pH 8.6).

SlaaapN (1 mg/ml; 2.2 mM) was then added to each well (100 µl) and substrate cleavage (production of p-anilide) measured using a BioTek Synergy HT spectrophotometer (410 nM; 25°C) every 5 minutes over 30-minute incubation.

Enzymatic action rate was calculated and plotted against molar ratio to determine functional activity.

4.2.5.4. *Functional Activity of SLPI*

Once the activity of NE was determined, it was used in an inhibition assay to derive the functional activity of SLPI using cleavage of N-methoxysuccinyl-Ala-Ala-Pro-Val p-nitroanilide (MSaapVN) (Maffía *et al.*, 2018).

Increasing amounts of NE buffer was added to duplicate wells in a flat-bottomed polystyrene 96-well plate starting from 75 µl to 100 µl in 5 µl increments. Each well was repeated in duplicate.

SLPI (BioTechne. MN, US) was diluted to 10 µg/ml (0.855 µM) in PBS and added in decreasing volumes with buffer to the above wells to make a total volume of 100 µl.

Then 10 µl of NE at 10 µg/ml (386.1 nM) was added to each well and the plate was incubated at 37°C with gentle shaking for 20 minutes.

MSaapVN was prepared to 0.2 mg/ml (338.6 µM) in PPE substrate buffer, and 100 µl was added to each well.

The plate was shaken for 8 seconds and the production of p-nitroanilide (the product of the reaction) was measured every minute for 30 minutes by a spectrophotometer (410 nm).

Molar ratio was then plotted against percentage uninhibited enzyme activity and the intercept on the x-axis was used to determine SLPI functional activity on NE.

$$\frac{known\ \mathrm{NE}\ activity}{x\ axis\ intercept} = SLPI\ activity\ on\ NE$$

4.3. Results

4.3.1. Porcine Pancreatic Elastase Activity

4.3.1.1. *Lineweaver-Burk double reciprocal plot analysis for PPE activity*

Prior to the application of inhibitors, the activity of PPE was determined by measuring substrate optical density over one hour (**Figure 4.4**), then the rate of reaction velocity and substrate cleavage was calculated (**Table 4.2**).

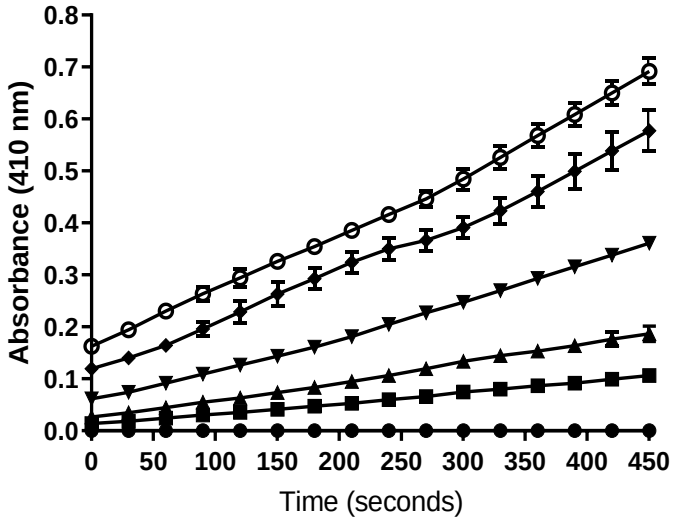

Figure 4.4. Absorbance over 30 minutes following addition of substrate to PPE.

Change in absorbance (410 nm) (y-axis) over a 30-minute incubation period (x-axis) following the addition of SlaaapN substrate to PPE. Each point indicates the value at increasing time intervals.

Table 4.2. PPE Reaction Velocities against SlaaapN.

[S] (mM/L)	1/[S] (mM/L-1)	v (mM/L/s)	0.1/v
0.5	2.00	0.00166	6.02E+02
1	1.00	0.00230	4.35E+02
2.5	0.40	0.00507	1.97E+02
5	0.20	0.00833	1.20E+02
7.5	0.13	0.00875	1.14E+02

Legend. Change in reaction velocities ([S] = substrate concentration, v = velocity) and kinetic derivatives (1/[S], 0.1/v) of PPE were determined following measurement of optical density (410 nm) following incubation for 30 minutes with 5 concentrations of the substrate SlaaapN; n=3.

This allowed the production of a Michaelis-Menten plot (**Figure 4.5**). This plot demonstrated a parabolic curve, so the reaction can be described by the usual Michaelis-Menten equation and is not cooperative or allosteric.

A Lineweaver-Burk plot was also produced (**Figure 4.6**). Using the axis crosspoints obtained computationally, the values for maximal rate (V_{max}) and the Michaelis constant (K_m) were calculated as below.

$$\frac{1}{V_{max}} = Y\ axis\ crosspoint = 85.86$$

$$\frac{1}{85.86} = 0.0116\ mM/s\ or\ 0.0000116\ M/s = V_{max}$$

$$-\frac{1}{K_m} = X\ axis\ crosspoint = 0.28$$

$$\frac{1}{0.28} = 3.6 = K_m$$

These results were consistent with the result computationally confirmed by the Michaelis-Menten plot**.**

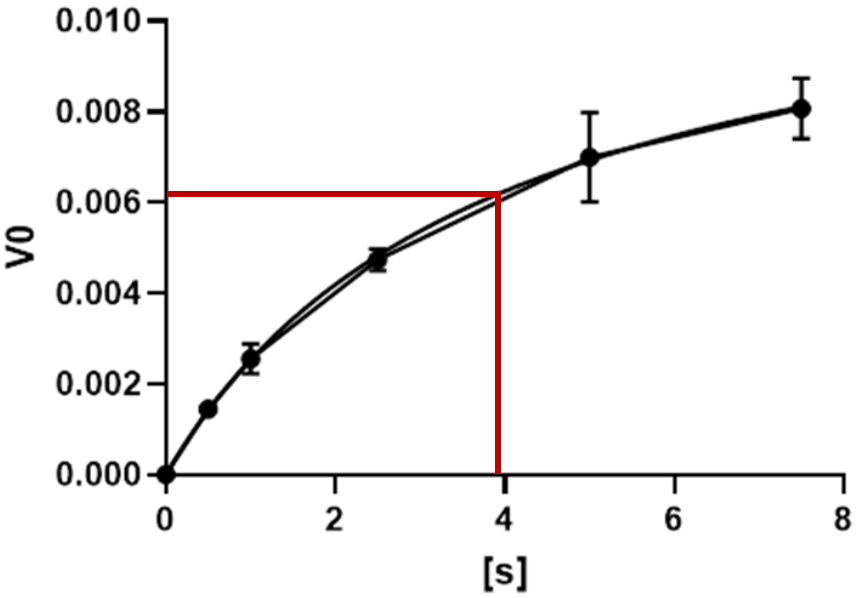

Figure 4.5. Michaelis-Menten plot of PPE activity.

Plot of initial velocity, V_0, as a function of the substrate concentration, [s], as described by Michaelis-Menten equation, n=3. The red line intercept of the y-axis indicates ½ V_{max} and the red line intercept of the x-axis indicates K_m.

Table 4.3 Computational best-fit values of V_{max} and K_m obtained from Michaelis-Menten plot.

Best-fit values	
Vmax	0.01228
Km	3.9

Legend. Table displays computational best-fit V_{max} and K_m values of axis intercepts and slopes obtained by Michaelis-Menten plot of kinetic data calculated using absorbance rate of PPE against SlaaapN.

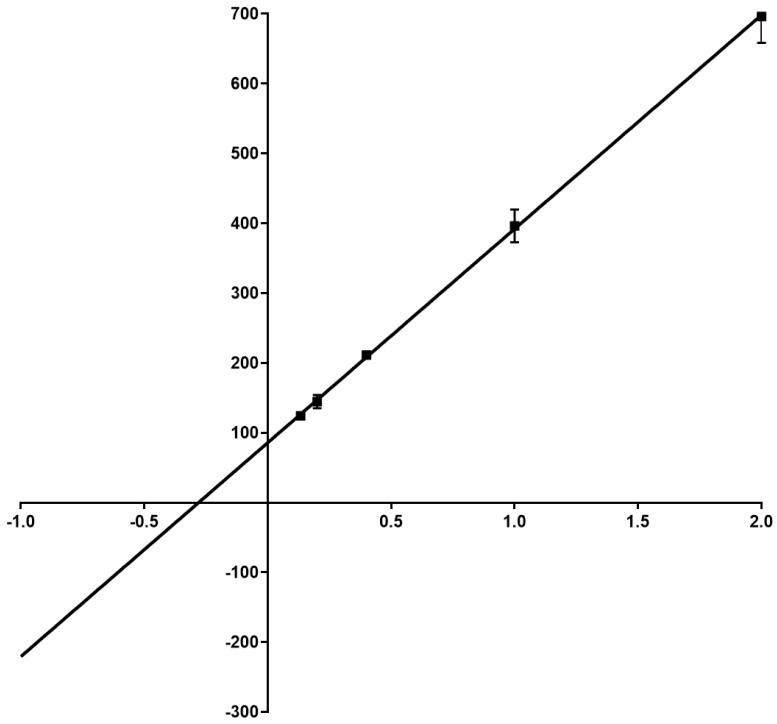

Figure 4.6. Lineweaver-Burk plot of PPE activity.

Plot of 1/[initial reaction velocity] (y-axis) against 1/[substrate concentration] (x-axis); n=3; line illustrates linear regression; error bars mean +/- SEM.

Table 4.4. Computational best-fit values of axis intercepts obtained from Lineweaver-Burk plot.

Best-fit values	
Y-intercept	85.86
X-intercept	-0.28

Legend. Table displays computational best-fit values of axis intercepts and slopes obtained by Lineweaver-Burk plot of kinetic data calculated using absorbance rate of PPE against SlaaapN.

Using these values and the known published value for catalytic efficiency (Nakajima *et al.*, 1979), the activity of PPE was determined.

$$V_{max} = K_{cat}[E]_T$$

$$K_{cat} = 37.0\ /s$$

$$V_{max} \div 37 = 3.148 \times 10^{-7}\ M$$

$$0.01\ mg/ml \times \frac{1\ ml}{25900\ Da} = 3.861 \times 10^{-7}\ M$$

$$\frac{3.148 \times 10^{-7}\ M}{3.861 \times 10^{-7}\ M} \times 100 = 81.5\%$$

4.3.1.2. *Assessment of PPE activity using PiMM plasma*

An alternative method was used to assess PPE activity by plotting the molar ratio of AAT determined by increasing volumes of plasma: a fixed amount of PPE determining remaining enzymatic activity (**Figure 4.7**). Extrapolation of the slope demonstrated that AAT inhibited PPE at a molar ratio of 1:1.223.

$$\frac{1}{1.223} \times 100 = 81.766\%$$

PPE activity using both methods was consistent and 81.7% was used in all subsequent experiments.

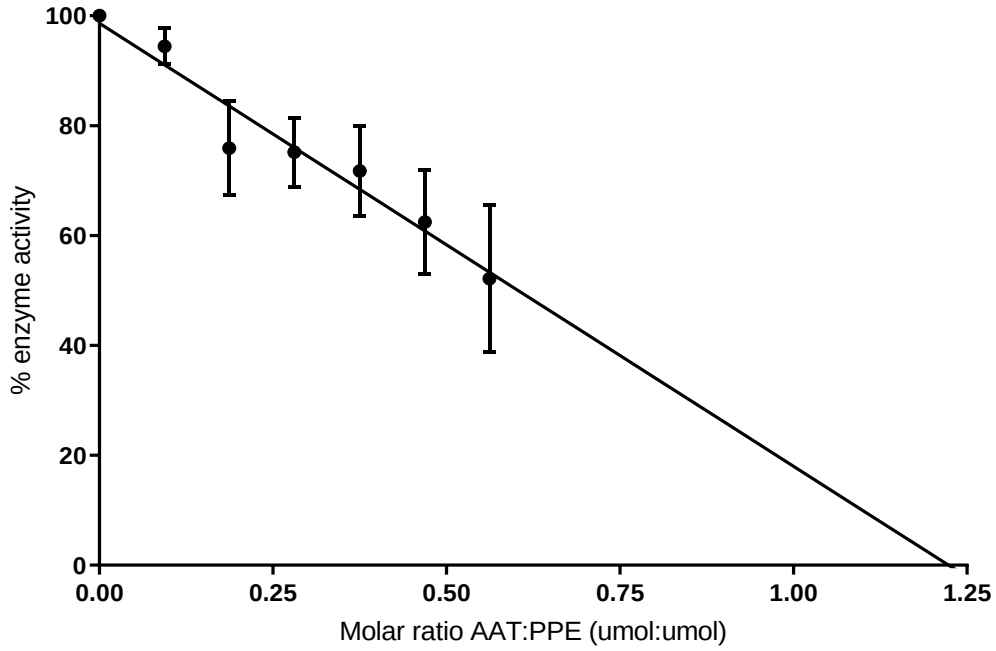

Figure 4.7. Assessment of PPE activity against PiMM plasma of known concentration.

Activity of PPE (y-axis) when in the presence of increasing concentrations of fresh, genetically-confirmed PiMM plasma; displayed as the molar ratio of AAT:PPE (x-axis); n=4; error bars mean +/-SEM; line of best fit calculated using simple linear regression.

Table 4.5. Computational best-fit values of axis intercepts and slope from assessment of PPE activity using PiMM plasma.

Best-fit values		
Slope	-80.63	(-102.3- -58.92)
Y-intercept	98.65	(91.31-106.0)
X-intercept	1.2	(1.019-1.576)

Legend. Table displays computational best-fit values of axis intercepts and slope, with 95% confidence intervals shown in parentheses, obtained by comparing AAT:PPE ratios against the calculated enzymatic activity of PPE against SlaaapN in the presence of AAT.

4.3.2. Alpha-1 Antitrypsin Inhibition of Proteinase Activity Kinetically

Functional activity of purified AAT was assessed kinetically by measuring SlaaapN cleavage by active PPE (as determined above), following incubation with AAT. Over time the amount of SlaaapN cleaved increased (**Figure 4.8**) and as the AAT:[active PPE] molar ratio increased, lower rates of substrate cleavage occurred.

Extrapolation of the AAT to PPE ratio to the x-axis intercept occurred with an AAT molar ratio to PPE occurred at 1.2:1 (**Figure 4.9** and **Table 4.6**). This should occur at 1:1 and indicated that the pure AAT was partly inactive and was therefore 67.8% functional. This value was used for subsequent experiments.

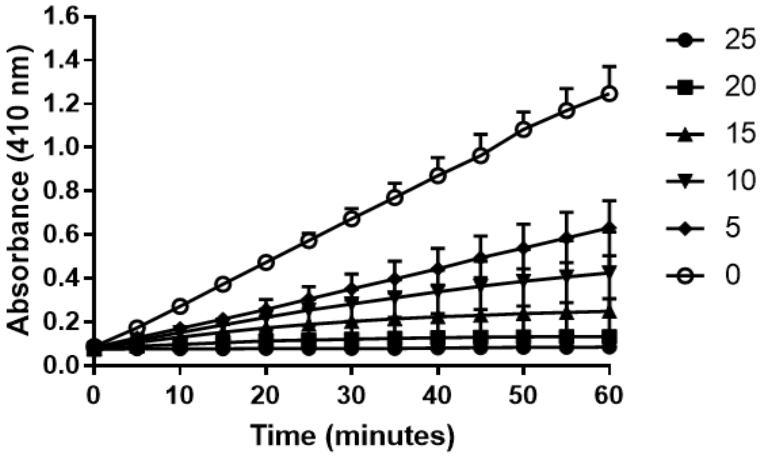

Figure 4.8 Inhibitory action of AAT on PPE.

Absorbance (410 nm) (y-axis) produced from PPE incubated with AAT and N-succinyl-Ala-Ala-Ala-p-nitroanilide substrate at increasing concentrations over 5-minute intervals up to 60 minutes (x-axis), n=3; error bars median +/- IQR.

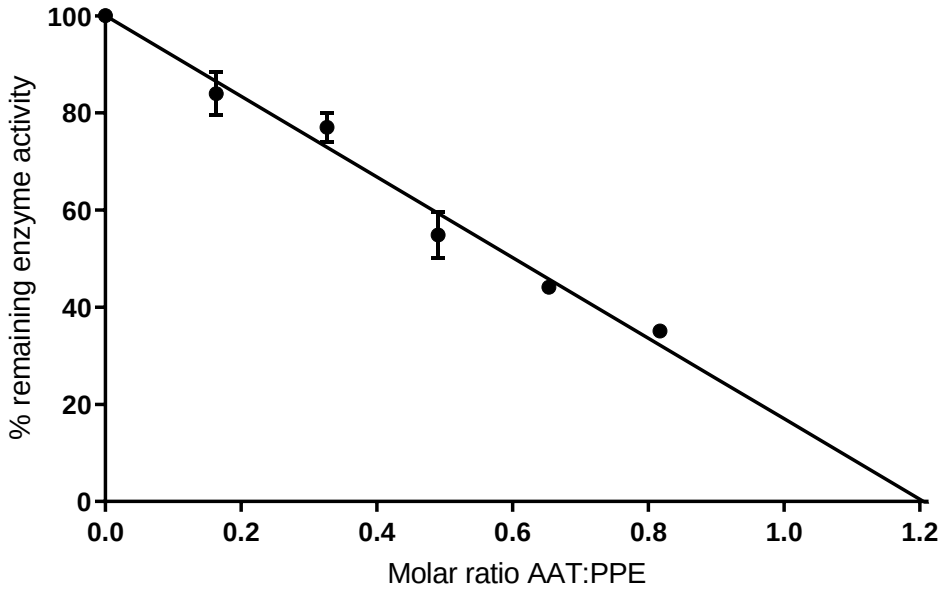

Figure 4.9 Assessment of AAT activity.

Graph shows the percentage of remaining PPE activity (y-axis) in the presence of increasing concentrations of AAT expressed as a molar ratio of pure AAT to active PPE, n=3; error bars +/- SD; line of best fit calculated using simple linear regression with the control at 100% and extrapolated to 0% PPE activity.

Table 4.6 Computational best-fit values of x-axis intercept and slope from assessment of AAT activity.

Best-fit values	
Slope	-82.97
X-intercept	1.2

Legend. Table displays computational best-fit values of x-axis intercept and the slope obtained using the average data from all 3 experiments.

4.3.3. Assessment of NE activity using AAT of known activity

Activity of NE was then assessed kinetically by measuring SlaaapN cleavage by NE when incubated with known active molar concentrations of AAT (**Figure 4.10**). Over time the amount of SlaaapN cleaved increased, but the rate decreased as the molar ratio of AAT increased.

Again, by extrapolation the line crossed the x-axis at a molar ratio of 0.99:1 indicating that the NE was fully active.

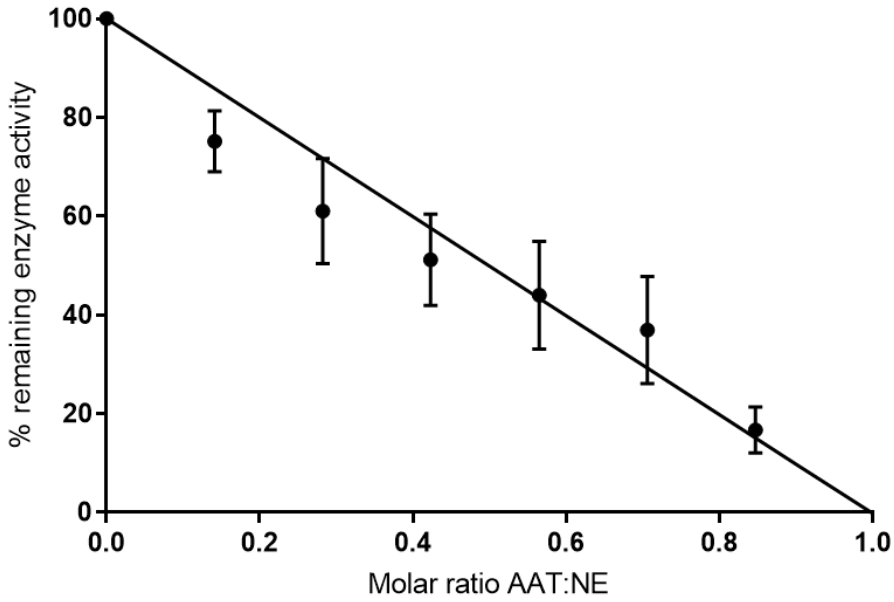

Figure 4.10 Assessment of NE activity.

Activity of NE (y-axis) when in the presence of AAT (x-axis); n=4; error bars mean +/- SEM; line of best fit calculated using simple linear regression.

Table 4.7 Computational best-fit values of x-axis intercept and slope from assessment of NE activity.

Best-fit values	
Slope	-100.3
X-intercept	0.99

Legend. Table displays computational best-fit values of x-axis intercept and the slope obtained using the average data from all 4 experiments.

4.3.4. SLPI Inhibition of Proteinase Activity Kinetically

Activity of purified SLPI was assessed kinetically by measuring SlaaapN cleavage by NE of a known activity, when incubated with increasing amount of SLPI.

Over time the amount of SlaaapN cleaved increased in the presence of NE. As SLPI:[active NE] molar ratio increased, lower rates of cleavage occurred (**Figure 4.11**).

Extrapolation of the rate of NE activity to the x intercept indicated that the pure SLPI inhibited NE at a molar ratio of 2.1:1, which is similar to kinetic data described in literature (Weldon *et al.*, 2009; Zabieglo *et al.*, 2015).

The results obtained here suggest that SLPI has an inhibitory activity of 47.6% against NE and this figure was used for subsequent studies.

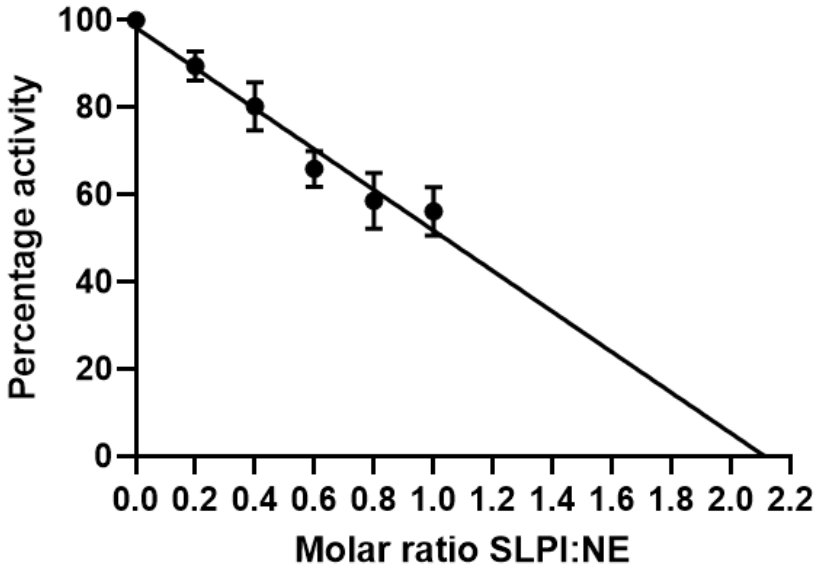

Figure 4.11. Assessment of SLPI activity.

Percentage remaining NE activity (y-axis) following incubation with increasing concentrations of SLPI shown as a ratio of SLPI to NE (x-axis), n=6; error bars +/- SEM; line of best fit calculated using simple linear regression and extrapolated to the x-intercept.

Table 4.8. Computational best-fit values of x-axis intercept and slope from assessment of SLPI activity.

Best-fit values	
Slope	-46.53
X-intercept	2.1

Legend. Table displays computational best-fit values of x-axis intercept and the slope obtained using the average data from all 6 experiments.

4.3.5. Alpha-1 Antitrypsin Inhibition of Proteinase Activity in an *in vitro* model

4.3.5.1. *Pre-treatment of neutrophils with active AAT*

Functional AAT was added in increasing concentrations to isolated neutrophils and incubated for 15 minutes at 37°C, before the addition of the substrate (fibrinogen, 550 nM) and the stimulus (fMLP, 10 µM) and incubation for a further 15-minutes (**Figure 4.12**). AAT concentrations were used to include different genotype plasma AAT concentrations as described by the American Thoracic and European Respiratory Societies, 2003: 0 µM represents the Pi ’*null’* genotype, 3-7 µM represents the PiZZ genotype, and 10-15 µM represents the Pi*SZ* genotype.

Proteinase activity footprint results generated are described as the concentration of Aα-Val^{360} or Aα-Val^{541} in nM.

The proteinase activity footprints generated decreased rapidly when incubated with AAT. PR3 activity fell to 78.5% (SEM +/- 13.6) with 3 µM AAT, before plateauing at 57.8% (+/- 4.7) with AAT concentrations above 10 µM. Similarly, NE activity fell to 70.6% (+/- 6.4) with 3 µM AAT, before plateauing at 44.5% (+/- 8.1) when AAT concentrations exceeded 10 µM.

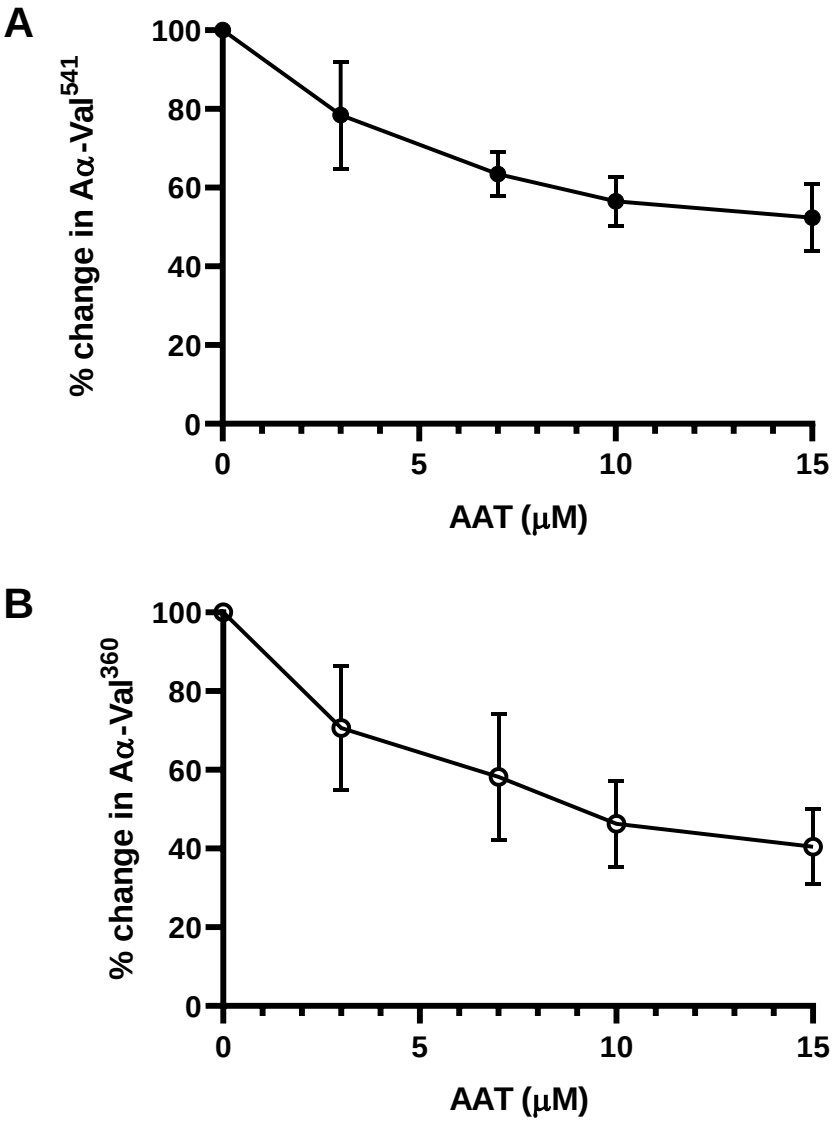

Figure 4.12. Incubation of neutrophils with AAT prior to stimulation and incubation with substrate reduces proteinase activity footprint.

Percentage change in generation of **A** PR3 and **B** NE footprints (y-axis) following prior incubation of isolated neutrophils ($2.5x10^6$/ml) with increasing concentrations of AAT (0-15 μM) (x-axis) for 15 minutes followed by stimulation with 10 μM fMLP in the presence of 550nM uncleaved fibrinogen 15 minutes; 0 μM set as 100% activity baseline; n=6; ●= PR3 activity footprint, o= NE activity footprint; error bars mean +/- SEM.

4.3.5.2. *Addition of AAT to neutrophils and fibrinogen with no pre-treatment*

To provide a model of pathogenesis, the pre-incubation stage was removed with AAT applied direct to the proteinase/anti-proteinase model rather than pre-incubating the AAT with neutrophils (as shown in **Figure 4.13**).

As concentration of the AAT increased, the proteinase footprints reduced for both PR3 and NE and plateaued around 10 µM. The change in activity footprint (baseline set at 0 µM as 100% active) indicated that the mean activity footprints reduced to 88.7% (+/- 36.3) for PR3 and 70.1% (+/- 9.0) for NE when exposed to 3 µM AAT, and to a plateau value of 38.3% (+/- 22.8) in the presence of 10 µM AAT. The median NE activity footprint also reduced by 42.0% (+/- 10.8) when exposed to 10 µM AAT.

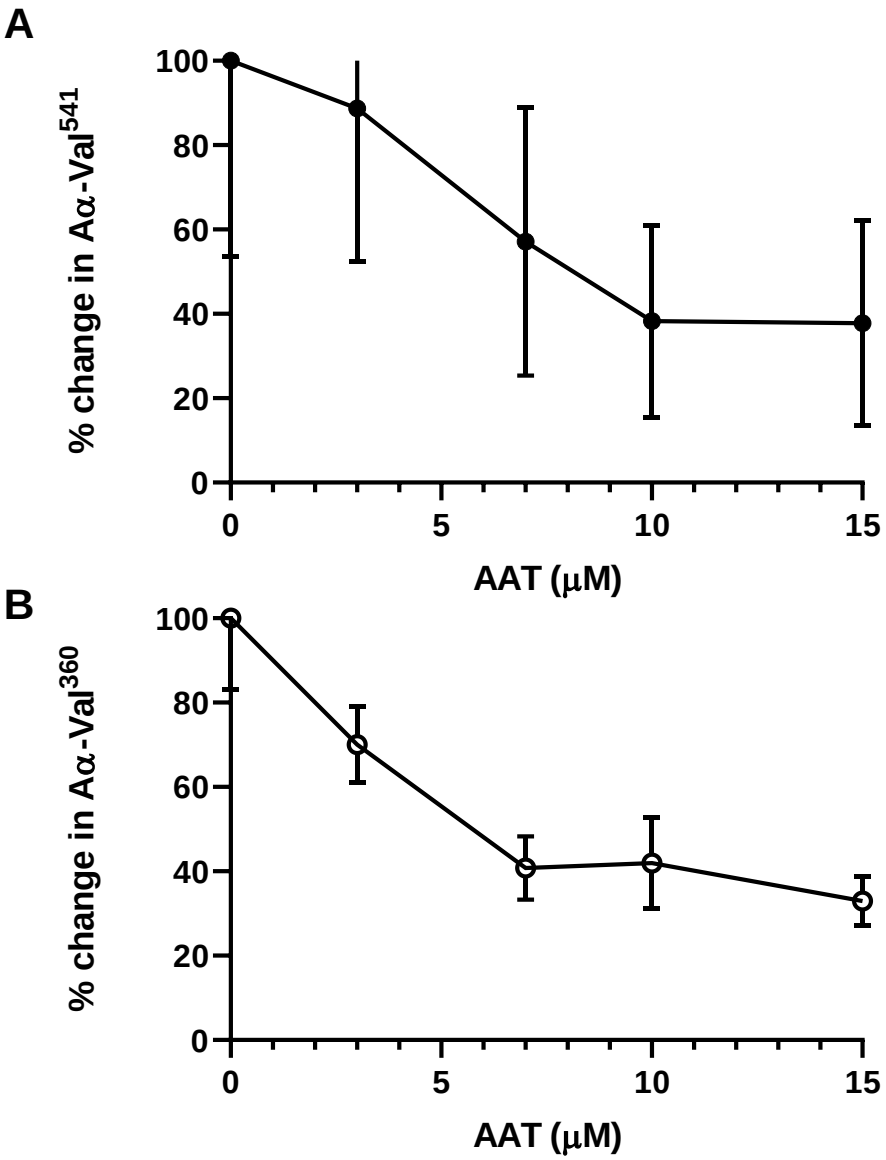

Figure 4.13. Incubation of neutrophils with AAT simultaneously to stimulation and incubation with substrate reduces proteinase activity footprint.

Percentage change in generation of **A** PR3 and **B** NE footprints (y-axis) following incubation of isolated neutrophils ($2.5x10^6$/ml) with increasing concentrations of AAT (0-15 μM) (x-axis) in the presence of 10 μM fMLP and 550nM uncleaved fibrinogen for 15 minutes; 0 μM set as 100% activity baseline; n=4; ●= PR3 activity footprint, o= NE activity footprint; error bars mean +/- SEM.

4.3.6. Effect of addition of SLPI into the model

Functional SLPI was added in increasing concentrations into the model, at the same time as the other reagents. Physiological lung concentrations were selected as described in the literature (van Wetering *et al.*, 2000; Sullivan *et al.*, 2008).

As the concentration of SLPI increased, the proteinase footprint generated by NE was reduced. The change in footprint (baseline set at 0 μM as 100%) indicated a decrease to 84.7% at 1.3 nM SLPI, then further to 74.8% at 2.56 nM and 58.2% at 3.85 nM.

As expected, there was no effect of SLPI on PR3 footprint.

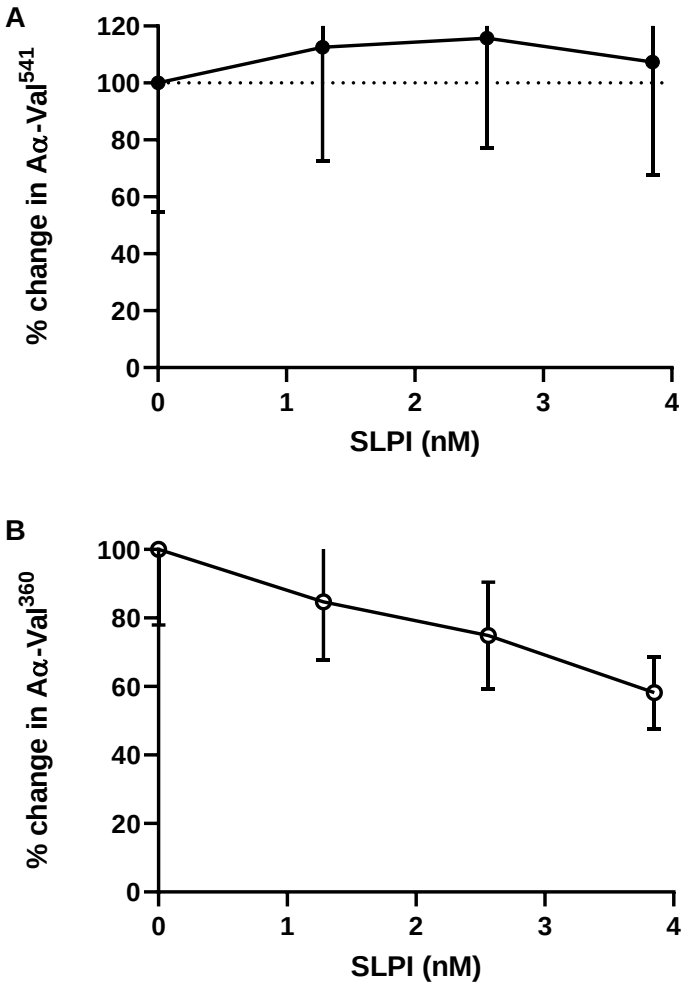

Figure 4.14. Incubation of neutrophils with SLPI prior to stimulation and incubation with substrate reduces NE activity footprint.

Percentage change in generation of **A** PR3 and **B** NE footprints (y-axis) following incubation of isolated neutrophils ($2.5x10^6$/ml) with increasing concentrations of SLPI (0-3.85 nM) (x-axis), 10 μM fMLP and 550 nM uncleaved fibrinogen for 15 minutes; with 0 nM set as 100% activity baseline; n=4; ●= PR3 activity footprint, o= NE activity footprint; error bars median +/- IQR.

4.3.7. Effect of normal and deficient plasma on footprint generation by healthy neutrophils.

Neutrophils from healthy young donors (henceforth called HY neutrophils) were incubated in a plasma pool with normal or deficient concentrations of AAT. The activity footprints generated by HY neutrophils incubated in AAT-deficient plasma were higher than when incubated in plasma from healthy donors or patients with COPD who had normal concentrations of AAT (**Figure 4.15**). As subject derived plasma already contains some of the footprint, the generation of footprint by HY neutrophils incubated in pooled plasma was determined as follows:

$$Activity\ footprint\ of\ HY\ neutrophils\ incubated\ in\ pooled\ plasma$$
$$-\ Activity\ footprint\ of\ baseline\ pooled\ plasma$$
$$= \boldsymbol{Change\ in\ footprint}$$

HY neutrophils incubated in healthy elderly plasma generated a median footprint increase for PR3 of 31.38 nM (IQR 22.6-37.7), and for NE of 4.3 nM (2.9-7.9). The change in footprint was similar by HY neutrophils in COPD plasma with footprint generation of 21.2 (12.3-26.7) for PR3 (p=0.7883) and 4.8 nM (3.4-5.6) for NE (p>0.99; Kruskal-Wallis test).

However, when incubated in AATD plasma, the activity footprint was significantly greater at 64.5 nM (59.2-70.2) for PR3 (versus healthy p=0.033; versus COPD p=0.001) and 8.3 nM (6.6-12.0) for NE (versus healthy p=0.038; versus COPD p=0.039).

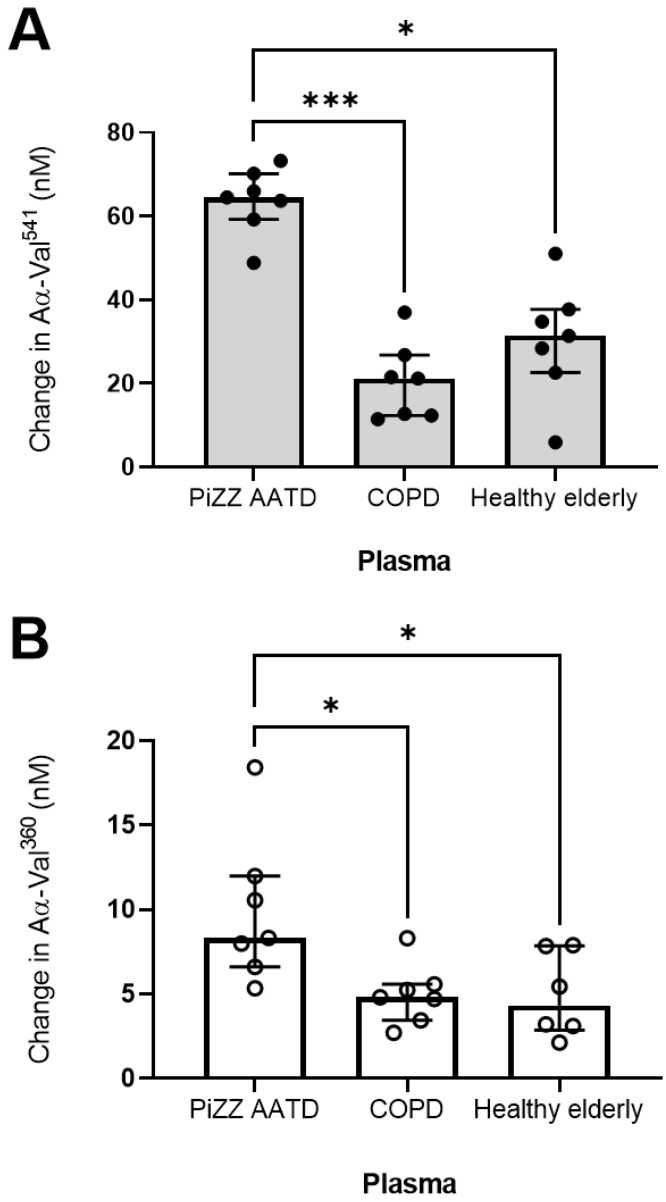

Figure 4.15. Proteinase footprint increases when neutrophils are incubated in AAT deficient plasma.

Median **A** PR3 and **B** NE footprints (y-axis) generated by neutrophils from healthy young subjects incubated in plasma from patients with non-deficient COPD (n=7) or AATD (n=7), or plasma from healthy elderly donors (n=6) (x-axis). ●= PR3 activity footprint, o= NE activity footprint; Error bars median +/- IQR; * = $p \leq 0.05$, *** = $p \leq 0.001$ determined by Kruskal-Wallis with multiple comparison.

4.4. Discussion

4.4.1. Determination of Enzyme kinetics

Biologically it is important to determine the kinetic activity of enzymes and inhibitors as accurately as possible. This is particularly true in determining any differences in experimental outcomes between inhibitors and footprint generation.

The cleavage of marker substrate over time was assessed using a baseline enzyme with known published kinetic markers. This is an accurate and well-validated method for the determination of enzymatic activity.

For this purpose, PPE was assessed over time with increasing concentrations of SlaaapN (Henri, 1902; Michaelis *et al.*, 1913).

The parabolic curve in the activity plot enables enzymatic behaviour to be defined by the Michaelis-Menten equation and hence, like previous kinetic studies, confirms that the reaction between PPE and the substrate was not cooperative or allosteric (Michaelis *et al.*, 1913; Berg *et al.*, 2002). Thus, an accurate assessment of the amount of active PPE in the purified protein was obtained. The calculated activity fits with what we know from the literature; during purification, enzyme manipulation results in loss of some activity, although activity should remain high.

The baseline enables us to assess the activity of purified AAT by enzyme inhibition curves as PPE and AAT interact on a 1:1 molar basis. The functional activity of the AATD preparation was then used to determine the activity of the NE protein using an

NE specific substrate (MSaapVN), again assuming a 1:1 molar inhibition. Subsequently, the active NE was also used to determine the SLPI activity.

AAT was added into the footprint model causing a dose-related decrease in NE and PR3 footprint generation.

The addition of SLPI was also able to decrease NE footprint generation, with no change to PR3 activity, as expected from its inhibitory profile (van Wetering *et al.*, 2000; Sullivan *et al.*, 2008).

4.4.2. Proteinase activity within the proteinase/anti-proteinase balance model as a biomarker of physiological inhibitor activity

AAT was used to replicate the proteinase environment that may occur *in vivo* on the footprint generation. As the AAT decreased, little change in the generation of the footprints occurred until the concentration fell below 10 µM, consistent with studies that suggest a treatment target of about 11 µM would largely protect local connective tissue from excess degradation in AATD (Brantly *et al.*, 1991; Campbell *et al.*, 2000a; Brantly *et al.*, 2018).

The data is also supported by studies in human plasma, it has been observed that levels of these footprints are increased in PiZZ AATD and relate to disease severity and augmentation therapy (Carter *et al.*, 2015; Newby *et al.*, 2019).

Pre-incubation of neutrophils with inhibitors (such as AAT) is considered more physiological. In the “pre-incubation model”, AAT was able to rapidly decrease proteinase activity. Furthermore, AAT added to neutrophils before their stimulation was

able to more effectively reduce proteinase activity (at a lower concentration) than when the AAT was added after neutrophil stimulation with fMLP.

In both experimental protocols the percentage change in proteinase footprint generation plateaued at the same AAT concentration and roughly the same percentage decrease compared to the control. This indicates that the relationship is non-linear, and some proteinase activity is protected from AAT.

SLPI was used as a further inhibitor to confirm this effect, as it should not influence PR3 footprint generation, but should influence NE footprint generation. The data confirmed that SLPI was effective at reducing NE, but not PR3 footprint generation which was consistent with its anti-proteinase characteristics.

When interpreting results from SLPI inhibition, the nature of its inhibitory action on proteinases must be taken into account. Unlike AAT, SLPI forms a reversible and unstable complex with NE which can be dissociated.

Of note, SLPI can form complexes with ECM bound NE, which may indicate that Aα-Val^{360} measurement is not representative of substrate cleavage or proteinase activity within the model (Morrison *et al.*, 1990).

It must be recognised that the action of SLPI is different in the lung to that of AAT, with SLPI being primarily located within the airway secretions. Therefore, although the effect of SLPI on proteinase activity footprints within the model can be used for validation, its effect within the model cannot be considered physiological or compared to that of AAT.

The proteinase/anti-proteinase model data, collected in this thesis, demonstrate that AAT suppresses the destructive actions of NE and PR3 which is highlighted in AATD.

4.4.3. Physiological concentrations of AAT in plasma determine proteinase footprint generation

Whilst this chapter has produced evidence that supports the impact of physiological concentrations of exogenous AAT on the activity of proteinases *in vitro*, the data presented also supports the effect of ambient AAT concentrations in plasma. It indicates that neutrophils obtained from healthy individuals can generate footprints when incubated in plasma and that this is enhanced when plasma from subjects with AATD is used. Again, the data is consistent with the effect of low AAT levels on the generation of specific enzyme footprints in the presence of activated neutrophils.

Despite the trends observed, this study cannot conclusively prove that concentration of AAT within the plasma results in the observed change in activity footprint. It could be argued that the presence of exogenous plasma and its molecular components may contribute towards cellular signalling cascades that indirectly alter the activity of proteinases.

4.4.4. Clinical relevance

This chapter supports the concept of an AAT “at-risk” threshold of 11 μM (Brantly *et al.*, 1991; Campbell *et al.*, 2000a; Brantly *et al.*, 2018). It presents evidence that supports the role of AAT in the inhibition of NSPs and demonstrates the importance of local AAT concentration on the subsequent generation of proteinase footprints.

It provides an *in vitro* model of the process in the presence of activated neutrophils and a susceptible substrate. The data provides evidence of a threshold below which neutrophilic activity is enhanced and a putative dose-ranging template for new compounds to be assessed for equivalence to AAT for therapeutic strategies.

4.5. Summary

This chapter describes the action of physiological NSP inhibitors on the proteinase/anti-proteinase balance model. Incubation with activated neutrophils provided a signal of substrate degradation typical of enzyme footprints detectable in plasma from healthy individuals and those with non-deficient COPD and AATD.

Initially, evaluation of the addition of AAT and SLPI provided evidence that the process of enzyme-specific degradation of fibrinogen can be both stimulated by cytokines and limited by the ambient concentration of inhibitors and their cognate enzyme targets. Furthermore, AAT was unable to completely abrogate the proteinase effect consistent with the high concentration of neutrophil related enzymes and the exponential effect was seen with decreasing AAT levels.

Of significance, the maximal inhibitory effect occurred around 10 μM consistent with other studies and the proteinase activity footprints generated are consistent with those seen in relevant patients.

Data also emphasised the role of circulating AAT concentration on proteinase activity footprint. Together, these data presented in this chapter support the clinical significance of the putative 11 μM threshold in AATD.

Finally, this chapter indicates that the model, alongside the in-house assays, can work accurately to indicate changes in proteinase activity following the addition of inhibitors and suggest the potential for the activity footprints to be used for *in vitro* test dose ranging of therapeutics.

CHAPTER 5: APPLICATION OF ALVELESTAT TO THE NEUTROPHIL/FIBRINOGEN-BUFFER MODEL

5.1. Brief Introduction

5.1.1. Background

AAT levels in healthy human tissues are usually at a concentration that facilitates an effective proteolytic response to immune challenges whilst enabling inhibition of excessive destructive proteinases such as PR3 and NE (Greene *et al.*, 2009; von Nussbaum *et al.*, 2015). The balance between proteinases and anti-proteinases was described in **1.1.1.7. Proteinase/anti-proteinase balance theory,** and in this thesis has been referred to as the proteinase/anti-proteinase balance.

In the tissues of patients with AATD, the concentration of the major anti-proteinase AAT is significantly reduced and, as other physiological proteinase inhibitors may not sufficiently block proteinase action at the site of airway tissue damage, excessive proteinase activity occurs (Stockley, 1999; Sinden *et al.*, 2013; Sinden *et al.*, 2015).

In many countries, healthcare systems approve exogenous AAT to augment endogenous AAT through intravenous therapy. The only therapeutic agent that has been shown statistically to provide a benefit in a placebo-controlled clinical trial is Respreeza (CSL Behring), which was not approved for use in the UK in 2018 by the National Institute for Health and Care Excellence (NICE), due to concerns about cost-effectiveness and limited evidence of clinical benefit in patients (National Institute for Health and Care Excellence, 2018).

Outside this clinical trial, meta-analyses of clinical observational data have suggested that AAT augmentation is associated with a reduction in the decline of lung function

(Chapman *et al.*, 2009; Edgar *et al.*, 2017). Currently, there is no evidence demonstrating patient response to augmentation in early disease. However, this reflects clinical trial design, which focuses on those with established impairment of lung function (Dirksen *et al.*, 2009; McElvaney *et al.*, 2017), where observational studies indicated a likely beneficial effect on FEV_1 decline was seen for those with an FEV_1 between 30-65% predicted (Alpha-1 Antitrypsin Deficiency Registry Study Group, 1994).

Current studies are limited by the sensitivity of outcome measures and patient recruitment issues for this 'rare' genetic disease. The use of imaging (lung densitometry) is by far the most sensitive to change, whereas lung function (specifically FEV_1), the frequency and severity of exacerbations, exercise capacity and health status are relatively insensitive. Studies designed to demonstrate clinically meaningful differences in these outcome measures, therefore require large patient numbers and long periods of observations, and this precludes their use in rare diseases such as AATD (Herpel *et al.*, 2006; Glaab *et al.*, 2010; Wielpütz *et al.*, 2014) although patient selection for the outcome of interest may reduce the numbers to manageable levels (Stockley *et al.*, 2018). Trials concentrating on lung density as a measure of the dominant clinical feature (emphysema) have provided statistical evidence, or at least a trend towards augmentation benefit, remaining concordant with controlled trials and being argued as the most specific measure of emphysema and its severity (Dirksen *et al.*, 2009; Parr *et al.*, 2009; Stockley *et al.*, 2010; Quinn *et al.*, 2020).

Augmentation therapy requires weekly infusions of plasma purified AAT and is not only expensive but also has a significant impact on health care delivery and patient acceptance (Stockley *et al.*, 2013c; Teschler, 2015). Alternative anti-proteinase

strategies might prove more acceptable, especially if the administration was not intravenous and more cost-effective. Orally available proteinase inhibitors might be an alternative to re-establish a proteinase/anti-proteinase balance.

The development of an *in vitro* cellular model of the putative proteinase/anti-proteinase balance in AATD was introduced in **Chapter 3,** and the effect of physiological concentrations of AAT on this model was further explored in **Chapter 4.**

The current chapter describes the effect of adding a novel Mereo Biopharma NE inhibitor AZD9668 into the stimulated neutrophil-fibrinogen buffer model to assess changes in proteinase activity by monitoring the release of proteinase specific footprints of the process as a predictor of potential therapeutic efficacy.

5.1.2. Alvelestat

The Mereo Biopharma compound Alvelestat (International non-proprietary name; also known as MPH966 and AZD9668; henceforth referred to as AZD9668) has been shown by pharmacokinetic analysis to be a potent, yet fully reversible 3rd generation small-molecule inhibitor of NE (Stevens *et al.*, 2011; von Nussbaum *et al.*, 2015).

AZD9668 has an N-([5-(methanesulfonyl)pyridine-2-yl]methyl)-6-methyl-5-(1-methyl-1H-pyrazol-5-yl)-2-oxo-1-[3-(trifluoromethyl)phenyl]-1,2-dihydropyridine-3-carboxamide structure (Stevens *et al.*, 2011). Analysis of congeners suggests that the possession of an *m*-(trifluoromethyl)phenyl binding motif alongside the pyridone scaffold enables inhibition of NE through binding in the S1 pocket inducing a conformational change which alters the S2 pocket structure (von Nussbaum *et al.*,

2015). Importantly, this structure allows the drug to be orally bioavailable, selective and provides a high binding affinity to NE (Stevens *et al.*, 2011; von Nussbaum *et al.*, 2015).

The exact mechanism of NE inhibition by AZD9668 *in vivo* or in a physiological model remains unpublished, however *in vitro* and whole blood studies have demonstrated that the compound can interact with both surface-bound and free NE (Stevens *et al.*, 2011). Binding with surface-bound NE potentially increases the compounds range of activity making it more potent than other physiological inhibitors, such as AAT which is relatively ineffective against membrane-bound NE (Korkmaz *et al.*, 2005). Despite having a similar association rate constant to AAT, AZD9668 is shown to be active at 10x lower concentrations in a cell-based assay, suggesting that it may have both extra benefit and the potential ability to work in synergy with AAT (Stevens *et al.*, 2011). In addition, pharmacokinetic data suggest that AZD9668 is less reactive to targets and less cytotoxic than Sivelestat, a similar NE inhibitor that has been investigated for use in ARDS (Stevens *et al.*, 2011).

In rodent models, AZD9668 reduced systemic inflammation following tobacco smoke exposure and prevented NE-induced damage (Stevens *et al.*, 2011). Similarly, data from a phase I study with healthy volunteers and a phase IIa study with patients with COPD (GOLD stage II and III, defined by 2013 guidelines) indicated that *ex vivo* zymosan-stimulated NE activity by neutrophils was reduced following oral treatment with the compound (Gunawardena *et al.*, 2013). Clinical markers of disease were reduced following treatment with the compound in a phase II study of patients with bronchiectasis, including a small but significant increase in FEV_1 (Stockley *et al.*, 2013a). However, lung function and NE activity were not altered in a study of

bronchiectasis patients with CF, although non-specific inflammatory biomarkers were reduced suggesting an anti-inflammatory benefit (Elborn *et al.*, 2012).

Analysis of inhibitory studies *in vitro* has suggested the inhibitor has a limited effect on other NSPs, including PR3 (Stevens *et al.*, 2011). No published research has assessed the role of the compound on other proteinase activity in a neutrophil-associated *in vitro* model of proteinase/anti-proteinase balance.

5.1.3. Hypotheses and Aims

It was hypothesised that the addition of experimental-phase pharmaceutical compounds, with known biochemical action, into the validated *in vitro* model of uninhibited proteinase activity (as described in **Chapter 3**) would provide relevant data on the effect of the drug on proteinase activity *in vitro* in a dose-dependent manner. This would provide supporting evidence of benefit before progressing to appropriate phase III clinical studies in patients with AATD.

The primary purpose of the model was to understand this potential interaction and provide evidence that proteinase footprints generated by neutrophils could be understood and used as biomarkers for early readout of a measurable effect *in vivo*, and hence putative clinical efficacy.

Secondly, this chapter was designed to assess the cellular response to the compound compared to and in addition to AAT at levels consistent with AATD and those generated by augmentation therapy.

5.2. Specific Methodology

5.2.1. Enzyme kinetics

Assessment of the biological activity of the enzymes and inhibitors was performed as described in **Chapter 4.** These activities were used for all subsequent experiments.

5.2.1.1. *Activity of AZD9668*

AZD9668 (Mereo Biopharma, US) has been shown to have functional activity *in vitro* at whole blood concentrations of 50 nM and 1 μM (Hopkins, 2008; Stevens *et al.*, 2011).

Having confirmed the NE activity (described in **Chapter 4**), the inhibitory function of AZD9668 (AstraZeneca) (dissolved in dimethyl sulfoxide (DMSO; Sigma-Aldrich, US); Mereo Biopharma, UK) was determined for all subsequent experiments as follows:

Increasing amounts of NE buffer was added to wells in a flat-bottomed polystyrene 96 well plate, starting from 57.5 μl to 100 μl, in duplicate wells.

AZD9668 was diluted to 1 mM in DMSO and added to the above wells to give final concentrations of 10 nM, 50, nM, 100 nM, 250 nM as well as a blank control. Then 10 μl of active NE (339 nM) was added to each well and the plate was incubated at 37°C with gentle shaking for 20 minutes.

N-methoxysuccinyl-ala-ala-pro-Val p-nitroanilide (MSaaapVN; Sigma-Aldrich) was prepared to 1 mg/ml in NE substrate buffer and 100 μl was added to each well. Control

wells lacking substrate were prepared, and the volumes made up to 210 µl with NE buffer.

The plate was shaken for 8 seconds and read every 5 minutes for 1 hour by a spectrophotometer (410 nm).

Molar ratio of AZD9668 to NE was plotted against the percentage of remaining enzyme activity and the x-axis intercept was determined by linear regression using GraphPad Prism software and used to determine AZD9668 functional activity. This value was used for all subsequent experiments.

$$\frac{known\ NE\ activity}{x\ axis\ intercept} = AZD9668\ activity$$

The molar ratio x-intercept was 0.87:1, indicating by extrapolation that 0.87 mole of AZD9668 is required to inhibit 1 mole of NE. Therefore, inhibitory activity was determined to be full within experimental error.

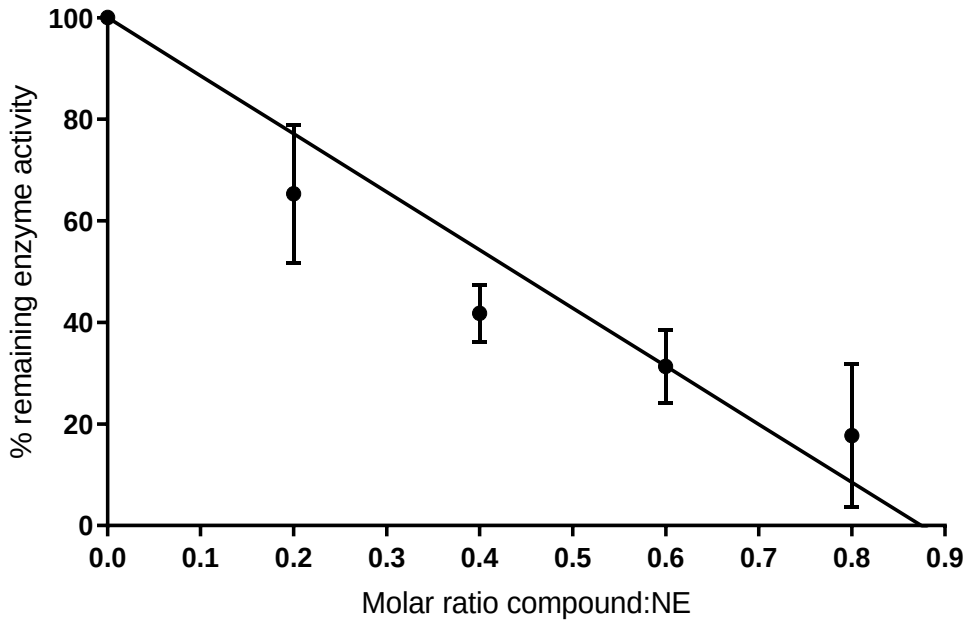

Figure 5.1. Assessment of AZD9668 activity.

Graph shows the activity of increasing concentrations of AZD9668 when in the presence of NE; n=4; error bars mean +/- SEM; line of best fit calculated using simple linear regression; normality determined using Shapiro-Wilk test.

Table 5.1. Computational best-fit values of x-axis intercept and slope from assessment of AZD9668 activity.

Best-fit values	
Slope	-114.4
X-intercept	0.8742

Table. Best-fit values of x-axis intercept and slope obtained by comparing AZD9668:NE ratios against the observed enzymatic activity of NE determined by SlaaapN cleavage in the presence of AZD9668.

5.2.2. Neutrophil treatment with pharmaceutical proteinase inhibitors

Isolated neutrophils obtained from healthy volunteers were incubated for 15 minutes at 37°C with 550 nM fibrinogen (Calbiochem, San Diego, CA, US), 10 μM fMLP (Sigma-Aldrich, St. Louis, MO, US), and simultaneously with increasing concentrations of functional AZD9668 (Mereo Biopharma) 0-700 nM and/or AAT 0-11 μM (Athens Research and Technology, Athens, GA, US) in RPMI (with L-glutamine and sodium bicarbonate) supplemented with Penicillin-streptomycin (1% v/v). See **Figure 5.2** for an experimental flow diagram.

Concentrations of AZD9668 were determined by titrating from active doses and measured plasma concentrations reported from clinical trials as well as previous *in vitro* studies (Hopkins, 2008; Stevens *et al.*, 2011; Elborn *et al.*, 2012; Gunawardena *et al.*, 2013; Stockley *et al.*, 2013a).

The supernatant was obtained through centrifugation at 300 *xg* for 5 minutes and NE and PR3 footprints were measured.

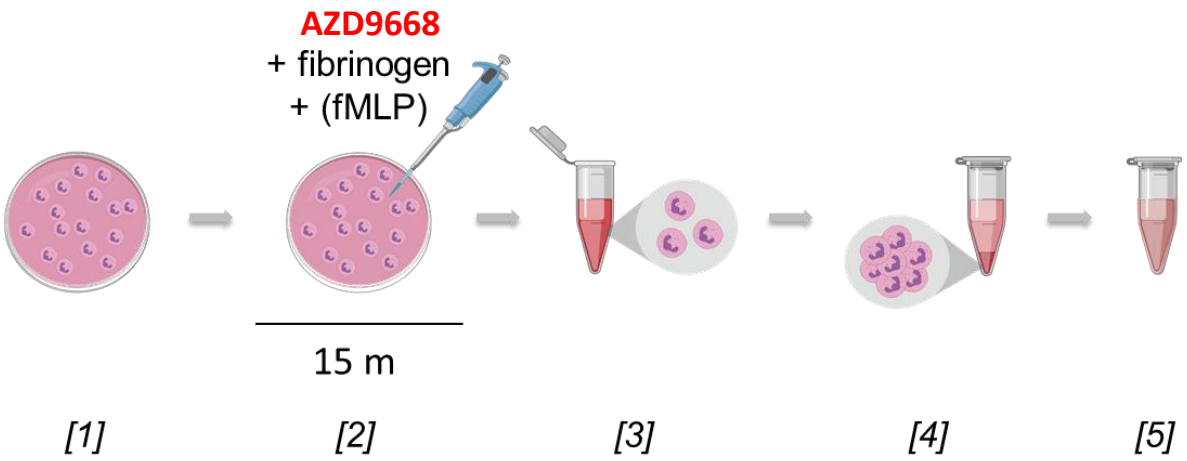

Figure 5.2. Visualisation of the model protocol.

Legend. [1] Isolated neutrophils were plated at $2.5x10^6$ cells/ml; [2] Substrate (fibrinogen) and stimulus (fMLP) was added at the beginning of a 15-minute incubation period; [3] treated cells were removed from the plate and spun down; [4-5] supernatant was transferred into a fresh Eppendorf and the cells disposed of. Red text indicates the point of AZD9668/AAT addition to plated neutrophils alongside the addition of substrate and stimulus. Figure produced using Biorender.com.

5.3. Results

5.3.1. The Generation of Proteinase Footprints by Increasing Concentrations of AZD9668

AZD9668 was added into the stimulated fibrinogen model, with neutrophils from HY controls, doses reflecting therapeutically relevant concentrations previously reported in the literature (10 nM to 700 nM). Each experiment took variable cell preparation into account by expressing control enzymatic generation as 100%. The effect of AZD9668 was determined for both PR3 and NE generated footprints and results were reported as percentage reduction (+/- SEM) in Aα-Val^{360} or Aα-Val^{541} generation compared to control.

Data showed that when 10 nM of the compound was added into the model, footprint generation decreased to 62.4% (+/- 10.8%) for NE footprint and continued to decrease at greater concentrations of AZD9668 until the NE activity footprint plateaued at 32.9% (+/- 11.4%) of the control at the pharmaceutical concentration of 300 nM.

However, the compound had little effect on PR3 footprint generation and remained between 92.0% (+/-16.5%) and 128.0% (+/-18.9%) of the control across all doses.

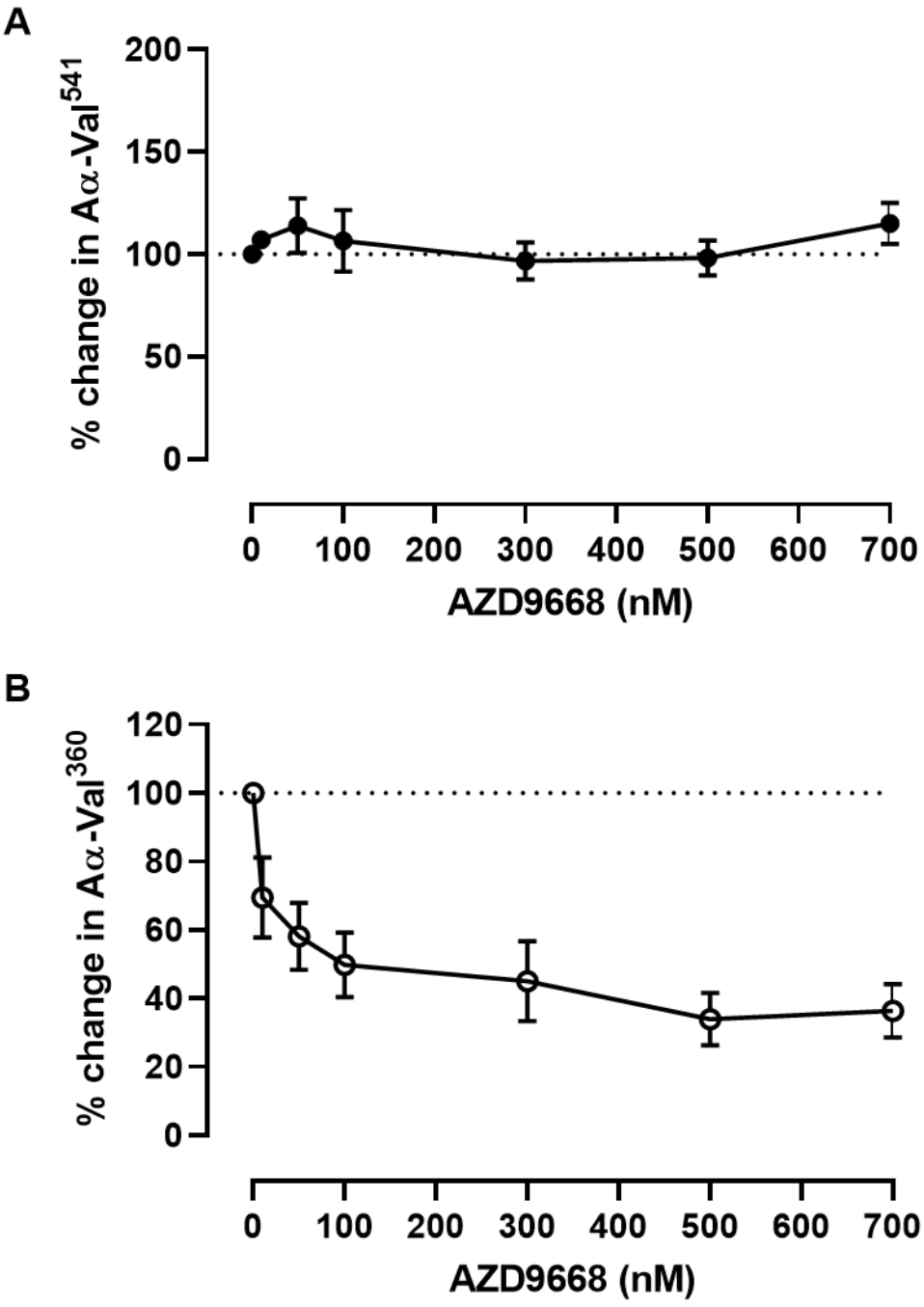

Figure 5.3. Inhibitory effect of AZD9668 on proteinase activity footprint.

Proteinase footprint expressed as % of the control (set at 100%, y-axis) produced by fMLP-stimulated neutrophils in the presence of increasing concentrations (10 nM-700 nM) of AZD9668 (x-axis); Percentage change in **A** PR3 footprint and **B** NE footprint; n=7. Dotted line at 100%; ●= PR3 activity footprint, o= NE activity footprint; error bars mean +/- SEM.

5.3.2. Effect of AZD9668 on proteinase activity with increasing AAT concentrations

Patients who are considered for this therapy and AAT augmentation have deficient concentrations of AAT within their blood. To address this scenario, pathophysiological concentrations of AAT were introduced to fMLP-stimulated neutrophils in fibrinogen-buffer to mimic patient levels as described in **1.4.2. Alpha-1 Antitrypsin Deficiency.**

Selected AAT concentrations used were 0 μM to represent a Pi 'null' genotype, 2.6-6.5 μM to represent a PiZZ genotype, and 10.4-14.3 μM to represent a PiSZ genotype (American Thoracic Society/European Respiratory Society, 2003). The concentration for AZD9668 (300 nM) was used to represent therapeutic levels confirmed in clinical trials. When cells were treated AZD9668, in conjunction with these concentrations of AAT a further decrease in NE and PR3 activity footprints were observed.

From an uninhibited control as baseline (100% active), the addition of AZD9668 to a sample with 5 μM AAT compared to inhibition with 5 μM AAT alone reduced the PR3 activity footprint by 37.5%, from 52.9% (SEM +/- 9.0) to 15.4% (+/- 9.5) ($p=0.067$; Mann-Whitney test), and the NE activity footprint by 52.6%, from 55.8% (+/- 9.3) to 3.2% (+/- 0.7) ($p=0.009$) (**Figure 5.4**).

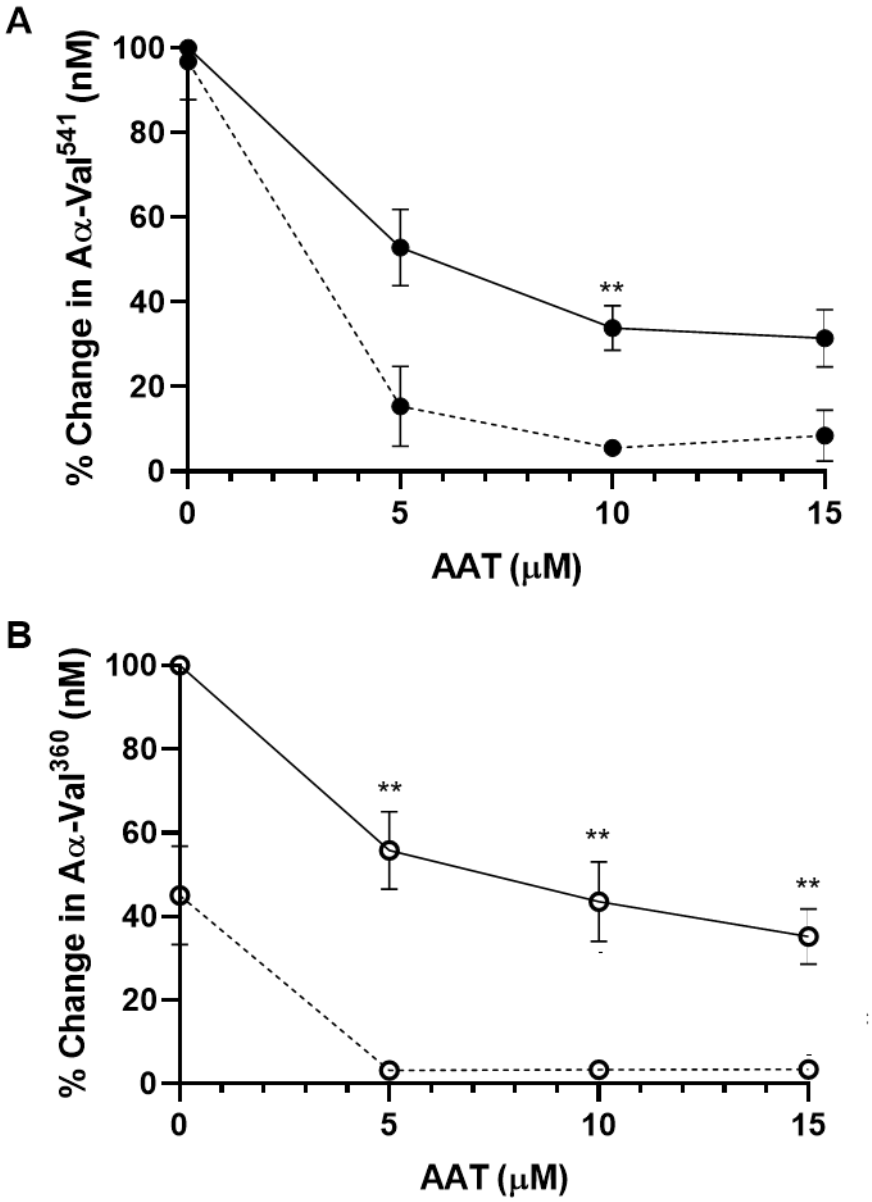

Figure 5.4. Comparison of proteinase activity footprint following application of AAT with and without AZD9668.

Percentage change in **A** PR3 and **B** NE activity footprint (y-axis) from fMLP-stimulated neutrophils ($2.5x10^6$/ml) in a fibrinogen buffer (550 nM) inhibited with AAT (x-axis) at 5, 10 or 15 μM (with solid line), compared to fMLP-stimulated neutrophils in a fibrinogen buffer with AZD9668 (300 nM) and AAT at 5, 10 or 15 μM (with dotted line). ●= PR3 activity footprint, o= NE activity footprint. Error bars mean +/- SEM. ** = $p \leq 0.01$ determined by Kruskal-Wallis test.

With 10 μM AAT, the PR3 activity footprint reduced by 28.3%, from 33.9% (+/- 5.3) to 5.6% (+/- 1.7) (p=0.009; Mann-Whitney test), and the NE activity footprint reduced by 40.1%, from 43.5% (+/- 9.5) to 3.4% (+/- 0.8) (p=0.009), whilst with 10 μM AAT, the PR3 activity footprint reduced by 23.0%, from 31.5% (+/- 6.7) to 8.5% (+/- 6.0) (p=0.067), and the NE activity footprint reduced by 31.8%, from 35.2% (+/- 6.6) to 3.4% (+/- 0.6) (p=0.009).

5.4. Discussion

5.4.1. The effect of AZD9668 on proteinase footprints generated by neutrophils in the absence and presence of AAT

The literature describes AZD9668 as a potent inhibitor of NE *in vitro* (Stevens *et al.*, 2011; Gunawardena *et al.*, 2013) and this is confirmed in this chapter using both inhibition of pure NE and inhibition of the proteinase footprint generation in the current cell model.

Alone AZD9668 reduced the generation of the NE footprint, and at a lower molar concentration than observed for AAT. This would imply that the compound inhibits NE which is not freely accessible to the larger AAT molecule indicating perhaps a fibrinogen bound component, cell membrane-bound or intracellular effect.

However, there is limited published data that describes the molecular/cellular interactions of AZD9668. Therefore, to fully understand the data with this compound the full mechanisms of its action should be explored.

As expected from kinetic analysis, the compound was unable to inhibit PR3 footprint generation. It has been hypothesised based upon association rate constants that there is a preferential binding of NE with AAT compared to PR3 (Sinden *et al.*, 2015). If the compound inhibited NE activity in its own right, it may preserve more AAT function making a proportion available to inhibit PR3 activity.

To test this concept, AZD9668 (300 nM) was given alongside pathophysiological concentrations (0, 5, 10 and 15 μM) of AAT, to determine whether there is such an effect reducing both PR3 and NE footprint generation.

5.4.2. Synergy between physiological and pharmaceutical proteinase inhibitors to normalise proteinase activity in the model

The addition of average pathophysiological concentrations of AAT and therapeutic concentrations of AZD9668 into the model produced greater inhibition of the proteolytic footprint generation by both NE and PR3 consistent with an additive effect on NE footprint generation and a sparing effect on AAT/NE interaction leading to a potential increasing effect on PR3.

Patients with PiZZ AATD generally have plasma AAT concentrations below the putative protective threshold of 11 μM, however other intermediate phenotypes, such as PiSZ, may also have plasma AAT concentrations below this threshold (Turino *et al.*, 1996; Franciosi *et al.*, 2020; Franciosi *et al.*, 2021).

In human plasma studies, higher levels of the proteinase activity footprints (NE and PR3) are associated with the ZZ genotypes which is consistent with this concept (Carter *et al.*, 2015; Newby *et al.*, 2019) and the footprints reflect disease severity (Carter *et al.*, 2015; Newby *et al.*, 2019). The latter study also described that the patients with the SZ genotype had a PR3 to NE footprint ratio that was significantly different to the non-deficient (MM genotype) footprint, suggesting that those with an SZ genotype may also have a risk of excessive proteinase activity.

In the current thesis, increasing the AAT level *in vitro*, led to a dose-dependent reduction in the generation of the NE footprint by neutrophils which plateaued at a level below the lowest point achieved by augmentation therapy. *In vivo* increasing the AAT dose given to patients as part of their augmentation therapy has been shown to reduce the NE footprint further (Campos *et al.*, 2005). Although the effect on PR3 activity footprint has yet to be studied.

Within the current model, AZD9668 would likely decrease the generation of the NE footprint by a direct effect, although the activity footprint was still not abrogated as seen in clinical studies with AAT augmentation (Carter *et al.*, 2011; Schouten *et al.*, 2021). The addition of AZD9668 has the potential of also reducing the NE footprint activity as well as assisting the ambient AAT to limit PR3 footprint activity. Investigating into whether a similar effect could be observed following augmentation therapy would be worthy of further study.

5.4.3. Clinical relevance

The data presented within this chapter suggests that AZD9668 may act as an effective inhibitor of excessive proteinase activity, together with AAT data suggest that the inhibitor is effective at the low concentrations seen in pharmacokinetic studies. The evidence supports its further exploration in phase III trials in AATD alone or in combination with AAT augmentation therapy.

5.5. Summary

This chapter demonstrates how this model can be utilised effectively to explore the proteinase/anti-proteinase balance in AATD and as a dose-ranging screening tool for new pharmaceutical therapies.

Specifically, this chapter assesses the effect of AZD9668 on proteinase activity as marked by a cleavage-product footprint. The data supports a role for AZD9668, as a potent inhibitor of NE activity, normalising key components driving the development and progression of AATD-associated disease.

CHAPTER 6: ADAPTION OF THE PROTEINASE/ANTI-PROTEINASE MODEL INTO WHOLE BLOOD

6.1. Brief Introduction

Data presented throughout this thesis provides evidence that the proteinase/anti-proteinase cell model could be used with proteinase footprint assays to assess both physiological and pharmaceutical proteinase inhibitor function relevant to AATD. As expected, both physiological and pharmaceutical proteinase inhibitors were able to reduce the proteinase activity footprints.

Whilst there is extensive evidence that neutrophils are involved in AATD pathophysiology, there are many other immune cells and blood components that are thought to be directly or indirectly involved in disease pathophysiology, including monocytes, eosinophils and platelets. These cells facilitate neutrophil recruitment, influence inflammatory feedback loops and release endogenous AAT. Studying neutrophils in isolation may not capture the complexities of AATD cellular interactions, and the potential impact of augmentation or other therapeutic strategies.

6.1.1. Monocytes and macrophages

Monocytes are large leukocytes with the potential to differentiate into macrophages and dendritic cells.

Monocytes secrete small amounts of AAT, and transcription of AAT mRNA has been shown to increase when NE is present (Perlmutter *et al.*, 1988). In patients with a ZZ genotype of AAT, AAT aggregates can form within monocytes which, in turn, can

upregulate pro-inflammatory mediators and activate inflammatory cascades (Carroll *et al.*, 2010).

Pulmonary macrophages isolated from the airways also produce AAT, with a 3X greater expression of AAT mRNA than monocytes (van 't Wout *et al.*, 2012). As with monocytes, in patients with AATD, secretion of AAT is impaired in macrophages and AAT aggregates form within the cell (Bazzan *et al.*, 2018). Further, the macrophages of deficient patients have been shown to have reduced ability to undertake both efferocytosis (Lee *et al.*, 2020) and phagocytosis (Belchamber *et al.*, 2021) which can induce a greater localised inflammatory environment but can be corrected *in vivo* with AAT augmentation therapy (Serban *et al.*, 2017).

6.1.2. Granulocytes

There remains limited evidence as to the role of non-neutrophil granulocytes in the pathophysiology of AATD.

A study by Low *et al.* reported that approximately 60% of patients with SZ and ZZ AATD genotype presented with intermittent or persistent blood eosinophilia (Low *et al.*, 2018). Moreover, eosinophils have been demonstrated to release preformed AAT from their granules (Johansson *et al.*, 2001). It is theorised that eosinophils may contribute towards an anti-proteinase environment, and hence increased inhibition of PR3 and NE. It has been suggested that the eosinophilia seen in some patients with AATD reflects a response to activated neutrophils (Nagata *et al.*, 2020).

6.1.3. Platelets

Platelets can instigate the release of mediators which promote neutrophil recruitment in lung disease (Hwaiz *et al.*, 2015). A recent study by Lacey *et al.* (2020) reported increased interactions between neutrophils and platelets in individuals with ZZ AATD compared to healthy MM controls, with more circulating aggregates and a higher proportion of platelet activation markers (Lacey *et al.*, 2020). The authors also reported that these defects were restored to normal following AAT augmentation therapy (60 mg/kg) which they proposed were a result of re-establishing homeostasis.

6.1.4. Proposal of a Whole Blood Model

The isolated neutrophil model removes any potential influence of these other cells into the inflammatory model and hence may limit its interpretation and the effect of any potential modifiers.

Furthermore, neutrophil isolation involves both physical and chemical manipulation which can result in their activation. Although the adapted Jepsen-Skottun method utilised within this project has been demonstrated to produce no/little activation when performed correctly. The sensitivity of neutrophils to external influences when studied *ex vivo* has been well documented by others (Thomas *et al.*, 2015b; Quach *et al.*, 2017).

A more physiological model using whole blood might overcome some of these issues.

6.1.5. Hypotheses and aims

It was hypothesised that the addition of inhibitors to stimulated whole blood and measuring the proteinase footprints would provide a more physiological model of the proteinase/anti-proteinase balance than the use of isolated neutrophils alone.

This chapter aimed to establish whether whole blood could be used to determine whether therapeutics impact footprint generation in a different way to that seen with isolated neutrophils.

6.2. Specific Methodology

6.2.1. Determining parameters for cellular stimulation

Blood was obtained from healthy volunteers using the plasma vacutainer techniques described in **Chapter 3.** It was incubated for 45 minutes with dextran (1:6) to facilitate erythrocyte sedimentation, then the erythrocyte/thrombocyte-sedimented blood product (henceforth termed erythrocyte-sedimented blood) layer was removed into a clean vessel.

To investigate any effect of temperature and incubation time, the erythrocyte-sedimented blood was incubated for 15 or 30 minutes at room temperature or 37^{o}C in an incubator. A non-incubated control was also collected at baseline (0 minutes). Tubes were then centrifuged at 300 *xg* for 10 minutes and the plasma was removed and frozen at -20^{o}C until analysis with the proteinase footprint assays described within **Chapter 3.**

Ideal parameters for incubation period and temperature were then selected, and stimuli and inhibitors were added to the model to assess the effects.

The erythrocyte-sedimented blood was stimulated before incubation with fMLP at concentrations of 0.1 µM, 0.5 µM and 1 µM, or left unstimulated as a control. These concentrations were chosen based upon titration from stimulating concentrations reported in the literature (Simchowitz *et al.*, 1980; Bréa *et al.*, 2012).

The methodology is presented as a flow chart in **Figure 6.1**.

6.2.2. Thin blood smear

A 1 µl droplet of erythrocyte-sedimented blood was placed on the lower half of a flat microscope slide, which had been cleaned with 70% ethanol. The side of a coverslip was angled at 45° against the slide below the droplet then dragged across the droplet along the surface of the slide.

The smear was left to air dry for 3 minutes, then labelled for 20 seconds each with diff-quik stains: methanol fixative, xanthene and thiazine/methyline blue/azure A (all Reastain, Reagena, Finland).

Smears were then visually assessed under light microscopy, and cells were identified through colour from diff-quik stain, for their size and morphology.

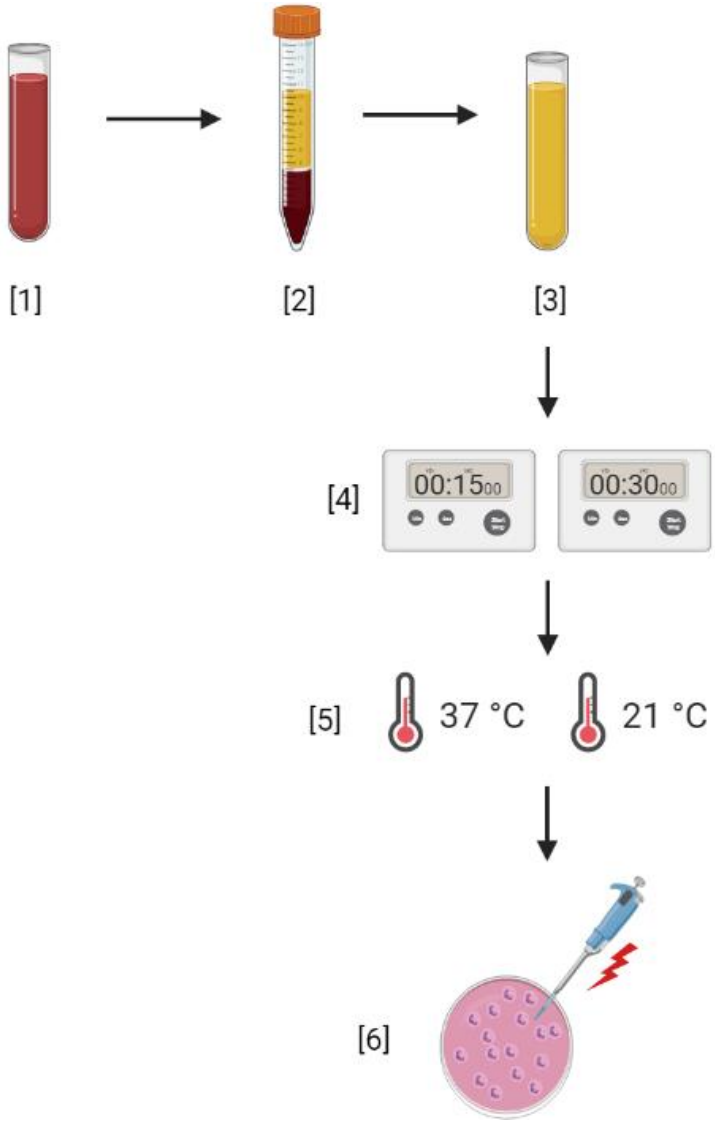

Figure 6.1. Flow chart diagram of methodological procedure used for the development of the whole blood model.

The procedure started with the sedimentation of erythrocytes from whole blood (collected in a lithium-heparin vacutainer [1]) using 2% dextran at a ratio of 1:6 [2]. The erythrocyte-sedimented blood [3] was used to determine parameters for incubation period (0, 15 or 30 minutes) [4] and temperature (at room temperature or 37°C) [5] were determined. The effect of stimulation by fMLP (0.1-1 µM) [6] was then assessed.

6.2.3. Assumptions in analysis

Analysis assumed that erythrocyte-sedimented blood contained mid-range physiological concentrations of fibrinogen at 3 g/L (8800 nM) (Chao *et al.*, 1974; Simchowitz *et al.*, 1980; Oswald *et al.*, 1983; Li *et al.*, 2002; Muller *et al.*, 2007; Bolliger *et al.*, 2009; Sapey, 2010; Amulic *et al.*, 2012; Valvi *et al.*, 2012; Pedrazzani *et al.*, 2016), AAT at 2 g/L (38 μM) (American Thoracic Society/European Respiratory Society, 2003) and neutrophil concentrations of $4x10^6$/ml (Li *et al.*, 2002; Sapey, 2010; Amulic *et al.*, 2012). These values were not measured in individual donor samples for this proof-of-concept work. To negate some of these differences, change in proteinase footprint was described as change from baseline.

6.3. Results

6.3.1. Model development

Validation experiments were carried out with blood from healthy young volunteers (<45 years).

6.3.1.1. *Haemolysis of Erythrocytes by Vehicle Diluent*

Initial experiments with whole blood resulted in haemolysis. This was thought to be a result of the vehicle DMSO used to dissolve the stimulus (**Figure 6.1**). To check for this, whole blood was incubated for 15 minutes at room temperature alone, or with 1 µl or 10 µl DMSO (equivalent to the volume of DMSO solution used), then centrifuged at 1000 *xg* for 10 minutes to obtain plasma and checked for absorbance (410nm). An increase in absorbance was observed with the increasing concentration of DMSO. With no DMSO, median absorbance (450 nm) was 0.33 (IQR:0.33-0.35), increasing to 0.52 (0.38-0.59) with 1 µl DMSO (p=0.25, Wilcoxon test), and 1.49 (0.6-1.7) with 10 µl DMSO (p=0.25, Wilcoxon test) demonstrating objectively increasing haemolysis.

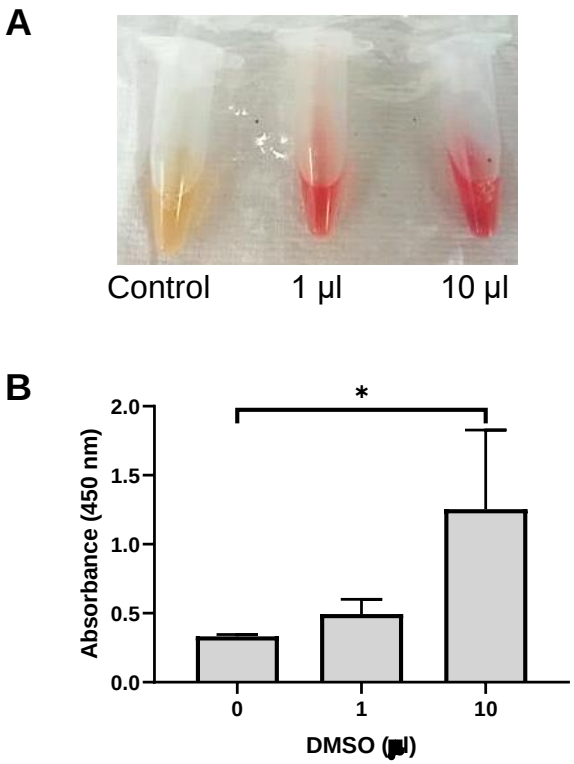

Figure 6.2 Haemolysis of erythrocytes following treatment of blood with DMSO.

A Visual representation of haemolysis occurring in a DMSO-free control, sample with 1 µl DMSO and 10 µl DMSO; **B** Absorbance values (450 nM) of each sample (control versus sample with 1 µl DMSO or 10 µl DMSO); n=3; median with error bars +/- IQR. * = $p \leq 0.05$ determined by Kruskal-Wallis test.

6.3.1.2. *Cellular composition of erythrocyte-sedimented blood*

Whole blood underwent dextran sedimentation to avoid haemolysis. During this process erythrocytes and platelets were sedimented and the remaining blood and cells were separated. A thin blood smear indicated that this blood product was composed of peripheral blood mononuclear cells, PMNs, and a smaller proportion of erythrocytes (<86%, n=5) (**Figure 6.3**)**.**

6.3.1.3. *Incubation period*

Changing the period of incubation before removal of supernatant did not statistically alter the proteinase footprint either at room temperature or at 37°C (**Figure 6.4**).

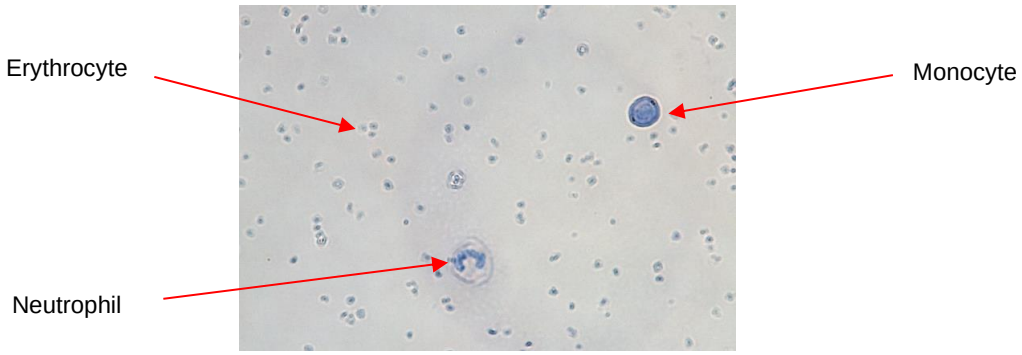

Figure 6.3. Components of erythrocyte-sedimented blood product.

A typical sample of erythrocyte-sedimented blood as seen under light microscopy with Reastain diff-quik staining. Key components are indicated with red arrows.

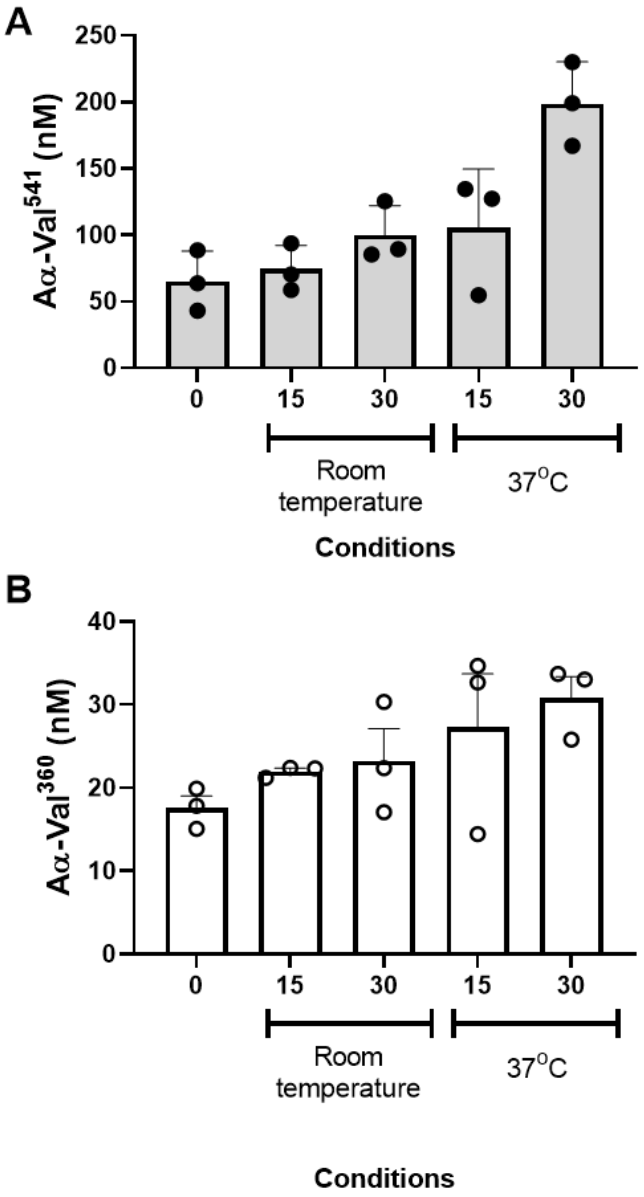

Figure 6.4. Effect of temperature and incubation period on proteinase footprints.

Proteinase activity footprints (y-axis) following incubation of erythrocyte-sedimented blood at baseline (0), 15 and 30 minutes at room temperature or 37°C (x-axis); A PR3 activity; B NE; n=3. ●= PR3 activity footprint, o= NE activity footprint; Error bars mean +/- SEM.

6.3.1.4. *Stimulation*

The erythrocyte-sedimented blood was stimulated with a range of fMLP concentrations. Results are the mean increase in footprint generation with SEM summarised in **Figure 6.5**.

A dose-response was seen following stimulation with ascending concentrations of fMLP for both the PR3 and NE footprints. Stimulation of the erythrocyte sedimented blood with 1 µM fMLP resulted in a 26.1 nM (+/- 11.4 nM) increase in PR3 activity footprint, rising by 39.7 nM (+/- 7.9) with 5 µM fMLP. A similar effect was seen with the NE footprint: stimulation of the erythrocyte-sedimented blood with 1 µM fMLP resulted in an 8.4 nM (+/- 8.8) increase, rising by 10.2 (+/- 9.2) with 5 µM and 19.6 nM (+/-11.1) with 10 µM (**Figure 6.5**).

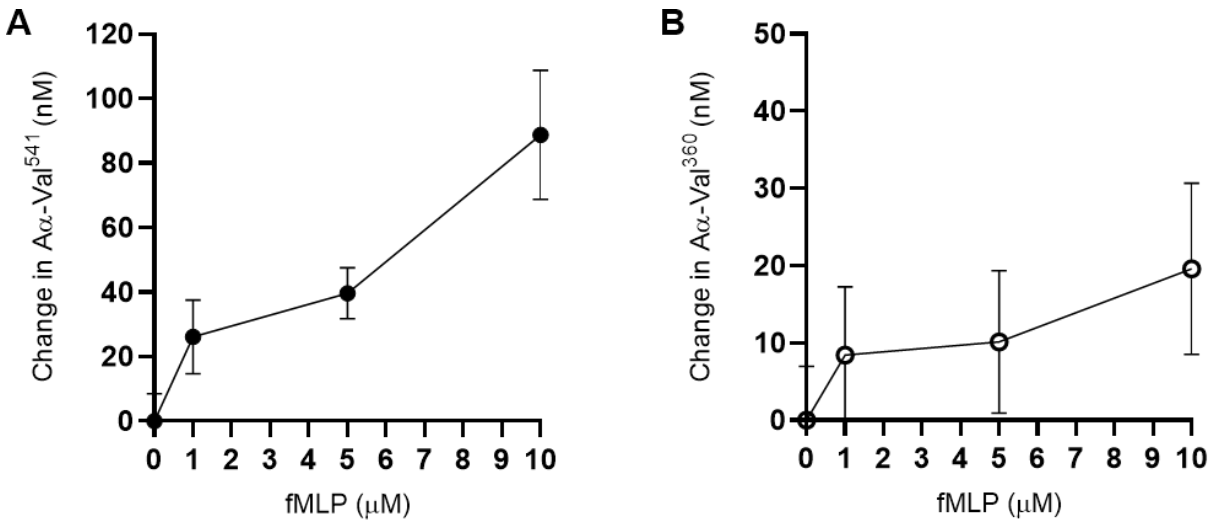

Figure 6.5. Effect of stimulation of erythrocyte-sedimented blood product on proteinase activity footprints.

Proteinase activity footprints (y-axis) before and following stimulation of erythrocyte-sedimented blood with fMLP at 1, 5 or 10 μM (x-axis), then incubated at 37°C for 15 minutes; A PR3 activity; B NE activity; n=6. ●= PR3 activity footprint, o= NE activity footprint; points are mean and error bars +/- SEM.

6.4. Discussion

6.4.1. Development of a whole blood model

This chapter reports the initial development of a model to test proteinase activity in whole blood, which can be manipulated using proteinase inhibitors for comparison with effects seen in clinical trials. Further work is needed to develop this model, but in general, cell sedimentation of whole blood produced similar data to the neutrophil-fibrinogen buffer system described in **Chapters 3, 4** and **5**.

6.4.1.1. *Haemolysis of Samples*

DMSO is a weak stimulator of neutrophil activation in this model. However, during initial establishment using whole blood, it was noticed that adding DMSO resulted in haemolysis, consistent with previous data (Yi *et al.*, 2017).

Variability of the footprint assays was observed during initial experimentation using haemolysed samples, which is similar to previous reports of haemolysis interfering with other ELISAs (Lucena *et al.*, 1998; Kurian *et al.*, 2012; Saracevic *et al.*, 2019).

Therefore, the methodology was adapted to include a step whereby erythrocytes and platelets were separated from the sample by dextran sedimentation for 45 minutes before experimentation on erythrocyte-sedimented blood using DMSO containing reagents.

6.4.1.2. *Period of sample incubation*

Proteinase footprint generation was not increased with longer incubations at 37°C but this likely reflected low numbers of experiments in this series.

Inter-person variation in footprint generation was still observed within the samples as before (including the initial baseline value), therefore data was presented as percentage change compared to the baseline to negate some of this variation.

6.4.1.3. *Stimulation of samples*

Stimulation of this cellular milieu allows for the creation of a more complex cellular environment likely to reflect disease. fMLP resulted in increases in the production of the PR3 and NE footprints in a dose-dependent manner which remained measurable and well within the assay limits. The concentration of fMLP used to treat the neutrophils should be increased until a plateau in proteinase activity is reached to fully assess this effect.

6.4.2. Clinical Relevance

The data collected in this chapter suggest that a more complex cellular model of the proteinase/anti-proteinase balance model can be developed. Although due to the haemolysis effect, the protein milieu would become changed and therefore the resulting data may not provide any further data than the initial model with isolated neutrophils for studying dose responses to inhibitors or as a template for the study of new pharmaceuticals. However, it may prove beneficial or confirmatory if used from patients before and during interventional studies.

6.5. Summary

This chapter describes preliminary evidence towards the development of a second novel *in vitro* model of the proteinase/anti-proteinase balance using whole blood. Although utilising a milieu of blood cells, the data is similar to that with isolated neutrophils alone. Repeating the studies with cells and plasma from patients with known AAT levels and genotypes would be important in directing its use in future clinical studies.

Validation identified that median PR3 and NE activity footprints did not statistically change with time or temperature, but increased following stimulation with fMLP, similarly to the neutrophil/fibrinogen-buffer model.

In conclusion, the data presented in this chapter suggest that a secondary model of proteinase/anti-proteinase balance to generate specific activity footprints can be developed and future studies should explore the use of a plasma cell model without haemolysis for comparison between different AAT genotypes and in the presence of non-AAT inhibitors.

CHAPTER 7: GENERAL DISCUSSION

7.1. Project Overview

COPD presents a significant health burden with 384 million people globally believed to be afflicted with the disease (Global Initiative for Chronic Obstructive Lung Disease, 2021). The pathogenesis of COPD is poorly understood, and this translates to the treatment options available to patients with no mechanistically specifica therapies. Due to the heterogeneity of COPD, it is important to consider treatable traits of the disease, for example, the genetic deficiency in AAT.

As described throughout this thesis, AATD represents a subset of COPD caused by a genetic defect to the major anti-proteinase AAT (Kidd *et al.*, 1983; Gettins, 2002). The emphysematous pathophysiology of AAT can be attributed to an imbalance between destructive proteinases and protective anti-proteinases in the airways (Stockley, 1999), but the exact mechanisms remain unclear.

The studies in this thesis aimed to assess the role of the NSPs in the lung through the development of a novel *in vitro* model of the putative proteinase/anti-proteinase balance, with particular reference to the roles of both NE and PR3.

Furthermore, using the model, the effect of anti-proteinases on inflammatory activity footprints of these enzymes and the validity of the putative AAT threshold that increases risk was assessed. Literature reported the significance of the AAT concentration being below 11 μM for the development of emphysema, although there remains some controversy concerning the exact level.

7.2. Development of *in vitro* models of proteinase/anti-proteinase balance

The development of the neutrophil/fibrinogen-buffer model in this thesis is intended to provide a template to allow the pathophysiology of the interaction of neutrophils and inhibitors to be studied specifically related to enzyme footprint generation relevant to clinical studies. To the best of our knowledge, this research presents a novel *in vitro* model of this proteinase/anti-proteinase balance to provide a better understanding of the underlying mechanisms relevant to AATD and its treatment.

The data presented in **Chapter 3** was able to validate *in vitro* parameters to replicate the proteinase environment in an unstimulated state with a low proteinase activity footprint and a stimulated state with a high-proteinase activity footprint. The low and high proteinase footprints were used to replicate the activity footprints observed in healthy donors and patients with AATD, with and without stimulation, reflected in plasma studies (Carter, 2013; Gudmann *et al.*, 2018; Newby *et al.*, 2019; Schouten *et al.*, 2021).

Furthermore, the parameters – neutrophil, fibrinogen, and stimulus concentrations - selected were chosen to resemble pathophysiology (Chao *et al.*, 1974; Simchowitz *et al.*, 1980; Oswald *et al.*, 1983; Li *et al.*, 2002; Muller *et al.*, 2007; Bolliger *et al.*, 2009; Sapey, 2010; Amulic *et al.*, 2012; Valvi *et al.*, 2012; Swarowska *et al.*, 2014; Pedrazzani *et al.*, 2016).

Chapter 6 introduced the development of a further novel erythrocyte-free blood model of the proteinase/anti-proteinase balance which aimed to provide a more physiological environment than the *in vitro* neutrophil/fibrinogen buffer cell model. An increasing body of evidence suggests that cellular interactions and signalling may be of importance in AATD, therefore this model aimed to preserve (at least in part) the cell-to-cell interactions in the blood *in vivo*. That said, it was necessary to remove erythrocytes from the blood sample by dextran sedimentation, due to sample haemolysis interfering with the result, which resulted in changes to the protein milieu.

The proteinase footprints in the plasma obtained following erythrocyte sedimentation were similar to the footprints obtained in the supernatants from the neutrophil/fibrinogen-buffer model, and ultimately provided no additional information when compared to the neutrophil/fibrinogen buffer model.

7.3. Application of the *in vitro* cell model to assess disease pathogenesis

When the stimulated neutrophil-fibrinogen buffer model was treated with AAT (**Chapter 4**) there was a reduction and normalisation in activity footprint.

These data suggest that the proteinase/anti-proteinase balance could be recovered by AAT. This is consistent with the concept that it represents an appropriate model of the balance.

The data indicated that AAT can limit excess proteinase activity but reaches a therapeutic plateau when AAT concentration exceeds 11 μM. Activity is unlikely to be eliminated as AAT is unlikely to be able to effectively bind all active proteinases. This finding supports evidence of the putative 'at-risk' or maximal treatment threshold as a therapeutic target.

The supporting evidence of the existence of an 11 μM threshold that was presented within this thesis may have wide-reaching clinical impact on how those with AATD are diagnosed and their risk of lung disease is assessed.

Although concentrations of AAT below this threshold increase risk of developing emphysema, it is not absolute and should only instigate treatment when evidence of progressive disease is also present. Early detection of physiological deterioration or other biomarkers of indicating high risk also helping in decision making (McElvaney *et al.*, 2020). Treatments such as AAT augmentation should be used to raise AAT concentrations at least above this threshold, however whether higher concentrations are beneficial requires further exploration.

The assessment of proteinase activity footprints obtained from healthy neutrophils incubated in AATD versus healthy plasma also supported the role of AAT in the abrogation of proteinase activity in proximity to a natural substrate. Higher proteinase activity footprints were generated when neutrophils were incubated in AAT-deficient (<11 µM) plasma than in normal AAT-sufficient plasma.

7.4. Application of the neutrophil/fibrinogen buffer model to assess the activity of a novel pharmaceutical neutrophil elastase inhibitor AZD9668

If the application of a treatment to the *in vitro* model can reduce the activity footprint, the data can be extrapolated to suggest that it may reduce proteinase activity *in vivo* and hence decrease the risk of pathological damage and emphysema development. Therefore, the proteinase activity obtained from the model has the potential to function as a pharmaceutical biomarker to assess the potential efficacy of newer compounds.

Data displayed in **Chapter 5** indicated how the model could be utilised to demonstrate the effect of drugs with different AAT plasma concentrations. This is important as different phenotypes of AATD have different levels of AAT which affects disease development and it is important to consider how this change in concentration will affect treatment response (American Thoracic Society/European Respiratory Society, 2003).

The study in this chapter focused upon the inhibitory effect of a novel NE inhibitor AZD9668 on the proteinase activity footprints. The drug was found to limit excessive NE activity at low concentrations, with a maximal effect plateau occurring at the dose and plasma concentrations found *in vivo*.

Although AZD9668 did not affect the PR3 footprint generation *in vitro* when used alone, it was able to significantly reduce both NE and PR3 activity when in the presence of average AAT concentrations found in PiZZ patients *in vivo*. These data suggest a synergy between AZD9668 and AAT, with most likely the preferential binding of NE by AAT being offset by the drug inactivating some of the elastase, preserving AAT function and leading to increased PR3 inhibition by PR3.

This is an important observation because an increasing body of evidence has highlighted the role of PR3 in the pathogenesis of COPD. Therefore, any reduction in PR3 activity footprint, alongside NE inhibition, may contribute towards normalising the overall NSP proteolytic profile and inflammatory environment of the airways, and hence potentially slow the development of lung disease.

There are currently no data on the proteinase activity footprint response to this drug in patients. However, there are several phase II studies reported (Gunawardena *et al.*, 2013; Stockley *et al.*, 2013a). Measurement of the plasma proteinase footprints in these studies should provide data to support or refute this observation in my model.

7.5. Limitations

There are some limitations to the work explored in this thesis that should be taken into account to make appropriate conclusions from the data.

7.5.1. General limitations

A limitation in the work described in this thesis is the low number of replicates in some experiments. Statistical significance and the magnitude of change would be more clearly determined by using these initial data to perform power calculations to inform sample size. Increasing the number of experiments would aid in the identification of outliers and the accurate interpretation of individual data, together with power calculations facilitating clinical and *in vitro* study design.

Limits of the *in vitro* data centre upon the variability of individual isolated neutrophil preparations. Variability may reflect differences between individuals, or differences in the preparation process including cell recovery, purity of preparations or activation status. This variability was observed during functional assessment and in the activity footprints produced by neutrophils used in the model. However, data was analysed as a fold or percentage change of a sample against the experimental control to normalised some of the inherent variability.

A further limitation presented was the variability of the assays themselves. A higher inter-assay CV value was produced by supernatants, from stimulated neutrophils incubated in the fibrinogen-buffer, than when the assays were performed on plasma. Measurement of samples in technical duplication both intra- and inter-plate allowed

identification of variable results for exclusion/repeated measurement, and where possible samples from each experiment were run together on the same plate to reduce variability for comparison between outcomes. However, this limitation is more relevant to the interpretation of individual data points rather than the overall interpretation of the data.

7.5.2. Limitations of the neutrophil-fibrinogen buffer model

7.5.2.1. *Model development*

There were some limitations associated with the neutrophil/fibrinogen-buffer model.

The strong activation of neutrophils stimulated with CaI before flow cytometry caused an issue as neutrophils became clumped together making them difficult to re-suspend in the PBS-BSA buffer used. This was not corrected by treatment with EDTA. Subsequently, observations on neutrophils stimulated with higher concentrations came from experiments where fewer neutrophils were collected. Nevertheless, the activation was so profound it still enabled decisions about maximum substrate required for results with less vigorous activation. Subsequently, a different stimulus with a milder effect was utilised.

7.5.2.2. *Model validation*

There are also some potential limitations to the kinetics methods used within this thesis that should be considered.

The Michaelis-Menten equation assumes the law of mass action and a steady state. This is accurate in a kinetic model but not so translatable to a heterogeneous cell environment (Briggs *et al.*, 1925; Zhou *et al.*, 2008). Therefore, any enzyme kinetic activity is not specifically applicable to an *in vitro* cellular model.

This caveat may result in inaccurate PPE interactions within the cellular model, which would affect the downstream kinetic analysis of AAT and SLPI. Ultimately, this may result in an inaccurate active quantity of AAT being added into the model. However, a second method was used to confirm PPE activity. The use of two methodologies showing comparable results supports their accuracy.

Beyond this, it would be beneficial to enhance the dose-response curve of the model used for AAT to accurately determine the point that the reduction in proteinase activity plateaued. Although data indicates that activity levels persist above 10 µM, the actual point of plateau may be between 7 and 10 µM, and hence further studies with smaller incremental increases in dose would be necessary to determine a more accurate threshold. This would provide data to support the findings of Campbell *et al.* (Liou and Campbell, 1996; Campbell, 1999; Turino, 1996), and Carter (2013) who identified a significant increase ($p<0.001$) in NE activity in those with an AAT concentration below 11 µM compared to those with with AAT above this.

That said, some patients with AAT concentrations below this threshold maintain good health. Although it remains controversial, the findings presented in this thesis support the use of an AAT concentration of 11 μM as a target threshold in those with progressing disease.

Further, the AAT phenotype of healthy and COPD donors was unknown but assumed to be PiMM (>90% UK Caucasian population), including those who donated plasma to the pools and those who donated neutrophils. A small proportion of the UK, Caucasian population (~3%) is likely to be PiMZ heterozygotes, although this would present low contamination in a pool.

The presence of the Z protein may, however, affect results as recent cellular studies indicate that AATD may result in a wider immunological phenotype, including changes in the function of neutrophils. Neutrophils from patients with AATD have been demonstrated to have reduced phagocytosis (Walton *et al.*, 2017), increased chemotactic ability (Bergin *et al.*, 2010) and production of ROS (Alfawaz *et al.*, 2013), and neutrophil apoptosis (Hurley *et al.*, 2014) when compared to the neutrophils from healthy individuals. Therefore neutrophil donors with this phenotype (even though healthy) may have an impact on a single set of experiments. This should be tested in the current model and the genotype of all donors checked to ensure homogeneity of the pool, and negate the effect of the Z protein on neutrophil activity.

The AAT concentration of the HE plasma pool was lower than has been reported for healthy individuals in the literature (American Thoracic Society/European Respiratory Society, 2003) with a healthy AAT concentration reported at 20-48 μM. Although unlikely, as explained above some donors may have had a non-PiMM phenotype. As the SARS-CoV-2 pandemic interrupted access to target cohorts the use of historically stored plasma pools was necessary not allowing individual data to be confirmed.

7.5.2.3. *Application of Alvelestat*

Alvelestat (AZD9668) appeared to be more potent in preventing the generation of the NE footprint than the natural inhibitor AAT despite adjustment for the inhibitory capacity using active site titrated NE.

Interpretation of the mechanism involved was limited by the lack of publications related to the mode of action. In addition, the data confirmed an additive effect in the presence of physiological concentrations of AAT found in AATD patients. Furthermore, although AZD9668 failed to affect the PR3 footprint on its own, there was an effect in the presence of AAT despite the prime target for AAT being NE. Based on this data, it was hypothesised that AZD9668 was able to inhibit NE that was not as accessible to AAT and by doing so released some AAT function to interact with PR3 in the same model. This may reflect AZD9668 directly inhibiting the NE released by neutrophils complementing inhibition by AAT, inhibiting NE on the cell membrane that is largely protected from inhibition by AAT, or by acting intracellularly before exocytosis of the enzyme.

To study this, confirmation of the effects of AZD9668 in the ongoing Phase II studies assessing both enzyme footprints may provide support for the *in vitro* data generated in this thesis. Localisation of AZD9668 on the cell membrane or in the cell cytoplasm may help. Finally, localisation of NE activity both intracellularly and on its surface using specific chromophores may provide supportive data.

These results may suggest a combination of treatment for AATD, with AAT augmentation therapy and AZD9668, for those with declining lung function despite replacement therapy, or those with rapidly declining lung health.

7.5.2.4. *Whole blood model development*

Whilst the erythrocyte-free blood model was a more physiological set-up, its limitations included that standardised components (such as AAT and neutrophil concentration) were not used which limits its comparability between donors. This is an issue because there is a high variation in neutrophil concentrations in the blood and in addition there may be disease specific components which could change the model. For example, it has been hypothesised that neutrophils have an increased propensity to degrade the extracellular matrix in AATD due to lower concentrations of AAT and the activation status of the cells.

7.5.2.5. *Impact of the SARS-CoV-2 Coronavirus (COVID-19) Pandemic*

The outbreak of the novel coronavirus SARS-CoV-2 negatively impacted the development of this thesis due to the mandatory closure of academic institutions making the laboratory inaccessible between March-July 2020, and cessation of patient attendances for sample collections.

In addition, the postponement of the phase II Alvelestat clinical trial meant some of the *in vivo* confirmatory data could not be obtained before the completion of my studentship. However, this represents a target for future supportive studies.

Adaptions required to access whole blood from healthy young subjects were described in the introduction. Specific procedures used to mitigate risk are described in detail in a publication by Walker et al. (2020).

Due to these major and unavoidable limitations, several initial aims of this thesis could not be completed as intended within the time frame of the studentship.

7.6. Recommendations for future direction

This thesis further describes the role of proteinases in the inflammation associated with AATD. It presents two novel models of proteinase/anti-proteinase balance and explains how the neutrophil/fibrinogen-buffer model can be utilised to investigate mechanisms of disease and as a pharmaceutical model.

Following comprehensive validation of the proof-of-concept *in vitro* model of proteinase/anti-proteinase balance, the data presented in this thesis suggest the following prospective projects:

1. Initially it would be important to continue the use of the neutrophil/fibrinogen-buffer model alongside the in-house proteinase activity assays for use as a biomarker of pharmaceutical efficacy. This should include the application of other inhibitory compounds of both NE and PR3, and exploration of the mechanisms involved in the influence of AZD9668 on proteolytic modulation such as any differential location of inhibitor-proteinase interactions.

2. Secondly the neutrophil/fibrinogen-buffer model should be replicated using the neutrophils of different at-risk patient groups, including those with MZ, SZ, and ZZ AATD phenotypes. Evidence that neutrophils from these different subgroups respond differently or similarly to stimulation and inhibition by both physiological and pharmaceutical inhibitors would support the use of this model for the interpretation of putative efficacy *in vivo* and design such interventional Phase II and III clinical trials.

3. The individual variability of the proteinase activity of neutrophils from donors should be investigated in more detail and in particular whether this is a factor that increases susceptibility to disease development. Replications from each donor would confirm whether the variability is subject-dependent or varies widely in each individual. Further, the incubation of neutrophils from those with AATD/COPD or healthy elderly donors with and without stimuli should be investigated to determine whether this affects variation in neutrophil proteinase footprints.

4. Measurement of proteinase activity footprints in the plasma of patients treated with pharmaceutical compounds designed to have an impact should become a validation marker to observe whether the effects on proteinase activity reduction persists *in vivo* and would also contribute towards the clinical relevance of the proteinase/anti-proteinase balance neutrophil/fibrinogen-buffer model.

7.7. Concluding statement

In conclusion, while understanding of the relationships between proteinases and the pathophysiology of AATD remains limited, the studies presented within this thesis have demonstrated evidence supporting the role of PR3 and NE as major mediators of lung damage observed in AATD.

A model of the balance between proteinases and anti-proteinases observed in AATD was produced using a novel neutrophil/fibrinogen buffer. This has the potential to advance our understanding of the mechanisms of interaction and putative role in disease pathophysiology. This thesis provides evidence to support the use of the putative safety threshold of 11 μM in the management of AATD and has outlined how this could be used effectively alongside therapeutic compounds as a marker of pharmaceutical efficacy. It has been well reported that there are inter-person differences in neutrophil function and the number of proteinases stored in neutrophil granules (Campbell, 2000b), and work presented here suggests that these factors may also affect the proteinase activity footprint of a sample and hence potential tissue destruction. There is a need for ongoing research to investigate the use of this model and explore the role of the proteinase/anti-proteinase balance in COPD and AATD.

CHAPTER 8: REFERENCES

Abboud, R.T., Nelson, T.N., Jung, B. and Mattman, A. (2011). "Alpha1-antitrypsin deficiency: A clinical-genetic overview." *The Application of Clinical Genetics* **4**: 55-65.

Adeloye, D., Chua, S., Lee, C., Basquill, C., Papana, A., Theodoratou, E., Nair, H., Gasevic, D., Sridhar, D., Campbell, H., Chan, K.Y., Sheikh, A. and Rudan, I. (2015). "Global and regional estimates of COPD prevalence: Systematic review and meta-analysis." *Journal of Global Health* **5**(2): 020415.

Afonina, I.S., Tynan, G.A., Logue, S.E., Cullen, S.P., Bots, M., Lüthi, A.U., Reeves, E.P., McElvaney, N.G., Medema, J.P., Lavelle, E.C. and Martin, S.J. (2011). "Granzyme b-dependent proteolysis acts as a switch to enhance the proinflammatory activity of IL-1α." *Molecular Cell* **44**(2): 265-78.

Ahmed, K., Ichinose, A., Dai, T.C., Takahashi, A., Utsunomiya, Y., Kawakami, K., Nagatake, T. and Matsumoto, K. (1993). "Neutrophil response to nontypable *Haemophilus influenzae* in respiratory infections." *Microbiology and Immunology* **37**(9): 671-7.

Al Ashry, H.S. and Strange, C. (2017). "COPD in individuals with the PiMZ alpha-1 antitrypsin genotype." *European Respiratory Review* **26**(146): 170068.

Alam, S., Li, Z., Janciauskiene, S. and Mahadeva, R. (2011). "Oxidation of Z α1-antitrypsin by cigarette smoke induces polymerization: A novel mechanism of early-onset emphysema." *American Journal of Respiratory Cell and Molecular Biology* **45**(2): 261-9.

Alfaidi, M., Wilson, H., Daigneault, M., Burnett, A., Ridger, V., Chamberlain, J. and Francis, S. (2015). "Neutrophil elastase promotes interleukin-1β secretion from human coronary endothelium." *Journal of Biological Chemistry* **290**(40): 24067-78.

Alfawaz, B., Bergin, D.A., McElvaney, N.G. and Reeves, E.P. (2013). "Alpha-1 antitrypsin regulates neutrophil reactive oxygen species production via inhibition of key players of the respiratory burst oxidase system." *BMC Proceedings* **7**(1): P7.

Allen, T.C. (2010). "Pathology of small airways disease." *Archives of Pathology and Laboratory Medicine* **134**(5): 702-18.

Alobaidi, N.Y., Stockley, J.A., Stockley, R.A. and Sapey, E. (2020). "An overview of exacerbations of chronic obstructive pulmonary disease: Can tests of small airways' function guide diagnosis and management?" *Annals of Thoracic Medicine* **15**(2): 54-63.

Alpha-1 Antitrypsin Deficiency Registry Study Group (1994). "A registry of patients with severe deficiency of alpha1-antitrypsin: Design and methods." *Chest* **106**(4): 1223-32.

American Thoracic Society/European Respiratory Society (2003). "American thoracic society/european respiratory society statement." *American Journal of Respiratory and Critical Care Medicine* **168**(7): 818-900.

Amulic, B., Cazalet, C., Hayes, G.L., Metzler, K.D. and Zychlinsky, A. (2012). "Neutrophil function: From mechanisms to disease." *Annual Review of Immunology* **30**(1): 459-89.

Armbruster, D.A. and Pry, T. (2008). "Limit of blank, limit of detection and limit of quantitation." *The Clinical Biochemist Reviews* **29 Suppl 1**(Suppl 1): S49-S52.

AstraZeneca *Par&d prenomination report for project Nei - compound AZ12301876 - including implication and issues for product design*.

Ataya, A. (2020). "Recurrence of emphysema post-lung transplantation in a patient with alpha 1 antitrypsin deficiency (AATD)." *Respiratory Medicine Case Reports* **31**: 101309.

Bafadhel, M., Umar, I., Gupta, S., Raj, J.V., Vara, D.D., Entwisle, J.J., Pavord, I.D., Brightling, C.E. and Siddiqui, S. (2011). "The role of CT scanning in multidimensional phenotyping of COPD." *Chest* **140**(3): 634-42.

Baici, A., Szedlacsek, S.E., Fruh, H. and Michel, B.A. (1996). "pH-dependent hysteretic behavior of human myeloblastin (leucocyte proteinase 3)." *Biochemical Journal* **317**: 901-5.

Baker, M., Mackenzie, I.R., Pickering-Brown, S.M., Gass, J., Rademakers, R., Lindholm, C., Snowden, J., Adamson, J., Sadovnivk, A.D., Rollinson, S., Cannon, A., Dwosh, E., Neary, D., Melquist, S., Richardon, A., Dickson, D., Berger, Z., Ericksen, J., Robinosn, T., Zehr, C., Dickey, C.A., Crook, R., McGowan, E., Mann, D., Boeve, B., Feldman, H. and Hutton, M. (2006). "Mutations in progranulin cause tau-negative frontotemporal dementia linked to chromosome 17." *Nature* **442**: 916-9.

Bals, R., Boyd, J., Esposito, S., Foronjy, R., Hiemstra, P.S., Jimenez-Ruiz, C.A., Katsaounou, P., Lindberg, A., Metz, C., Schober, W., Spira, A. and Blasi, F. (2019). "Electronic cigarettes: A task force report from the european respiratory society." *European Respiratory Journal* **53**(2).

Barnes, P.J. (2016a). "Sex differences in chronic obstructive pulmonary disease mechanisms." *American Journal of Respiratory and Critical Care Medicine* **193**(8): 813-4.

Barnes, P.J. (2016b). "Inflammatory mechanisms in patients with chronic obstructive pulmonary disease." *Journal of Allergy and Clinical Immunology* **138**(1): 16-27.

Baur, X., Manuwald, U. and Wilken, D. (2010). "[does long-term asbestos exposure cause an obstructive ventilation pattern?]." *Pneumologie* **64**(12): 736-44.

Bazzan, E., Tinè, M., Biondini, D., Benetti, R., Baraldo, S., Turato, G., Fagiuoli, S., Sonzogni, A., Rigobello, C., Rea, F., Calabrese, F., Foschino-Barbaro, M.P., Miranda,

E., Lomas, D.A., Saetta, M. and Cosio, M.G. (2018). "A(1)-antitrypsin polymerizes in alveolar macrophages of smokers with and without α(1)-antitrypsin deficiency." *Chest* **154**(3): 607-16.

Beatty, K., Bieth, J. and Travis, J. (1980). "Kinetics of association of serine proteinases with native and oxidized alpha-1-proteinase inhibitor and alpha-1-antichymotrypsin." *Journal of Biological Chemistry* **255**(9): 3931-4.

Beilke, M.A., Collins-Lech, C. and Sohnle, P.G. (1987). "Effects of dimethyl sulfoxide on the oxidative function of human neutrophils." *Journal of Laboratory and Clinical Medicine* **110**(1): 91-6.

Beiter, K., Wartha, F., Albiger, B., Normark, S., Zychlinsky, A. and Henriques-Normark, B. (2006). "An endonuclease allows *streptococcus pneumoniae* to escape from neutrophil extracellular traps." *Current Biology* **16**(4): 401-7.

Belchamber, K. and Sapey, E. (2021). "S51 hungry hungry macrophages: How multiple prey affects macrophage phagocytosis." *Thorax* **76**(Suppl 1): A31-A.

Belchamber, K.B.R., Walker, E., Stockley, R.A. and Sapey, E. (2020). "Monocytes and macrophages in alpha-1 antitrypsin deficiency." *International Journal of Chronic Obstructive Pulmonary Disease* **15**: 3183-92.

Belorgey, D., Hägglöf, P., Karlsson-Li, S. and Lomas, D.A. (2007). "Protein misfolding and the serpinopathies." *Prion* **1**(1): 15-20.

Benarafa, C., Priebe, G.P. and Remold-O'Donnell, E. (2007). "The neutrophil serine protease inhibitor serpinB1 preserves lung defence functions in *pseudomonas aeruginosa* infection." *The Journal of Experimental Medicine* **204**(8): 1901-9.

Beran, D., Zar, H.J., Perrin, C., Menezes, A.M. and Burney, P. (2015). "Burden of asthma and chronic obstructive pulmonary disease and access to essential medicines in low-income and middle-income countries." *Lancet Respiratory Medicine* **3**(2): 159-70.

Berend, N. (2016). "Contribution of air pollution to COPD and small airway dysfunction." *Respirology* **21**(2): 237-44.

Berg, J.M., Tymoczko, J.L. and Stryer, L. (2002). *Biochemistry*. New York, W.H. Freeman.

Bergenfeldt, M., Axelsson, L. and Ohlsson, K. (1992). "Release of neutrophil proteinase 4(3) and leukocyte elastase during phagocytosis and their interaction with proteinase inhibitors." *Scandinavian Journal of Clinical and Laboratory Investigation* **52**(8): 823-9.

Bergin, D.A., Reeves, E.P., Meleady, P., Henry, M., McElvaney, O.J., Carroll, T.P., Condron, C., Chotirmall, S.H., Clynes, M., O'Neill, S.J. and McElvaney, N.G. (2010). "A-1 antitrypsin regulates human neutrophil chemotaxis induced by soluble immune complexes and IL8." *Journal of Clinical Investigation* **120**(12): 4236-50.

Berman, H.M., Westbrook, J., Feng, Z., Gilliland, G., Bhat, T.N., Weissig, H., Shindyalov, I.N. and Bourne, P.E. (2000). *The protein data bank*. Nucleic Acids Research. **28:** 235-42.

Bhatta, D.N. and Glantz, S.A. (2020). "Association of e-cigarette use with respiratory disease among adults: A longitudinal analysis." *American Journal of Preventive Medicine* **58**(2): 182-90.

Bigna, J.J., Kenne, A.M., Asangbeh, S.L. and Sibetcheu, A.T. (2018). "Prevalence of chronic obstructive pulmonary disease in the global population with HIV: A systematic review and meta-analysis." *Lancet Global Health* **6**(2): e193-e202.

Bio-Rad (2019). *Principles of fluorescence*. Flow cytometry basics guide.

Black, P.N., Ching, P.S.T., Beaumont, B., Ranasinghe, S., Taylor, G. and Merrilees, M.J. (2008). "Changes in elastic fibres in the small airways and alveoli in COPD." *European Respiratory Journal* **31**(5): 998.

Blanco, I. (2014). "Oxidant-mediated aggregation of Z α1-antitrypsin in pulmonary epithelial cells amplifies lung inflammation." *American Journal of Respiratory and Critical Care Medicine* **189**(8): 877-9.

Blanco, I., Lipsker, D., Lara, B. and Janciauskiene, S. (2016). "Neutrophilic panniculitis associated with alpha-1-antitrypsin deficiency: An update." *British Journal of Dermatology* **174**(4): 753-62.

Blanco, I., Diego, I., Bueno, P., Casas-Maldonado, F. and Miravitlles, M. (2019). "Geographic distribution of copd prevalence in the world displayed by geographic information system maps." *European Respiratory Journal* **54**(1): 1900610.

Bode, W., Wei, A.Z., Huber, R., Meyer, E., Travis, J. and Neumann, S. (1986). "X-ray crystal structure of the complex of human leukocyte elastase (PMN elastase) and the third domain of the turkey ovomucoid inhibitor." *The EMBO Journal* **5**(10): 2453-8.

Bolliger, D., Szlam, F., Molinaro, R.J., Rahe-Meyer, N., Levy, J.H. and Tanaka, K.A. (2009). "Finding the optimal concentration range for fibrinogen replacement after severe haemodilution: An *in vitro* model." *British Journal of Anaesthesia* **102**(6): 793-9.

Borel, F., Sun, H., Zieger, M., Cox, A., Cardozo, B., Li, W., Oliveira, G., Davis, A., Gruntman, A., Flotte, T.R., Brodsky, M.H., Hoffman, A.M., Elmallah, M.K. and Mueller, C. (2018). "Editing out five serpinA1 paralogs to create a mouse model of genetic emphysema." *Proceedings of the National Academy of Sciences of the United States of America*.

Boulet, L.P., Turcotte, H., Turcot, O. and Chakir, J. (2003). "Airway inflammation in asthma with incomplete reversibility of airflow obstruction." *Respiratory Medicine* **97**(6): 739-44.

Bradford, E., Jacobson, S., Varasteh, J., Comellas, A.P., Woodruff, P., O'Neal, W., DeMeo, D.L., Li, X., Kim, V., Cho, M., Castaldi, P.J., Hersh, C., Silverman, E.K., Crapo, J.D., Kechris, K. and Bowler, R.P. (2017). "The value of blood cytokines and chemokines in assessing COPD." *Respiratory Research* **18**(1): 180.

Brantly, M.L., Paul, L.D., Miller, B.H., Falk, R.T., Wu, M. and Crystal, R.G. (1988). "Clinical features and history of the destructive lung disease associated with alpha-1-antitrypsin deficiency of adults with pulmonary symptoms." *American Review of Respiratory Disease* **138**(2): 327-36.

Brantly, M.L., Wittes, J.T., Vogelmeier, C.F., Hubbard, R.C., Fells, G.A. and Crystal, R.G. (1991). "Use of a highly purified alpha-1-antitrypsin standard to establish ranges for the common normal and deficient alpha-1-antitrypsin phenotypes." *Chest* **100**(3): 703-8.

Brantly, M.L., Lascano, J.E. and Shahmohammadi, A. (2018). "Intravenous alpha-1 antitrypsin therapy for alpha-1 antitrypsin deficiency: The current state of the evidence." *Chronic Obstructive Pulmonary Diseases* **6**(1): 100-14.

Bréa, D., Meurens, F., Dubois, A.V., Gaillard, J., Chevaleyre, C., Jourdan, M.-L., Winter, N., Arbeille, B., Si-Tahar, M., Gauthier, F. and Attucci, S. (2012). "The pig as a model for investigating the role of neutrophil serine proteases in human inflammatory lung diseases." *Biochemical Journal* **447**(3): 363-70.

Briggs, G.E. and Haldane, J.B. (1925). "A note on the kinetics of enzyme action." *Biochemical Journal* **19**(2): 338-9.

Brinkmann, V., Reichard, U., Goosmann, C., Fauler, B., Uhlemann, Y., Weiss, D.S., Weinrauch, Y. and Zychlinsky, A. (2004). "Neutrophil extracellular traps kill bacteria." *Science* **303**(5663): 1532-5.

Brinkmann, V. (2018). "Neutrophil extracellular traps in the second decade." *Journal of Innate Immunity* **10**(5-6): 414-21.

Brown, G.B. and Roth, J.A. (1991). "Comparison of the response of bovine and human neutrophils to various stimuli." *Veterinary Immunology and Immunopathology* **28**(3): 201-18.

Brubaker, M.J., Groutas, W.C., Hoidal, J.R. and Rao, N.V. (1992). "Human neutrophil proteinase 3: Mapping of the substrate binding site using peptidyl thiobenzyl esters." *Biochemical and Biophysical Research Communications* **188**(3): 1318-24.

Buist, A.S., McBurnie, M.A., Vollmer, W.M., Gillespie, S., Burney, P., Mannino, D.M., Menezes, A.M.B., Sullivan, S.D., Lee, T.A., Weiss, K.B., Jensen, R.L., Marks, G.B., Gulsvik, A. and Nizankowska-Mogilnicka, E. (2007). "International variation in the prevalence of COPD (the BOLD study): A population-based prevalence study." *Lancet* **370**(9589): 741-50.

Burnett, D. and Stockley, R.A. (1981). "Serum and sputum alpha 2 macroglobulin in patients with chronic obstructive airways disease." *Thorax* **36**(7): 512-6.

Burnett, D., Chamba, A., Hill, S.L. and Stockley, R.A. (1987). "Neutrophils from subjects with chronic obstructive lung disease show enhanced chemotaxis and extracellular proteolysis." *Lancet* **2**(8567): 1043-6.

Burns, A.R., Smith, C.W. and Walker, D.C. (2003). "Unique structural features that influence neutrophil emigration into the lung." *Physiological Reviews* **83**(2): 309-36.

Bustamante-Marin, X.M. and Ostrowski, L.E. (2017). "Cilia and mucociliary clearance." *Cold Spring Harbor Perspectives in Biology* **9**(4).

Butcher, S., Chahel, H. and Lord, J.M. (2000). "Review article: Ageing and the neutrophil: No appetite for killing?" *Immunology* **100**(4): 411-6.

Byrne, A.L., Marais, B.J., Mitnick, C.D., Lecca, L. and Marks, G.B. (2015). "Tuberculosis and chronic respiratory disease: A systematic review." *International Journal of Infectious Diseases* **32**: 138-46.

Cadwallader, K.A., Uddin, M., Condliffe, A.M., Cowburn, A.S., White, J.F., Skepper, J.N., Ktistakis, N.T. and Chilvers, E.R. (2004). "Effect of priming on activation and localization of phospholipase D-1 in human neutrophils." *European Journal of Biochemistry* **271**(13): 2755-64.

Calabrese, F., Baraldo, S., Bazzan, E., Lunardi, F., Rea, F., Maestrelli, P., Turato, G., Lokar-Oliani, K., Papi, A., Zuin, R. and Sfriso, P. (2008). "IL-32, a novel proinflammatory cytokine in chronic obstructive pulmonary disease." *American Journal of Respiratory and Critical Care Medicine* **178**(9): 894-901.

Calverley, P.M.A., Anderson, J.A., Celli, B., Ferguson, G.T., Jenkins, C., Jones, P.W., Yates, J.C. and Vestbo, J. (2007). "Salmeterol and fluticasone propionate and survival in chronic obstructive pulmonary disease." *New England Journal of Medicine* **356**(8): 775-89.

Campanelli, D., Detmers, P.A., Nathan, C.F. and Gabay, J.E. (1990). "Azurocidin and a homologous serine protease from neutrophils. Differential antimicrobial and proteolytic properties." *Journal of Clinical Investigation* **85**(3): 904-15.

Campbell, E.J., Campbell, M.A., Boukedes, S.S. and Owen, C.A. (2000a). "Quantum proteolysis by neutrophils: Implications for pulmonary emphysema in α1-antitrypsin deficiency." *Chest* **117**(5): 303S.

Campbell, E.J., Campbell, M.A. and Owen, C.A. (2000b). "Bioactive proteinase 3 on the cell surface of human neutrophils: Quantification, catalytic activity, and susceptibility to inhibition." *The Journal of Immunology* **165**: 3366-74.

Campos, M.A., Wanner, A., Zhang, G. and Sandhaus, R.A. (2005). "Trends in the diagnosis of symptomatic patients with alpha1-antitrypsin deficiency between 1968 and 2003." *Chest* **128**(3): 1179-86.

Candas, B., Cusan, L., Gomez, J.L., Diamond, P., Suburu, R.E., Levesque, J., Brousseau, G., Belanger, A. and Labrie, F. (2000). "Evaluation of prostatic specific

antigen and digital rectal examination as screening tests for prostate cancer." *Prostate* **45**(1): 19-35.

Carrell, R.W. and Lomas, D.A. (2003). "Alpha1-antitrypsin deficiency — a model for conformational diseases." *The New England Journal of Medicine* **346**: 45-53.

Carroll, T.P., Greene, C.M., O'Connor, C.A., Nolan, A.M., O'Neill, S.J. and McElvaney, N.G. (2010). "Evidence for unfolded protein response activation in monocytes from individuals with alpha-1 antitrypsin deficiency." *Journal of Immunology* **184**(8): 4538-46.

Carter, R.I., Mumford, R.A., Treonze, K.M., Finke, P.E., Davies, P., Si, Q., Humes, J.L., Dirksen, A., Piitulainen, E., Ahmad, A. and Stockley, R.A. (2011). "The fibrinogen cleavage product Aα-val360, a specific marker of neutrophil elastase activity in vivo." *Thorax* **66**(8): 686-91.

Carter, R.I. (2013). *Biomarkers of disease activity in COPD and emphysema*. Doctor of Philosophy, University of Birmingham.

Carter, R.I., Ungers, M.J., Mumford, R.A. and Stockley, R.A. (2013). "Aa-Val360: A marker of neutrophil elastase and COPD disease activity." *European Respiratory Journal* **41**(1): 8.

Carter, R.I., Ungers, M.J., Pillal, A., Mumford, R.A. and Stockley, R.A. (2015). "The relationship of the fibrinogen cleavage biomarker Aa-Val360 with disease severity and activity in alpha-1-antitrypsin deficiency." *Chest* **148**(2): 7.

Cepinskas, G., Sandig, M. and Kvietys, P.R. (1999). "Paf-induced elastase-dependent neutrophil transendothelial migration is associated with the mobilization of elastase to the neutrophil surface and localization to the migrating front." *Journal of Cell Science* **112 (Pt 12)**: 1937-45.

Chao, F.C., Tullis, J.L., Kenney, D.M., Conneely, G.S. and Doyle, J.R. (1974). "Concentration effects of platelets, fibrinogen and thrombin on platelet aggregation and fibrin clotting." *Thrombosis et Diathesis Haemorrhagica* **32**(1): 216-31.

Chapman, K.R., Stockley, R.A., Dawkins, C., Wilkes, M.M. and Navickis, R.J. (2009). "Augmentation therapy for alpha1 antitrypsin deficiency: A meta-analysis." *COPD* **6**(3): 177-84.

Chelladurai, P., Seeger, W. and Pullamsetti, S.S. (2012). "Matrix metalloproteinases and their inhibitors in pulmonary hypertension." *European Respiratory Journal* **40**: 766-82.

Chen, L.W. and Jan, C.R. (2001). "Mechanisms and modulation of formyl-methionyl-leucyl-phenylalanine (fMLP)-induced CA2+ mobilization in human neutrophils." *International Immunopharmacology* **1**(7): 1341-9.

Cichy, J., Potempa, J. and Travis, J. (1997). "Biosynthesis of alpha1-proteinase inhibitor by human lung-derived epithelial cells." *Journal of Biological Chemistry* **272**(13): 8250-5.

Cockayne, D.A., Cheng, D.T., Waschki, B., Sridhar, S., Ravindran, P., Hilton, H., Kourteva, G., Bitter, H., Pillai, S.G., Visvanathan, S., Müller, K.-C., Holz, O., Magnussen, H., Watz, H. and Fine, J.S. (2012). "Systemic biomarkers of neutrophilic inflammation, tissue injury and repair in copd patients with differing levels of disease severity." *PLOS ONE* **7**(6): e38629-e.

Coeshott, C., Ohnemus, C., Pilyavskaya, A., Ross, S., Wieczorek, M., Kroona, H., Leimer, A.H. and Cheronis, J. (1999). "Converting enzyme-independent release of tumor necrosis factor alpha and IL-1beta from a stimulated human monocytic cell line in the presence of activated neutrophils or purified proteinase 3." *Proceedings of the National Academy of Sciences of the United States of America* **96**(11): 6261-6.

Cole, A.M., Shi, J., Ceccarelli, A., Kim, Y.H., Park, A. and Ganz, T. (2001). "Inhibition of neutrophil elastase prevents cathelicidin activation and impairs clearance of bacteria from wounds." *Blood* **97**(1): 297-304.

Condliffe, A.M., Hawkins, P.T., Stephens, L.R., Haslett, C. and Chilvers, E.R. (1998). "Priming of human neutrophil superoxide generation by tumour necrosis factor-α is signalled by enhanced phosphatidylinositol 3,4,5-trisphosphate but not inositol 1,4,5-trisphosphate accumulation." *FEBS Letters* **439**(1): 147-51.

Cooley, J., Takayama, T.K., Shapiro, S.D., Schechter, N.M. and Remold-O'Donnell, E. (2001). "The serpin MNEI inhibits elastase-like and chymotrypsin-like serine proteases through efficient reactions at two active sites." *Biochemistry* **40**(51): 15762-70.

Couto, M.A., Harwig, S.S., Cullor, J.S., Hughes, J.P. and Lehrer, R.I. (1992). "ENAP-2, a novel cysteine-rich bactericidal peptide from equine leukocytes." *Infection and Immunity* **60**(12): 5042-7.

Crisford, H., Sapey, E. and Stockley, R.A. (2018). "Proteinase 3; a potential target in chronic obstructive pulmonary disease and other chronic inflammatory diseases." *Respiratory Research* **19**(180).

Crisford, H., Sapey, E., Rogers, G.B., Taylor, S., Nagakumar, P., Lokwani, R. and Simpson, J.L. (2021). "Neutrophils in asthma: The good, the bad and the bacteria." *Thorax*: thoraxjnl-2020-215986.

Csernok, E., Ernst, M., Schmitt, W., Bainton, D.F. and Gross, W.L. (1994). "Activated neutrophils express proteinase 3 on their plasma membrane *in vitro* and *in vivo*." *Clinical and Experimental Immunology* **95**(2): 244-50.

Currie, D.C., Pavia, D., Agnew, J.E., Lopez-Vidriero, M.T., Diamond, P.D., Cole, P.J. and Clarke, S.W. (1987). "Impaired tracheobronchial clearance in bronchiectasis." *Thorax* **42**(2): 126-30.

da Silva, F.M., Massart-Leën, A.M. and Burvenich, C. (1994). "Development and maturation of neutrophils." *Veterinary Quarterly* **16**(4): 220-5.

Dahl, M., Vestbo, J., Lange, P., Bojesen, S.E., Tybjærg-Hansen, A. and Nordestgaard, B.G. (2007). "C-reactive protein as a predictor of prognosis in chronic obstructive pulmonary disease." *American Journal of Respiratory and Critical Care Medicine* **175**(3): 250-5.

Damiano, V.V., Tsang, A., Kucich, U., Abrams, W.R., Rosenbloom, J., Kimbel, P., Fallahnejad, M. and Weinbaum, G. (1986). "Immunolocalization of elastase in human emphysematous lungs." *Journal of Clinical Investigation* **78**(2): 482-93.

Dancey, J.T., Deubelbeiss, K.A., Harker, L.A. and Finch, C.A. (1976). "Neutrophil kinetics in man." *Journal of Clinical Investigation* **58**(3): 705-15.

Dasaraju, P.V. and Liu, C. (1996). *Infections of the respiratory system*. Medical microbiology. S. Baron. Galveston, Texas, University of Texas Medical Branch at Galveston.

de Bont, C.M., Koopman, W.J.H., Boelens, W.C. and Pruijn, G.J.M. (2018). "Stimulus-dependent chromatin dynamics, citrullination, calcium signalling and ros production during net formation." *Biochimica et Biophysica Acta Molecular Cell Research* **1865**(11 Pt A): 1621-9.

de Serres, F.J., Blanco, I. and Fernández-Bustillo, E. (2006). "Estimating the risk for alpha-1 antitrypsin deficiency among copd patients: Evidence supporting targeted screening." *Journal of Chronic Obstructive Pulmonary Disease* **3**(3): 133-9.

deCathelineau, A.M. and Henson, P.M. (2003). "The final step in programmed cell death: Phagocytes carry apoptotic cells to the grave." *Essays in Biochemistry* **39**: 105-17.

Delain, E., Pochon, F., Barray, M. and Van Leuven, F. (1992). "Ultrastructure of alpha 2-macroglobulins." *Electron Microscopy Reviews* **5**(2): 231-81.

Delgado-Rizo, V., Martinez-Guzman, M.A., Iniguez-Gutierrez, L., Garcia-Orozco, A., Alvarado-Navarro, A. and Fafutis-Morris, M. (2017). "Neutrophil extracellular traps and its implications in inflammation: An overview." *Frontiers in Immunology* **2017**(8): 1-20.

Ding, Z.M., Babensee, J.E., Simon, S.I., Lu, H., Perrard, J.L., Bullard, D.C., Dai, X.Y., Bromley, S.K., Dustin, M.L., Entman, M.L., Smith, C.W. and Ballantyne, C.M. (1999). "Relative contribution of LFA-1 and MAC-1 to neutrophil adhesion and migration." *The Journal of Immunology* **163**(9): 5029-38.

Dirksen, A., Piitulainen, E., Parr, D.G., Deng, C., Wencker, M., Shaker, S.B. and Stockley, R.A. (2009). "Exploring the role of CT densitometry: A randomised study of augmentation therapy in alpha1-antitrypsin deficiency." *European Respiratory Journal* **33**(6): 1345-53.

Domon, H., Nagai, K., Maekawa, T., Oda, M., Yonezawa, D., Takeda, W., Hiyoshi, T., Tamura, H., Yamaguchi, M., Kawabata, S. and Terao, Y. (2018). "Neutrophil elastase subverts the immune response by cleaving toll-like receptors and cytokines in pneumococcal pneumonia." *Frontiers in Immunology* **9**(732).

Duranton, J. and Bieth, J.G. (2003). "Inhibition of proteinase 3 by [alpha]1-antitrypsin in vitro predicts very fast inhibition *in vivo*." *American Journal of Respiratory Cell and Molecular Biology* **29**(1): 57-61.

Duvoix, A., Dickens, J., Haq, I., Mannino, D., Miller, B., Tal-Singer, R. and Lomas, D.A. (2013). "Blood fibrinogen as a biomarker of chronic obstructive pulmonary disease." *Thorax* **68**(7): 670.

Edgar, R.G., Patel, M., Bayliss, S., Crossley, D., Sapey, E. and Turner, A.M. (2017). "Treatment of lung disease in alpha-1 antitrypsin deficiency: A systematic review." *International Journal of Chronic Obstructive Pulmonary Disease* **12**: 1295-308.

Ekeowa, U.I., Freeke, J., Miranda, E., Gooptu, B., Bush, M.F., Pérez, J., Teckman, J., Robinson, C.V. and Lomas, D.A. (2010). "Defining the mechanism of polymerization in the serpinopathies." *Proceedings of the National Academy of Sciences of the United States of America* **107**(40): 17146-51.

Ekpenyong, A.E., Toepfner, N., Chilvers, E.R. and Guck, J. (2015). "Mechanotransduction in neutrophil activation and deactivation." *Biochimica et Biophysica Acta Molecular Cell Research* **1853**(11, Part B): 3105-16.

Elborn, J.S., Perrett, J., Forsman-Semb, K., Marks-Konczalik, J., Gunawardena, K. and Entwistle, N. (2012). "Efficacy, safety and effect on biomarkers of AZD9668 in cystic fibrosis." *European Respiratory Journal* **40**(4): 969-76.

Esnault, V.L.M., Testa, A., Audrain, M., Rogé, C., Hamidou, M., Barrier, J.H., Sesboüé, R., Martin, J.-P. and Lesavre, P. (1993). "Alpha1-antitrypsin genetic polymorphism in anca-positive systemic vasculitis." *Kidney International* **43**(6): 1329-32.

Faull, S.V., Elliston, E.L.K., Gooptu, B., Jagger, A.M., Aldobiyan, I., Redzej, A., Badaoui, M., Heyer-Chauhan, N., Rashid, S.T., Reynolds, G.M., Adams, D.H., Miranda, E., Orlova, E.V., Irving, J.A. and Lomas, D.A. (2020). "The structural basis for Z α(1)-antitrypsin polymerization in the liver." *Science Advances* **6**(43).

Ferrarotti, I., Thun, G.A., Zorzetto, M., Ottaviani, S., Imboden, M., Schindler, C., von Eckardstein, A., Rohrer, L., Rochat, T., Russi, E.W., Probst-Hensch, N.M. and Luisetti, M. (2012). "Serum levels and genotype distribution of α1-antitrypsin in the general population." *Thorax* **67**(8): 669.

Fietta, A., Bersani, C., De Rose, V., Grassi, F.A., Mangiarotti, P., Uccelli, M. and Grassi, C. (1988). "Evaluation of systemic host defense mechanisms in chronic bronchitis." *Respiration* **53**(1): 37-43.

Franciosi, A.N., Hobbs, B.D., McElvaney, O.J., Molloy, K., Hersh, C., Clarke, L., Gunaratnam, C., Silverman, E.K., Carroll, T.P. and McElvaney, N.G. (2020). "Clarifying

the risk of lung disease in SZ alpha-1 antitrypsin deficiency." *American Journal of Respiratory and Critical Care Medicine* **202**(1): 73-82.

Franciosi, A.N., Alkhunaizi, M.A., Woodsmith, A., Aldaihani, L., Alkandari, H., Lee, S.E., Fee, L.T., McElvaney, N.G. and Carroll, T.P. (2021). "Alpha-1 antitrypsin deficiency and tobacco smoking: Exploring risk factors and smoking cessation in a registry population." *Journal of Chronic Obstructive Pulmonary Disease* **18**(1): 76-82.

Fregonese, L. and Stolk, J. (2008). "Hereditary alpha-1-antitrypsin deficiency and its clinical consequences." *Orphanet Journal of Rare Diseases* **3**.

Fujinaga, M., Chernaia, M.M., Halenbeck, R., Koths, K. and James, M.N.G. (1996). "The crystal structure of PR3, a neutrophil serine proteinase antigen of Wegener's granulomatosis antibodies." *Journal of Molecular Biology* **261**: 267-77.

Gadek, J.E., Klein, H.G., Holland, P.V. and Crystal, R.G. (1981). "Replacement therapy of alpha 1-antitrypsin deficiency. Reversal of protease-antiprotease imbalance within the alveolar structures of PiZ subjects." *Journal of Clinical Investigation* **68**(5): 1158-65.

Gagnon, P., Guenette, J.A., Langer, D., Laviolette, L., Mainguy, V., Maltais, F., Ribeiro, F. and Saey, D. (2014). "Pathogenesis of hyperinflation in chronic obstructive pulmonary disease." *International Journal of Chronic Obstructive Pulmonary Disease* **9**: 187-201.

Gane, J. and Stockley, R.A. (2012). "Mechanisms of neutrophil transmigration across the vascular endothelium in COPD." *Thorax* **67**(6): 553.

GE Healthcare (2016). *Effects of multiple freeze/thaw cycles on trypsin activity*.

Gershon, A.S., Warner, L., Cascagnette, P., Victor, J.C. and To, T. (2011). "Lifetime risk of developing chronic obstructive pulmonary disease: A longitudinal population study." *Lancet* **378**(9795): 991-6.

Gettins, P.G. (2002). "Serpin structure, mechanism, and function." *Chemical Reviews* **102**(12): 4751-804.

Gibbs, L.S., Lai, L. and Malik, A.B. (1990). "Tumor necrosis factor enhances the neutrophil-dependent increase in endothelial permeability." *Journal of Cellular Physiology* **145**(3): 496-500.

Glaab, T., Vogelmeier, C. and Buhl, R. (2010). "Outcome measures in chronic obstructive pulmonary disease (COPD): Strengths and limitations." *Respiratory Research* **11**(1): 79.

Global Initiative for Chronic Obstructive Lung Disease (2021). *Global strategy for the diagnosis, management and prevention of chronic obstructive pulmonary disease*.

Gough, J. (1965). "The pathology of emphysema." *Postgraduate Medical Journal* **41**: 392-400.

Grabcanovic-Musija, F., Obermayer, A., Stoiber, W., Krautgartner, W.D., Steinbacher, P., Winterberg, N., Bathke, A.C., Klappacher, M. and Studnicka, M. (2015). "Neutrophil extracellular trap (NET) formation characterises stable and exacerbated COPD and correlates with airflow limitation." *Respiratory Research* **16**(1): 59.

Grabiec, A.M. and Hussell, T. (2016). "The role of airway macrophages in apoptotic cell clearance following acute and chronic lung inflammation." *Seminars in Immunopathology* **38**(4): 409-23.

Graham, K.S., Le, A. and Sifers, R.N. (1990). "Accumulation of the insoluble PiZ variant of human alpha 1-antitrypsin within the hepatic endoplasmic reticulum does not elevate the steady-state level of GRP78/BIP." *Journal of Biological Chemistry* **265**(33): 20463-8.

Green, C.E., Vayalapra, S., Hampson, J.A., Mukherjee, D., Stockley, R.A. and Turner, A.M. (2015). "PiSZ alpha-1 antitrypsin deficiency (AATD): Pulmonary phenotype and prognosis relative to PiZZ AATD and PiMM COPD." *Thorax* **70**(10): 939-45.

Greene, C.M. and McElvaney, N.G. (2009). "Proteases and antiproteases in chronic neutrophilic lung disease - relevance to drug discovery." *British Journal of Pharmacology* **158**(4): 1048-58.

Guarino, C., Gruba, N., Grzywa, R., Dyguda-Kazimierowicz, E., Hamon, Y., Legowska, M., Skorenski, M., Dallet-Choisy, S., Marchand-Adam, S., Kellenberger, C., Jenne, D.E., Sienczyk, M., Lesner, A., Gauthier, F. and Korkmaz, B. (2018). "Exploiting the s4-s5 specificity of human neutrophil proteinase 3 to improve the potency of peptidyl di(chlorophenyl)-phosphonate ester inhibitors: A kinetic and molecular modeling analysis." *Journal of Medicinal Chemistry* **61**(5): 1858-70.

Gudmann, N.S., Manon-Jensen, T., Sand, J.M.B., Diefenbach, C., Sun, S., Danielsen, A., Karsdal, M.A. and Leeming, D.J. (2018). "Lung tissue destruction by proteinase 3 and cathepsin G mediated elastin degradation is elevated in chronic obstructive pulmonary disease." *Biochemical and Biophysical Research Communications*.

Guillot, L., Nathan, N., Tabary, O., Thouvenin, G., Le Rouzic, P., Corvol, H., Amselem, S. and Clement, A. (2013). "Alveolar epithelial cells: Master regulators of lung homeostasis." *The International Journal of Biochemistry & Cell Biology* **45**(11): 2568-73.

Gunawardena, K.A., Gullstrand, H. and Perrett, J. (2013). "Pharmacokinetics and safety of AZD9668, an oral neutrophil elastase inhibitor, in healthy volunteers and patients with COPD." *International Journal of Clinical Pharmacology and Therapeutics* **51**(4): 288-304.

Guyot, N., Wartelle, J., Malleret, L., Todorov, A.A., Devouassoux, G., Pacheco, Y., Jenne, D.E. and Belaaouaj, A. (2014). "Unopposed cathepsin G, neutrophil elastase, and proteinase 3 cause severe lung damage and emphysema." *American Journal of Pathology* **184**(8): 2197-210.

Hajjar, E., Korkmaz, B., Gauthier, F., Brandsdal, B.O., Witko-Sarsat, V. and Reuter, N. (2006). "Inspection of the binding sites of proteinase 3 for the design of a highly specific substrate." *Journal of Medicinal Chemistry* **49**(4): 1248-60.

Hajjar, E., Broemstrup, T., Kantari, C., Witko-Sarsat, V. and Reuter, N. (2010). "Structures of human proteinase 3 and neutrophil elastase - so similar yet so different." *The FEBS Journal* **277**: 2238-54.

Halbert, R.J., Natoli, J.L., Gano, A., Badamgarav, E., Buist, A.S. and Mannino, D.M. (2006). "Global burden of COPD: Systematic review and meta-analysis." *European Respiratory Journal* **28**(3): 523.

Halbwachs-Mecarelli, L., Bessou, G., Lesavre, P., Lopez, S. and Witko-Sarsat, V. (1995). "Bimodal distrubution of proteinase 3 (PR3) surface expression reflects a constitutive heterogeneity in the polymorphonuclear neutrophil pool." *FEBS Letters* **374**(1): 29-33.

Hallett, M.B. and Lloyds, D. (1995). "Neutrophil priming: The cellular signals that say 'amber' but not 'green'." *Immunology Today* **16**(6): 264-8.

Han, S. and Mallampalli, R.K. (2015). "The role of surfactant in lung disease and host defense against pulmonary infections." *Annals of the American Thoracic Society* **12**(5): 765-74.

Haq, I., Irving, J.A., Saleh, A.D., Dron, L., Regan-Mochrie, G.L., Motamedi-Shad, N., Hurst, J.R., Gooptu, B. and Lomas, D.A. (2016). "Deficiency mutations of alpha-1 antitrypsin. Effects on folding, function, and polymerization." *American Journal of Respiratory Cell and Molecular Biology* **54**(1): 71-80.

Harpel, P.C. (1973). "Studies on human plasma alpha 2-macroglobulin-enzyme interactions. Evidence for proteolytic modification of the subunit chain structure." *Journal of Experimental Medicine* **138**(3): 508-21.

Harris, H. (1954). "Role of chemotaxis in inflammation." *Physiological Reviews* **34**(3): 529-62.

Hayden, L.P., Hobbs, B.D., Cohen, R.T., Wise, R.A., Checkley, W., Crapo, J.D. and Hersh, C.P. (2015). "Childhood pneumonia increases risk for chronic obstructive pulmonary disease: The copdgene study." *Respiratory Research* **16**(1): 115.

Hazeldine, J., Harris, P., Chapple, I.L., Grant, M., Greenwood, H., Livesey, A., Sapey, E. and Lord, J.M. (2014). "Impaired neutrophil extracellular trap formation: A novel defect in the innate immune system of aged individuals." *Aging Cell* **13**(4): 690-8.

Henri, V. (1902). *Théorie générale de l'action de quelques diastases*, Gauthier-Villars.

Henry, C.M., Sullivan, G.P., Clancy, D.M., Afonina, I.S., Kulms, D. and Martin, S.J. (2016). "Neutrophil-derived proteases escalate inflammation through activation of IL-36 family cytokines." *Cell Reports* **14**(4): 708-22.

Herpel, L.B., Kanner, R.E., Lee, S.M., Fessler, H.E., Sciurba, F.C., Connett, J.E. and Wise, R.A. (2006). "Variability of spirometry in chronic obstructive pulmonary disease: Results from two clinical trials." *American Journal of Respiratory and Critical Care Medicine* **173**(10): 1106-13.

Hill, A.T., Campbell, E.J., Hill, S.L., Bayley, D.L. and Stockley, R.A. (2000). "Association between airway bacterial load and markers of airway inflammation in patients with stable chronic bronchitis." *The American Journal of Medicine* **109**(4): 288-95.

Hof, D.G., Repine, J.E., Peterson, P.K. and Hoidal, J.R. (1980). "Phagocytosis by human alveolar macrophages and neutrophils: Qualitative differences in the opsonic requirements for uptake of *Staphylococcus aureus* and *Streptococcus pneumoniae in vitro*." *American Review of Respiratory Disease* **121**(1): 65-71.

Hogg, J.C. (2004). "Pathophysiology of airflow limitation in chronic obstructive pulmonary disease." *Lancet* **364**(9435): 709-21.

Holme, J. and Stockley, R.A. (2009). "Ct scan appearance, densitometry, and health status in protease inhibitor SZ alpha1-antitrypsin deficiency." *Chest* **136**(5): 1284-90.

Hong, W., Juneau, R.A., Pang, B. and Swords, W.E. (2009). "Survival of bacterial biofilms within neutrophil extracellular traps promotes nontypeable *haemophilus influenzae* persistence in the chinchilla model for otitis media." *Journal of Innate Immunity* **1**(3): 215-24.

Hopkins, J.E. (2008). *Azd9668: Determination of neutrophil elastase activity in zymosan-stimulated human plasma samples from clinical study number d0520c00004.*, AstraZeneca.

Hruby, J. and Butler, J. (1975). "Variability of routine pulmonary function tests." *Thorax* **30**(5): 548-53.

Hughes, J., Johnson, R.J., Mooney, A., Hugo, C., Gordon, K. and Savill, J. (1997). "Neutrophil fate in experimental glomerular capillary injury in the rat. Emigration exceeds *in situ* clearance by apoptosis." *American Journal of Pathology* **150**(1): 223-34.

Hughes, M.J., McGettrick, H.M. and Sapey, E. (2020). "Shared mechanisms of multimorbidity in copd, atherosclerosis and type-2 diabetes: The neutrophil as a potential inflammatory target." *European Respiratory Review* **29**(155): 190102.

Hughes, M.J. (2021). *Accelerated ageing as a cause of disease pathogenesis, progression and mulit-morbidity in chronic obstructive pulmonary disease*. PhD, University of Birmingham.

Hurley, K., Lacey, N., O'Dwyer, C.A., Bergin, D.A., McElvaney, O.J., O'Brien, M.E., McElvaney, O.F., Reeves, E.P. and McElvaney, N.G. (2014). "Alpha-1 antitrypsin augmentation therapy corrects accelerated neutrophil apoptosis in deficient individuals." *The Journal of Immunology* **193**(8): 3978-91.

Hurst, S.M., Wilkinson, T.S., McLoughline, R.M., Jones, S., Horiuchi, S., Yamamoto, N., Rose-john, S., Fuller, G.M., Topley, N. and Jones, S.A. (2001). "IL-6 and its soluble receptor ochestrate a temportal switch in the pattern of leukocyte recruitment seen during acute inflammation." *Immunity* **14**(6): 705-14.

Hutchison, D.C. (1998). "Alpha 1-antitrypsin deficiency in europe: Geographical distribution of Pi types S and Z." *Respiratory Medicine* **92**(3): 367-77.

Hwaiz, R., Rahman, M., Zhang, E. and Thorlacius, H. (2015). "Platelet secretion of CXCL4 is RAC1-dependent and regulates neutrophil infiltration and tissue damage in septic lung damage." *British Journal of Pharmacology* **172**(22): 5347-59.

Iiri, T., Tohkin, M., Morishima, N., Ohoka, Y., Ui, M. and Katada, T. (1989). "Chemotactic peptide receptor-supported adp-ribosylation of a pertussis toxin substrate GTP-binding protein by cholera toxin in neutrophil-type HL-60 cells." *Journal of Biological Chemistry* **264**(35): 21394-400.

Irving, J.A., Pike, R.N., Lesk, A.M. and Whisstock, J.C. (2000). "Phylogeny of the serpin superfamily: Implications of patterns of amino acid conservation for structure and function." *Genome Research* **10**(12): 1845-64.

Iwamoto, H., Gao, J., Pulkkinen, V., Toljamo, T., Nieminen, P. and Mazur, W. (2014). "Soluble receptor for advanced glycation end-products and progression of airway disease." *BMC Pulmonary Medicine* **14**: 68.

James, A.L. (2002). "Peripheral airways in asthma." *Current Allergy and Asthma Reports* **2**(2): 166-74.

James, H.L. and Cohen, A.B. (1978). "Mechanism of inhibition of porcine elastase by human alpha-1-antitrypsin." *Journal of Clinical Investigation* **62**(6): 1344-53.

Janciauskiene, S., Eriksson, S., Callea, F., Mallya, M., Zhou, A., Seyama, K., Hata, S. and Lomas, D.A. (2004). "Differential detection of PAS-positive inclusions formed by the Z, Siiyama, and Mmalton variants of alpha1-antitrypsin." *Hepatology* **40**(5): 1203-10.

Janciauskiene, S., Wrenger, S., Immenschuh, S., Olejnicka, B., Greulich, T., Welte, T. and Chorostowska-Wynimko, J. (2018). "The multifaceted effects of alpha1-antitrypsin on neutrophil functions." *Frontiers in Pharmacology* **9**: 341-.

Janoff, A., Sloan, B., Weinbaum, G., Damiano, V., Sandhaus, R.A., Elias, J. and Kimbel, P. (1977). "Experimental emphysema induced with purified human neutrophil elastase: Tissue localization of the instilled protease." *American Review of Respiratory Disease* **115**(3): 461-78.

Jayes, L., Haslam, P.L., Gratziou, C.G., Powell, P., Britton, J., Vardavas, C., Jimenez-Ruiz, C. and Leonardi-Bee, J. (2016). "Smokehaz: Systematic reviews and meta-analyses of the effects of smoking on respiratory health." *Chest* **150**(1): 164-79.

Jepsen, L.V. and Skottun, T. (1982). "A rapid one-step method for the isolation of human granulocytes from whole blood." *Scandinavian Journal of Clinical and Laboratory Investigation* **42**(3): 235-8.

Jha, P., Ranson, M.K., Nguyen, S.N. and Yach, D. (2002). "Estimates of global and regional smoking prevalence in 1995, by age and sex." *American Journal of Public Health* **92**(6): 1002-6.

Jiang, Y.-Y., Xiao, W., Zhu, M.-X., Yang, Z.-H., Pan, X.-J., Zhang, Y., Sun, C.-C. and Xing, Y. (2012). "The effect of human antibacterial peptide lL-37 in the pathogenesis of chronic obstructive pulmonary d+isease." *Respiratory Medicine* **106**(12): 1680-9.

Jin, J., Li, S., Yu, W., Liu, X. and Sun, Y. (2018). "Emphysema and bronchiectasis in copd patients with previous pulmonary tuberculosis: Computed tomography features and clinical implications." *International Journal of Chronic Obstructive Pulmonary Disease* **13**: 375-84.

Johansson, B., Malm, J., Persson, T., Janciauskiene, S., Andersson, P., Carlson, J. and Egesten, A. (2001). "Alpha-1-antitrypsin is present in the specific granules of human eosinophilic granulocytes." *Clinical and Experimental Allergy* **31**(3): 379-86.

Johns, D.P., Walters, J.A. and Walters, E.H. (2014). "Diagnosis and early detection of COPD using spirometry." *Journal of Thoracic Disease* **6**(11): 1557-69.

Joo, S.Y., Kim, J.E., Kim, J.Y., Han, K.S. and Kim, H.K. (2010). "Usefulness of circulating vascular endothelial growth factor and neutrophil elastase as diagnostic markers of disseminated intravascular coagulation in non-cancer patients." *Korean Journal of Hematology* **45**(1): 23-8.

Jugniot, N., Duttagupta, I., Rivot, A., Massot, P., Cardiet, C., Pizzoccaro, A., Jean, M., Vanthuyne, N., Franconi, J.M., Voisin, P., Devouassoux, G., Parzy, E., Thiaudiere, E., Marque, S.R.A., Bentaher, A., Audran, G. and Mellet, P. (2018). "An elastase activity reporter for electronic paramagnetic resonance (EPR) and overhauser-enhanced magnetic resonance imaging (OMRI) as a line-shifting nitroxide." *Free Radical Biology and Medicine* **126**: 101-12.

Kallquist, L., Hansson, M., Persson, A.M., Janssen, H., Calafat, J., Tapper, H. and Olsson, I. (2008). "The tetraspanin CD63 is involved in granule targeting of neutrophil elastase." *Blood* **112**(8): 3444-54.

Kao, R.C., Wehner, N.G., Skubitz, K.M., Gray, B.H. and Hoidal, J.R. (1988). "Proteinase 3. A distinct human polymorphonuclear leukocyte proteinase that produces emphysema in hamsters." *Journal of Clinical Investigation* **82**(6): 1963-73.

Karatepe, K. and Luo, H.R. (2015). "Proteinase 3 is expressed in stem cells and regulates bone marrow hematopoiesis." *Blood* **126**(23): 1159.

Keatings, V.M., Collins, P.D., Scott, D.M. and Barnes, P.J. (1996). "Differences in interleukin-8 and tumour necrosis factor-alpha in induced sputum from patients with

chronic obstructive pulmonary disease or asthma." *American Journal of Respiratory and Critical Care Medicine* **153**(2): 512-21.

Kessenbrock, K., Frohlich, L., Sixt, M., Lammermann, T., Pfister, H., Bateman, A., Belaaouaj, A., Ring, J., Ollert, M., Fassler, R. and Jenne, D.E. (2008). "Proteinase 3 and neutrophil elastase enhance inflammation in mice by inactivating anti-inflammatory progranulin." *Journal of Clinical Investigation* **118**(7): 2438-47.

Kessenbrock, K., Krumbholz, M., Schonermarck, U., Back, W., Gross, W.L., Werb, Z., Grone, H.-J., Brinkmann, V. and Jenne, D.E. (2009). "Netting neutrophils in autoimmune small-vessel vasculitis." *Nature Medicine* **15**(6): 623-5.

Kessenbrock, K., Dau, T. and Jenne, D.E. (2011). "Tailor-made inflammation: How neutrophil serine proteases modulate the inflammatory response." *Journal of Molecular Medicine* **89**: 23-8.

Kida, K., Mizuuchi, T., Takeyama, K., Hiratsuka, T., Jinno, S., Hosoda, K., Imaizumi, A. and Suzuki, Y. (1992). "Serum secretory leukoprotease inhibitor levels to diagnose pneumonia in the elderly." *American Review of Respiratory Disease* **146**(6): 1426-9.

Kidd, V.J., Wallace, R.B., Itakura, K. and Woo, S.L.C. (1983). "A1-antitrypsin deficiency detection by direct analysis of the mutation in the gene." *Nature* **304**(5923): 230-4.

Kim, S.-H., Han, S.-Y., Azam, T., Yoon, D.-Y. and Dinarello, C.A. (2005). "Interleukin-32: A cytokine and inducer of TNFα." *Immunity* **22**: 131-42.

Kim, S., Lee, S., Her, E., Bae, S., Choi, J., Hong, J., Jaekal, J., Yoon, D., Azam, T., Dinarello, C.A. and Kim, S. (2008). "Proteinase 3-processed form of the recombinant IL-32 separate domain." *BMB Reports* **41**(11): 6.

Kim, V. and Criner, G.J. (2013). "Chronic bronchitis and chronic obstructive pulmonary disease." *American Journal of Respiratory and Critical Care Medicine* **187**(3): 228-37.

Klebanoff, S.J., Vadas, M.A., Harlan, J.M., Sparks, L.H., Gamble, J.R., Agosti, J.M. and Waltersdorph, A.M. (1986). "Stimulation of neutrophils by tumor necrosis factor." *The Journal of Immunology* **136**(11): 4220.

Knudsen, L. and Ochs, M. (2018). "The micromechanics of lung alveoli: Structure and function of surfactant and tissue components." *Histochemistry and Cell Biology* **150**(6): 661-76.

Koizumi, M., Fujino, A., Fukushima, K., Kamimura, T. and Takimoto-Kamimura, M. (2008). "Complex of human neutrophil elastase with 1/2 SLPI." *Journal of Synchrotron Radiation* **15**(Pt 3): 308-11.

Koj, A., Regoeczi, E., Toews, C.J., Leveille, R. and Gauldie, J. (1978). "Synthesis of antithrombin III and alpha-1-antitrypsin by the perfused rat liver." *Biochimica et Biophysica Acta* **539**(4): 496-504.

Kokot, K., Teschner, M., Schaefer, R.M. and Heidland, A. (1987). "Stimulation and inhibition of elastase release from human neutrophil-dependence on the calcium messenger system." *Mineral and Electrolyte Metabolite* **13**(3): 189-95.

Kolonin, A.G., Sergeeva, A., Staquicini, D.I., Smith, T.L., Tarleton, C.A., Molldrem, J.J., Sidman, R.L., Marchio, S., Pasqualini, R. and Arap, W. (2017). "Interaction between tumour cell surface receptor rage and proteinase 3 mediates prostate cancer matastasis to bone." *Cancer Research* **77**(12): 3144-50.

Koo, H.-K., Kang, H.K., Song, P., Park, H.K., Lee, S.-S. and Jung, H. (2017). "Systemic white blood cell count as a biomarker associated with severity of chronic obstructive lung disease." *Tuberculosis and Respiratory Diseases* **80**(3): 304-10.

Korkmaz, B., Poutrain, P., Hazouard, E., de Monte, M., Attucci, S. and Gauthier, F.L. (2005). "Competition between elastase and related proteases from human neutrophil for binding to α1-protease inhibitor." *American Journal of Respiratory Cell and Molecular Biology* **32**(6): 553-9.

Korkmaz, B., Moreau, T. and Gauthier, F. (2008). "Neutrophil elastase, proteinase 3 and cathepsin g: Physiochemical properties, activity and physiopathologcal functions." *Biochemie* **90**: 227-42.

Korkmaz, B., Jaillet, J., Jourdan, M.-L., Gauthier, A., Gauthier, F. and Attucci, S. (2009). "Catalytic activity and inhibition of wegener antigen proteinase 3 on the cell surface of human polymorphonuclear neutrophils." *Journal of Biological Chemistry* **284**(30): 19896-902.

Korkmaz, B., Horwitz, M.S., Jenne, D.E. and Gauthier, F. (2010). "Neutrophil elastase, proteinase 3, and cathepsin g as therapeutic targets in human diseases." *Pharmacological Reviews* **62**(4): 726-59.

Korkmaz, B., Lesner, A., Letast, S., Mahdi, Y.K., Jourdan, M.L., Dallet-Choisy, S., Marchand-Adam, S., Kellenberger, C., Viaud-Massuard, M.C., Jenne, D.E. and Gauthier, F. (2013). "Neutrophil proteinase 3 and dipeptidyl peptidase I (cathepsin c) as pharmacological targets in granulomatosis with polyangiitis (wegener granulomatosis)." *Seminars in Immunopathology* **35**(4): 411-21.

Kouchi, I., Yasuoka, S., Ueda, Y. and Ogura, T. (1993). "Analysis of secretory leukocyte protease inhibitor (slpi) in bronchial secretions from patients with hypersecretory respiratory diseases." *Tokushima Journal of Experimental Medicine* **40**(1-2): 95-107.

Krieger, E. and Vriend, G. (2014). "Yasara view - molecular graphics for all devices - from smartphones to workstations." *Bioinformatics* **30**: 2981-2.

Kristensen, J.H., Karsdal, M.A., Sand, J.M., Willumsen, N., Diefenbach, C., Svensson, B., Hägglund, P. and Oersnes-Leeming, D.J. (2015). "Serological assessment of neutrophil elastase activity on elastin during lung ECM remodeling." *BMC Pulmonary Medicine* **15**: 53.

Kuckleburg, C.J., Tilkens, S.M., Santoso, S. and Newman, P.J. (2012). "Proteinase 3 contributes to transendothelial migration of NB1-positive neutrophils." *The Journal of Immunology* **188**(5): 2419-26.

Kuebler, W.M., Kuhnle, G.E. and Goetz, A.E. (1999). "Leukocyte margination in alveolar capillaries: Interrelationship with functional capillary geometry and microhemodynamics." *Journal of Vascular Research* **36**(4): 282-8.

Kurian, A., Neumann, E.J., Hall, W.F. and Marks, D. (2012). "Effects of blood sample mishandling on ELISA results for infectious bronchitis virus, avian encephalomyelitis virus and chicken anaemia virus." *The Veterinary Journal* **192**(3): 378-81.

Kuroda, K., Okumura, K., Isogai, H. and Isogai, E. (2015). "The human cathelicidin antimicrobial peptide lL-37 and mimics are potential anti-cancer drugs." *Frontiers in Oncology* **5**: 10.

Lacey, N., McElvaney, O.J., Hawkins, P., McEnery, T., Lee, M.Q., Hoo, M., Reeves, E.P. and McElvaney, N.G. (2020). "Increased neutrophil-platelet interactions in alpha-1 antitrypsin deficient individuals is corrected post augmentation therapy." *American Journal of Respiratory and Critical Care Medicine* (201): A4783-A.

Lacoste, J.Y., Bousquet, J., Chanez, P., Van Vyve, T., Simony-Lafontaine, J., Lequeu, N., Vic, P., Enander, I., Godard, P. and Michel, F.B. (1993). "Eosinophilic and neutrophilic inflammation in asthma, chronic bronchitis, and chronic obstructive pulmonary disease." *Journal of Allergy and Clinical Immunology* **92**(4): 537-48.

Lacy, P. (2006). "Mechanisms of degranulation in neutrophils." *Allergy, asthma, and clinical immunology : official journal of the Canadian Society of Allergy and Clinical Immunology* **2**(3): 98-108.

Lamprecht, B., McBurnie, M.A., Vollmer, W.M., Gudmundsson, G., Welte, T., Nizankowska-Mogilnicka, E., Studnicka, M., Bateman, E., Anto, J.M., Burney, P., Mannino, D.M. and Buist, S.A. (2011). "COPD in never smokers: Results from the population-based burden of obstructive lung disease study." *Chest* **139**(4): 752-63.

Laurent, P. and Bieth, J.G. (1989). "Kinetics of the inhibition of free and elastin-bound human pancreatic elastase by alpha 1-proteinase inhibitor and alpha 2-macroglobulin." *Biochimica et Biophysica Acta* **994**(3): 285-8.

Lee, J., Taneja, V. and Vassallo, R. (2012). "Cigarette smoking and inflammation: Cellular and molecular mechanisms." *Journal of Dental Research* **91**(2): 142-9.

Lee, J., Lu, Y., Oshins, R., West, J., Moneypenny, C.G., Han, K. and Brantly, M.L. (2020). "Alpha 1 antitrypsin-deficient macrophages have impaired efferocytosis of apoptotic neutrophils." *Frontiers in Immunology* **11**: 574410.

Lee, W.L., Harrison, R.E. and Grinstein, S. (2003). "Phagocytosis by neutrophils." *Microbes and Infection* **5**(14): 1299-306.

Lefrancais, E., Roga, S., V., G., Gonzalez-de-Peredo, A., Monsarrat, B., Girard, J.-P. and Cayrol, C. (2012). "IL-33 is processed into mature biosactive forms by neutrophil elastase and cathepsin g." *Proceedings of the National Academy of Sciences of the United States of America* **109**(5): 6.

Lefrançais, E., Mallavia, B., Zhuo, H., Calfee, C.S. and Looney, M.R. (2018). "Maladaptive role of neutrophil extracellular traps in pathogen-induced lung injury." *Journal of Clinical Investigation Insight* **3**(3).

Li, Y., Karlin, A., Loike, J.D. and Silverstein, S.C. (2002). "A critical concentration of neutrophils is required for effective bacterial killing in suspension." *Proceedings of the National Academy of Sciences of the United States of America* **99**(12): 8289-94.

Lien, D.C., Henson, P.M., Capen, R.L., Henson, J.E., Hanson, W.L., Wagner, W.W. and Worthen, G.S. (1991). "Neutrophil kinetics in the pulmonary microcirculation during acute inflammation." *Laboratory investigation; a journal of technical methods and pathology* **65**(2): 145-59.

Lindblad, D., Blomenkamp, K. and Teckman, J. (2007). "Alpha-1-antitrypsin mutant Z protein content in individual hepatocytes correlates with cell death in a mouse model." *Hepatology* **46**(4): 1228-35.

Linden, M., Rasmussen, J.B., Piitulainen, E., Tunek, A., Larson, M., Tegner, H., Venge, P., Laitinen, L.A. and Brattsand, R. (1993). "Airway inflammation in smokers with nonobstructive and obstructive chronic bronchitis." *American Review of Respiratory Disease* **148**(5): 1226-32.

Lineweaver, H. and Burk, D. (1934). *The determination of enzyme dissociation constants*. The Fertilizer Investigations Unit, Bureau of Chemistry and Soils, United States, Department of Agriculture. **56:** 658-66.

Liu, X., Ma, S., Turino, G. and Cantor, J. (2017). "The pattern of elastic fiber breakdown in bleomycin-induced pulmonary fibrosis may reflect microarchitectural changes." *Lung* **195**(1): 93-9.

Loison, F., Zhu, H., Karatepe, K., Kason, A., Liu, P., Ye, K., Zhou, J., Cao, S., Gong, H., Jenne, D.E., Remold-O'Donnell, E., Xu, Y. and Luo, H.R. (2014). "Proteinase 3-dependent caspase-3 cleavage modulates neutrophil death and inflammation." *Journal of Clinical Investigation* **124**(10): 14.

Lomas, D.A., Evans, D.L., Finch, J.T. and Carrell, R.W. (1992). "The mechanism of Z alpha 1-antitrypsin accumulation in the liver." *Nature* **357**(6379): 605-7.

Lomas, D.A., Silverman, E.K., Edwards, L.D., Miller, B.E., Coxson, H.O. and Tal-Singer, R. (2008). "Evaluation of serum CC-16 as a biomarker for copd in the eclipse cohort." *Thorax* **63**(12): 1058.

Lombard, C., Bouchu, D., Wallach, J. and Saulnier, J. (2005). "Proteinase 3 hydrolysis of peptides derived from human elastin exon 24." *Amino Acids* **28**: 403-8.

Long, G.L., Chandra, T., Woo, S.L., Davie, E.W. and Kurachi, K. (1984). "Complete sequence of the cdna for human alpha 1-antitrypsin and the gene for the S variant." *Biochemistry* **23**(21): 4828-37.

Louhelainen, N., Rytilä, P., Haahtela, T., Kinnula, V.L. and Djukanović, R. (2009). "Persistence of oxidant and protease burden in the airways after smoking cessation." *BMC Pulmonary Medicine* **9**(1): 25.

Low, E.V., Hughes, S.M., Zaffarullah, S., Kantas, D., Stockley, R.A. and Turner, A.M. (2018). "ICS use may modify FEV1 decline in α1-antitrypsin deficiency patients with relatively high blood eosinophils." *Respiration* **95**(2): 114-21.

Lucena, R., Moreno, P., Pérez-Rico, A. and Ginel, P.J. (1998). "Effects of haemolysis, lipaemia and bilirubinaemia on an enzyme-linked immunosorbent assay for cortisol and free thyroxine in serum samples from dogs." *The Veterinary Journal* **156**(2): 127-31.

Luisetti, M., Ma, S., Iadarola, P., Stone, P.J., Viglio, S., Casado, B., Lin, Y.Y., Snider, G.L. and Turino, G.M. (2008). "Desmosine as a biomarker of elastin degradation in copd: Current status and future directions." *European Respiratory Journal* **32**(5): 1146-57.

Magnussen, H., Vaz Fragoso, C.A., Miller, M.R. and Brusasco, V. (2017). "Spirometry variability must be critically interpreted before negating a clinical diagnosis of chronic obstructive pulmonary disease." *American Journal of Respiratory and Critical Care Medicine* **197**(6): 835-6.

Mahadeva, R., Atkinson, C., Li, Z., Stewart, S., Janciauskiene, S., Kelley, D.G., Parmar, J., Pitman, R., Shapiro, S.D. and Lomas, D.A. (2005). "Polymers of Z alpha1-antitrypsin co-localize with neutrophils in emphysematous alveoli and are chemotactic in vivo." *American Journal of Pathology* **166**(2): 377-86.

Mahomed, A.G. and Anderson, R. (2000). "Activation of human neutrophils with chemotactic peptide, opsonized zymosan and the calcium ionophore A23187, but not with a phorbol ester, is accompanied by efflux and store-operated influx of calcium." *Inflammation* **24**(6): 559-69.

Mannino, D.M., Tal-Singer, R., Lomas, D.A., Vestbo, J., Graham Barr, R., Tetzlaff, K., Lowings, M., Rennard, S.I., Snyder, J., Goldman, M., Martin, U.J., Merrill, D., Martin, A.L., Simeone, J.C., Fahrbach, K., Murphy, B., Leidy, N. and Miller, B. (2015). "Plasma fibrinogen as a biomarker for mortality and hospitalized exacerbations in people with COPD." *Chronic Obstructive Pulmonary Diseases* **2**(1): 23-34.

Marc, M.M., Korosec, P., Kosnik, M., Kern, I., Flezar, M., Suskovic, S. and Sorli, J. (2004). "Complement factors C3a, C4a, and C5a in chronic obstructive pulmonary disease and asthma." *American Journal of Respiratory Cell and Molecular Biology* **31**(2): 216-9.

Marchand, V., Tournier, J.M., Polette, M., Nawrocki, B., Fuchey, C., Pierrot, D., Burlet, H. and Puchelle, E. (1997). "The elastase-induced expression of secretory leukocyte protease inhibitor is decreased in remodelled airway epithelium." *European Journal of Pharmacology* **336**(2-3): 187-96.

Martin, T.R. and Frevert, C.W. (2005). "Innate immunity in the lungs." *Proceedings of the American Thoracic Society* **2**(5): 403-11.

Martínez-García, M.A., Soler-Cataluña, J.J., Donat Sanz, Y., Catalán Serra, P., Agramunt Lerma, M., Ballestín Vicente, J. and Perpiñá-Tordera, M. (2011). "Factors associated with bronchiectasis in patients with COPD." *Chest* **140**(5): 1130-7.

Mathias, J.R., Perrin, B.J., Liu, T.X., Kanki, J., Look, A.T. and Huttenlocher, A. (2006). "Resolution of inflammation by retrograde chemotaxis of neutrophils in transgenic zebrafish." *Journal of Leukocyte Biology* **80**(6): 1281-8.

McCarthy, C., Reeves, E.P. and McElvaney, N.G. (2016). "The role of neutrophils in alpha-1 antitrypsin deficiency." *Annals of the American Thoracic Society* **13**(Supplement_4): S297-S304.

McDonough, J.E., Yuan, R., Suzuki, M., Seyednejad, N., Elliott, W.M., Sanchez, P.G., Wright, A.C., Gefter, W.B., Litzky, L., Coxson, H.O., Pare, P.D., Sin, D.D., Pierce, R.A., Woods, J.C., McWilliams, A.M., Mayo, J.R., Lam, S.C., Cooper, J.D. and Hogg, J.C. (2011). "Small-airway obstruction and emphysema in chronic obstructive pulmonary disease." *The New England Journal of Medicine* **365**(17): 1567-75.

McElvaney, N.G., Stoller, J.K., Buist, A.S., Prakash, U.B., Brantly, M.L., Schluchter, M.D. and Crystal, R.D. (1997). "Baseline characteristics of enrollees in the national heart, lung and blood institute registry of alpha 1-antitrypsin deficiency. Alpha 1-antitrypsin deficiency registry study group." *Chest* **111**(2): 394-403.

McElvaney, N.G., Burdon, J., Holmes, M., Glanville, A., Wark, P.A., Thompson, P.J., Hernandez, P., Chlumsky, J., Teschler, H., Ficker, J.H., Seersholm, N., Altraja, A., Mäkitaro, R., Chorostowska-Wynimko, J., Sanak, M., Stoicescu, P.I., Piitulainen, E., Vit, O., Wencker, M., Tortorici, M.A., Fries, M., Edelman, J.M. and Chapman, K.R. (2017). "Long-term efficacy and safety of α1 proteinase inhibitor treatment for emphysema caused by severe α1 antitrypsin deficiency: An open-label extension trial (RAPID-OLE)." *Lancet Respiratory Medicine* **5**(1): 51-60.

McElvaney, N.G., Sandhaus, R.A., Miravitlles, M., Turino, G.M., Seersholm, N., Wencker, M. and Stockley, R.A. (2020). "Clinical considerations in individuals with α(1)-antitrypsin Pi*SZ genotype." *European Respiratory Journal* **55**(6).

McGee, D., Schwarz, L., McClure, R., Peterka, L., Rouhani, F., Brantly, M. and Strange, C. (2010). "Is PiSS alpha-1 antitrypsin deficiency associated with disease?" *Pulmonary Medicine* **2010**: 570679.

McGrath, J.J.C. and Stampfli, M.R. (2018). "The immune system as a victim and aggressor in chronic obstructive pulmonary disease." *Journal of Thoracic Disease* **10**(Suppl 17): S2011-S7.

McLoughlin, R.M., Hurst, S.M., Nowell, M.A., Harris, D.A., Horiuchi, S., Morgan, L.W., Wilkinson, T.S., Yamamoto, N., Topley, N. and Jones, S.A. (2004). "Differential regulation of neutrophil-activating chemokines by IL-6 and its soluble receptor isoforms." *The Journal of Immunology* **172**(9): 5676-83.

Mead, J., Turner, J.M., Macklem, P.T. and Little, J.B. (1967). "Significance of the relationship between lung recoil and maximum expiratory flow." *Journal of Applied Physiology* **22**(1): 95-108.

Mehraban, S., Gu, G., Ma, S., Liu, X., Turino, G. and Cantor, J. (2020). "The proinflammatory activity of structurally altered elastic fibers." *American Journal of Respiratory Cell and Molecular Biology*.

Mercado, N., Ito, K. and Barnes, P.J. (2015). "Accelerated ageing of the lung in copd: New concepts." *Thorax* **70**(5): 482.

Michaelis, L. and Menten, M.L. (1913). "Die kinetik der invertinwirkung." *Biochemische Zeitschrift* **26**: 333-69.

Mihaila, A. and Tremblay, G.M. (2001). "Human alveolar macrophages express elafin and secretory leukocyte protease inhibitor." *Zeitschrift fur Naturforschung. C, Journal of Biosciences* **56**(3-4): 291-7.

Miller, M.R., Quanjer, P.H., Swanney, M.P., Ruppel, G. and Enright, P.L. (2011). "Interpreting lung function data using 80% predicted and fixed thresholds misclassifies more than 20% of patients." *Chest* **139**(1): 52-9.

Miralda, I., Uriarte, S.M. and McLeish, K.R. (2017). "Multiple phenotypic changes define neutrophil priming." *Frontiers in Cellular and Infection Microbiology* **7**: 217-.

Miravitlles, M., Mayordomo, C., Artés, M., Sánchez-Agudo, L., Nicolau, F. and Segu, J.L. (1999). "Treatment of chronic obstructive pulmonary disease and its exacerbations in general practice." *Respiratory Medicine* **93**(3): 173-9.

Miravitlles, M., Garcia-Sidro, P., Fernandez-Nistal, A., Buendia, M.J., Espinosa de Los Monteros, M.J., Esquinas, C. and Molina, J. (2015). "The chronic obstructive pulmonary disease assessment test improves the predictive value of previous exacerbations for poor outcomes in COPD." *International Journal of Chronic Obstructive Pulmonary Disease* **10**: 2571-9.

Miravitlles, M., Dirksen, A., Ferrarotti, I., Koblizek, V., Lange, P., Mahadeva, R., McElvaney, N.G., Parr, D., Piitulainen, E., Roche, N., Stolk, J., Thabut, G., Turner, A., Vogelmeier, C. and Stockley, R.A. (2017). "European respiratory society statement: Diagnosis and treatment of pulmonary disease in α-1 antitrypsin deficiency." *European Respiratory Journal* **50**(5): 1700610.

Modest, E.J. and Sengupta, S.K. (1974). "7-substituted actinomycin D (NSC-analogs as fluorescent DNA-binding and experimental antitumor agents." *Cancer Chemotherapy Reports* **58**(1): 35-48.

Molloy, K., Hersh, C.P., Morris, V.B., Carroll, T.P., O'Connor, C.A., Lasky-Su, J.A., Greene, C.M., O'Neill, S.J., Silverman, E.K. and McElvaney, N.G. (2014). "Clarification of the risk of chronic obstructive pulmonary disease in α1-antitrypsin deficiency pimz heterozygotes." *American Journal of Respiratory and Critical Care Medicine* **189**(4): 419-27.

Montanelli, A., Mainardi, E., Pini, L., Corda, L. and Grassi, V. (2002). "Alpha-1-antitrypsin deficiency and nephropathy." *Nephron* **90**(1): 114-5.

Mornex, J.F., Chytil-Weir, A., Martinet, Y., Courtney, M., LeCocq, J.P. and Crystal, R.G. (1986). "Expression of the alpha-1-antitrypsin gene in mononuclear phagocytes of normal and alpha-1-antitrypsin-deficient individuals." *Journal of Clinical Investigation* **77**(6): 1952-61.

Morrison, H.M., Welgus, H.G., Stockley, R.A., Burnett, D. and Campbell, E.J. (1990). "Inhibition of human leukocyte elastase bound to elastin: Relative ineffectiveness and two mechanisms of inhibitory activity." *American Journal of Respiratory Cell and Molecular Biology* **2**(3): 263-9.

Mottola, C. and Romeo, D. (1982). "Calcium movement and membrane potential changes in the early phase of neutrophil activation by phorbol myristate acetate: A study with ion-selective electrodes." *The Journal of cell biology* **93**(1): 129-34.

Mulgrew, A.T., Taggart, C.C., Lawless, M.W., Greene, C.M., Brantly, M.L., O'Neill, S.J. and McElvaney, N.G. (2004). "Z α1-antitrypsin polymerizes in the lung and acts as a neutrophil chemoattractant." *Chest* **125**(5): 1952-7.

Muller, A., Voswinkel, J., Gottschlich, S. and Csernok, E. (2007). "Human proteinase 3 (PR3) and its binding molecules: Implications for inflammatory and PR3-related autoimmune responses. ." *Annals of the New York Academy of Sciences* **1109**: 84-92.

Murray, J.F. and Mason, R.J. (2010). *Anatomy and development of the respiratory tract*. Murray and nadel's textbook of respiratory medicine. Philadelphia, Saunders Elsevier.

Nagata, M., Nakagome, K. and Soma, T. (2020). "Mechanisms of eosinophilic inflammation." *Asia Pacific Allergy* **10**(2): e14.

Nakajima, K., Powers, J.C., Ashe, B.M. and Zimmerman, M. (1979). "Mapping the extended substrate binding site of cathepsin g and human leukocyte elastase. Studies with peptide substrates related to the alpha 1-protease inhibitor reactive site." *Journal of Biological Chemistry* **254**(10): 4027-32.

Narasaraju, T., Yang, E., Samy, R.P., Ng, H.H., Poh, W.P., Liew, A.-A., Phoon, M.C., van Rooijen, N. and Chow, V.T. (2011). "Excessive neutrophils and neutrophil

extracellular traps contribute to acute lung injury of influenza pneumonitis." *American Journal of Pathology* **179**(1): 199-210.

National Institute for Health and Care Excellence (2018). *Evaluation consultation document –human alpha1-proteinase inhibitor for treating emphysema*. National Institute for Health and Care Excellence.

Navia, M.A., McKeever, B.M., Springer, J.P., Lin, T.Y., Williams, H.R., Fluder, E.M., Dorn, C.P. and Hoogsteen, K. (1989). "Structure of human neutrophil elastase in complex with a peptide chloromethyl ketone inhibitor at 1.84-a resolution." *Proceedings of the National Academy of Sciences of the United States of America* **86**(1): 7-11.

Nemeth, T. and Mocsai, A. (2016). "Feedback amplification of neutrophil function." *Cell* **37**(6): 412-24.

Newby, P.R., Carter, R.I. and Stockley, R.A. (2017). *Aα-val^{541} a novel biomarker of proteinase 3 activity* American Thoracic Society 2017, American Thoracic Society**:** A5247-A.

Newby, P.R., Crossley, D., Crisford, H., Stockley, J.A., Mumford, R.A., Carter, R.I., Sapey, E., Bolton, C.E., Hopkinson, N.S., Mahadeva, R., Steiner, M.C., Wilkinson, T.M.A. and Stockley, R.A. (2019). "A specific proteinase 3 activity footprint in alpha-1 antitrypsin deficiency." *European Respiratory Journal Open Research*.

Ng, M., Freeman, M.K., Fleming, T.D., Robinson, M., Dwyer-Lindgren, L., Thomson, B., Wollum, A., Sanman, E., Wulf, S., Lopez, A.D., Murray, C.J. and Gakidou, E. (2014). "Smoking prevalence and cigarette consumption in 187 countries, 1980-2012." *Journal of Vascular Research* **311**(2): 183-92.

Ni, Y., Shi, G., Yu, Y., Hao, J., Chen, T. and Song, H. (2015). "Clinical characteristics of patients with chronic obstructive pulmonary disease with comorbid bronchiectasis: A systemic review and meta-analysis." *International Journal of Chronic Obstructive Pulmonary Disease* **10**: 1465-75.

Nick, J.A., Avdi, N.J., Young, S.K., Knall, C., Gerwins, P., Johnson, G.L. and Worthen, G.S. (1997). "Common and distinct intracellular signaling pathways in human neutrophils utilized by platelet activating factor and fMLP." *Journal of Clinical Investigation* **99**(5): 975-86.

Norberg, B., Bandmann, U. and Rydgren, L. (1977). "Amoeboid movement in human leucocytes: Basic mechanisms, cytobiological and clinical significance." *Journal of Mechanochemistry & Cell Motility* **4**(1): 37-53.

Nyon, M.P., Segu, L., Cabrita, L.D., Lévy, G.R., Kirkpatrick, J., Roussel, B.D., Patschull, A.O., Barrett, T.E., Ekeowa, U.I., Kerr, R., Waudby, C.A., Kalsheker, N., Hill, M., Thalassinos, K., Lomas, D.A., Christodoulou, J. and Gooptu, B. (2012). "Structural dynamics associated with intermediate formation in an archetypal conformational disease." *Structure* **20**(3): 504-12.

O'Brien, C., Guest, P.J., Hill, S.L. and Stockley, R.A. (2000). "Physiological and radiological characterisation of patients diagnosed with chronic obstructive pulmonary disease in primary care." *Thorax* **55**(8): 635-42.

O'Donnell, A.E. (2011). "Bronchiectasis in patients with COPD: A distinct COPD phenotype?" *Chest* **140**(5): 1107-8.

O'Shaughnessy, T.C., Ansari, T.W., Barnes, N.C. and Jeffery, P.K. (1997). "Inflammation in bronchial biopsies of subjects with chronic bronchitis: Inverse relationship of CD8+ t lymphocytes with FEV1." *American Journal of Respiratory and Critical Care Medicine* **155**(3): 852-7.

Obermayer, A., Stoiber, W., Krautgartner, W.-D., Klappacher, M., Kofler, B., Steinbacher, P., Vitkov, L., Grabcanovic-Musija, F. and Studnicka, M. (2014). "New aspects on the structure of neutrophil extracellular traps from chronic obstructive pulmonary disease and in vitro generation." *PLOS ONE* **9**(5): e97784.

Oelsner, E.C., Carr, J.J., Enright, P.L., Hoffman, E.A., Folsom, A.R., Kawut, S.M., Kronmal, R.A., Lederer, D.J., Lima, J.A.C., Lovasi, G.S., Smith, B.M., Shea, S.J. and Barr, R.G. (2016). "Per cent emphysema is associated with respiratory and lung cancer mortality in the general population: A cohort study." *Thorax* **71**(7): 624.

Ogawa, K., Suzuki, K., Okutsu, M., Yamazaki, K. and Shinkai, S. (2008). "The association of elevated reactive oxygen species levels from neutrophils with low-grade inflammation in the elderly." *Immunity & Ageing* **5**: 13-.

Ostrowski, S. and Barud, W. (2006). "Factors influencing lung function: Are the predicted values for spirometry reliable enough?" *Journal of Physiology and Pharmacology* **57 Suppl 4**: 263-71.

Oswald, M.W., Hunt, H.H. and Lazarchick, J. (1983). "Normal range of plasma fibrinogen." *American Journal of Medical Technology* **49**(1): 57-9.

Owen, C.A., Campbell, M.A., Sannes, P.L., Boukedes, S.S. and Campbell, E.J. (1995). "Cell surface-bound elastase and cathepsin G on human neutrophils: A novel, non-oxidative mechanism by which neutrophils focus and preserve catalytic activity of serine proteinases." *Jounal of Cell Biology* **131**(3): 775-89.

Owen, C.A. (2008). "Roles for proteinases in the pathogenesis of chronic obstructive pulmonary disease." *International Journal of Chronic Obstructive Pulmonary Disease* **3**(2): 253-68.

Palmer, R.M. and Salmon, J.A. (1983). "Release of leukotriene B4 from human neutrophils and its relationship to degranulation induced by n-formyl-methionyl-leucyl-phenylalanine, serum-treated zymosan and the ionophore A23187." *Immunology* **50**(1): 65-73.

Pandey, K.C., De, S. and Mishra, P.K. (2017). "Role of proteases in chronic obstructive pulmonary disease." *Frontiers in Pharmacology* **8**: 9.

Papayannopoulos, V. (2018). "Neutrophil extracellular traps in immunity and disease." *Nature Reviews Immunology* **18**(2): 134-47.

Park, J.A., He, F., Martin, L.D., Li, Y., Chorley, B.N. and Adler, K.B. (2005). "Human neutrophil elastase induces hypersecretion of mucin from well-differentiated human bronchial epithelial cells in vitro via a protein kinase C{delta}-mediated mechanism." *American Journal of Pathology* **167**(3): 651-61.

Parr, D.G., Dirksen, A., Piitulainen, E., Deng, C., Wencker, M. and Stockley, R.A. (2009). "Exploring the optimum approach to the use of ct densitometry in a randomised placebo-controlled study of augmentation therapy in alpha 1-antitrypsin deficiency." *Respiratory Research* **10**(1): 75.

Patel, I.S., Vlahos, I., Wilkinson, T.M., Lloyd-Owen, S.J., Donaldson, G.C., Wilks, M., Reznek, R.H. and Wedzicha, J.A. (2004). "Bronchiectasis, exacerbation indices, and inflammation in chronic obstructive pulmonary disease." *American Journal of Respiratory and Critical Care Medicine* **170**(4): 400-7.

Pedersen, F., Marwitz, S., Holz, O., Kirsten, A., Bahmer, T., Waschki, B., Magnussen, H., Rabe, K.F., Goldmann, T., Uddin, M. and Watz, H. (2015). "Neutrophil extracellular trap formation and extracellular DNA in sputum of stable COPD patients." *Respiratory Medicine* **109**(10): 1360-2.

Pedrazzani, C., Mantovani, G., Salvagno, G.L., Baldiotti, E., Ruzzenente, A., Iacono, C., Lippi, G. and Guglielmi, A. (2016). "Elevated fibrinogen plasma level is not an independent predictor of poor prognosis in a large cohort of western patients undergoing surgery for colorectal cancer." *World Journal of Gastroenterology* **22**(45): 9994-10001.

Perlmutter, D.H., Travis, J. and Punsal, P.I. (1988). "Elastase regulates the synthesis of its inhibitor, alpha 1-proteinase inhibitor, and exaggerates the defect in homozygous PiZZ alpha 1 PI deficiency." *Journal of Clinical Investigation* **81**(6): 1774-80.

Petersen, C.M. (1993). "Alpha 2-macroglobulin and pregnancy zone protein. Serum levels, alpha 2-macroglobulin receptors, cellular synthesis and aspects of function in relation to immunology." *Danish Medical Bulletin* **40**(4): 409-46.

Pham, C.T.N. (2006). "Neutrophil serine proteases: Specific regulators of inflammation." *Nature Reviews Immunology* **6**: 541.

Phillips, B., Veljkovic, E., Peck, M.J., Buettner, A., Elamin, A., Guedj, E., Vuillaume, G., Ivanov, N.V., Martin, F., Boue, S., Schlage, W.K., Schneider, T., Titz, B., Talikka, M., Vanscheeuwijck, P., Hoeng, J. and Peitsch, M.C. (2015). "A 7-month cigarette smoke inhalation study in C57BL/6 mice demonstrates reduced lung inflammation and emphysema following smoking cessation or aerosol exposure from a prototypic modified risk tobacco product." *Food and Chemical Toxicology* **80**: 328-45.

Pierce, R.A., Mariani, T.J. and Senior, R.M. (1995). "Elastin in lung development and disease." *Ciba Foundation Symposium* **192**: 199-212.

Popa, C., Netea, M.G., van Riel, P.L.C.M., van der Meer, J.W.M. and Stalenhoef, A.F.H. (2007). "The role of tnf-a in chronic inflammatory conditions, intermediary metabolism, and cardiovascular risk." *Journal of Lipid Research* **48**: 751-62.

Postma, D.S., Reddel, H.K., ten Hacken, N.H. and van den Berge, M. (2014). "Asthma and chronic obstructive pulmonary disease: Similarities and differences." *Clinics in Chest Medicine* **35**(1): 143-56.

Poulter, L.W. (1997). "Basic concepts in lung immunology." *Research in Immunology* **148**(1): 8-13.

Pouwels, S.D., Klont, F., Bischoff, R. and ten Hacken, N.H.T. (2019). "Confounding factors affecting srage as a biomarker for chronic obstructive pulmonary disease." *American Journal of Respiratory and Critical Care Medicine* **200**(1): 114-.

Pride, N.B. (2001). "Smoking cessation: Effects on symptoms, spirometry and future trends in COPD." *Thorax* **56**(suppl 2): ii7.

Punekar, Y.S., Shukla, A. and Mullerova, H. (2014). "Copd management costs according to the frequency of COPD exacerbations in UK primary care." *International Journal of Chronic Obstructive Pulmonary Disease* **9**: 65-73.

Qizilbash, A. and Young-Pong, O. (1983). "Alpha 1 antitrypsin liver disease differential diagnosis of PASiastase-resistant globules in liver cells." *American Journal of Clinical Pathology* **79**(6): 697-702.

Quach, A. and Ferrante, A. (2017). "The application of dextran sedimentation as an initial step in neutrophil purification promotes their stimulation, due to the presence of monocytes." *Journal of Immunology Research* **2017**: 1254792.

Quinn, M., Ellis, P., Pye, A. and Turner, A.M. (2020). "Obstacles to early diagnosis and treatment of alpha-1 antitrypsin deficiency: Current perspectives." *Therapeutics and Clinical Risk Management* **16**: 1243-55.

Quint, J.K. and Wedzicha, J.A. (2007). "The neutrophil in chronic obstructive pulmonary disease." *Journal of Allergy and Clinical Immunology* **119**(5): 1065-71.

Rani, L., Minz, R.W., Sharma, A., Anand, S., Gupta, D., Panda, N.K. and Sakhuja, V.K. (2015). "Predominance of PR3 specific immune response and skewed Th17 vs. T-regulatory miliew in active granfulomatosis with polyangiitis." *Cytokine* **71**: 7.

Rao, N.V., Wehner, N.G., Marshall, B.C., Gray, W.R., Gray, B.H. and Hoidal, J.R. (1991). "Characterisation of proteinase 3 (PR-3), a neutrophil serine proteinase: Structural and functional properties." *Journal of Biological Chemistry* **266**(15): 9540-8.

Rao, N.V., Marshall, B.C., Gray, B.H. and Hoidal, J.R. (1993). "Interaction of secretory leukocyte protease inhibitor with proteinase-3." *American Journal of Respiratory Cell and Molecular Biology* **8**(6).

Raundhal, M., Morse, C., Khare, A., Oriss, T.B., Milosevic, J., Trudeau, J., Huff, R., Pilewski, J., Holguin, F., Kolls, J., Wenzel, S., Ray, P. and Ray, A. (2015). "High IFN-γ and low SLPI mark severe asthma in mice and humans." *Journal of Clinical Investigation* **125**(8): 3037-50.

Remold-O'Donnell, E., Nixon, J.C. and Rose, R.M. (1989). "Elastase inhibitor. Characterization of the human elastase inhibitor molecule associated with monocytes, macrophages, and neutrophils." *Journal of Experimental Medicine* **169**(3): 1071-86.

Ren, K. and Torres, R. (2009). "Role of interleukin-1beta during pain and inflammation." *Brain Research Reviews* **60**(1): 57-64.

Ribeiro, L.I. and Ind, P.W. (2016). "Effect of cannabis smoking on lung function and respiratory symptoms : A structured literature review." *NPJ Primary Care Respiratory Medicine* **26**: 16071-.

Richardson, R.H., Guenter, C.A., Welch, M.H., Hyde, R.M. and Hammarsten, J.F. (1969). "The pattern of inheritance of alpha1 antitrypsin deficiency and associated pulmonary disease." *American Review of Respiratory Disease* **100**(5): 619-25.

Robache-Gallea, S., Morand, V., Bruneau, J.M., Schoot, B., Tagat, E., Realo, E., Chouaib, S. and Roman-Roman, S. (1995). "In vitro processing of human tumour necrosis factor-alpha." *Journal of Biological Chemistry* **270**(40): 23688-92.

Roberts, H.R., Wells, A.U., Milne, D.G., Rubens, M.B., Kolbe, J., Cole, P.J. and Hansell, D.M. (2000). "Airflow obstruction in bronchiectasis: Correlation between computed tomography features and pulmonary function tests." *Thorax* **55**(3): 198-204.

Ron, D. and Walter, P. (2007). "Signal integration in the endoplasmic reticulum unfolded protein response." *Nature Reviews Molecular Cell Biology* **8**(7): 519-29.

Sadhra, S., Kurmi, O.P., Sadhra, S.S., Lam, K.B.H. and Ayres, J.G. (2017). "Occupational COPD and job exposure matrices: A systematic review and meta-analysis." *International Journal of Chronic Obstructive Pulmonary Disease* **12**: 725-34.

Saetta, M., Finkelstein, R. and Cosio, M.G. (1994). "Morphological and cellular basis for airflow limitation in smokers." *European Respiratory Journal* **7**(8): 1505.

Saetta, M., Turato, G., Facchini, F.M., Corbino, L., Lucchini, R.E., Casoni, G., Maestrelli, P., Mapp, C.E., Ciaccia, A. and Fabbri, L.M. (1997). "Inflammatory cells in the bronchial glands of smokers with chronic bronchitis." *American Journal of Respiratory and Critical Care Medicine* **156**(5): 1633-9.

Sallenave, J.M., Shulmann, J., Crossley, J., Jordana, M. and Gauldie, J. (1994). "Regulation of secretory leukocyte proteinase inhibitor (SLPI) and elastase-specific inhibitor (ESI/elafin) in human airway epithelial cells by cytokines and neutrophilic enzymes." *American Journal of Respiratory Cell and Molecular Biology* **11**(6): 733-41.

Sallenave, J.M., Si Tahar, M., Cox, G., Chignard, M. and Gauldie, J. (1997). "Secretory leukocyte proteinase inhibitor is a major leukocyte elastase inhibitor in human neutrophils." *Journal of Leukocyte Biology* **61**(6): 695-702.

Sallenave, J.M. (2002). "Antimicrobial activity of antiproteinases." *Biochemical Society Transactions* **30**(2): 111-5.

Sandhaus, R.A. and Turino, G. (2013). "Neutrophil elastase-mediated lung disease." *Journal of Chronic Obstructive Pulmonary Disease* **10 Suppl 1**: 60-3.

Sapey, E. (2010). *Inflammation and neutrophil recruitment in ageing subjects and patients with chronic obstructive pulmonary disease*, University of Birmingham.

Sapey, E., Stockley, J.A., Greenwood, H., Ahmad, A., Bayley, D., Lord, J.M., Insall, R.H. and Stockley, R.A. (2011). "Behavioral and structural differences in migrating peripheral neutrophils from patients with chronic obstructive pulmonary disease." *American Journal of Respiratory and Critical Care Medicine* **183**(9): 1176-86.

Sapey, E., Greenwood, H., Walton, G., Mann, E., Love, A., Aaronson, N., Insall, R.H., Stockley, R.A. and Lord, J.M. (2014). "Phosphoinositide 3-kinase inhibition restores neutrophil accuracy in the elderly: Toward targeted treatments for immunosenescence." *Blood* **123**(2): 239.

Sapey, E., Patel, J.M., Greenwood, H.L., Walton, G.M., Hazeldine, J., Sadhra, C., Parekh, D., Dancer, R.C.A., Nightingale, P., Lord, J.M. and Thickett, D.R. (2017). "Pulmonary infections in the elderly lead to impaired neutrophil targeting, which is improved by simvastatin." *American Journal of Respiratory and Critical Care Medicine* **196**(10): 1325-36.

Saracevic, A., Dukic, L. and Simundic, A.M. (2019). "Haemolysis and lipemia interfere with resistin and myeloperoxidase biovendor elisa assays." *Biochemia Medica* **29**(2): 020703.

Saragih, H., Zilian, E., Jaimes, Y., Paine, A., Figueiredo, C., Eiz-Vesper, B., Blascysk, R., Larmann, J., Theilmeier, G., Burg-Roderfeld, M., Andrei-Selmer, L.-C., Becker, J.U., Santaso, S. and Immenschuh, S. (2014). "PECAM-1-dependent heme oxygenase-1 regulation via an NRF2-mediated pathway in endothelial cells." *Thrombosis and Haemostasis* **111**(6): 1077-88.

Sato, T., Hongu, T., Sakamoto, M., Funakoshi, Y. and Kanaho, Y. (2013). "Molecular mechanisms of n-formyl-methionyl-leucyl-phenylalanine-induced superoxide generation and degranulation in mouse neutrophils: Phospholipase D is dispensable." *Molecular and Cellular Biology* **33**(1): 136-45.

Sauce, D., Dong, Y., Campillo-Gimenez, L., Casulli, S., Bayard, C., Autran, B., Boddaert, J., Appay, V. and Elbim, C. (2017). "Reduced oxidative burst by primed neutrophils in the elderly individuals is associated with increased levels of the CD16bright/CD62Ldim immunosuppressive subset." *The Journals of Gerontology. Series A, Biological Sciences and Medical Sciences.* **72**(2): 163-72.

Savran, O. and Ulrik, C.S. (2018). "Early life insults as determinants of chronic obstructive pulmonary disease in adult life." *International Journal of Chronic Obstructive Pulmonary Disease* **13**: 683-93.

Schechter, I. and Berger, A. (1967). "On the size of the active site in proteases. I. Papain." *Biochemical and Biophysical Research Communications* **27**(2): 157-62.

Schleede, S., Meinel, F.G., Bech, M., Herzen, J., Achterhold, K., Potdevin, G., Malecki, A., Adam-Neumair, S., Thieme, S.F., Bamberg, F., Nikolaou, K., Bohla, A., Yildirim, A.Ö., Loewen, R., Gifford, M., Ruth, R., Eickelberg, O., Reiser, M. and Pfeiffer, F. (2012). "Emphysema diagnosis using x-ray dark-field imaging at a laser-driven compact synchrotron light source." *Proceedings of the National Academy of Sciences of the United States of America* **109**(44): 17880.

Schouten, I.G.M., Mumford, R.A., Moes, D., Hiemstra, P.S. and Stolk, J. (2021). "The course of AαVal541 as a proteinase 3 specific neo-epitope after alpha-1-antitrypsin augmentation in severe deficient patients." *Int J Mol Sci* **22**(15).

Segal, A.W. (2005). "How neutrophils kill microbes." *Annual Review of Immunology* **23**: 197-223.

Serban, K.A., Petrusca, D.N., Mikosz, A., Poirier, C., Lockett, A.D., Saint, L., Justice, M.J., Twigg, H.L., 3rd, Campos, M.A. and Petrache, I. (2017). "Alpha-1 antitrypsin supplementation improves alveolar macrophages efferocytosis and phagocytosis following cigarette smoke exposure." *PLOS ONE* **12**(4): e0176073.

Şerifoğlu, İ. and Ulubay, G. (2019). "The methods other than spirometry in the early diagnosis of COPD." *Tuberkuloz ve Toraks* **67**(1): 63-70.

Sevenoaks, M.J. and Stockley, R.A. (2006). "Chronic obstructive pulmonary disease, inflammation and co-morbidity--a common inflammatory phenotype?" *Respiratory Research* **7**(1): 70-.

Shi, J. and Ganz, T. (1998). "The role of protegrins and other elastase-activated polypeptides in the bactericidal properties of porcine inflammatory fluids." *Infection and Immunity* **66**(8): 3611.

Shock, A. and Baum, H. (1988). "Inactivation of alpha-1-proteinase inhibitor in serum by stimulated human polymorphonuclear leucocytes. Evidence for a myeloperoxidase-dependent mechanism." *Cell Biochemistry and Function* **6**(1): 13-23.

Shoji, S., Ertl, R.F., Koyama, S., Robbins, R., Leikauf, G., Von Essen, S. and Rennard, S.I. (1995). "Cigarette smoke stimulates release of neutrophil chemotactic activity from cultured bovine bronchial epithelial cells." *Clinical Science* **88**(3): 337-44.

Siddharthan, T., Grigsby, M.R., Goodman, D., Chowdhury, M., Rubinstein, A., Irazola, V., Gutierrez, L., Miranda, J.J., Bernabe-Ortiz, A., Alam, D., Kirenga, B., Jones, R., van Gemert, F., Wise, R.A. and Checkley, W. (2018). "Association between household air pollution exposure and chronic obstructive pulmonary disease outcomes in 13 low- and

middle-income country settings." *American Journal of Respiratory and Critical Care Medicine* **197**(5): 611-20.

Silva, G.E., Sherrill, D.L., Guerra, S. and Barbee, R.A. (2004). "Asthma as a risk factor for COPD in a longitudinal study." *Chest* **126**(1): 59-65.

Simchowitz, L., Spilberg, I. and Atkinson, J.P. (1980). "Superoxide generation and granule enzyme release induced by ionophore A23187. Studies on the early events of neutrophil activation." *Journal of Laboratory and Clinical Medicine* **96**(3): 408-24.

Sinden, N.J. (2012). *The role of proteinase 3 in chronic obstructive pulmonary disease*. Doctor of Philosophy, The University of Birmingham.

Sinden, N.J. and Stockley, R.A. (2013). "Proteinase 3 activity in sputum from subjects with alpha-1 anti-trypsin deficiency and COPD." *European Respiratory Journal* **41**: 1042-50.

Sinden, N.J., Baker, M.J., Smith, D.J., Kreft, J.-U., Dafforn, T.R. and Stockley, R.A. (2015). "Alpha-1-antitrypsin variants and the proteinase/anti-proteinase imbalance in chronic obstructive pulmonary disease." *American Journal of Physiology, Lung Cellular and Molecular Physiology* **308**: 12.

Singh, D., Edwards, L., Tal-Singer, R. and Rennard, S. (2010). "Sputum neutrophils as a biomarker in copd: Findings from the eclipse study." *Respiratory Research* **11**(1): 77.

Singh, D. (2017). "Small airway disease in patients with chronic obstructive pulmonary disease." *Tuberculosis and respiratory diseases* **80**(4): 317-24.

Sluis, K.B., Darlow, B.A., Vissers, M.C. and Winterbourn, C.C. (1994). "Proteinase-antiproteinase balance in tracheal aspirates from neonates." *European Respiratory Journal* **7**(2): 251.

Smallman, L.A., Hill, S.L. and Stockley, R.A. (1984). "Reduction of ciliary beat frequency in vitro by sputum from patients with bronchiectasis: A serine proteinase effect." *Thorax* **39**(9): 663-7.

Smith, C.R. (2015). "Diagnosis in chronic obstructive pulmonary disease-"too little, too late?"." *Chronic Respiratory Disease* **12**(4): 281-3.

Solovyev, M. and Gisbert, E. (2016). "Influence of time, storage temperature and freeze/thaw cycles on the activity of digestive enzymes from gilthead sea bream (Sparus aurata)." *Fish Physiology and Biochemistry* **42**(5): 1383-94.

Sorensen, O.E., Follin, P., Johnsen, A.H., Calafat, J., Tjabringa, G.S., Hiemstra, P.S. and Borregaard, N. (2001). "Human cathelicidin, hCAP-18, is processed to the antimicrobial peptide lL-37 by extracellular cleavage with proteinase 3." *Blood* **97**(12): 3951-9.

Sørheim, I.C., Johannessen, A., Gulsvik, A., Bakke, P.S., Silverman, E.K. and DeMeo, D.L. (2010). "Gender differences in COPD: Are women more susceptible to smoking effects than men?" *Thorax* **65**(6): 480.

Sottrup-Jensen, L. (1989). "Alpha-macroglobulins: Structure, shape, and mechanism of proteinase complex formation." *Journal of Biological Chemistry* **264**(20): 11539-42.

Stevens, T., Ekholm, K., Gränse, M., Lindahl, M., Kozma, V., Jungar, C., Ottosson, T., Falk-Håkansson, H., Churg, A., Wright, J.L., Lal, H. and Sanfridson, A. (2011). "AZD9668: Pharmacological characterization of a novel oral inhibitor of neutrophil elastase." *Journal of Pharmacology and Experimental Therapeutics* **339**(1): 313.

Stockley, J.A., Ismail, A.M., Hughes, S.M., Edgar, R., Stockley, R.A. and Sapey, E. (2017). "Maximal mid-expiratory flow detects early lung disease in α(1)-antitrypsin deficiency." *European Respiratory Journal* **49**(3).

Stockley, R.A. (1995). "Role of inflammation in respiratory tract infections." *The American Journal of Medicine* **99**(6b): 8s-13s.

Stockley, R.A. (1999). "Neutrophils and protease/antiprotease imbalance." *American Journal of Respiratory and Critical Care Medicine* **160**: S49-S52.

Stockley, R.A. (2001). "Proteases and antiproteases." *Novartis Found Symp* **234**: 189-99; discussion 99-204.

Stockley, R.A. (2002). "Neutrophils and the pathogenesis of COPD." *Chest* **121**(5 Suppl): 151s-5s.

Stockley, R.A. (2007). "Biomarkers in COPD: Time for a deep breath." *Thorax* **62**(8): 657.

Stockley, R.A., Parr, D.G., Piitulainen, E., Stolk, J., Stoel, B.C. and Dirksen, A. (2010). "Therapeutic efficacy of α-1 antitrypsin augmentation therapy on the loss of lung tissue: An integrated analysis of 2 randomised clinical trials using computed tomography densitometry." *Respiratory Research* **11**(1): 136.

Stockley, R.A., De Soyza, A., Gunawardena, K., Perrett, J., Forsman-Semb, K., Entwistle, N. and Snell, N. (2013a). "Phase II study of a neutrophil elastase inhibitor (AZD9668) in patients with bronchiectasis." *Respiratory Medicine* **107**(4): 524-33.

Stockley, R.A., Dirksen, A. and Stolk, J. (2013b). "Alpha-1 antitrypsin deficiency: The european experience." *Journal of Chronic Obstructive Pulmonary Disease* **10**(sup1): 50-3.

Stockley, R.A., Miravitlles, M. and Vogelmeier, C. (2013c). "Augmentation therapy for alpha-1 antitrypsin deficiency: Towards a personalised approach." *Orphanet Journal of Rare Diseases* **8**(1): 149.

Stockley, R.A., Edgar, R.G., Starkey, S. and Turner, A.M. (2018). "Health status decline in α-1 antitrypsin deficiency: A feasible outcome for disease modifying therapies?" *Respiratory Research* **19**(1): 137.

Stockley, R.A., Halpin, D.M.G., Celli, B.R. and Singh, D. (2019). "Chronic obstructive pulmonary disease biomarkers and their interpretation." *American Journal of Respiratory and Critical Care Medicine* **199**(10): 1195-204.

Stockley, R.A. (2020a). "Alpha-1 antitrypsin deficiency: Have we got the right proteinase?" *Chronic Obstructive Pulmonary Diseases* **7**(3): 163-71.

Stockley, R.A. (2020b). "Alpha-1 antitrypsin deficiency: The learning goes on." *American Journal of Respiratory and Critical Care Medicine* **202**(1): 6-7.

Stolk, J., Aggarwal, N., Hochnadel, I., Wrenger, S., Martinez-Delgado, B., Welte, T., Yevsa, T. and Janciauskiene, S. (2019). "Blood monocyte profiles in COPD patients with pimm and pizz α1-antitrypsin." *Respiratory Medicine* **148**: 60-2.

Stoller, J.K., Lacbawan, F.L. and Aboussouan, L.S. (1993). "Alpha-1 antitrypsin deficiency." *GeneReviews*.

Stone, H., McNab, G., Wood, A.M., Stockley, R.A. and Sapey, E. (2012). "Variability of sputum inflammatory mediators in COPD and α-1 antitrypsin deficiency." *European Respiratory Journal* **40**(3): 561-9.

Stone, H., Pye, A. and Stockley, R.A. (2014). "Disease associations in alpha-1-antitrypsin deficiency." *Respiratory Medicine* **108**(2): 338-43.

Stone, P.J., Calore, J.D., Snider, G.L. and Franzblau, C. (1982). "Role of alpha-macroglobulin-elastase complexes in the pathogenesis of elastase-induced emphysema in hamsters." *Journal of Clinical Investigation* **69**(4): 920-31.

Sugawara, A., Uehara, A., Nochi, T., Yamaguchi, T., Ueda, H., Sugiyama, A., Hanzawa, K., Kumagai, K., Okamura, H. and Takada, H. (2001). "Neutrophil proteinase 3-mediated induction of bioactive IL-18 secretion by human oral epithelial cells." *The Journal of Immunology* **167**(11): 6568-75.

Sukkar, M.B., Ullah, M.A., Gan, W.J., Wark, P.A.B., Chung, K.F., Hughes, J.M., Armour, C.L. and Phipps, S. (2012). "RAGE: A new frontier in chronic airways disease." *British Journal of Pharmacology* **167**(6): 1161-76.

Sullivan, A.L., Dafforn, T., Hiemstra, P.S. and Stockley, R.A. (2008). "Neutrophil elastase reduces secretion of secretory leukoproteinase inhibitor (SLPI) by lung epithelial cells: Role of charge of the proteinase-inhibitor complex." *Respiratory Research* **9**(1): 60.

Summers, C., Rankin, S.M., Condliffe, A.M., Singh, N., Peters, A.M. and Chilvers, E.R. (2010). "Neutrophil kinetics in health and disease." *Trends in Immunology* **31**(8): 318-24.

Summers, C., Singh, N.R., White, J.F., Mackenzie, I.M., Johnston, A., Solanki, C., Balan, K.K., Peters, A.M. and Chilvers, E.R. (2014). "Pulmonary retention of primed neutrophils: A novel protective host response, which is impaired in the acute respiratory distress syndrome." *Thorax* **69**(7): 623.

Suratt, B.T., Young, S.K., Lieber, J., Nick, J.A., Henson, P.M. and Worthen, G.S. (2001). "Neutrophil maturation and activation determine anatomic site of clearance from circulation." *American Journal of Physiology Lung Cellular and Molecular Physiology* **281**(4): L913-21.

Sveger, T. (1976). "Liver disease in alpha1-antitrypsin deficiency detected by screening of 200,000 infants." *The New England Journal of Medicine* **294**(24): 1316-21.

Sveger, T., Piitulainen, E. and Arborelius, M. (1995). "Clinical features and lung function in 18-year-old adolescents with alpha 1-antitrypsin deficiency." *Acta Paediatrica* **84**(7): 815-6.

Swarowska, M., Janowska, A., Polczak, A., Klimkowicz-Mrowiec, A., Pera, J., Slowik, A. and Dziedzic, T. (2014). "The sustained increase of plasma fibrinogen during ischemic stroke predicts worse outcome independently of baseline fibrinogen level." *Inflammation* **37**(4): 1142-7.

Tak, T., Wijten, P., Heeres, M., Pickkers, P., Scholten, A., Heck, A.J.R., Vrisekoop, N., Leenen, L.P., Borghans, J.A.M., Tesselaar, K. and Koenderman, L. (2017). "Human CD62Ldim neutrophils identified as a separate subset by proteome profiling and in vivo pulse-chase labeling." *Blood* **129**(26): 3476-85.

Takahashi, H., Nukiwa, T., Yoshimura, K., Quick, C.D., States, D.J., Holmes, M.D., Whang-Peng, J., Knutsen, T. and Crystal, R.G. (1988). "Structure of the human neutrophil elastase gene." *Journal of Biological Chemistry* **263**(29): 14739-47.

Tanash, H.A. and Piitulainen, E. (2019). "Liver disease in adults with severe alpha-1-antitrypsin deficiency." *Journal of Gastroenterology* **54**(6): 541-8.

Teschler, H. (2015). "Long-term experience in the treatment of α1-antitrypsin deficiency: 25 years of augmentation therapy." *Eur Respir Rev* **24**(135): 46-51.

The Torch Study Group (2004). "The torch (towards a revolution in COPD health) survival study protocol." *European Respiratory Journal* **24**(2): 206.

Thelin, T., Sveger, T. and McNeil, T.F. (1996). "Primary prevention in a high-risk group: Smoking habits in adolescents with homozygous alpha-1-antitrypsin deficiency (ATD)." *Acta Paediatrica* **85**(10): 1207-12.

Thomas, G., Tacke, R., Hedrick, C.C. and Hanna, R.N. (2015a). "Nonclassical patrolling monocyte function in the vasculature." *Arteriosclerosis, Thrombosis, and Vascular Biology* **35**(6): 1306-16.

Thomas, H.B., Moots, R.J., Edwards, S.W. and Wright, H.L. (2015b). "Whose gene is it anyway? The effect of preparation purity on neutrophil transcriptome studies." *PLOS ONE* **10**(9): e0138982.

Thomas, M., Decramer, M. and O'Donnell, D.E. (2013). "No room to breathe: The importance of lung hyperinflation in COPD." *Primary Care Respiratory Journal* **22**: 101.

Thore, M., Löfgren, S., Tärnvik, A., Monsen, T., Selstam, E. and Burman, L.G. (1985). "Anaerobic phagocytosis, killing, and degradation of streptococcus pneumoniae by human peripheral blood leukocytes." *Infection and Immunity* **47**(1): 277-81.

Torén, K., Schiöler, L., Lindberg, A., Andersson, A., Behndig, A.F., Bergström, G., Blomberg, A., Caidahl, K., Engvall, J.E., Eriksson, M.J., Hamrefors, V., Janson, C., Kylhammar, D., Lindberg, E., Lindén, A., Malinovschi, A., Lennart Persson, H., Sandelin, M., Eriksson Ström, J., Tanash, H., Vikgren, J., Johan Östgren, C., Wollmer, P. and Sköld, C.M. (2020). "The ratio FEV1/FVC and its association to respiratory symptoms—a swedish general population study." *Clinical Physiology and Functional Imaging*.

Totti, N., McCusker, K.T., Campbell, E.J., Griffin, G.L. and Senior, R.M. (1984). "Nicotine is chemotactic for neutrophils and enhances neutrophil responsiveness to chemotactic peptides." *Science* **223**(4632): 169-71.

Townend, J., Minelli, C., Mortimer, K., Obaseki, D.O., Al Ghobain, M., Cherkaski, H., Denguezli, M., Gunesekera, K., Hafizi, H., Koul, P.A., Loh, L.C., Nejjari, C., Patel, J., Sooronbayev, T., Buist, S.A. and Burney, P.G.J. (2017). "The association between chronic airflow obstruction and poverty in 12 sites of the multinational bold study." *European Respiratory Journal* **49**(6): 1601880.

Tregay, N., Begg, M., Cahn, A., Farahi, N., Povey, K., Madhavan, S., Simmonds, R., Gillett, D., Solanki, C., Wong, A., Maison, J., Lennon, M., Bradley, G., Jarvis, E., de Groot, M., Wilson, F., Babar, J., Peters, A.M., Hessel, E.M. and Chilvers, E.R. (2019). "Use of autologous 99m technetium-labelled neutrophils to quantify lung neutrophil clearance in COPD." *Thorax* **74**(7): 659.

Tsukishiro, S., Suzumori, N., Nishikawa, H., Arakawa, A. and Suzumori, K. (2005). "Use of serum secretory leukocyte protease inhibitor levels in patients to improve specificity of ovarian cancer diagnosis." *Gynecologic Oncology* **96**(2): 516-9.

Tsutsui, Y., Kuri, B., Sengupta, T. and Wintrode, P.L. (2008). "The structural basis of serpin polymerization studied by hydrogen/deuterium exchange and mass spectrometry*." *Journal of Biological Chemistry* **283**(45): 30804-11.

Tubío-Pérez, R.A., Blanco-Pérez, M., Ramos-Hernández, C. and Torres-Durán, M. (2018). "Alpha-1 antitrypsin deficiency associated with the PI*Q0(ourém) allele in a 2-year-old girl and family study. An unusual case." *Arch Bronconeumol* **54**(4): 228-30.

Turino, G.M., Barker, A.F., Brantly, M.L., Cohen, A.B., Connelly, R.P., Crystal, R.G., Eden, E., Schluchter, M.D. and Stoller, J.K. (1996). "Clinical features of individuals with

pi*sz phenotype of alpha 1-antitrypsin deficiency. Alpha 1-antitrypsin deficiency registry study group." *Am J Respir Crit Care Med* **154**(6 Pt 1): 1718-25.

Twigg, M.S., Brockbank, S., Lowry, P., FitzGerald, S.P., Taggart, C. and Weldon, S. (2015). "The role of serine proteases and antiproteases in the cystic fibrosis lung." *Mediators of Inflammation* **2015**: 10.

Ungers, M.J., Sinden, N.J. and Stockley, R.A. (2014). "Progranulin is a substrate for neutrophil-elastase and proteinase-3 in the airway and its concentration correlates with mediators of airway inflammation in COPD." *American Journal of Physiology, Lung Cellular and Molecular Physiology* **306**(1): L80-L7.

Urban, C.F., Ermert, D., Schmid, M., Abu-Abed, U., Goosmann, C., Nacken, W., Brinkmann, V., Jungblut, P.R. and Sycglinsky, A. (2009). "Neutrophil extracellular traps contain calprotectin, a cytosolic protein complex involved in host defense against candida albicans." *PLOS Pathogens* **5**(10): e1000639.

Valenzuela-Fernández, A., Planchenault, T., Baleux, F., Staropoli, I., Le-Barillec, K., Leduc, D., Delaunay, T., Lazarini, F., Virelizier, J.-L., Chignard, M., Pidard, D. and Arenzana-Seisdedos, F. (2002). "Leukocyte elastase negatively regulates stromal cell-derived factor-1 (SDF-1)/CXCR4 binding and functions by amino-terminal processing of SDF-1 and CXCR4." *Journal of Biological Chemistry* **277**(18): 15677-89.

Valvi, D., Mannino, D.M., Müllerova, H. and Tal-Singer, R. (2012). "Fibrinogen, chronic obstructive pulmonary disease (COPD) and outcomes in two united states cohorts." *International Journal of Chronic Obstructive Pulmonary Disease* **7**: 173-82.

van 't Wout, E.F., van Schadewijk, A., Savage, N.D., Stolk, J. and Hiemstra, P.S. (2012). "A1-antitrypsin production by proinflammatory and antiinflammatory macrophages and dendritic cells." *American Journal of Respiratory Cell and Molecular Biology* **46**(5): 607-13.

van der Berg, C.W., Tambourgi, D.V., Clark, H.W., Hoong, S.J., Spiller, O.B. and McGreal, E.P. (2014). "Mechanism of neutrophil dysfunction: Neutrophil serine proteases cleave and inactivate the C5a receptor." *The Journal of Immunology* **192**(4): 1787-95.

van Dijk, M., Gan, C.T., Koster, T.D., Wijkstra, P.J., Slebos, D.J., Kerstjens, H.A.M., van der Vaart, H. and Duiverman, M.L. (2020). "Treatment of severe stable COPD: The multidimensional approach of treatable traits." *ERJ open research* **6**(3): 00322-2019.

van Rossum, A.P., Rarok, A.A., Huitema, M.G., Fassina, G., Limburg, P.C. and Kallenberg, C.G. (2004). "Constitutive membrane expression of proteinase 3 (PR3) and neutrophil activation by anti-PR3 antibodies." *Journal of Leukocyte Biology* **76**(6): 1162-70.

van Wetering, S., van der Linden, A.C., van Sterkenburg, M.A., Rabe, K.F., Schalkwijk, J. and Hiemstra, P.S. (2000). "Regulation of secretory leukocyte proteinase inhibitor

(slpi) production by human bronchial epithelial cells: Increase of cell-associated SLPI by neutrophil elastase." *Journal of Investigative Medicine* **48**(5): 359-66.

Vatić, S., Mirković, N., Milošević, J.R., Jovčić, B. and Polović, N.Đ. (2020). "Trypsin activity and freeze-thaw stability in the presence of ions and non-ionic surfactants." *Journal of Bioscience and Bioengineering*.

Virca, G.D. and Travis, J. (1984). "Kinetics of association of human proteinases with human alpha 2-macroglobulin." *Journal of Biological Chemistry* **259**(14): 8870-4.

Vogt, K.L., Summers, C., Chilvers, E.R. and Condliffe, A.M. (2018). "Priming and de-priming of neutrophil responses in vitro and in vivo." *European Journal of Clinical Investigation* **48 Suppl 2**: e12967.

von Nussbaum, F. and Li, V.M.J. (2015). "Neutrophil elastase inhibitors for the treatment of (cardio)pulmonary diseases: Into clinical testing with pre-adaptive pharmacophores." *Bioorganic & Medicinal Chemistry Letters* **25**(20): 4370-81.

Vonk, J.M., Jongepier, H., Panhuysen, C.I., Schouten, J.P., Bleecker, E.R. and Postma, D.S. (2003). "Risk factors associated with the presence of irreversible airflow limitation and reduced transfer coefficient in patients with asthma after 26 years of follow up." *Thorax* **58**(4): 322-7.

Voynow, J.A., Fischer, B.M., Malarkey, D.E., Burch, L.H., Wong, T., Longphre, M., Ho, S.B. and Foster, W.M. (2004). "Neutrophil elastase induces mucus cell metaplasia in mouse lung." *American Journal of Physiology-Lung Cellular and Molecular Physiology* **287**(6): L1293-L302.

Walker, E.M., Jasper, A.E., Davis, L., Yip, K.P., Faniyi, A.A., Hughes, M.J., Crisford, H.A., Spittle, D.A., Sapey, E., Belchamber, K.B.R. and Scott, A. (2020). "Mitigating health risks to reopen a clinical research laboratory during the covid-19 pandemic: A framework." *JMIR Research Protocols* **9**(12): e22570-e.

Walton, G., Butler, A., Stockley, R., Donnelly, L. and Sapey, E. (2017). "Impaired serum opsonisation of non typeable haemophilus influenzae in copd and alpha-1 anti-trypsin deficiency. A potential mechanism for reduced bacterial clearance?" *European Respiratory Journal* **50**(suppl 61): PA993.

Walton, G.M. (2018). *Neutrophil migration and phagocytosis in chronic obstructive pulmonary disease*. PhD, University of Birmingham.

Wang, S., Dangerfield, J.P., Young, R.E. and Nourshargh, S. (2005). "Pecam-1, α6 integrins and neutrophil elastase cooperate in mediating neutrophil transmigration." *Journal of Cell Science* **118**(9): 2067-76.

Wang, Z., Yao, W.Z., Xia, G.G. and Sun, D.J. (2008). "[the expression and implications of human alpha-defensin 1-3 in serum and induced sputum in patients with chronic obstructive pulmonary disease]." *Zhonghua Jie He He Hu Xi Za Zhi* **31**(6): 410-3.

Weibel, E.R. (1963). *Morphometry of the human lung*, Springer-Verlag Berlin Heidelberg.

Weldon, S., McNally, P., McElvaney, N.G., Elborn, J.S., McAuley, D.F., Wartelle, J., Belaaouaj, A., Levine, R.L. and Taggart, C.C. (2009). "Decreased levels of secretory leucoprotease inhibitor in the pseudomonas-infected cystic fibrosis lung are due to neutrophil elastase degradation." *The Journal of Immunology* **183**(12): 8148-56.

Wewers, M.D., Casolaro, M.A., Sellers, S.E., Swayze, S.C., McPhaul, K.M., Wittes, J.T. and Crystal, R.G. (1987). "Replacement therapy for alpha 1-antitrypsin deficiency associated with emphysema." *The New England Journal of Medicine* **316**(17): 1055-62.

WHO (1993). "Who international programme on chemical safety biomarkers and risk assessment: Concepts and principles.".

Wiedow, O. and Meyer-Hoffert, U. (2005). "Neutrophil serine proteases: Potential key regulators of cell signalling during inflammation." *Journal of Internal Medicine* **257**: 319-28.

Wielpütz, M.O., Bardarova, D., Weinheimer, O., Kauczor, H.U., Eichinger, M., Jobst, B.J., Eberhardt, R., Koenigkam-Santos, M., Puderbach, M. and Heussel, C.P. (2014). "Variation of densitometry on computed tomography in COPD--influence of different software tools." *PLOS ONE* **9**(11): e112898.

Willemse, B.W., ten Hacken, N.H., Rutgers, B., Lesman-Leegte, I.G., Postma, D.S. and Timens, W. (2005). "Effect of 1-year smoking cessation on airway inflammation in copd and asymptomatic smokers." *European Respiratory Journal* **26**(5): 835-45.

Witko-Sarsat, V., Halbwachs-Mecarelli, L., Schuster, A., Nusbaum, P., Ueki, I., Canteloup, S., Lenoir, G., Descamps-Latscha, B. and Nadel, J.A. (1999). "Proteinase 3, a potent secretagogue in airways, is present in cystic fibrosis sputum." *American Journal of Respiratory Cell and Molecular Biology* **20**(4): 729-36.

Wright, T.K., Gibson, P.G., Simpson, J.L., McDonald, V.M., Wood, L.G. and Baines, K.J. (2016). "Neutrophil extracellular traps are associated with inflammation in chronic airway disease." *Respirology* **21**(3): 467-75.

Wu, Y., Swulius, M.T., Moremen, K.W. and Sifers, R.N. (2003). "Elucidation of the molecular logic by which misfolded alpha 1-antitrypsin is preferentially selected for degradation." *Proceedings of the National Academy of Sciences of the United States of America* **100**(14): 8229-34.

Yamasaki, M., Li, W., Johnson, D.J. and Huntington, J.A. (2008). "Crystal structure of a stable dimer reveals the molecular basis of serpin polymerization." *Nature* **455**(7217): 1255-8.

Yamasaki, M., Sendall, T.J., Pearce, M.C., Whisstock, J.C. and Huntington, J.A. (2011). "Molecular basis of α1-antitrypsin deficiency revealed by the structure of a domain-swapped trimer." *EMBO Reports* **12**(10): 1011-7.

Yang, L., Mei, Y., Fang, Q., Wang, J., Yan, Z., DSong, Q., Lin, Z. and Ye, G. (2017). "Identification and characterization of serine protease inhibitors in a parasitic wasp, pteromalus puparum." *Scientific Reports* **7**.

Yang, P., Sun, Z., Krowka, M.J., Aubry, M.-C., Bamlet, W.R., Wampfler, J.A., Thibodeau, S.N., Katzmann, J.A., Allen, M.S., Midthun, D.E., Marks, R.S. and de Andrade, M. (2008). "Alpha1-antitrypsin deficiency carriers, tobacco smoke, chronic obstructive pulmonary disease, and lung cancer risk." *Archives of Internal Medicine* **168**(10): 1097-103.

Yi, X., Liu, M., Luo, Q., Zhuo, H., Cao, H., Wang, J. and Han, Y. (2017). "Toxic effects of dimethyl sulfoxide on red blood cells, platelets, and vascular endothelial cells in vitro." *FEBS Open Bio* **7**(4): 485-94.

Ying, Q.L. and Simon, S.R. (1993). "Kinetics of the inhibition of human leukocyte elastase by elafin, a 6-kilodalton elastase-specific inhibitor from human skin." *Biochemistry* **32**(7): 1866-74.

Yipp, B.G. and Kubes, P. (2013). "NETosis: How vital is it?" *Blood* **122**(16): 2784-94.

Yonchuk, J.G., Silverman, E.K., Bowler, R.P., Agusti, A., Lomas, D.A., Miller, B.E., Tal-Singer, R. and Mayer, R.J. (2015). "Circulating soluble receptor for advanced glycation end products (sRAGE) as a biomarker of emphysema and the rage axis in the lung." *American Journal of Respiratory and Critical Care Medicine* **192**(7): 785-92.

Yoshida, H., Matsui, T., Hosokawa, N., Kaufman, R.J., Nagata, K. and Mori, K. (2003). "A time-dependent phase shift in the mammalian unfolded protein response." *Developmental Cell* **4**(2): 265-71.

Yu, W.C., Fu, S.N., Tai, E.L., Yeung, Y.C., Kwong, K.C., Chang, Y., Tam, C.M. and Yiu, Y.K. (2013). "Spirometry is underused in the diagnosis and monitoring of patients with chronic obstructive pulmonary disease (COPD)." *International Journal of Chronic Obstructive Pulmonary Disease* **8**: 389-95.

Zabieglo, K., Majewski, P., Majchrzak-Gorecka, M., Wlodarczyk, A., Grygier, B., Zegar, A., Kapinska-Mrowiecka, M., Naskalska, A., Pyrc, K., Dubin, A., Wahl, S.M. and Cichy, J. (2015). "The inhibitory effect of secretory leukocyte protease inhibitor (SLPI) on formation of neutrophil extracellular traps." *Journal of leukocyte biology* **98**(1): 99-106.

Zaky, D.S.E., Naiem, M., Eid, H.A., Adawy, Z.R., Abd-Elraheem, S.E. and Mohamed, Z.A.Z. (2014). "Circulating surfactant protein-D as a biomarker of severity in stable chronic obstructive pulmonary diseases." *Egyptian Journal of Chest Diseases and Tuberculosis* **63**(3): 553-9.

Zani, M.-L., Baranger, K., Guyot, N., Dallet-Choisy, S. and Moreau, T. (2009). "Protease inhibitors derived from elafin and SLPI and engineered to have enhanced specificity towards neutrophil serine proteases." *Protein Science* **18**(3): 579-94.

Zani, M.-L., Nobar, S.M., Lacour, S.A., Lemoine, S., Boudier, C., Bieth, J.G. and Moreau, T. (2004). "Kinetics of the inhibition of neutriophil proteinases by recombinant

elafin and pre-elafin (trappin-2) expressed in pichia pastoris." *European Journal of Biochemistry* **271**: 2370-8.

Zhang, J.-M. and An, J. (2007). "Cytokines, inflammation and pain." *International Anesthesiology Clinics* **45**(2): 27-37.

Zhang, Y., Jiang, Y., Sun, C., Wang, Q., Yang, Z., Pan, X., Zhu, M. and Xiao, W. (2014). "The human cathelicidin IL-37 enhances airway mucus production in chronic obstructive pulmonary disease." *Biochemical and Biophysical Research Communications* **443**(1): 103-9.

Zhou, H.-X., Rivas, G. and Minton, A.P. (2008). "Macromolecular crowding and confinement: Biochemical, biophysical, and potential physiological consequences." *Annual Review of Biophysics* **37**(1): 375-97.

Zhu, J., Nathan, C., Jin, W., Sim, D., Ashcroft, G.S., Wahl, S.M., Lacomis, L., Erdujument-Bromage, H., Tempst, P., Wright, C.D. and Ding, A. (2002). "Conversion of proepithelin to epithelins: Roles of SLPI and elastase in host defense and wound repair." *Cell* **111**(6): 867-78.

Zimmer, M., Medcalf, R.L., Fink, T.M., Mattmann, C., Lichter, P. and Jenne, D.E. (1992). "Three human elastase-like genes coordingately expressed in the myelomonocyte lineage are organised as a single genetic locus on 19pter." *Proceedings of the National Academy of Sciences of the United States of America* **89**: 5.

Zorzetto, M., Russi, E., Senn, O., Imboden, M., Ferrarotti, I., Tinelli, C., Campo, I., Ottaviani, S., Scabini, R., von Eckardstein, A., Berger, W., Brändli, O., Rochat, T., Luisetti, M. and Probst-Hensch, N. (2008). "SerpinA1 gene variants in individuals from the general population with reduced α1-antitrypsin concentrations." *Clinical Chemistry* **54**(8): 1331.